Thèse de doctorat de l'Université Paris-Est

Présentée par

Masoud Fallah Shorshani

pour l'obtention du diplôme de docteur
de l'Université Paris-Est
Spécialité : SIE – Sciences, Ingénierie et Environnement

Modélisation de l'impact du trafic routier sur la pollution de l'air et des eaux de ruissellement

---

Soutenue le 4 juillet 2014

Jury composé de

Ludovic Leclercq, IFSTTAR	Président du jury & examinateur
Isabelle Braud, IRSTEA	Rapporteur
Lionel Soulhac, École Centrale de Lyon	Rapporteur
Frédéric Mahé, AIRPARIF	Examinateur
Guido Petrucci, Vrije Universiteit Brussel	Examinateur
Céline Bonhomme, LEESU	Co-encadrante
Michel André, IFSTTAR	Co-directeur de thèse
Christian Seigneur, CEREA	Directeur de thèse

Abstract: Road traffic emissions are a major source of pollution in cities. Modeling of air and stormwater pollution due to on-road vehicles is essential to understand the processes that lead to the pollution and provide the necessary information for the development of effective public policy in order to reducing pollution. This thesis aimed to evaluate the feasibility and relevance of chain models to simulate the impact of road traffic on air and stormwater pollution. The first part was to achieve a state of the art modeling tools for different phenomena (traffic, emissions, atmospheric dispersion, and stormwater), highlighting the integration of the different models to to create a coherent chain in terms of pollutants and spatio-temporal scales. Two examples of modeling chain have been proposed, one static with hourly time-step, the second considering a dynamic approach to traffic and associated pollution. In the second part of the thesis, different interface tools have been developed to link the models in the modeling chains. These modeling chains were tested with different case studies : (1) coupling traffic / emissions with a simulation of an urban street using a dynamic model of traffic with instantaneous and averaged emission models (2) coupling emissions / air pollution along a freeway , (3) couplings traffic / emissions / air pollution near a freeway, (4) coupling emissions / air pollution in suburban neighborhood (5) coupling atmospheric deposition / stormwater quality for a urban catchment, and finally (6) a complete modeling chain with traffic / emissions / air and stormwater quality models for urban catchment drainage. This work allows to identify different possibility of models integration for calculate the air and stormwater pollution due to road traffic in urban areas. Moreover, they provide a solid basis for the future development of integrated numerical models of urban pollution.

Résumé: Les émissions du trafic routier sont une des sources majeures de pollution dans les villes. La modélisation de la pollution de l'air et des eaux de ruissellement due aux émissions du trafic routier est essentielle pour comprendre les processus qui mènent à cette pollution et fournir les éléments d'information nécessaires au développement de politiques publiques efficaces pour la réduction des niveaux de pollution. L'objectif de cette thèse est d'évaluer la faisabilité et la pertinence de chaînes de modèles pour simuler l'impact du trafic routier sur la pollution de l'air et des eaux de ruissellement. La première partie a consisté à réaliser un état de l'art des outils de modélisation des différents phénomènes (trafic, émissions, pollution atmosphérique, qualité des eaux de ruissellement), mettant en exergue les enjeux liés à l'intégration des différents modèles pour constituer une chaîne cohérente en termes de polluants et d'échelles spatio-temporelles. Deux exemples de chaînes de modélisation ont été proposés, l'une statique avec des pas de temps horaires, la seconde envisageant une approche dynamique du trafic et des pollutions associées. Dans la deuxième partie de la thèse, des outils automatisés d'interfaçage ont été développés pour construire des chaînes de modèles. Ces chaînes de modèles ont ensuite été testées avec différents cas d'étude : (1) Couplage trafic / émissions avec une simulation d'une voie urbaine utilisant un modèle dynamique de trafic en lien avec des modèles d'émissions instantané et moyenné, (2) couplage émissions / pollution atmosphérique en bordure d'une autoroute, (3) couplages trafic / émissions / pollution atmosphérique en bordure d'une autoroute urbaine, (4) couplage émissions / pollution atmosphérique pour un quartier suburbain, (5) couplage dépôts atmosphériques / qualité des eaux de ruissellement pour un bassin versant suburbain, et finalement (6) une chaîne de modélisation complète avec couplages trafic / émissions /qualité de l'air et des eaux de ruissellement pour un bassin versant suburbain. Ces travaux ont permis à travers ces différents cas d'étude d'identifier les enjeux associés à l'intégration de modèles pour le calcul de la pollution de l'air et des eaux de ruissellement due au trafic routier en zone urbaine. Par ailleurs, ils fournissent une base solide pour le développement futur de modèles numériques intégrés de la pollution urbaine.

Remerciement

Je tiens tout d'abord à remercier très fortement mes directeurs de thèse, Christian Seigneur qui m'accompagné tout au long de ce travail avec ses idées et solutions toujours pertinentes et Michel André pour le grand intérêt et la curiosité qu'il a portés à mes travaux. J'adresse de chaleureux remerciements à ma co-encadrante de thèse, Céline Bonhomme pour sa grande disponibilité, son dynamisme et son efficacité.

Je tiens à remercier également les membres de mon jury, Ludovic Leclercq, Isabelle Braud, Lionel Soulhac, Frédéric Mahé et Guido Petrucci d'avoir bien voulu lire et juger ces travaux. Ils ont également contribué par leurs nombreuses remarques et suggestions à améliorer la qualité de ce travail, et je leur en suis très reconnaissant.

Merci à Mathieu Goriaux et stéphanie Deschamps avec qui j'ai partagé un bureau, des difficultés et des sourires.

Je tiens aussi à mentionner le plaisir que j'ai eu à travailler au sein des CEREA, LTE et LEESU; et j'en remercie tous ses membres. Des remerciements particuliers à : Régis Briant pour m'avoir familliarisé avec son code, Eduardo Redondo-Iglesias, Philippe DUPUY, Serge Pélissier, Yelva Roustan, Vivien Mallet, Christine Buisson, Hervé Chanut, Bruno Tassin, Ghassan Chebbo, Stefano Malfettani, Sylvain Doré, Luci Polo, Véronique Dehlinger, Aurélie Charron, Youngseob Kim, Nora Duhanyan, Marc Bocquet, Antoine Waked, Florian Couvidat, Mohammad Reza Koohkan, Eve Lecoeur, Nicolas Cherin, Arnaud Quérel, Yiguo Wang, Victor Winiarek, Vincent Loizeau, Jean-Matthieu Haussaire, Laetitia Girault, Laëtitia Thouron Pierre Tran, Nicolas Yan, Giuliana Becerra, Karine Sartelet, Jean-Luc Jaffrezo, Mohamed Houacine, Eugénie Brutti-Mairesse, Anaïs Pasquier, Antoine Montenon, Jérôme Drevet, Pascal Gastineau, Paul Kreczanik, Daniel Olivier...

A mes amis et particulièrement les Mehdis, Abbas, Aude, Marine et Saeed.

Enfin, un grand merci à l'ensemble de ma famille : mes frères, sœur, belle sœur, beaux parents. Merci particuliérement à mes parents sans qui cette thèse n'aurait pu débuter et à Samaneh qui m'a soutenu tout le temps inconditionnellment même durant ma thése.

Sommaire

Chapitre 1

1 Introduction

L'augmentation de la population urbaine et de la forte concentration de nombreuses activités humaines dans certaines zones des territoires mène à des problèmes de pollution de l'air et de l'eau. Par conséquent, étudier l'impact anthropique sur l'environnement urbain est nécessaire. Les impacts sanitaires de la pollution atmosphérique urbaine ont été étudiés dans 25 villes européennes dans le cadre du projet Aphekom (Improving Knowledge and Communication for Decision Making on Air Pollution and Health in Europe) dont neuf villes françaises. Ce projet a montré qu'une diminution des concentrations moyennes de particules fines ($PM_{2.5}$) jusqu'au seuil recommandé (10 μgm^{-3}) par l'Organisation Mondiale de la Santé (OMS) pourrait rallonger l'espérance de vie de 22 mois pour les personnes de 30 ans. De plus, 16 500 décès prématurés seraient attribuables chaque année en France liés à la pollution urbaine (Declercq et al., 2012). Par ailleurs, les polluants atmosphériques peuvent se déposer sur les bassins versants urbains et être transférés dans les eaux de ruissellement qui se chargent de polluants lors de leur précipitation sur les surfaces urbaines.

La gestion de l'environnement urbain est complexe. Une première étape consiste à comprendre les phénomènes de pollution, les mesurer, quantifier leurs niveaux et identifier leurs sources. Dans un second temps, on peut proposer des modèles qui simulent l'impact des émissions de polluants sur la qualité de l'environnement pour des études d'impact, des scénarios de prospective ou de la prévision à court terme. Grace à ces modèles, différents scénarios peuvent être testés dans le but de réduire ou d'optimiser les émissions de polluants. Ces études de modélisation peuvent alors fournir les bases scientifiques nécessaires pour élaborer des politiques publiques environnementales efficaces.

Une grande partie de la pollution dans les villes est due au trafic routier et sa contribution est susceptible d'augmenter encore car plus de 70% de la population mondiale en 2050 habitera dans les villes. L'objectif de ce travail est d'améliorer nos connaissances par la modélisation de l'impact des pollutions liées à la circulation automobile sur la qualité de l'air et des eaux de ruissellement. Pour cela, ce travail de thèse se propose de relier quatre composantes qui sont: (1) la position et les paramètres cinématiques des véhicules (modèle de trafic), (2) les quantités de différents types de polluants émis par les véhicules (modèle d'émission), (3) la dispersion et la transformation de ces polluants dans l'air ainsi que le transfert de ces polluants vers les surfaces par dépôts sec et humide (modèle de dispersion atmosphérique), et (4) la propagation des polluants qui entrent dans les eaux de ruissellement (modèle hydrologique et qualité de l'eau). Les couplages entre ces modèles au moyen d'interfaces et d'harmonisation des échelles spatio-temporelles conduisent au développement d'une chaîne

de modélisation qui permet alors de simuler l'impact des polluants émis par les véhicules sur la pollution de l'air et des eaux de ruissellement.

Cette thèse est donc consacrée à la construction de telles chaînes de modélisation, de leur évaluation avec des mesures expérimentales, de l'identification des difficultés qui peuvent être rencontrées et de la réalisation d'un ensemble de recommandations pour des travaux futurs sur cette problématique.

Le reste de ce chapitre est organisé comme suit. Les processus d'émissions de polluants par les véhicules sont brièvement décrits, puis les principaux polluants sont documentés. Ensuite, les effets sanitaires et les réglementations concernant la qualité de l'air et de l'eau sont exposés. Les systèmes de mesures de la pollution en zone urbaine et les stratégies de surveillance des concentrations de polluants dans l'air et l'eau sont brièvement présentés. Enfin, les objectifs généraux, la stratégie et les méthodologies adoptées dans cette thèse pour répondre à ces questions sont exposés.

Le second chapitre présente brièvement les modèles utilisés lors de ces travaux. Il s'agit des modèles Symuvia pour le trafic, CopCETE et PHEM pour les émissions de polluants, Polyphemus-Gaussien pour la dispersion atmosphérique et SWMM pour la modélisation de la quantité et de la qualité de l'eau. Une formulation améliorée d'un modèle gaussien de source linéique a aussi été appliquée pour la modélisation de la dispersion atmosphérique des particules.

Le chapitre trois présente un état de l'art des différents modèles de trafic, d'émission, de dispersion atmosphérique et d'hydrologie existants. Ensuite, différentes catégories de modèles sont considérées afin de développer des chaînes de modélisation en fonction des échelles spatio-temporelles. Ce chapitre aborde aussi de manière spécifique les couplages entre trafic et émissions, émissions et qualité de l'air, et qualité de l'air et qualité de l'eau à travers trois cas d'études.

Le chapitre 4 est consacré à la simulation de la qualité de l'air à proximité d'une autoroute urbaine à l'aide de données mesurées de trafic et des modèles d'émission et de dispersion atmosphérique. Le modèle d'émissions a été modifié pour tenir compte de la resuspension de particules par le trafic et le modèle de dispersion a été amélioré pour des conditions de vents faibles. Les résultats de cette chaîne de modélisation ont été comparés avec les mesures de concentrations de polluants atmosphériques obtenues dans le cadre des projets MOCOPO et PM-DRIVE.

Le chapitre 5 présente trois méthodes différentes pour modéliser l'impact du trafic sur la qualité des eaux de ruissellement. La première méthode utilise des données expérimentales de dépôts atmosphériques liés au trafic à proximité de routes. La deuxième méthode est basée sur l'utilisation d'un modèle boîte (0D) qui calcule les concentrations de polluants et les dépôts de manière uniforme sur le domaine de l'étude. La troisième méthode crée une chaîne de modélisation complète qui inclut les modèles de trafic, d'émission, de qualité de l'air et de

qualité de l'eau. Cette chaîne de modélisation est évaluée avec les données expérimentales du bassin versant de Grigny en région parisienne.

Un dernier chapitre présente les conclusions générales qui résument les principaux résultats mis en avant dans cette thèse ainsi qu'une discussion des perspectives à donner à ce travail.

1.1 Les émissions de polluants

Les émissions de polluants liés à la circulation automobile peuvent être catégorisées en quatre types selon les différents phénomènes qui génèrent ces émissions :

- **les émissions à l'échappement** : Ces émissions (ci-après dénommées simplement « émissions échappement ») sont liées au fonctionnement d'un moteur à explosion et aux phénomènes chimiques qui en découlent. Les émissions de certains polluants au cours de la période de chauffe (moteur froid) sont beaucoup plus élevées que pendant le fonctionnement à chaud du moteur ; il est donc nécessaire de distinguer ces deux types de production de polluants. Lorsque le moteur n'est pas suffisamment chaud (température inférieure à 80°C environ), il ne fonctionne pas à son rendement optimal, ce qui affecte les émissions liées au processus de combustion. Les émissions à chaud et à froid sont principalement liées aux technologies, motorisations, carburants, huiles, dispositifs de dépollution, et surtout aux modes d'utilisation du véhicule (vitesse et charge par exemple). Alors que les surémissions à froid peuvent être négligeables sur de longs trajets routiers ou autoroutiers, elles peuvent être majoritaires sur de courts trajets urbains.
- **les émissions par évaporation de carburant** : ce sont les émissions par évaporation dues aux systèmes de carburant des véhicules à essence (réservoir, système d'injection et conduites de carburant). Les émissions par évaporation provenant des véhicules diesel sont négligeables en raison de la présence d'hydrocarbures plus lourds et, par conséquent, d'une pression de vapeur du carburant diesel qui est relativement faible. Le processus d'évaporation est dû à la variation de température, soit par changement de température dans la journée, soit par évolution de celle du moteur des véhicules pendant la conduite et le stationnement. Une autre source importante est la perméation du carburant : diverses études montrent la fuite de carburant au travers de composants plastiques. Les évaporations sont de trois types : les évaporations au cours des déplacements, les évaporations lors du refroidissement du véhicule et les évaporations journalières dues aux variations de température ambiante.
- **les émissions « non-échappement »** : Les émissions « non-échappement » incluent des particules (PM), y compris des métaux lourds émis par l'usure des pneus, des plaquettes de freins et de l'embrayage des véhicules ainsi que des gaz émis suite à des fuites de gaz frigorigènes, carburant, huile, liquide de frein, etc. On inclut aussi dans ces émissions, l'usure de la chaussée par les véhicules. Ces émissions dépendent de la vitesse moyenne et du kilométrage parcouru par le véhicule.
- **les émissions par remise en suspension de particules** : La resuspension est la remise en état de suspension dans l'atmosphère de particules préalablement déposées sur le

sol. Cette resuspension peuvent représenter une bonne part des émissions de particules du trafic routier, jusqu'à environ 50% (par exemple, Polo, 2013).

1.2 Pollution émise par le trafic routier

Le trafic automobile contribue à la pollution atmosphérique à la fois par l'émission directe de polluants liée à l'utilisation des véhicules (polluants primaires) et par les polluants dérivés ou secondaires formés après réactions chimiques dans l'atmosphère à partir d'espèces chimiques (dites précurseurs) émises par les véhicules (e.g., ozone et la fraction secondaire des particules fines). Les polluants se classent en deux grandes catégories : les particules (émises à l'échappement ou issues de l'usure des véhicules, de la chaussée et de la resuspension.), et les polluants gazeux (échappement et évaporation des carburants). Certains polluants de l'échappement peuvent être semi-volatils et être par conséquent présents en tant que particules et gaz.

Plus précisément, les polluants émis par les véhicules roulants sont principalement :

- **Le dioxyde de carbone** (CO_2, aussi appellé gaz carbonique) qui est émis par la combustion de carburants fossiles (émission échappement). Le dioxyde de carbone n'a pas d'impact sur la santé publique (sauf à des concentrations très élevées), mais il intervient dans l'effet de serre qui mène au changement climatique.

- **Le monoxyde de carbone** (CO) qui résulte d'une combustion incomplète (émission échappement). Il s'oxyde lentement en dioxyde de carbone dans l'atmosphère avec une durée de vie de l'ordre d'un mois. Il s'agit d'un polluant bien connu du point de vue de son effet néfaste sur la santé.

- **Les oxydes d'azote** (NO_x), qui se forment à des températures de combustion élevées par recombinaison de l'azote et de l'oxygène de l'air. Ils incluent le monoxyde d'azote (NO), qui est majoritaire, et le dioxyde d'azote (NO_2). On définit $NO_x = NO + NO_2$; les fractions relatives de ces deux espèces chimiques dépendent du type de véhicule, du mode de conduite et du système de dépollution. L'origine de ces polluants était à 75 % due au trafic routier en 2005 (http://www.citepa.org/fr/). Les oxydes d'azote interviennent dans la formation d'ozone, de particules, de pluies acides et de dépôts azotés. NO_2 présente aussi des effets néfastes pour la santé.

- **L'ozone** (O_3) qui est un polluant secondaire issu de la réaction des oxydes d'azote et des composés organiques volatils (COV) sous l'effet du soleil (photochimie). La formation de l'ozone est un mécanisme complexe faisant intervenir de nombreux aspects chimiques et climatiques (température, ensoleillement, etc.). L'ozone n'est pas un polluant de proximité car il se forme au cours de plusieurs heures. Il réagit presque instantanément avec le monoxyde d'azote (NO) émis par les véhicules automobiles pour former le dioxyde d'azote (NO_2). L'ozone est un polluant à caractère plutôt

régional. C'est un oxydant qui a des effets néfastes sur la santé et la végétation ; c'est aussi un gaz à effet de serre.

- **Le dioxyde de soufre** (SO_2) est lié à la teneur en soufre dans le carburant diesel et dans une moindre mesure dans les essences. Il est émis par l'échappement. Pendant de nombreuses années, les véhicules diesel ont contribué à la pollution par SO_2, mais les décrets réduisant la teneur en soufre des carburants ont permis de réduire de façon importante les émissions des automobiles. SO_2 a des effets néfastes sur la santé et est aussi un précurseur de sulfate, qui contribue aux niveaux de particules fines et aux pluies acides.

- L'**ammoniac** (NH_3) qui est émis par l'échappement. Il n'a pas d'incidence sur la santé, mais il joue un rôle actif dans le phénomène de neutralisation des acides, dans la formation des particules atmosphériques, et dans les dépôts azotés sur les eaux de surface et les sols. Il faut noter qu'il est faiblement présent dans le secteur des transports ; bien que les technologies de dépollution tendent à en augmenter l'émission, ses émissions sont actuellement dominées par l'agriculture.

- Le **protoxyde d'azote** (N_2O) : Une petite partie des émissions de protoxyde d'azote est attribuée au trafic routier, en particulier aux pots catalytiques. C'est un des plus importants gaz à effet de serre contribuant au réchauffement de la planète après la vapeur d'eau (H_2O), le dioxyde de carbone (CO_2) et le méthane (CH_4).

- **Les particules** (PM) proviennent de l'échappement (principalement des véhicules diesel sans filtre à particules), des émissions non-échappement et du phénomène de resuspension. Les particules fines provenant de l'échappement sont formées de noyaux solides carbonés sur lesquels d'autres composés sont fixés, tels que les hydrocarbures imbrûlés semi-volatils provenant des huiles et du carburant, et des produits de combustion oxydés et / ou aromatiques. Les particules ultra-fines provenant de l'échappement sont formées à partir d'une nucléation d'acide sulfurique suivie de condensation de produits semi-volatils (acide sulfurique, composés organiques) ; elles coagulent ensuite avec des particules fines. A noter qu'il convient de distinguer les particules de diamètre aérodynamique inférieur à 10 µm (PM_{10}) et celles avec un diamètre inférieur à 2.5 µm ($PM_{2,5}$). Par ailleurs, les particules contiennent des substances toxiques comme des métaux lourds, du carbone suie et des composés organiques.

- **Composés Organiques Volatils** (COV), qui résultent d'une part (et principalement) d'une combustion incomplète et se retrouvent à l'échappement (notamment à froid), et d'autre part de l'évaporation de carburant. Les émissions de COV par évaporation représentent environ 9% contre 91% d'émission par échappement (André et al., 2012). Les COV incluent tous les composés organiques gazeux de l'atmosphère. On distingue (COVNM) COV non méthaniques (e.g., propane, propène, benzène, formaldéhyde, acroléine, etc.) et méthane (CH_4). Les COVNM contribuent, avec les NO_x, à la

formation de l'ozone et de particules secondaires. Le méthane est peu réactif mais est un gaz à effet de serre. Les hydrocarbures sont des COV qui ne contiennent que du carbone et de l'hydrogène. Ils comprennent les hydrocarbures aliphatiques et hydrocarbures aromatiques. Ces derniers peuvent être monocycliques (HAM, tels que le benzène et le toluène) ou polycycliques (HAP) ; 16 principaux HAP sont présentés dans le Tableau 1.1.

Tableau 1.1. Liste des 16 principaux HAP (d'après Deletraz, 2002)

HAP légers, principalement sous forme gazeuse	HAP lourds, principalement sous forme particulaire
Naphtalène Acénaphtylène Acénaphtène Fluorène Phénanthrène Anthracène Fluoranthène Pyrène (P) Chrysène Benzo(a)anthracène (BaA)	Benzo(a) pyrène (BaP) Benzo(b)fluoranthène (BbF) Benzo(k)fluoranthène (BkF) Dibenzo anthracène Indéno (1,2,3) pyrène (IP) Benzo(g,h,i)pérylènr (BghiP)

- Les **métaux** sont émis par émission échappement ainsi que par émission non-échappement sous forme de particules (à l'exception du mercure qui est principalement sous forme gazeuse, mais émis en très faible quantité par les véhicules). Les métaux principaux impliqués dans la pollution automobile sont :
    - **Le plomb** (Pb) : Après la disparition des essences à base de plomb une baisse significative des concentrations moyennes annuelles a été notée. Le plomb atmosphérique ne représente donc plus un enjeu fort pour la qualité de l'air. Toutefois, compte tenu des émissions non-échappement et de la remise en suspension des particules dans les eaux, de l'absorption par les plantes et dans les sols, sa prise en compte dans les études d'impact est encore obligatoire.
    - **Le cadmium** (Cd) : En milieu interurbain, l'automobile émet très peu de cadmium par rapport aux autres activités (industrielles, agricoles). On en trouve essentiellement dans les additifs des lubrifiants et dans les pneumatiques et aussi dans les émissions échappement. En milieu urbain, le trafic peut être sa principale source de pollution de l'air et de l'eau. Ce métal a des effets sur des plantes à vocation alimentaire, ce qui peut entraîner un risque indirect pour l'homme.
    - **Le zinc** (Zn) : Les émissions du zinc liées au trafic sont essentiellement dues aux fuites de lubrifiants, à l'émission par échappement et à l'érosion des glissières de sécurité. On peut donc en retrouver dans les émissions échappement sous forme de particules. Le zinc n'est pas un métal qui sera réglementé dans les années à venir au titre de la loi sur l'air. Actuellement, on

suit sa présence surtout dans les eaux de ruissellement des routes. On peut trouver des quantités importantes dans les sols des emprises routières.

- Les métaux **fer** (Fe), **cuivre** (Cu), **antimoine** (Sb), **chrome** (Cr), **nickel** (Ni), **sélénium** (Se), **baryum** (Ba), **arsenic** (As), **mercure** (Hg), etc., peuvent être produits par les émissions échappement, non-échappement et par resuspension. Les métaux lourds des différentes sources véhiculaires sont listés par exemple par Polo (2013).

1.3 Effets sanitaires

1.3.1 Enjeux sanitaires de la pollution atmosphérique

L'impact de la pollution atmosphérique sur la santé publique est devenu un problème majeur. En effet, elle est la cause principale de près de 7 millions de décès dans le monde en 2012 selon l'Organisation Mondiale de la Santé (OMS) : "Ces chiffres représentent plus du double des estimations précédentes et confirment que la pollution de l'air est désormais le principal risque environnemental pour la santé dans le monde". L'exemple de l'étude de Bell et Davis (2001) montre le lien entre les concentrations de dioxyde de soufre (SO2) et la mortalité lors du fameux épisode de pollution à Londres en 1952 (voir Figure 1.1).

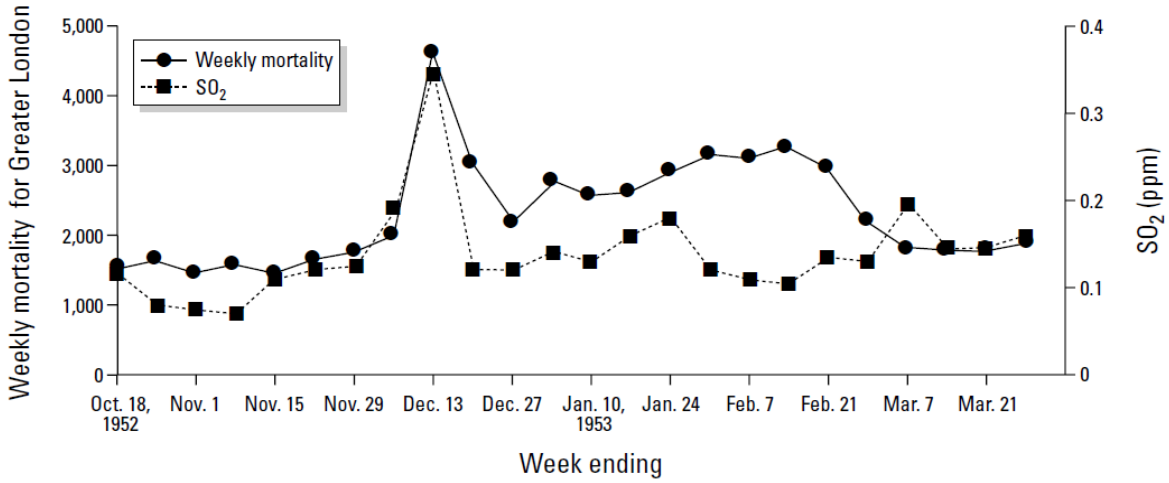

Figure 1.1. Nombre de décès et évolution de la concentration en dioxyde de souffre lors de l'épisode de smog de l'hiver 1952 à Londres. Source: Bell et Davis, 2001.

1.3.2 Enjeux sanitaires de la pollution des eaux

Les polluants qui sont transportés par les eaux de ruissellement affectent la qualité des eaux des milieux récepteurs. Ils occasionnent différents problèmes pour les écosystèmes, touchant à la fois les espèces animales et les espèces végétales, et peuvent par ailleurs limiter les activités humaines. Par exemple, l'augmentation de la toxicité des eaux de ruissellement entrant au barrage Fashafuyeh, due aux activités urbaines d'une banlieue de Téhéran, Iran, a tué 2 millions poissons en avril 2014 (voir Figure 1.2). Ce barrage est utilisé aussi pour la pisciculture.

Figure 1.2. L'effet toxique des eaux de ruissellement sur les espèces aquatiques (barrage Fashafuyeh, Iran)

1.3.3 Effets sur la santé des polluants émis par les véhicules

Les effets des principaux polluants liés au trafic routier sur la santé sont brièvement présentés dans cette partie.

CO_2 est un gaz peu toxique à faible dose mais il est un des principaux gaz à effet de serre. A très forte concentration, il peut cependant provoquer des malaises et des maux de tête.

CO se fixe sur l'hémoglobine du sang, avec une affinité 200 fois supérieure à celle de l'oxygène, ce qui peut influencer le cerveau et le cœur. L'inhalation de CO entraîne des maux de tête et des vertiges et peut mener à la mort.

NO_2 provoque une hyperréactivité bronchique chez les asthmatiques. Le dioxyde d'azote se transforme dans l'atmosphère en acide nitrique, qui retombe au sol assez rapidement (durée de vie atmosphérique de l'ordre d'une journée), et la pluie en ruisselant va entraîner cet acide dans les eaux de ruissellement et les milieux récepteurs. Par ailleurs, NO_x (NO et NO_2) sont des précurseurs de O_3 et de particules.

O_3 est capable de pénétrer profondément dans les poumons. Il affecte les voies respiratoires car c'est un oxydant puissant. Il affecte aussi la végétation car il détériore la surface des feuilles et aiguilles des plantes.

SO_2 est un gaz irritant, notamment pour l'appareil respiratoire. Les fortes pointes de pollution peuvent déclencher une gêne respiratoire chez les personnes sensibles (asmathiques, jeunes enfants). L'étude de Tertre et al. (2014) montre qu'il y a un rapport linéaire entre l'augmentation de concentration de SO_2 et la mortalité. Le dioxyde de soufre se transforme principalement en acide sulfurique qui contamine les eaux de ruissellement et contribue à la formation de particules fines.

NH_3 est un gaz incolore et odorant, qui est très irritant pour le système respiratoire, la peau, et les yeux à très fortes concentrations. Ce n'est pas un polluant primaire aux concentrations atmosphériques observées mais il est un précurseur de particules. Il est peu généré par le transport routier. Sa présence dans les eaux de l'ammoniac affecte la vie aquatique. Pour les eaux douces courantes, sa toxicité aiguë provoque chez les poissons notamment des lésions branchiales et une asphyxie des espèces sensibles. Pour les eaux douces stagnantes, le risque d'intoxication aiguë est plus marqué en été car la hausse des températures entraine l'augmentation de la photosynthèse. Ce phénomène, s'accompagne d'une augmentation du pH qui privilégie la forme NH_3 (toxique) aux ions ammonium (NH_4^+).

Les particules sont un des polluants majeurs dans les villes (An et al., 2013). La toxicité des particules dépend de leur taille et de leur composition. Leur rôle a été démontré dans certaines atteintes fonctionnelles respiratoires, le déclenchement de crises d'asthme et la hausse du nombre de décès pour cause cardio-vasculaire ou respiratoire. Les particules fines, $PM_{2.5}$, sont les plus dangereuses (voir Figure 1.3). Les particules fines sont capables de pénétrer au plus profond de l'appareil respiratoire, elles atteignent les voies aériennes terminales et peuvent pénétrer dans le système sanguin. Ces particules peuvent véhiculer des composés toxiques, allergènes, mutagènes ou cancérigènes, comme des polluants organiques persistants (POP) tels que les HAP et des métaux lourds (tels que Fe, As, Cd, Cr, Cu, Hg, Ni, Pb, Se et Zn). Il faut noter que HAP et métaux sont les principaux polluants dans les eaux. Les phénomènes de ruissellement et de lessivage des sols sont à l'origine de la contamination des cours d'eau et des nappes phréatiques et à plus long terme des eaux potables.

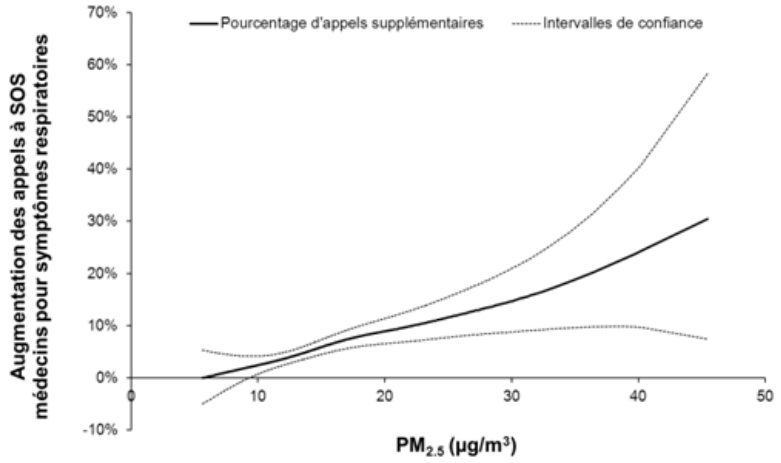

Figure 1.3. Illustration d'appels à SOS médecins en fonction de la concentration de $PM_{2.5}$. Source : ORS Île-de-France

Les métaux lourds s'accumulent dans les organismes vivants et ont des effets toxiques à court et long terme. Certains, comme le cadmium et le chrome hexavalent sont cancérigènes.

Certains COV ont des effets irritants sur la peau, les yeux et le système respiratoire. Certains COV comme le benzène et le formaldéhyde sont cancérigènes (Vlachokostas et al., 2012).

Les HAP sont des molécules biologiquement actives qui, une fois accumulées dans les tissus organiques, se prêtent à des réactions de transformation en métabolite. Ces métabolites ainsi formés peuvent avoir un effet plus ou moins marqué en se liant à des molécules telles que les protéines, l'ARN ou l'ADN, menant à des dysfonctionnements cellulaires. Le benzo(a)pyrène est un des composés les plus toxiques de cette famille car il est mutagène et fortement cancérigène.

Le trafic routier est une des sources majeures de la pollution urbaine. L'étude de Yim and Barrett (2012) suggère qu'environ 7500 morts par an résultent des émissions liées au transport routier en Angleterre. Plusieurs études comparent généralement l'apparition d'effets indésirables sur la santé des populations qui vivent, travaillent ou vont à l'école près de routes très fréquentées. Baldauf et al. (2008) présentent 26 études différentes concernant les effets du trafic routier sur la santé qui incluent l'asthme et d'autres symptômes respiratoires, le poids des nouveaux nés, la mortalité prématurée, des effets cardiovasculaires et des cancers. Cet état de fait a amené les pouvoirs publics à considérer l'urgence de la mise en place de moyens visant à réduire ce type de pollution.

1.4 Réglementations de la qualité des eaux et de l'air ambiant

Les effets de la pollution atmosphérique et des eaux pluviales polluées sur la santé ainsi que sur les écosystèmes engendrent une pression pour la mise en place de réglementations.

Les règlementations européennes portant sur la qualité de l'air sont : la Directive n° 2004/107/CE du 15 décembre 2004 concernant l'arsenic, le cadmium, le mercure, le nickel et les hydrocarbures aromatiques polycycliques dans l'air ambiant et la Directive n° 2008/50/CE du 21 mai 2008 concernant la qualité de l'air ambiant et un air pur pour l'Europe. Cette directive est transposée par le décret n°2010-1250 du 21 octobre 2010.

La Directive cadre sur l'eau (DCE 2000/60/CE) fixe au niveau européen et la circulaire du 7 mai 2007 au niveau national des NQEp (normes de qualité environnementale provisoires) pour les objectifs de réduction des émissions pour l'eau. Les substances polluantes pour l'eau et la réglementation de la qualité des eaux en milieu urbain ont été étudiées par Zgheib (2009). Les NQEp sont établies pour trois types d'eaux : les eaux de surfaces intérieures (cours d'eau, plans d'eau, canaux, réservoirs), les eaux de transition (eaux de surface situées a proximité des embouchures de rivières ou de fleuves) et les eaux marines intérieures et territoriales.

Ces réglementations pour différents polluants liés au trafic sont illustrées dans le Tableau 1.2 pour les eaux de surfaces intérieures et l'air ambiant. Dans ce tableau NQE-MA représente la norme de qualité environnementale pour une concentration moyenne annuelle, SEI est le seuil d'évaluation inférieur, c'est-à-dire un niveau en deçà duquel il est suffisant, pour évaluer la qualité de l'air ambiant, d'utiliser des techniques de modélisation ou d'estimation objective, et SES est le seuil d'évaluation supérieur, c'est-à-dire un niveau en deçà duquel il est permis,

pour évaluer la qualité de l'air ambiant, d'utiliser une combinaison de mesures fixes et de techniques de modélisation et/ou de mesures indicatives. Une valeur limite est un niveau à atteindre dans un délai donné et à ne pas dépasser (plus d'un certain nombre de fois pour les valeurs portant sur des périodes courtes), et fixé sur la base des connaissances scientifiques afin d'éviter, de prévenir ou de réduire les effets nocifs sur la santé humaine ou sur l'environnement dans son ensemble. Une valeur cible est un niveau à atteindre, dans la mesure du possible, dans un délai donné, et fixé afin d'éviter, de prévenir ou de réduire les effets nocifs sur la santé humaine ou l'environnement dans son ensemble. Il faut noter que 14 COV (éthylbenzène, isopropylbenzène, toluène, xylènes, 1,2-dichloroéthane, chlorure de méthylène, hexachlorobutadiène, chloroforme, tétrachlorure de carbone, tétrachloroéthylène, trichloréthylène, 1,2,4-trichlorobenzène, 1,2,3-trichlorobenzène, 1,3,5-trichlorobenzène) possèdent des NQEp fixées par la circulaire du 7 mai 2007 mais l'émission de ces polluants n'est pas encore étudiée pour le trafic routier.

La réduction de la pollution due au trafic est nécessaire afin de respecter les niveaux de polluants ci-dessus. Plusieurs générations de directives (70/220/EEC et 98/69/EC) se sont succédées en coordination avec les États, les constructeurs automobiles et les producteurs de pétrole pour déterminer 6 niveaux d'émissions (appelés normes Euro). Ces normes s'expriment en unité de masse par distance (g/km) pour les véhicules légers et en unité de masse par énergie (g/kWh) pour les poids lourds ; elles sont définies pour des cycles de conduite bien définis. Les véhicules les plus récents respectent la norme Euro 5 en vigueur depuis 2011, et plus contraignante que les réglementations antérieures. La norme Euro 6 est prévue pour septembre 2014, avec des émissions en particules réduites de 97% en masse par rapport à celles d'un véhicule Euro 1 pour un moteur diesel. La Figure 1.4 montre l'évolution des émissions en fonction des normes Euro pour les véhicules légers.

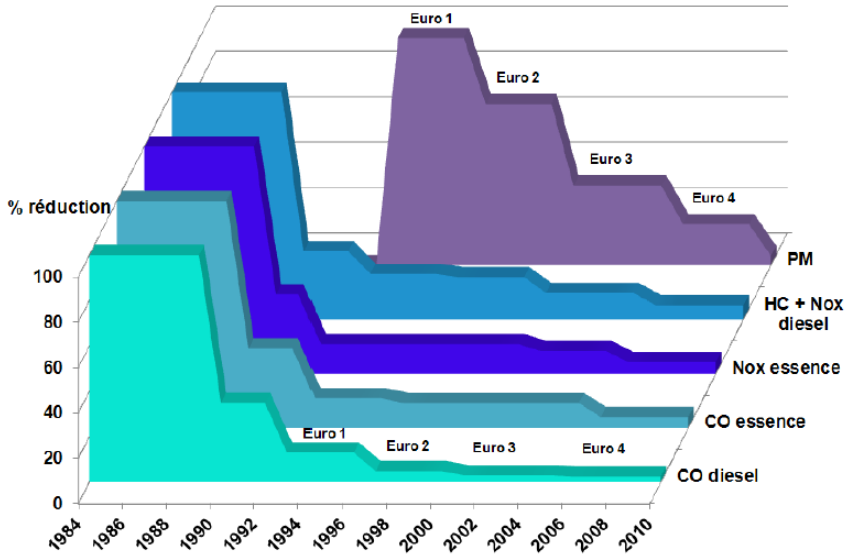

Figure 1.4. Évolution des émissions CO, NO_x, PM (masse) en fonction des normes européennes pour les véhicules légers (www.senat.fr).

Tableau 1.2. Réglementations des polluants dus au trafic pour les eaux de surfaces intérieures et l'air ambiant.

Polluants	Directives 2004/107/CE et 2008/50/CE et décret n°2010-1250 du 21 octobre 2010 air ambiant				Directive 2008/105/CE et la circulaire du 7 mai 2007 pour les eaux de surfaces intérieures (µg/L)	
	Moyenne critique – air	SEI	SES	Valeurs limites Valeurs cibles*	NQE-MA	NQEp
CO	Moyenne sur 8 heures	5 mg/m^3	7 mg/m^3	10 mg/m^3		
NO_x	Moyenne annuelle (protection de la végétation)	19,5 $µg/m^3$	24 $µg/m^3$		-	-
NO_2	Moyennes horaires à ne pas dépasser plus de 18 fois par année civile (protection de la santé humaine)	100 $µg/m^3$	140 $µg/m^3$	200 $µg/m^3$	-	-
	Moyenne annuelle (protection de la santé humaine)	26 µg/m3	32 µg/m3	40 $µg/m^3$	-	-
SO_2	Moyennes journalières à ne pas dépasser plus de 3 fois par année (protection de la santé humaine)	50 $µg/m^3$	75 $µg/m^3$	125 $µg/m^3$	-	-
	Moyenne hivernale (protection des écosystèmes)	8 $µg/m^3$	12 $µg/m^3$		-	-
PM_{10}	Moyennes sur 24 heures à ne pas dépasser plus de 35 fois par année civile	25 $µg/m^3$	35 $µg/m^3$	40 $µg/m^3$	-	-
	Moyenne annuelle	20 $µg/m^3$	28 $µg/m^3$	50 $µg/m^3$	-	-
$PM_{2.5}$	Moyenne annuelle	12 $µg/m^3$	17 $µg/m^3$	26, 20* $µg/m^3$	-	-
Benzène (C_6H_6)	Moyenne annuelle	2 $µg/m^3$	3.5 $µg/m^3$	5 $µg/m^3$	10	10
Benzo[a]pyrene	Moyenne annuelle	0.4 ng/m^3	0.6 ng/m^3	1* ng/m^3	0,05	0,05
Benzo[b]fluoranthene Benzo[k]fluoranthene	-	-	-		Σ = 0,03	Σ= 0,03
Benzo[g,h,i]perylene Indeno[1,2,3cd]pyrene	-	-	-		Σ = 0,002	Σ = 0,002
Pb	Moyenne annuelle	0.25 $µg/m^3$	0.35 $µg/m^3$	0.5 $µg/m^3$	7,2	7,2
Cd	Moyenne annuelle	2 ng/m^3	3 ng/m^3	5* ng/m^3	0,15	5
As	Moyenne annuelle	2,4 ng/m^3	3,6 ng/m^3	6* ng/m^3	-	-
Ni	Moyenne annuelle	10 ng/m^3	14 ng/m^3	20* ng/m^3	20	20
Hg	-	-	-		0,05	1

La réduction des polluants par les constructeurs automobiles et les pétroliers inclut plusieurs systèmes : (1) la conception de systèmes de combustion efficaces pour réduire les émissions à l'échappement, (2) l'utilisation de systèmes de récupération des vapeurs d'essence d'évaporation, (3) l'utilisation des technologies informatiques pour surveiller et contrôler les performances du moteur, (4) les technologies efficaces de « post-traitement » ou de dépollution, comme les convertisseurs catalytiques et filtres à particules, et dispositifs de réduction des oxydes d'azotes (SCR, De-NOx) qui éliminent ou convertissent les polluants avant leur émission dans l'atmosphère et (5) l'amélioration de la qualité du carburant (suppression / remplacement de composés toxiques, utilisation de carburants de substitution).

1.5 Surveillance des concentrations

1.5.1 Air

En réponse aux enjeux sanitaires, la loi française est « codifiée aux articles L220-1 et suivants du Code de l'Environnement » ; c'est la loi sur l'air et l'utilisation rationnelle de l'énergie (LAURE), parue le 30 décembre 1996, qui vise à rationaliser l'utilisation de l'énergie et à définir une politique publique intégrant l'air en matière de développement urbain. Elle invoque le droit de respirer un air qui ne nuise pas à la santé. Elle rend obligatoires : (1) la définition de normes de qualité de l'air (voir plus haut), (2) la surveillance de la qualité de l'air, et (3) l'information du public, dont l'État est le garant, qui doit être réalisée périodiquement et le déclenchement d'une alerte en cas de dépassement de seuil réglementaire. Le dispositif de surveillance de la qualité de l'air regroupe l'ensemble des acteurs impliqués dans ce domaine : le Ministère de l'Écologie, du Développement Durable et de l'Énergie (MEDDE), les DREAL, l'ADEME, les AASQA et le LCSQA. Pour garantir la qualité des mesures, l'État a mis en place le Laboratoire Central de Surveillance de la Qualité de l'Air (LCSQA). Les Associations Agréées de Surveillance de Qualité de l'Air (AASQA) comprennent 26 associations (http://www.lcsqa.org/aasqa) qui sont chargées de surveiller la qualité de l'air dans les différentes régions françaises. Les cartes de synthèse de la pollution enregistrée pour chaque région sont disponibles sur le lien suivant : http://www.lcsqa.org/surveillance/dispositif/plans_surveillance. La loi prescrit également l'élaboration pour les agglomérations de plus de 250 000 habitants de Plans de Protection de l'Atmosphère (PPA) et pour les agglomérations de plus de 100 000 habitants de Plans de Déplacements Urbains (PDU). Le PDU vise à développer les transports collectifs et les modes de transport propres, à organiser le stationnement et à aménager la voirie (http://www.developpement-durable.gouv.fr). Il affecte donc indirectement la qualité de l'air.

Un indice de qualité de l'air est un chiffre utilisé par les agences gouvernementales pour communiquer au public le niveau de pollution. Différents pays ont leurs propres indices de qualité de l'air qui ne sont pas tous compatibles. En France, pour les agglomérations de plus de 100 000 habitants, il s'agit de l'indice Atmo et pour les agglomérations de moins de 100 000 habitants, il s'agit de l'indice IQA (« indice de qualité de l'air simplifié ») calculé sur la base d'un à quatre sous-indices. L'indice européen est aussi communiqué par les AASQA.

L'indice de qualité de l'air croît de 1 (très bon) à 10 (très mauvais). Il permet de caractériser de manière simple et globale la qualité de l'air d'une agglomération urbaine. L'indice est déterminé par le maximum d'un ensemble de sous-indices, chacun d'entre eux étant représentatif d'un polluant de l'air : dioxyde de soufre (SO_2), dioxyde d'azote (NO_2), ozone (O_3) et poussières respirables (PM_{10}). Les sites de mesure sélectionnés pour son calcul caractérisent la pollution atmosphérique de fond des zones fortement peuplées (sites urbains) ou sites périurbains (http://www.atmo-france.org). La Figure 1.5**. Cartographies de l'indice de qualité de l'air** montre un exemple des informations fournies par l'indice de qualité de l'air.

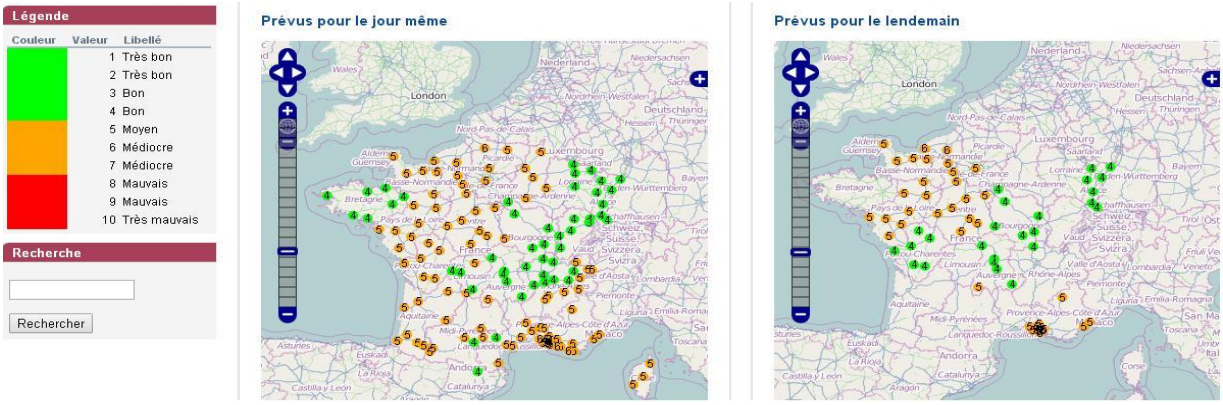

Figure 1.5. Cartographies de l'indice de qualité de l'air (source : http://www.lcsqa.org/)

Des prévisions de qualité de l'air sont fournies à la population pour l'informer et l'aider à minimiser les risques pour la santé publique. Elles peuvent par ailleurs être utilisées par les pouvoirs publies pour mettre en place des actions ponctuelles de réduction de la pollution (par exemple circulation alternée). Le système PREV'AIR (http://www.prevair.org/fr/index.php) a été mis en place en 2003 à l'initiative du Ministère de l'écologie (MEDDE) afin de générer et de diffuser quotidiennement des prévisions et des cartographies de qualité de l'air par simulation numérique à différents échelles spatiales. Par ailleurs, les AASQA ont leur propre système de prévision (par exemple, www.airparif.asso.fr) et certains laboratoires, tels que le CEREA, fournissent aussi des prévisions (http://cerea.enpc.fr/).

1.5.2 Eau

L'Office national de l'eau et des milieux aquatiques (Onema) a été créé pour une gestion globale et durable de la ressource en eau et des écosystèmes aquatiques et la reconquête de la qualité des eaux. En France, des programmes de surveillance (DCE) de l'état des eaux - cours d'eau, plans d'eau, eaux de transition, eaux côtières, eaux souterraines - ont été mis en œuvre dans chaque bassin hydrographique depuis 2007. Le réseau de contrôle de surveillance est constitué de l'ordre de 1500 sites pérennes « cours d'eau » répartis sur le territoire français (métropole). Les méthodes de surveillance et les substances prioritaires de l'état physico-chimique (température, oxygène, salinité, matières en suspension…), et l'état chimique (micropolluants tels que métaux lourds, pesticides, hydrocarbures…) sont prescrites pour les eaux douces de surface par la circulaire du 29 janvier 2013. Les observations de chaque bassin versant sont accessibles sur le lien suivant : http://www.surveillance.eaufrance.fr/.

L'état chimique est l'appréciation de la qualité d'une eau sur la base des concentrations de 41 substances incluant des polluants liés au trafic tels que des métaux lourds et certains HAP. Les concentrations ne doivent pas dépasser les NQE établies par la directive de 2008/105/CE. Le dépassement de la norme pour une seule substance suffit à déclarer une station du réseau en mauvais état chimique, quelle que soit la situation des autres substances sur cette même station. Il n'existe donc que deux classes de l'état chimique : bon état ou mauvais état.

Par ailleurs, les plans d'urbanisme doivent être compatibles avec les objectifs de protection définis par le SAGE (schéma d'aménagement et de gestion des eaux). Le SAGE est un document de planification de la gestion de l'eau à l'échelle d'un bassin versant qui fixe des objectifs de protection quantitative et qualitative de la ressource en eau et il doit être compatible avec le schéma directeur d'aménagement et de gestion des eaux (SDAGE).

1.6 Objectifs généraux du travail de thèse

Les enjeux environnementaux et sanitaires liés à la circulation automobile nous obligent à connaitre et surveiller ses impacts. Les mesures de polluants liés au trafic dans l'air et dans l'eau peuvent nous informer sur les niveaux de concentrations dans ces milieux mais cette méthode reste limitée à certains points. En revanche, la modélisation est complémentaire des mesures et essentielle pour comprendre les processus en jeu et fournir les éléments d'information nécessaires au développement de politiques publiques. En effet, la modélisation permet d'estimer les concentrations dans des gammes d'échelles spatio-temporelles plus vastes que celles possibles pour les mesures. La modélisation peut aussi être utilisée pour prévoir l'émergence d'enjeux environnementaux liés aux transports, contribuer à l'objectif de maîtrise de la qualité de l'air et de l'eau (étude de prospective) ou bien simuler l'impact de nouvelles émissions (étude d'impact). Par ailleurs, la modélisation est généralement moins coûteuse que la réalisation de mesures expérimentales.

Différents outils de modélisation ont été utilisés pour cette thèse. Ils couvrent la modélisation du trafic, des émissions de polluants, des concentrations des polluants dans l'atmosphère et des concentrations de polluants dans les eaux de ruissellement. Ces outils permettent d'obtenir les données d'entrées nécessaires pour l'outil simulant les phénomènes suivants ; par exemple, un modèle de trafic fournit les informations nécessaires pour calculer les émissions de polluants liés au trafic. Nous avons donc ciblé notre recherche pour développer une chaîne de modélisation qui permet de quantifier les impacts environnementaux du trafic routier sur la pollution atmosphérique et la contamination des bassins versants urbaines en prenant en compte le trafic, les émissions des véhicules, les processus de transport et de transformation atmosphériques, les dépôts atmosphériques sur les bassins versants et les processus de transport et de transformation dans les eaux de ruissellement. Il s'agit également d'évaluer la faisabilité et pertinence de ces chaînes de modèles à différentes échelles et pour différentes conditions.

La première partie de cette thèse a consisté à réaliser un état de l'art des outils de modélisation des différents phénomènes pertinents (trafic, émissions, pollution atmosphérique, qualité des

eaux de ruissellement), mettant en exergue les enjeux liés à l'intégration des différents modèles pour constituer une chaîne cohérente en termes de polluants et d'échelles spatio-temporelles. Deux exemples de chaînes de modélisation sont proposés, l'une statique avec des pas de temps horaires, la seconde envisageant une approche dynamique du trafic et des pollutions associées. Ces chaines de modèles ont été testées pour trois configurations partielles : (1) Couplage trafic / émissions avec une simulation d'une voie urbaine utilisant un modèle dynamique de trafic en lien avec des modèles d'émissions instantané et moyenné, (2) couplage émissions / pollution atmosphérique en bordure d'une autoroute, et (3) couplage dépôts atmosphériques / qualité des eaux de ruissellement pour un bassin versant urbain. Dans la suite du travail de thèse, des outils automatisés d'interfaçage ont été développés pour construire une chaîne de modèles simulant la qualité de l'air et aussi différentes méthodes pour estimer la qualité de l'eau en fonction des données détaillées disponibles sur un bassin versant. Les résultats de ces chaines de modélisation ont été comparés aux mesures obtenues lors de cinq campagnes de mesures : MOCOPO et PM-DRIVE à Grenoble, SIVOA à Grigny, Promeyrat (2001) à Metz (Autoroute A31), et INOGEV à Sucy-en-Brie.

Cette thèse aura permis une avancée significative dans la connaissance et l'intégration de l'ensemble des modèles permettant le calcul des concentrations atmosphériques et dans les eaux de certains contaminants liés au trafic routier, mettant en avant certaines limites et recommandant certaines précautions lors de la réalisation de telles chaînes de modélisation. Par ailleurs, la nécessité de données expérimentales robustes pour la validation de l'ensemble apparaît comme un point important qui doit être adressé dans les futurs programmes de recherche.

Chapitre 2

2 Description des modèles

Nous avons argumenté dans l'introduction l'intérêt de développer des chaînes pertinentes de modèles pour étudier les phénomènes influençant les pollutions de l'air et de l'eau induites par le trafic routier. Plusieurs outils ont été utilisés pour ces quatre phénomènes : trafic, émission, qualité de l'air et de l'eau.

Le choix du modèle dépendra de l'échelle spatio-temporelle à modéliser mais aussi de la résolution des données d'entrées et de sorties des modèles ou encore de la compatibilité des modèles disponibles pour le mettre en œuvre. Par exemple pour modéliser la qualité de l'eau, nous ne pouvons pas utiliser une chaîne de modèles dynamique à petite échelle temporelle car les modèles d'émissions instantanés actuels n'estiment pas encore les émissions non-échappement et les particules ayant un diamètre supérieur à 10 µm ; or, ces particules peuvent être la source principale de certains polluants dans les eaux de ruissellement (diamètre médian 30 µm). Il convient aussi de choisir des modèles en fonction des cas d'étude et de la précision attendue. Ces questions sont traitées dans le chapitre 3 qui présente un état de l'art des modèles disponibles pour simuler le trafic, les émissions de polluants, la qualité de l'air et la qualité des eaux de ruissellement.

Ce chapitre est consacré à la description des modèles utilisés dans les chaînes de modélisation construites dans cette thèse, particulièrement les chapitres 3, 4, et 5. Ils incluent le modèle dynamique de trafic (Symuvia), le modèle d'émissions pour vitesse moyennées (CopCETE), le modèle d'émissions instantanées (PHEM), le modèle de dispersion atmosphérique (Polyphemus), et le modèle de quantité et qualité de l'eau (SWMM).

2.1 Modèle de trafic (Symuvia)

Le modèle de trafic Symuvia de l'IFSTTAR est un modèle microscopique à loi macroscopique du 1er ordre de type LWR (Leclercq et al., 2007). Le modèle LWR de Lighthill et Whitham (1955) et Richards (1956) calcule trois variables macroscopiques du trafic (le débit Q, la concentration K et la vitesse V) par deux lois de la mécanique des fluides et la relation du diagramme fondamentale qui décrit le comportement des véhicules.

$$\frac{\partial K}{\partial t} + \frac{\partial Q}{\partial x} = 0 \qquad 2.1$$

$$Q = KV \qquad 2.2$$

Les modèles du 1er ordre de type LWR supposent que le système est en permanence à l'équilibre et que la vitesse n'est fonction que de la concentration : $Q = KV_{eq}(k(x,t))$, donc le système se réduit à une seule équation hyperbolique scalaire de la variable K (Godlewski et Raviart, 1991).

$$\frac{\partial K}{\partial t} + \frac{\partial Q_{eq}(K)}{\partial x} = 0 \qquad 2.3$$

Cette équation est généralement calculée au moyen du schéma numérique de Godunov (Godunov, 1959) en tenant compte de la condition CFL ($V_{max}\ \Delta t \leq \Delta x$).

Le modèle Symuvia a été enrichi avec diverses extensions de manière à décrire plus finement les diverses situations de trafic en milieu urbain et notamment l'accélération bornée pour améliorer la reproduction de la cinématique des véhicules, les différentes classes de véhicules, la gestion particulière des transports collectifs et les conflits aux carrefours urbains (giratoire, feux, les interactions entre les piétons et les véhicules, etc.) (Leclercq et Laval, 2007 ; Laval et Leclercq, 2008 ; Chevallier et Leclercq, 2008 ; Chevallier et Leclercq, 2008b).

Les données d'entrée du modèle incluent : la matrice origine-destination (O/D), les niveaux de demandes aux entrées (veh/h), les réglages des cycles de feux aux carrefours ainsi que les types de véhicules (véhicules légers, bus, trolleys bus, tramways, etc.). Ce modèle est susceptible de calculer à chaque instant la position, la vitesse et l'accélération de chaque véhicule présent sur le réseau.

2.2 Modèle d'émission basé sur la vitesse moyenne (CopCETE)

CopCETE a été développé pour des cas d'études français par le Ministère de l'Écologie (MEDDE) et coordonné par le CETE (Centre d'études techniques de l'équipement ; actuellement CEREMA) Normandie-Centre. CopCETE est un outil basé sur les méthodologies et équations de COPERT (Ntziachristos et al., 2009), avec en plus certains facteurs d'émissions spécifiques dérivés de travaux français. Le logiciel COPERT est orienté sur le calcul d'inventaire macroscopique (inventaires nationaux d'émissions) alors que CopCETE permet de travailler à partir d'une grande série de tronçons ou segments routiers, plutôt que les 3 seuls cas urbain / rural / autoroutier envisagés par l'outil COPERT.

Les méthodologies de COPERT4 sont présentées brièvement à l'Annexe A et de manière détaillée à http://www.emisia.com/copert/Documentation.html.

CopCETE offre la plupart des possibilités de calcul abordées dans la méthodologie COPERT : (source, Notice CopCETE, 2010)

- les émissions à chaud pour les véhicules légers et lourds ;
- les surémissions à froid pour les véhicules légers ;
- les surémissions liées à la pente pour les poids lourds ;

- les surémissions liées à la charge des poids lourds ;
- les corrections liées aux améliorations des carburants ;
- les corrections liées au vieillissement des catalyseurs et leur maintenance ;
- les émissions par évaporation pour les véhicules légers ;
- les émissions hors échappement ;

Il faut noter que le logiciel CopCETEv3 a été utilisé pour calculer les émissions échappement et évaporation en utilisant des données COPERT, or l'approche des émissions de démarrage à froid et par évaporation n'est pas toujours appropriée au niveau du tronçon. Par ailleurs, pour les émissions non échappement, le document « Sélection des agents dangereux à prendre en compte dans l'évaluation des risques sanitaires liés aux infrastructures routières et ferroviaires » a été utilisé (http://www.sante.gouv.fr).

Pour appliquer le modèle, if faut connaître les paramètres suivants : (1) pas de temps (horaire, journalier, mensuel, annuel), (2) la période (mois) renvoyant aux conditions de température, (3) le chargement des véhicules lourds (0, 50% ou 100%), (4) la longueur des trajets (ou un facteur de démarrage à froid) et leur nombre journalier pour la détermination des surémissions de démarrage à froid et par évaporation de carburant, (5) la longueur du tronçon et sa pente moyenne (par classe de 2% jusqu'à ±6), (6) le milieu (urbain diffus, urbain dense, campagne, autoroute), (7) les nombres de véhicules légers et lourds ayant circulé pendant la période sur ce tronçon, un pourcentage du VUL dans le flux VL, le nombre de bus et de camions, (8) la vitesse de circulation des VL, PL et bus, (9) des données liées au démarrage à froid et aux évaporations (taux de froid, nombre d'arrêt au cours de la période) et (10) le parc automobile français élaboré par l'Ifsttar-LTE (version 2011) qui a été intégré dans CopCETE (cependant, le modèle peut utiliser des parcs différents selon le cas d'étude). Le calcul d'émissions sur un réseau routier peut être effectué pour chaque tronçon et pas de temps, on ne définit qu'une vitesse moyenne par groupe de véhicules ; en conséquence, tous les véhicules circulent à la même vitesse sur le tronçon, stable au cours de la période, et on ne capte pas plus finement qu'à ce niveau la dynamique du trafic.

Le modèle fournit des émissions échappement et non échappement par tronçon et par catégorie détaillée de véhicules pour un pas de temps choisi par l'utilisateur (horaire, journalier, mensuel, annuel). COPCETE peut également agréger les résultats par grandes catégories (VP, VUL, PL, etc.), par tronçon, et pour l'ensemble des tronçons. Les données fournis par CopCETE comprennent la consommation de carburant et les émissions de 26 polluants qui incluent CO_2, CO, NO_x, COV, benzène, PM, SO_2, Pb, Cd, CH_4, COVNM, N_2O, NH_3, HAP, Cu, Cr, Ni, Se, Zn, Ba, As, acroléine, formaldéhyde, 1,3-butadiène, acétaldéhyde et benzo(a)pyrène. La liste des types d'émissions pris en compte pour chaque polluant est présentée en Annexe B.

Il faut noter que les facteurs d'émission non-échappement de COPERT 4 ont été utilisés ici pour les polluants qui ne sont pas inclus dans modèle CopCETE.

2.3 Modèle d'émissions instantanées (PHEM)

Le modèle PHEM (Passenger Car and Heavy Duty Emission Model) est développé par Graz University of Technology, Autriche (Zallinger et al., 2008). Ce modèle calcule la consommation de carburant et l'émission instantanée des véhicules sur la base de cycles de conduite donnés et de cartes du moteur du véhicule. Ces cartes du moteur sont produites par la puissance et la vitesse de moteur (1 Hz) pour chaque norme Euro. Les données d'entrées (cycle de conduite et caractéristiques du véhicule) calculent à la fois la puissance du moteur liée à la résistance du véhicule et la perte de transmission, et aussi la vitesse du moteur basée sur le taux de transmission, le diamètre de roue et le modèle de changement de vitesse. En effet, les différents paramètres tels que les charges des véhicules, la pente de la route en combinaison avec les variations de la vitesse et de l'accélération peuvent être illustrés dans le modèle par différents effets de changement de vitesse. La Figure 2.1 montre différents paramètres mis en jeu avec le modèle PHEM.

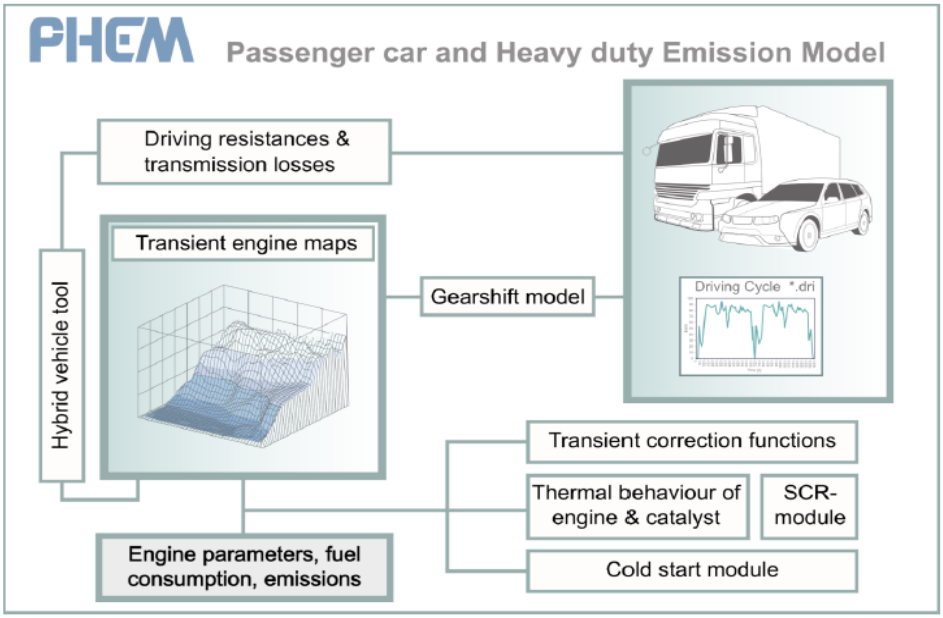

Figure 2.1. Schéma du modèle PHEM.

Il existe trois versions de ce modèle : (1) PHEM Standard simule l'émission d'un véhicule individuel à l'aide de ses caractéristiques et de son cycle de conduite, (2) PHEM Batch peut être utilisé pour un groupe des véhicules ; cette version utilise aussi les caractéristiques du véhicule et le cycle de conduite, (3) PHEM Advance calcule les émissions d'un parc automobile dans les réseaux routiers. Pour PHEM Advance, l'utilisateur n'a besoin d'entrer que les positions et les vitesses des véhicules en chaque instant (e.g., GPS) ou les laisser être calculées par le modèle de trafic.

Nous sommes intéressés ici par la version PHEM Advance qui est capable de calculer les émissions à petites échelles spatio-temporelles et peut aussi être couplé grâce à une interface avec le modèle de trafic. Ce modèle nécessite 4 fichiers entrés pour la mise en œuvre opérationnelle : (1) données de trafic (FZP) qui incluent le temps, la position, la vitesse, la

catégorie de véhicule, et le numéro de tronçon et sa pente. Ces données peuvent être fournies par le modèle de trafic (e.g., VISSIM), (2) la composition du parc automobile (FLT), (3) les données de température (TEM) et (4) la segmentation de réseaux (STR). Une compatibilité de la segmentation avec celle d'un modèle de qualité de l'air facilite le transfert des résultats. Les résultats de PHEM se présentent sous trois formes : (1) résultats seconde par seconde d'information sur les véhicules: les coordonnées, les identifications de véhicules, la puissance, la vitesse, l'accélération, les émissions de plusieurs polluants (NO, NO_x, CO, HC, PM, PN (nombre de particule)) et la consommation du carburant, (2) les valeurs moyennes d'émissions de chaque véhicule en fonction du temps de conduite, (3) des résultats qui peuvent être importés dans le modèle de qualité de l'air (e.g., MISKAM) et qui incluent NO_x, CO, HC, CO_2, PM_{10}, benzène, carbone suie (soot) et SO_2.

2.4 Dispersion atmosphérique (Polyphemus-Gaussien)

La plateforme de modélisation Polyphemus (Mallet et al., 2007) est développée par le CEREA. Cette plateforme propose différents modèles de simulation de qualité de l'air tels que des modèles Eulérien, Lagrangien, Plume-in-Grid et Gaussien. Ce dernier a été largement utilisé pour modéliser la dispersion atmosphérique à l'échelle locale grâce à ses formulations simples qui offrent l'avantage d'être une bonne approximation pour un grand nombre de cas proches des sources avec des temps de calcul convenables. La formulation gaussienne peut s'appliquer à des rejets instantanés (modèle à bouffées) et à des rejets continus (modèle de panache) ; par ailleurs, un rejet continu peut être discrétisé dans le temps pour être représenté par une série de bouffées. Un modèle à bouffées permet d'avoir une meilleurs représentation de la trajectoire d'un panache sur de longues distances où la direction du vent peut varier. Le modèle Gaussien de panache est utilisé pour les émissions du trafic routier car un modèle à bouffées est coûteux en temps de calcul du fait de la longueur des sources (routes) et un modèle de panache est approprié car les impacts ont lieu à seulement quelques centaines de mètres de la source. Les modèles gaussiens supposent que les conditions météorologiques sont uniformes et stationnaires ce qui est acceptable à l'échelle locale. La formule analytique de dispersion gaussienne est valable pour une source ponctuelle si l'on tient compte des hypothèses sur la stationnarité et l'homogénéité. Elle est aussi valable pour une source linéique dans le cas où vent est perpendiculaire à la route. Une autre formulation a été ajoutée au modèle gaussien de Polyphemus par Briant et al. (2011, 2013) ; elle est basée sur la formulation de Venkatram et Horst (2006) qui consiste à évaluer l'intégrale en approximant l'intégrande et en excluant du calcul certaines portions de la source. Cette formulation induit des erreurs sous le vent par rapport à la source linéique et aussi par rapport aux deux extrémités de la source. Les erreurs induites par cette approche ont été minimisées en ajoutant deux sources ponctuelles à chaque extrémité de la source linéique pour l'erreur sous le vent par rapport aux deux extrémités. L'erreur sous le vent par rapport à la source linéique est minimisée selon trois régime définis en fonction de l'angle du vent par rapport à la route. Pour des angles de 0° à 40°, (0° représente un vent perpendiculaire à la route), l'erreur est négligeable, pour des angles de 40° à 75° l'erreur peut être minimisée avec des fonctions gaussiennes, et pour des angles de 75° à 90° l'erreur est minimisée en utilisant une fonction

exponentielle. Par ailleurs, l'équation gaussienne diverge lorsque la direction du vent est parallèle à la source ; par conséquent, pour les cas où l'angle est supérieur à 80°, une combinaison de concentrations calculées par la formulation pour une source linéique et de concentrations calculées par la discrétisation de la source en sources ponctuelles est utilisée. Un coefficient qui dépend de l'angle du vent définit les fractions relatives de ces deux concentrations. Par ailleurs, le modèle a été amélioré pour modéliser la largeur de la route au moyen d'une intégration de Romberg. La formulation a été développée à l'origine pour des polluants gazeux. Dans le cadre de cette thèse, le modèle a été modifié pour traiter les particules.

Ce modèle donne de bons résultats pour les cas où la vitesse du vent est importante (>1 m/s), mais a des mauvaises performances pour les cas où la vitesse du vent est faible, car la direction du vent est alors mal définie. Une solution a été proposée par Venkatram et al. (2013) qui suppose que les polluants peuvent être dispersés sur 360° lorsque la météorologie est calme. Cette approche est développée et évaluée au chapitre 4.

Les données d'entrées nécessaires pour la simulation des concentrations des polluants et les dépôts atmosphériques comprennent les éléments suivants: (1) les coordonnées et longueurs des sources (tronçons de route), (2) les taux d'émissions horaires associées au trafic, (3) les positions des points récepteurs où sont calculées (et parfois mesurées) les concentrations, (4) les données météorologiques qui comprennent la vitesse et la direction du vent, la température et la nébulosité (la stabilité atmosphérique est estimé à partir de la période (jour ou nuit), vitesse du vent et nébulosité). Par ailleurs, les précipitations sont nécessaires pour le calcul des dépôts humides et des hypothèses doivent être faites sur la granulométrie des particules pour estimer les vitesses de dépôts secs et les coefficients de lessivage par la pluie.

2.5 Hydrologie (SWMM)

Le modèle SWMM 5 (Rossmann, 2004) simule à la fois la quantité (débit à l'exutoire d'un bassin versant) et aussi la qualité des eaux de ruissellement. Il s'agit d'un modèle assez répandu pour les études d'hydrologie urbaine pour des périodes continues et longues ou à l'échelle d'évènements de pluie. Ce modèle représente le bassin versant sous la forme de trois objets principaux : les sous-bassins versants en surface, les nœuds et les conduits du réseau d'assainissement. Dans ce modèle, le bassin versant est divisé en plusieurs sous-bassins pour mieux estimer la quantité et la qualité des eaux de ruissellement en fonction de la variabilité spatiale de la topographie, des ouvrages de drainage, de l'occupation de sol, etc.

La transformation pluie-débit est modélisée par un réservoir non-linéaire qui comprend l'infiltration, le stockage sous forme de pertes initiales et l'évaporation. Le transfert sur la surface est modélisé en suivant l'approche de l'écoulement d'une onde cinématique sur un plan (Singh, 1988). Les équations correspondantes sont:

$$\frac{dV}{dt} = A\left(p - perm * i - e\right) - Q\left(V\right) \qquad 2.4$$

$$Q(V) = kWn^{-1}\left(d - d_p\right)^{5/3} s^{-1/2} \qquad 2.5$$

où, V (m^3) est le volume stocké dans un sous-bassin versant, Q (m^3) est le volume d'eau sortant du sous-bassin versant, A (m^2) est la surface du sous-bassin versant, W (m) est la largeur moyenne du sous-bassin versant, p (m) est la hauteur de pluie, d (m) est la hauteur d'eau (*V/A*), perm est la pourcentage de surface perméable, d_p (m) est la hauteur des pertes initiales, i (m) est l'infiltration, n est la constante de Manning qui dépend de la typologie de la surface, e (m) est l'évaporation et s est la pente moyenne du sous-bassin versant.

L'écoulement est transporté dans les conduits représentant le réseau sur la base des équations de Saint-Venant.

La modélisation de la qualité des eaux nécessite la modélisation de l'accumulation de la pollution sur le sol durant le temps sec, du lessivage des polluants durant les pluies et du transport des polluants dans le réseau. Pour cela, le modèle a besoin que soient définies des informations telles que le type de polluant, les catégories d'occupation de sols qui produisent ces polluants et les concentrations des polluants dans les précipitations et dans les eaux souterraines. Les méthodes de calcul de ces paramètres seront expliquées au chapitre 5.

Ce modèle nécessite de fournir les discrétisations et de définir les caractéristiques des sous-bassins versants (surface, largeur, pente, surface imperméable, coefficient de rugosité), l'occupation des sols, les réseaux de conduits, les données de précipitation, le modèle d'infiltration, ainsi que l'accumulation de polluant et le lessivage. En sortie, l'utilisateur peut récupérer les résultats de débit, de hauteur d'eau, et la concentration des polluants en chaque nœud du réseau.

Chapitre 3

3 Chaînes de modélisation

La nécessité de développer une chaîne de modélisation pour simuler la pollution de l'air et des eaux pluviales due au trafic routier a été expliquée au chapitre 1. Ce chapitre présente un état de l'art des outils de modélisation des différents phénomènes (trafic, émissions, pollution atmosphérique, qualité des eaux de ruissellement), mettant en exergue les enjeux liés à l'intégration des différents modèles et le choix de modèles pour constituer une chaîne cohérente en termes de polluants et d'échelles spatio-temporelles.

Les modèles de trafic sont classés en 3 grandes catégories : statique, dynamique agrégée, et dynamique. Les méthodes et outils sont présentés pour différentes échelles, données d'entrée et résultats. Par exemple, un modèle statique tel que VISUM estime le débit et la vitesse moyenne sur un tronçon, alors qu'un modèle dynamique microscopique tel que Symuvia est capable de déterminer la position des véhicules, leurs vitesse et accélération sur l'ensemble du réseau de routes considéré. Les modèles d'émissions relèvent de 7 catégories en fonction des données nécessaires pour calculer les taux d'émissions ainsi que les différents types de polluants émis par les véhicules. Par exemple, le modèle CopCETE peut utiliser les résultats d'un modèle de trafic statique (donnant des flux de véhicules horaires et des vitesses moyennes) pour simuler les taux d'émissions de nombreux polluants issus de diverses sources d'émissions (échappement, non-échappement et évaporation). Si l'on souhaite connaître les émissions avec plus de précision, le modèle PHEM peut estimer l'émission à l'échappement à chaque instant et sur chaque segment de route. De nombreux types de modèles de dispersion atmosphérique faisant appel à diverses techniques de modélisation et couvrant différents échelles spatiales sont présentés. Le choix du modèle dépendra du cas d'étude local, régional ou continental. Les modèles de chimie-transport basés sur une approche Eulérienne ou Lagrangienne peuvent être utilisés aux échelles régionales et continentales (voire globales). À l'échelle locale sans obstacle et avec des données d'entrée uniformes spatialement (e.g., météorologie), les modèles Gaussiens sont appropriés. Les modèles de type « street-canyon » ont été développés pour tenir compte de l'effet des bâtiments sur la dispersion en milieu urbain. Pour les cas avec des géométries complexes, les modèles CFD peuvent être choisis, cependant, leurs besoins en temps de calcul limitent leurs applications à des domaines limités (quartier) et des courtes périodes (journée). Les modèles hydrologiques sont classées en 4 catégories selon le degré d'homogénéisation des données d'entrée spatiales qui peuvent caractériser un bassin versant (localisé), un sous-bassin versant (partiellement distribué), une surface avec des données d'entrée hydrologiques similaires (HRU) ou une région avec un maillage spatial (distribué). La disponibilité de données telles que celles d'occupation des sols et d'intensité de la pluie et la résolution désirée des données d'entrée déterminent le choix du

modèle. Les limitations et les incertitudes associées à ces modèles sont aussi brièvement présentées dans ce chapitre.

Le lien entre les émissions du la circulation, les dépôts atmosphériques et la contamination des eaux de ruissellement n'a pas encore été traité d'une manière globale. C'est pourquoi différents couplages entre modèles sont étudiés dans ce chapitre séparément à travers trois cas d'étude.

Le premier cas d'étude considère le couplage entre un modèle de trafic (Symuvia) et deux modèles d'émissions distincts : l'un utilisant des vitesses moyennées et l'autre des vitesses instantanées (PHEM). La comparaison des résultats de ces deux couplages montrent des émissions plus importantes pour la plupart des polluants avec le modèle d'émissions utilisant les vitesses instantanées pour une voie urbaine lorsque les vitesses de circulation sont faibles.

Le deuxième cas d'étude considère le couplage des modèles d'émissions et de qualité de l'air. Une application de ce couplage a été réalisée pour un segment de l'autoroute A31 près de Metz avec une comparaison des résultats de la simulation avec des mesures de dépôts de cadmium obtenues à différentes distances des deux côtés de l'autoroute pendant février 1997. Les émissions ont été calculées avec le modèle CopCETE. Le modèle Gaussien de Polyphemus, alimenté par ces émissions, a alors été utilisé pour calculer la dispersion et les dépôts secs et humides de cadmium. Les résultats des simulations sont satisfaisants sauf pour les zones proches de la bordure de l'autoroute où des particules grossières non-prises en compte dans les émissions pourraient contribuer significativement aux dépôts.

Le troisième cas d'étude considère le couplage entre les modèles de qualité de l'air et des eaux de ruissellement. En particulier, la cohérence et les interfaces des modèles sont discutées. Le cas d'étude réalisé traite le calcul du dépôt avec des données expérimentales de dépôt, de trafic et de conditions météorologiques. Une comparaison entre deux scénarios, l'un qui inclut les émissions du trafic local et les concentrations de fond et l'autre qui traite seulement les concentrations de fond, montre que les concentrations de métaux dans les eaux de ruissellement sont jusqu'à six fois plus élevées en considérant explicitement le trafic local pour les sous-bassins versants situés au voisinage des routes très fréquentées.

Cette étude a permis de proposer deux configurations de chaînes de modélisation, l'une statique avec des pas de temps horaires, la seconde envisageant une approche dynamique. La première chaîne peut estimer à la fois les concentrations de polluants dans l'air et aussi dans les eaux de ruissellement, grâce à son modèle d'émission (CopCETE) qui détermine une large variétés des polluants émis par les véhicules. Des facteurs d'émission de COPERT peuvent en particulier être utilisés pour les particules de diamètre supérieures à 10 µm, car celles-ci sont des polluants potentiellement importants dans les eaux de ruissellement. Une application de cette chaîne de modélisation sera présentée en détail au chapitre 5.

La seconde chaîne considère les émissions et la dispersion des polluants de manière plus détaillée, en analysant le comportement individuel des véhicules, l'effet du régime moteur sur les émissions du véhicule, ainsi que la turbulence créée par les obstacles et les véhicules. Cette seconde approche conviendrait pour une simulation précise de la qualité de l'air mais

pas pour la qualité de l'eau car les modèles d'émissions instantanés ne traitent pas encore les polluants d'intérêt pour l'eau tels que les HAP, métaux lourds, et la fraction grossière des PM produites par les émissions non-échappement (usure des freins et des pneus).

Ce chapitre est constitué de Fallah Shorshani et al., (2014) :

Fallah Shorshani M., André M., Bonhomme C., Seigneur C. (2014). Modelling chain for the effect of road traffic on air and water quality: Techniques, current status and future prospects. Submited to Environmental Modelling & Software.

Abstract

Modelling approaches for simulating air and stormwater pollution due to on-road vehicles in an urban environment are reviewed and discussed. Models for traffic, emissions, atmospheric dispersion and stormwater contamination are studied with particular emphasis on their couplings to create a modelling chain. The models must be carefully selected according to the requirements and level of necessary details required for the integrated modelling chain. Although a fair amount of research has been conducted to link air pollution and road traffic, many questions related to spatio-temporal scales, domains of validity, consistency among models, uncertainties of model simulation results and interfaces between models remain open. Furthermore, the link between traffic emissions, atmospheric deposition and the contamination of stormwater runoff in urban areas has not yet been treated in a comprehensive manner. The aim of this work is to review the current status of the relationships between traffic, emissions, and air and water quality models, to recommend modelling approaches and to propose some directions for improving the state of the art. The difficulties and challenges associated with model coupling are illustrated with specific examples.

3.1 Introduction

It is expected that in 2050 more than 70 percent of the world's population will live in urban areas. The growing amount of vehicles in densely populated areas increases traffic congestion and contributes to the deterioration of air (e.g., Zmirou et al., 2004) and stormwater quality (e.g., Obropta and Kardos, 2007). Thus, traffic is a major source of pollution in cities. Currently, traffic models can predict the position and kinematic parameters of the vehicles and emission models can estimate the amount of different types of pollutants emitted by vehicles, albeit with some uncertainty. Then, the dispersion and transformation of pollutants in the atmosphere can be modelled using atmospheric dispersion models and/or chemical-transport models. A fraction of the air pollutants deposits to surfaces by dry and wet processes. These pollutants may be entrained by the water runoff during rainfall events, which can be simulated by stormwater models. They may also be resuspended in the atmosphere due to mechanical disturbance (e.g., traffic, wind). Various models have been designed to simulate each of these phenomena; however, little work has been done to develop integrated modelling systems that can simulate the impact of traffic on both the air and water

environments in urban areas. It is essential that such capabilities be developed and evaluated as their needs are primordial for the planning of the sustainable cities of the future. Thus, there is a need for a global and systemic approach of pollutant mitigation policies in urban areas in order to decrease globally their pressure on the environment and human health.

Traffic pollutants are emitted by the internal combustion engine of the vehicles, tyre, clutch and brake wear, fuel evaporation, and road wear. Exhaust emissions consist mostly of carbon dioxide (CO_2), carbon monoxide (CO), nitrogen oxides (NO_x: NO and NO_2), volatile organic compounds (VOC), particulate matter (PM), nitrous oxide (N_2O), ammonia (NH_3), persistent organic pollutants (POP) including polycyclic aromatic hydrocarbons (PAH), and metals. VOC are also emitted by evaporation. Non-exhaust emissions such as brake and tyre wear are also sources of PM. PM includes inorganic species, trace metals, and carbonaceous compounds. Emission factors are available only for the major air pollutants and large uncertainties exist for many air pollutant emissions.

First, we present and classify the models for each phenomenon (traffic, emissions, air quality, and water quality) according to their input data and scales of application. Next, we discuss the strengths and weaknesses of these models. Then, we address the development of modelling chains and various approaches to link these models. Finally, we present recommendations for further model development and suggest alternative models that could be considered as integrated modelling systems. Specific issues such as differences in PM size ranges relevant to air and water quality are identified and actions to resolve those issues are proposed. This work provides the basis to improve the integrated modelling approach to relate traffic to air and water pollution, which today is typically limited to spatially or temporally averaged conditions (average fleet composition, average traffic speed, stationary atmospheric conditions) and separate media (i.e., either air or water).

3.2 Model description

3.2.1 Traffic models

Three major classes of models can represent the behaviour of vehicles for various applications to an urban network:

i) Static models rely on the spatial distribution of population and calculate average traffic volumes in different areas of a network. Such models (e.g., VISUM, Fellendorf et al., 2000) are typically divided into four steps: trip generation, trip distribution, modal split and assignment. The numbers of trips in each area of the network are estimated based on housing, office density, and their locations. These trips are used to construct an origin-destination (OD) matrix. The OD matrix, in combination with information such as the different modes of transport and speed flow curves, is used to calculate the travel times on the road network. Thus, they provide the vehicle flux for each link of the road network. These models are highly simplified, but they are useful to provide a static description of the road traffic in terms of flow and speed over large spatial scales (e.g., city scales).

ii) Dynamic models describe the temporal variations of traffic conditions and how they affect vehicle movement. These models use an explicit representation of congestion and operate at a smaller spatio-temporal scale than the static models. They calculate the location and kinematic parameters of vehicles, which can subsequently be used to predict pollutant emissions and traffic noise as a function of space and time. They are discussed in grater detail below.

iii) Aggregated dynamic models (e.g., Daganzo, 2007) keep an explicit representation of congestion by describing the temporal evolution of traffic states of a simplified road network (spatial aggregation). These models divide the city into neighbourhood-sized reservoirs (commensurate with a trip length) and shift the modelling emphasis from microscopic predictions to macroscopic monitoring. Upon the assumption of a homogeneous distribution of the traffic, it is possible to estimate the average speed and the congestion level as a function of time. These models are based on relationships between the amount of displacement per unit of time (generation) and the number of vehicles on the network (accumulation), which are denoted MFD (Macroscopic Fundamental Diagram), and traffic demand (OD-matrix) among different neighbourhoods. The typical application of such models is the evaluation of the level of congestion to reduce traffic.

We are interested here in dynamic models that provide appropriate traffic conditions for a more accurate estimation of air pollution. Dynamic models can be classified into three categories according to different aspects of traffic flow operations:

(1) The macroscopic models (e.g., METACOR, Diakaki and Papageorgiou, 1996) use an aggregate representation of vehicles and the assumption of continuous traffic flow. They are, therefore, characterized by variables such as traffic flow and vehicles density.

(2) The microscopic models take into account the time-space behaviour of individual vehicles under the influence of other vehicles in their proximity. These models determine vehicle location, speed, and acceleration.

(3) Mesoscopic models represent the behaviour of vehicles without explicitly distinguishing their time-space behaviour, but instead taking into account the behaviour of groups of several vehicles.

Macroscopic dynamic modelling is based on the collective behaviour of vehicles; therefore, vehicles are not followed individually. The point of view is rather that of a continuum. The Euler and Navier-Stokes equation of fluid dynamics describing the flow of fluids may also describe the motion of cars along a road. The three main variables of traffic (flow, vehicle density, and average speed) are connected by two fluid laws proposed by Lighthill and Whitham (1955) and Richards (1956) (LWR). This model can be adapted to represent the diversity of urban traffic situations (e.g., Leclerq and Bécarie, 2012). This system must be supplemented by an independent third equation (fundamental diagram of traffic flow) which describes a relationship between traffic flow and traffic density. Two classes of macroscopic models can be identified. The first class uses the sole mass conservation equation supplemented by suitable closure relations that represent equilibrium states (first-order models). The second class uses a coupled system of mass conservation and momentum balance equations that represent equilibrium states or the behaviour of the flow acceleration (relaxation flow velocity) (second-order models). The main parameters for the

implementation of macroscopic models include the fundamental diagram of traffic flow, OD-matrices, and the traffic control devices (e.g., traffic lights). The simulation outputs are traffic density in each cell as a function of time as well as the traffic flows simulated across the model cells.

Dynamic microscopic traffic models (e.g., VISSIM, Fellendorf and Vortisch, 2010) consider individual vehicle interactions with other vehicles and the road network. There are two main classes of microscopic models: (1) microscopic models with macroscopic law, which in fact correspond to a Lagrangian representation of macroscopic models, (2) microscopic models that are built up using submodels that control specific tasks in the simulation process. The car-following model is one of the most important submodels. A car-following model controls the driver's behaviour with respect to the interactions between two successive vehicles. These models can be completed by other submodels. In such models, typical submodels include the effect of overtaking as a function of vehicle categories and incoming traffic. For example, another submodel will allow one to simulate the response of vehicles to the control systems such as traffic lights, and an intersection submodel will manage the conflicts and the priorities at crossroad intersections and the arrival of new vehicles on the road network. These microscopic models calculate instantaneously the location, speed, and acceleration of the vehicles on the road network.

The mesoscopic models are intermediate between the macroscopic and the microscopic approaches. The objective is to describe the traffic given by aggregate laws. For example, vehicles may be grouped in packs, which then move on the road network (e.g., CONTRAM, Leonard et al., 1989). Table 3.1summarizes the classification of traffic models and provides an example for each category. An exhaustive list of available models cannot be provided here. Various traffic models, including their strengths and weaknesses, have been reviewed by Boxill and Yu (2000).

Table 3.1. Summary of traffic model categories.

<table>
<tr><th colspan="2">Models</th><th>Solving method</th><th>Application domain</th><th>Results</th><th>Example</th></tr>
<tr><td colspan="2">Static</td><td>O/D matrix</td><td>Urban area</td><td>Average quantity of vehicles</td><td>VISUM
(Fellendorf et al., 2000)</td></tr>
<tr><td colspan="2">Aggregated dynamic</td><td>Relation
flow-density</td><td>Several neighbourhoods</td><td>Average speed, congestion</td><td>Daganzo, 2007</td></tr>
<tr><td rowspan="4">Dynamic</td><td rowspan="2">Macroscopic</td><td>First order (LWR)</td><td rowspan="2">Neighbourhood

Highway</td><td rowspan="2">Density & speed of vehicles</td><td rowspan="2">METACOR
(Diakaki & Papageorgiou, 1996)</td></tr>
<tr><td>Second order (AZR)</td></tr>
<tr><td>Mesoscopic</td><td>Aggregate flows
Traffic details</td><td>Neighbourhood</td><td>Vehicle trajectory</td><td>CONTRAM
(Leonard et al., 1989)</td></tr>
<tr><td rowspan="2">Microscopic</td><td>Macroscopic Lagrangian</td><td rowspan="2">Urban network</td><td rowspan="2">Location, speed, acceleration per second</td><td rowspan="2">VISSIM
(Fellendorf et al., 2010)</td></tr>
<tr><td>Car following</td></tr>
</table>

Uncertainties of traffic models

The different types of errors that may cause incorrect estimations of traffic have been studied by Ortuzar and Willumsen (2011). These errors are summarized below

1) Measurement errors: Those are network measurement errors or errors due to information incorrectly registered by the interviewer.

2) Sampling errors: These errors depend on the number of observations. Optimal sampling strategies are defined by Daganzo (1980).

3) Computational errors: These errors are based on the iterative procedures of most models; they are typically small in comparison with other errors.

4) Specification errors: These errors are due to simplifications of processes in the models or the omission or misrepresentation of a phenomenon that is not well understood (e.g., using linear function to represent non-linear effects)

5) Transfer errors: They refer to cases when a model developed in one context (time and/or place) is applied in a different one.

6) Aggregation errors: They result from data aggregation that overlooks the individual behaviour.

A remaining question is whether complex models produce better results than simpler ones. Ortuzar and Wilumsen (2011) argued that if the complexity of a model with more variables reduces specification error (e_s), data measurement error (e_m) will probably increase with model complexity. As shown in Figure 3.1, the more realistic results that include a minimum of total modelling error ($E=\sqrt{(e_s^2+e_m^2)}$) are generally obtained for an optimal level of model complexity.

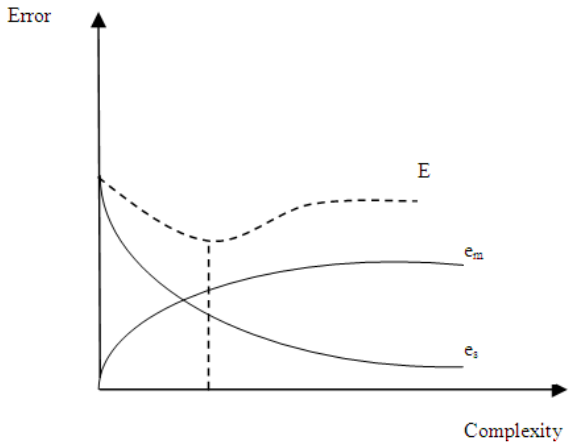

Figure 3.1. Variation of error with complexity, source: after Ortuzar and Wilumsen, 2011.

3.2.2 Emission models

There is a large variety of tools to calculate emissions and to develop on-road transportation emission inventories. Emissions from traffic are estimated by multiplying emission factors with appropriate activity data for different vehicle classes. The emission factors are measured in a laboratory using a chassis or engine dynamometer according to several specific driving cycles. A driving cycle is representative of driving behaviour for specific categories of vehicles, roads and speeds experienced.

Traffic emissions can be divided into four types: exhaust emissions, evaporative emissions, non-exhaust vehicle-wear emissions (mostly vehicle tyre and brake wear), and road wear and dust resuspension caused by vehicle traffic. Different categories of emission models are presented below. They can be classified according to the input data, the spatio-temporal scale of the study and the type of pollutants being considered.

1. Models based on fuel quantities

Models such as IPCC (Houghton et al., 1996) use fuel consumption as input data (i.e., fuel sale data) and the categories of vehicles. Such models can only be used for large-scale (e.g., national) emission inventories.

2. Models based on average traffic volumes per categories of vehicles

These models, such as NAEI (Choudrie et al., 2008) and IVE (Davis et al., 2005), use a single emission factor to represent a particular type of vehicle and driving cycle. The emission factors are calculated as mean values of measurements on a number of vehicles over given driving cycles and are usually stated in terms of the mass of pollutant emitted per vehicle distance or fuel consumption. The user only needs to provide the number of vehicles and the annual mileage per category. These models are mostly used in national and regional emission inventories.

3. Models based on average traffic speed

These models (e.g., COPERT; Ntziachristos et al., 2009, MOBILE, U.S. EPA; 1994) predict average emission factors for a vehicle class that is driven over a number of different driving patterns, which are a function of the mean travelling speed. The total emissions can be calculated as the sum of the exhaust emissions (hot and cold), evaporative emissions and for some models (e.g., COPERT) emissions due to vehicle tyre and brake wear as well as road wear resulting from the traffic. These models are based on time-averaged inputs (traffic mean speed) that may not be representative of actual traffic conditions because a given mean speed may correspond to different conditions. Nevertheless, they cover the major emission processes and most pollutants of interest and, accordingly, they are widely used in air quality modeling studies.

4. Models requiring detailed descriptions of traffic situations

These models (e.g., HBEFA, 2010) use distinct emission factors for predefined traffic situations (e.g. stop-and-go, saturated, heavy, free flow) and road configurations. Corresponding emission factors are available for pollutants emitted by the hot and cold exhaust emissions as well as by fuel evaporation. The methodologies were also developed for small scales such as for a single street (André et al., 2006). Traffic situation models require vehicle-kilometer-travelled (VKT) data per traffic-situation as input, which can be acquired from traffic models. It is important to note that there is no universal definition of traffic situation, which is to some extent a subjective concept. These models provide emissions for a large number of different regulated and non-regulated pollutants.

5. Models based on traffic-related variables

Emission factors obtained from traffic-variable models (e.g., Matzoros, 1990) are estimated from traffic flow variables such as average speed, traffic density, queue length and signal

settings. In fact, they use a correction of the average speed to assume the effects of the traffic onto pollutant emissions, Previous work (Smit, 2006) suggests that this approach is approximate and that the consideration of the impact of the congestion on emissions is not entirely correct.

6. Models representing a detailed description of the speeds experienced

These emission models (e.g., VERSIT+, Smit et al., 2007) are based on tests conducted on a large number of vehicles according to various driving cycles to calculate exhaust emission inventories. Within the model, each driving cycle used is characterized by a large number of descriptive parameters (e.g., average speed, number of stops per km, kinematics of vehicles such as acceleration, cruising, etc.). For each pollutant and vehicle category, a regression model is fitted to the average emission values over the different driving cycles. These models require detailed information on the movement of the vehicles (instantaneous speed, acceleration), which can be obtained from microscopic traffic models or from traffic measurements.

7. Model based on chronological speeds (instantaneous models)

These models (e.g., PHEM, Zallinger et al., 2008; CMEM, Barth et al., 2000) represent explicitly the vehicle emission behaviour by relating emission rates to vehicle operation during a series of short time steps. In some models, vehicle operation is defined in terms of a relatively small number of modes (idle, acceleration, deceleration, and cruise). For each of the modes, the emission rate for a given vehicle category and pollutant is fixed and the total emission rate is calculated by weighting each emission rate by the time spent in each mode. Several instantaneous models relate vehicle engine power, speed and acceleration to each point of a driving cycle. These models estimate exhaust emissions only. This type of model can be coupled with a dynamic traffic model, which estimates the kinematics of vehicles (using typically 1 second time steps).

Models of categories 1 and 2 are not appropriate for considering traffic variation since they are based on average traffic volumes and do not account for vehicle speed. Models of categories 3 and 4 account for traffic condition (but only via average values) and cover the major emission processes and most pollutants from a single road up to a city. Models of category 5 require traffic flow variables for each road and category 6 is defined by individual vehicle movement data. However, both types of models use databases, which are limited to specific conditions and pollutants. Models of category 7 represent explicitly the vehicle emission behaviour by relating emission rates to vehicle operation (engine power, speed, and acceleration) during a series of short time steps. They require detailed information on vehicle movements, which can only be acquired from on-board measurements, or derived from microscopic traffic models. However, they use databases of emission factors, which are limited to specific emission processes and pollutants.

Table 3.2. Summary of emission model categories.

Categories of Models	Application domain	Input	Example
Models based on fuel quantities	Country	Fuel consumption	IPCC Houghton et al. 1996
Models based on average traffic volumes per categories of vehicles	Country Region	Number of vehicles Average kilometer travel	NAEI Choudrie et al., 2008
Models based on average traffic speed	City Neighbourhood	Average speed	COPERT Ntziachristos et al., 2009
Models requiring detailed descriptions of traffic situations	Neighbourhood	Average speed Traffic condition	HBEFA, 2010
Models based on traffic-related variables	Intersection area	Driving cycles	Matzoros, 1990
Models based on a detailed description of the speeds experienced		Driving cycles	VERSIT+ Smit et al., 2007
Models based on chronological speed (instantaneous models)		Driving cycles Vehicle characteristics	PHEM Zallinger et al., 2008

Limitations and uncertainties of emission models

The model output uncertainty depends on the uncertainties in the model internal parameters (emission factors) and input data. The most typical sources of uncertainty in emission models include: (1) ambient conditions, (2) parameters with temporal variation (e.g., temperature) , (3) vehicle fleet composition, (4) vehicle mileage, (5) traffic data, (6) estimation methods of emissions based on steady-state emissions that ignore transient vehicle operation (for some emission models), and (7) emission factors.

The uncertainty of the emission factors can be divided into random sampling error (statistical error), measurement errors (imperfections in sampling and analytical methods), different conditions between the case study and the source test (e.g., vehicle aging or modification of car equipment by users), averaging time for measured or reference data, omissions (missing data), surrogate data (estimated data when data are not available), and in the absence of relevant data or surrogate data, other approaches (e.g., conversion of a trace species in a fuel to an air pollutant, Frey, 2007).
Most European countries (22 out of 27) use the COPERT model for emission inventory estimation. Uncertainties associated with this model have been studied by Kouridis et al. (2010). They calculated the contribution of four sources of errors for two case studies (Italy and Poland) by considering fifty-one uncertainty inputs. The most important inputs were (1)

meteorological and temporal parameters (e.g., temperature, time series, vapour pressure), (2) the activity data (e.g. vehicle fleet composition and mileage), (3) traffic and model parameters (e.g., vehicle velocity, driving shares among cycles, load factor for heavy-duty vehicles, average trip length and fuel properties), and (4) cold-start emissions and emission factors, which were all identified as influential parameters. A limitation of this study is that the parameters have been considered separately. For example, the emission factors cannot be considered as true input data as they may change depending on other parameters.
The limited number of measurements made for various emission processes and pollutants are insufficient to provide all the necessary data needed for most advanced emission models, for example, instantaneous emission models are limited to a few pollutants from exhaust emissions. In addition, emission models are not able to consider completely the processes associated with mechanical abrasion and corrosion (tyre, brake, clutch, and road surface wear, corrosion of chassis and body work). Particles greater than 10 µm in diameter are not considered in those emission models because current air quality regulations apply only to particles with an aerodynamic diameter below 10 µm. However, tracking PM above 10 µm is essential when modelling water contamination.

3.2.3 Air quality models

Air quality models calculate pollutant concentrations and deposition fluxes at various locations and times using mathematical equations describing the atmospheric transport processes and chemical and physical transformation processes between the point(s) of emissions and the receptor location(s). The different approaches available differ in terms of inputs and levels of spatial and temporal resolution of the results.

1. Box models

Box models consider that the concentrations are homogeneous within the modelling domain (i.e., the box). Pollutants are emitted, undergo chemical and physical processes, and are advected in and out of the box. These models are not used operationally, but they are useful to investigate specific processes under simple configurations (e.g., single airshed, Pun and seigneur, 2001) under controlled conditions (e.g., smog chamber experiments, Goliff at al., 2013) or to obtain annual average deposition fluxes, which can be used to estimate water contamination due to air pollutants (e.g., Petrucci et al., 2014).

2. Near-source dispersion models

Near-source dispersion models use parameterizations to represent the transport and dispersion of pollutants from one or a selected number of sources. In the absence of obstacles to atmospheric transport and under stationary atmospheric conditions, the atmospheric dispersion process can be approximated by a Gaussian distribution of the time-averaged pollutant concentrations. Therefore, Gaussian dispersion models, which are based on the assumption that atmospheric dispersion leads to a Gaussian distribution of the concentrations of the emitted pollutant in the vertical and horizontal directions are widely used (Csanady, 1973). In the case of steady-state atmospheric conditions, the impact of a source is

represented by a Gaussian plume model. In the case where atmospheric conditions are variable, one may represent the atmospheric dispersion process by releasing distinct puffs from the source at successive intervals of time; Gaussian puff models present the advantage over Gaussian plume models that they are not limited to steady-state conditions (e.g., constant wind speed and direction); however, the computational requirements are greater for puff models than for plume models. Gaussian plume models are not designed to model atmospheric dispersion under low wind-speed conditions and the wind is assumed to be constant in time and space. Hybrid models, which use a combination of the Gaussian plume and puff models, can provide better estimates of concentrations under low wind-speed conditions (Sharan et al., 1996; Thomson and Manning, 2001). Gaussian plume models treat deposition processes and can treat simple chemical reaction systems (i.e., first-order kinetics and steady-state systems). Gaussian puff models can treat complex chemically reacting systems (Karamchandani et al., 2000). Algorithms have been developed for some Gaussian models to treat atmospheric dispersion around buildings; the effect of wakes from buildings can be achieved by modifying the dispersion coefficients. However, the Gaussian equation is not able to calculate recirculation effects caused by multiple buildings or atmospheric flow at street intersections (Holmes and Morawska, 2006) and other formulations must then be used (e.g., Soulhac et al., 2011). Gaussian plume models may be used to estimate concentrations up to 50 km from the source and are typically applied with averaging times of one hour (or less) so that the assumptions of constant and uniform meteorology hold. Gaussian puff models have been used for long-range impacts, when coupled with an appropriate meteorological model; they are however limited to the impacts of a few specific sources.

For situations where the atmospheric dispersion of pollutants is constrained by obstacles such as buildings, noise-barriers or vegetation, other parameterizations must be used. For street-canyon situations, parameterizations based on the assumption of a well-mixed zone within the canyon can be used. One widely-used approach is the Operational Street Pollution Model (OSPM) (Hertel et Berkowicz, 1989 a, b, c).
Another method proposed for road pollution is SIRANE (Soulhac et al., 2011, 2012), which simulates each street with a box model and calculates the corresponding advective fluxes balance at intersections. This model accounts for three important transport mechanisms within the urban canopy to better estimate the effect of the complex street configuration in urban area: 1) advective mass transfer along the street due to the mean wind along their axis, 2) turbulent mass transfer across the interface between the street and the overlying atmospheric boundary layer, and 3) advective transport at street intersections (this last term is not treated by OSPM). The simulation at street level is completed by a standard Gaussian plume model for atmospheric transport and dispersion above roof level.

3. Lagrangian trajectory models

Lagrangian trajectory models (which include Gaussian dispersion models) consist in following the trajectory of an air mass along the mean wind flow. In addition to Gaussian models, we can mention the numerical particle models and the grid-based Lagrangian models (e.g., AUSTAL2000, Graff, 2002; Hysplit, Draxler and Hess, 1998; FLEXPART, Stohl et al., 1998). In a particle-trajectory model, the model particles are advected and dispersed as the air

mass moves along the trajectory by advection and pollutants are dispersed by turbulent diffusion. Thus, particle models work well for both stationary conditions over flat terrain and variable conditions over complex terrain (e.g., Holmes and Morawska, 2006). Grid-based trajectory models consist of a column (1D) or a wall (2D) of cells that is advected by the mean wind; turbulent dispersion spreads the air pollutants among those cells as the air mass moves downwind from the source along the trajectory (e.g., Seigneur et al., 1997). Because of the gridded nature of the model, it is possible to model non-linear chemistry, as discussed below for Eulerian models. However, complex meteorological conditions such as wind shear, land-sea breezes and mountain-valley winds are poorly represented by grid-based Lagrangian models.

4. Eulerian models

An Eulerian model considers an element of volume of homogeneous properties (air pollutant concentrations, meteorological variables) and studies the flow of those variables through a 3-D gridded mesh of such volumes, i.e., grid cells. The atmosphere is discretized into cells and the equations of mass conservation are solved iteratively for each grid cell. Such models take as input the meteorological variables that have been calculated previously using a meteorological model; they are typically referred to as chemical-transport models (CTM) (e.g., Polair3D, Sartelet et al., 2007; CHIMERE, Bessagnet et al., 2009; CMAQ, Byun and Ching, 1999; CAMx, ENVIRON., 2011. Alternatively, the Reynolds-Averaged Navier-Stokes (RANS) equations of the meteorology may be solved jointly with the chemical-transport equations; such a modelling approach is referred to as integrated on-line meteorology air quality modelling (WRF-Chem, Grell et al., 2005; Zhang, 2008; Zhang et al., 2012; Baklanov et al., 2014). The on-line approach is well suited to the study of feedbacks between air quality and meteorology (e.g., the effect of PM on clouds) and air quality forecasting. Eulerian models can handle a large number of sources, complex chemistry and, given the appropriate meteorological fields, complex atmospheric transport phenomena. They are used to simulate air quality from the urban scale to regional, continental, hemispheric and global scales. One class of Eulerian models combines the advantages of Eulerian models (large domain and multiple sources) and Lagrangian models (fine resolution near sources); these models, which are referred to as plume-in-grid models (PinG), simulate selected sources using a Lagrangian model (such as a puff model) imbedded within the 3D Eulerian model, which simulates the fate and transport of all other emissions (Karamchandani et al., 2011; Briant and Seigneur, 2013; Kim et al., 2014).

5. CFD models

The most common CFD (Computational Fluid Dynamics) techniques are direct numerical simulation (DNS), large-eddy simulation (LES), and Reynolds-averaged Navier-Stokes (RANS) equations with turbulence closure models. Each technique handles turbulence in a different manner. DNS solves the Navier-Stokes equation without approximations. It requires a very fine grid resolution to catch the smallest eddies in the flow. This makes the calculations extremely time consuming. DNS for either indoor or outdoor environment simulations is not realistic in the near future. LES separates turbulent motions into large and small eddies. The small eddies are modeled independently from the flow geometry with parameterizations and

large eddies are simulated explicitly for time-dependent flow. LES is a more practical technique than DNS; nevertheless, it is still time consuming and its application has been mostly limited to meteorology with no operational applications to air pollution yet to date. RANS is the fastest approach since the computational burden is significantly less than those of LES and DNS. It solves the time-averaged Navier-Stokes equations by using approximations to simplify the calculation of turbulent flow. RANS is useful for applications in air quality (e.g., Code_Saturne, Milliez and Carissimo, 2007; MISKAM, Eichhorn and Kniffka, 2010), which are limited to local applications, such as the impact of a single pollution source in complex terrain or in a built environment, where the flow characteristics are complex (e.g., Milliez and Carissimo, 2007; Yuan et al., 2014). Chemical transformations have recently been incorporated into RANS models. A comparison of two different modeling approaches (RANS and LES) has been presented by Gousseau et al., (2011) for an actual urban area.

Table 3.3. Summary of air quality model categories

Models	Application domain	Solution method	Examples
Chemical Transport Models (CTM)	Urban to global (from 1 km to several 100 km resolution)	Some Lagrangian models	Flexpart, Hysplit AUSTAL2000
		Eulerian models	Polair3D, CMAQ, WRF-Chem, CAMx CHIMERE
		Plume-in-Grid models	PinG , CMAQ-Urban
Near source dispersion models	Local impact (up to 1 km)	Gaussian models & some Lagrangian	Polyphemus, ADMS, SIRANE, AERMOD
		Street-canyon models	SIRANE, OSPM
Computational Fluid Dynamics models (CFD)	Complex environment Local scale (up to 10 km)	RANS	Code_Saturne, MISKAM
	Research (turbulence)	LES	FAST3D-CT (Patnaik and Boris, 2010)

Limitation and uncertainties of air quality models

The limitations of most models are as follows: (1) dispersion in urban areas is complicated by the aerodynamic effects of street/building geometry and traffic-induced turbulence., (2) air quality impacts of traffic include a local component as well as an urban background component, which differ in terms of pollutants, temporal and spatial scales, (3) the estimation of wet and dry atmospheric deposition fluxes strongly depends on the particle size

distribution; wet scavenging and dry deposition velocities still remain difficult to estimate as a function of particle size, atmospheric conditions and, for dry deposition, surface configuration and types (e.g., Sportisse, 2007, Duhanian and Roustan, 2011).

The major source of uncertainties is typically due to model inputs (e.g., emissions, meteorology and boundary conditions). The sensitivity and uncertainty analysis of model applications have been reviewed by Russel and Dennis (2000). Some studies found that the uncertainty of all input data can reach 50%, but can be greater for emission data (Hanna et al., 1998, Hanna et al., 2001). The second source of uncertainties is the mathematical representation of the physico-chemical processes simulated by the model; for example, chemical mechanisms include many simplifying assumptions and atmospheric turbulences is highly parameterized. Another significant source of uncertainty lies in the necessary numerical approximations including numerical schemes, time steps, and the horizontal and vertical resolutions.

3.2.4 Stormwater models

Several hydrological models are commonly used to model pollutant transport in waters. First of all, the models must simulate the water flow (quantity) in order to model water quality (i.e., pollutant concentrations and loads). These models may be classified in terms of their functionality, accessibility, water quantity and quality components included in the model, and their temporal and spatial scales. State-of-the-art reviews of stormwater models, including discussions of their capability, strengths and weaknesses have been conducted by Elliott et al., (2007), Zoppou (2001), Cheah (2009), and Jacobson (2011). Hydrological models may be classified according to their spatial distribution:

1. Lumped models (e.g., SLAMM, Pitt and Voorhees, 2002): A lumped model is based on spatial averaging of the input parameters over the catchment. Therefore, these models provide outputs only at the outlet of the catchment without an explicit consideration of spatial variability.
2. Semi-distributed models (e.g., SWMM, Rossman, 2010): Semi-distributed models take into account the variability inside the catchment by dividing a catchment into several subcatchments. Therefore, spatial resolution is related to the size and number of subcatchments.
3. Hydrological Response Unit models (e.g., URBS, Rodriguez et al., 2008): An HRU represents an area of similar runoff generation. The hydrological processes, which can be determined by different factors depending on the catchment and scale, should be similar in one HRU and must characterize the greatest variation in the dominant hydrologic process.
4. Fully-distributed models (e.g., MIKE-SHE, Refshaard et al, 1995; El-Tabach, 2010): They represent surface flow by using physical laws on a grid mesh. They often include spatial and temporal variability (such as soil properties, land use, etc.) depending on the grid size.

These models were listed above from the lowest to the highest spatial resolution. A lumped model often needs to be calibrated. On the contrary, a fully-distributed model is supposed to be based on more physical concepts and may not need to be calibrated. These different models have different aims in terms of temporal and spatial scales and model outputs. Fully-distributed models are mostly used to model individual storm events at the intra-event scale, whereas lumped models are used to simulate water and/or pollutant fluxes over long periods (annual scale). Many of these water quality models have been reviewed by Obropta and Kardos (2007), Vassilios et al. (1997), Elliot and Trowsdale (2007), and Cheah (2009).

Depending on the model type, processes related to pollutant behaviour may be described by deterministic or stochastic laws. Deterministic, stochastic, and hybrid (combination of deterministic and stochastic approaches) stormwater quality models have been presented by Obropta and Kardos (2007). In deterministic models, the transport and transformation of pollutants are mostly modeled by using an advection-diffusion equation and/or the conservation of mass coupled to different reaction rates involving the pollutants in different forms (particles, colloids, dissolved matter). In urban areas, these models couple hydrologic (for surface water) and hydraulic (for water flow through channels) modules. Surface flow is modeled with the shallow water wave equation or its simplified version (kinematic, diffusion wave equation). In lumped models, water contaminants are simply transferred from one compartment to another depending on rainfall intensity and flow rates among the modeled compartments. Another classification of models distinguishes conceptual and empirical models (Zoppou, 2001).

There is added complexity when modelling water quality in addition to water quantity because pollutant forms are highly diverse and variable: some pollutants may be transferred from the dissolved phase to suspended solids during their transport (thereby having a different dynamics of transport) and/or they may be degraded during their transport. Moreover, the phenomena involved in their build-up on urban surfaces and their wash-off are still poorly understood. Therefore, several processes in water quality models must often be simplified using empirical parameterizations. For example, four types of build-up models are generally used: linear, power, exponential, and Michaelis-Menten. Wash-off is usually modeled as a first-order decay function of runoff or with simpler methods such as a constant concentration and rating curves (graph of discharge versus stage for a given point on a stream). The prediction of pollutant transport and transformation in water is very complex and its simulation by current models includes large uncertainties (Kanso et al., 2004).
Atmospheric pollutants are introduced into the stormwater runoff by two processes: dry deposition under the effect of turbulence and, for particles only, gravity, and wet deposition via the scavenging of particles and gaseous pollutants by water droplets. These processes can be modelled by several parameterizations (Sportisse, 2007, Duhanian and Roustan, 2011). Other processes such as road surface abrasion and tyre wear also bring pollutants onto the road surface (Boulter, 2007).
Although these atmospheric processes are well-known, their impact on water quality is rarely treated in current water quality models.

Table 3.4. Summary of urban water quality model categories

Models	Scales	example
Lumped	Spatial average of the input for catchment	SLAMM Pitt and Voorhees, 2002
Semi-distributed	Spatial average for each sub-catchment	SWMM Rossman, 2010
Hydrological Response Units	Spatial average at HRU scale (be create by combined different factors)	URBs Rodriguez et al. 2008
Fully-distributed	Explicity spatial variability (mesh)	MIKE-SHE Refshaard et al. 1995

Water pollutants associated with on-road traffic include mainly polycyclic aromatic hydrocarbons (PAHs) and heavy metals such as Pb, Zn, Cd, Sb, Pt and Cu. Some of these pollutants may exist in a dissolved form. They may be complexed with organic matter or attached to suspended solids (SS), which can then be considered as pollution vectors.

Limitations and uncertainties of stormwater models

It is challenging to implement all these processes in a model and simplifications are needed, which may induce errors. The uncertainty of water quality model outputs is typically greater than that of water quantity because of the additional treatment of pollutants in an urban catchment. Moreover, there is a lack of knowledge on most pollutant emissions relevant to water quality impacts of traffic, which include a component caused by direct deposition on the roadway (road abrasion and tyre wear) and a component resulting from atmospheric processes, followed by water runoff. These processes are particularly difficult to model in water quality models.

Three major uncertainty sources are model parameter values, model formulation, and data (which are used for input, calibration and validation). The uncertainty of a flow measurement in a pipe is estimated to be about 20% and that of a suspended solid concentration is around 30 to 40%. Several studies have discussed the issue of uncertainties in urban hydrology, (e.g., Lindblom et al., 2007; Willems, 2008; Kanso et al., 2003; Dotto et al., 2010). The discussion of uncertainty and validation with special reference to the development and use of models was reviewed by Beck et al. (1987) and Mannina et al., (2006). Other studies (Kanso et al., 2004; Freni et al., 2011) investigated parameter uncertainties in urban runoff quality models. Uncertainty of the model inputs and calibration data have been presented by Freni et al. (2009), Park et al. (2012), and Sun et al. (2013). Finally, different uncertainty techniques in urban stormwater modelling have been compared by Dotto et al. (2012).

3.3 Modelling chain

The main building blocks of such a simulation framework are (1) the structure of the modelling chain which contains traffic, emission, air quality and water quality models (Figure 2) and (2) the interfaces between the output from a model and the input to the next model. Examples of modelling systems to link traffic flow, emission and air quality modelling tools have been described by Lim et al. (2005), Schmidt and Schäfer (1998) and Hatzopoulou (2010). Modelling the effects of atmospheric pollutant dispersion on water quality has been studied mostly at regional scales to address the impact of air pollutants on ecosystems (e.g., Burian et al., 2002, Vijayaraghavan et al., 2010, Gunawardena, 2012). However, there have been few studies of atmospheric deposition on urban watersheds (e.g., Sabin et al., 2005; Fallah Shorshani et al., 2014). We focus below on the interfaces between the various models.

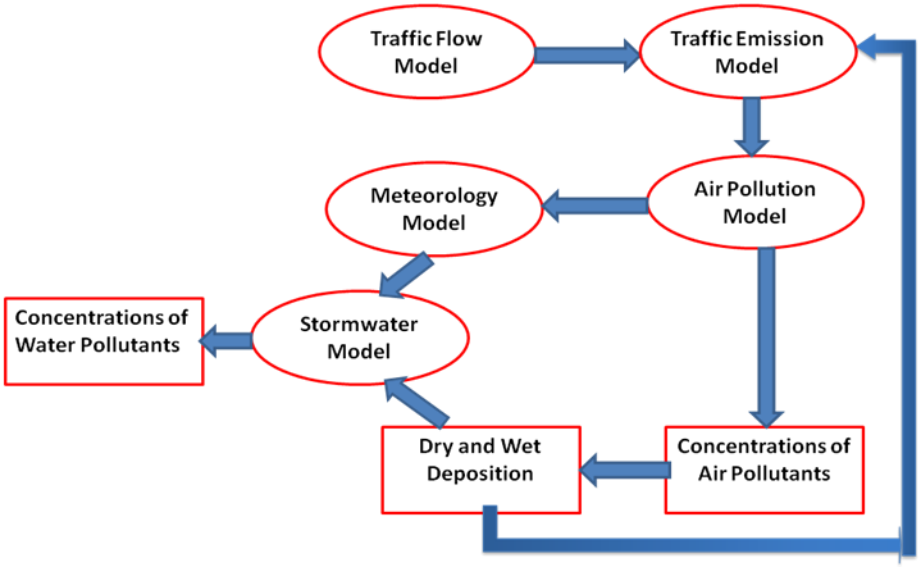

Figure 3.2. Schematic representation of the modelling chain (components are represented with ellipses) with expected input and output data (represented with boxes).

3.3.1 Coupling of traffic and emissions models

The factors relevant to the estimation of vehicle emissions are the vehicle operation (e.g. speed, acceleration, and engine load), the traffic flow conditions and the road and vehicle characteristics. These parameters can be determined by traffic models, so an appropriate coupling is examined here to link the input requirements of emission models with the outputs of traffic models. A traffic model must be chosen according to its capacity to produce the inputs of the emission model: road type and gradient, vehicle category, kinematic parameters (speed, acceleration, idling). Vehicle category information required by emission models is based in Europe on the Euro standard (Kousoulidou et al., 2008) and the capacity of the engine. The traffic models do not provide these data because they only require vehicle types (passenger cars, heavy-duty vehicles, motorcycles, etc.). Therefore, the fractions of different vehicles must be defined by a vehicle fleet composition estimated separately from the traffic model. The variety of traffic/emission models can be presented according to four major types:

- **Macroscopic (static traffic models and aggregated emission models)**

Macroscopic emission models (models based on average vehicle speeds) are combined with a static traffic model or an aggregated dynamic traffic model. Vehicle fleet composition must be provided. Macroscopic traffic flow and emission models are used for large road networks. Static models simply calculate the traffic volume that provides the number of vehicles and average speed on each link needed by average-speed emission models. Such coupling can induce a high level of uncertainty due to several parameters: (1) the OD matrix, which is a central element of the traffic, (2) the parameters and mathematical formulation of the traffic model such as speed-flow curves (which determine the free-flow and congested branches), and (3) the vehicle fleet composition, which has a significant impact on pollutant emissions. In general, both static traffic and average speed emission models use aggregate methods that include significant uncertainty due to the averaging process.

Situation-traffic emission models, such as HBEFA and MOBILE, can also be coupled with aggregated dynamic models of traffic, which can provide the average speed and degree of congestion. It is possible to use average-speed emission models with aggregated dynamic models but one needs to provide a sub-model that defines the level of congestion based on vehicle speed and speed limit. There has been a large number of studies that have integrated macroscopic traffic flow and exhaust emissions (Schmidt and Schafer, 1998; TEMMS project, Namdeo et al., 2002; TEIS, Xia and Shao, 2005). These couplings provide long-run estimates of vehicle emissions for large-scale applications, which would be challenging to calculate with more detailed models.

- **Mesoscopic (macroscopic traffic model and microscopic emission model)**

Emissions can be modeled more accurately with both vehicle speed and acceleration as inputs. Macroscopic traffic models do not provide the acceleration, unlike microscopic models. However, microscopic traffic models need large inputs and computational times when applied to a large road network. We are interested in finding a way to integrate macroscopic traffic models with instantaneous emission models so that the macroscopic variables can be used to produce estimates of the instantaneous emissions on large scales. Cappiello et al. (2002) proposed a combination of a probabilistic acceleration approach and a dynamic emission model (EMIT). The proposed model uses random variables distributed according to some known distribution, for a given speed range and other parameters. In spite of the use of an instantaneous emission model, the emissions calculated with this approach cannot represent accurately second-by-second emissions. The combined model must be used for cases where vehicles have homogenous characteristics within a given speed range.

Another study by Zegeye et al., (2010) proposed integrating the macroscopic traffic flow model METANET and the microscopic emission model VT-micro. METANET is a macroscopic traffic model that describes the average behaviour of vehicles into a number of segments by a system of discrete-time dynamic equations (average traffic density, flow and speed for each segment). VT-micro is a microscopic dynamic emission model that yields emissions of individual vehicles using second-by-second speed and acceleration. Since

METANET is discrete in both space and time, there are two possible accelerations: "temporal" (acceleration of the vehicle flow within a given segment) and "spatial" (acceleration of the vehicles flowing from one segment to another in one simulation time step). The temporal and spatial accelerations of vehicles in a segment are obtained from speed variation. The number of vehicles corresponding to each acceleration can be obtained according to density, flow, length of the segment, and time step. These spatial and temporal speed-acceleration pairs determine the spatial and temporal emissions using VT-micro. The combination of emissions and number of vehicles gives the total traffic emissions.
Information on vehicle category, which is needed by emission models, is not available in macroscopic traffic models. Therefore, the applicability of this approach is limited to cases where vehicles have homogenous characteristics within a given speed range.
These approaches may include important uncertainties associated with the coupling of the traffic and pollutant emission models.

- **Mesoscopic (microscopic traffic model and macroscopic emission model)**

The parameters of macroscopic emissions (average speed and traffic situation) can be precisely estimated by microscopic traffic models but may require large computation times for a large-scale network. To get a balanced trade-off between computational burden and accuracy, one may want to combine a microscopic traffic model with a macroscopic emission model. The main advantage of this coupling is the ability to simulate a large number of pollutants, because macroscopic emission models have a more complete pollutant database compared to instantaneous models. A study by Chanut and Chevallier (2012) compared different macroscopic and microscopic emission models (IMPACT, ARTEMIS, INST (EMIT)) coupled with a microscopic traffic model (AIMSUN). The three models provide very similar temporal evolution of CO_2 emissions in free-flow traffic. However, in congestion, the emissions of the instantaneous model (INST) are 2.5 times greater than those of the model based on average-speed (IMPACT) and 1.5 times greater than those of the model based on traffic-situation (ARTEMIS). Accordingly, the emission-averaged model cannot estimate correctly the emissions of CO_2 in stop & go situations.

- **Microscopic (microscopic traffic flow simulation and instantaneous emission model)**

Emission rates for vehicle operation during a series of short time steps can be predicted by coupling a microscopic traffic model with an instantaneous emission model. The main advantages are the prediction of individual vehicle emission rates as a function of time and the use of driver behaviour. Therefore, this coupling allows one to model traffic emissions at a great level of spatial and temporal detail. The drawback of this type of coupling is that detailed input data for instantaneous emission models are not usually provided by microscopic traffic models (vehicle category) and must be specified by the user. We present below several studies in which a microscopic traffic model has been combined with an instantaneous emission model.

One example is the coupling of VISSIM with PHEM. The instantaneous emission model (PHEM) calculates the emission of road vehicles with 1 s time steps for a given driving cycle

based on emission maps, that is emission level as a function of engine speed and engine power (Zallinger et al, 2008). The traffic flow model in VISSIM is a discrete, stochastic, time-step based microscopic model, with a psycho-physical car-following model. PHEM takes as input time, speed and vehicle characteristics of every single vehicle with other information defining vehicle location from VISSIM and calculates the emissions of each vehicle. The vehicle and engine data required by PHEM are taken from the data base developed from average vehicle data. The classification into Euro classes is chosen automatically in PHEM according to the fleet composition defined by the user. Hirschmann et al, (2010) have proposed to calibrate the traffic data calculated by VISSIM. For example, the maximum acceleration rates have been calibrated to perform the simulation. They assumed that the majority of the calibration effort carried out within their research project can be used also in other urban applications. The time resolution in the VISSIM simulation should be at least 0.3 s to achieve realistic speed profiles (Fellendorf and Vortisch, 2011).
The integrated VISSIM-CMEM traffic emission coupling was developed by Nam et al (2003), Chevallier (2005), Noland and Quddus (2006), Chen and Yu (2007), Stevanovic et al. (2009). The output of VISSIM is converted into the required input file for the CMEM and US vehicle emission standards are converted into European Union standards. VISSIM is currently the most widely used package. Beside this model, PARAMICS (Quadstone, 2002), AIMSUN (Bacelo and Casas, 2005) and DRACULA (Liu, 2005) have been used. Recently, a new microscopic model, Symuvia (Leclercq et al., 2007), has been developed to provide location, speed, and acceleration of each vehicle on a network at any simulation time. This model takes into account initial acceleration, line changing, and vehicle interaction and changes inputs over time. Other similar model coupling studies have been done by Park et al. (2001) with VISSIM and MODEM, Barth et al. (2001) and Boriboonsomsin and Barth (2008) with PARAMICS and CMEM, Tate et al. (2005) with DRACULA and CMEM, and Panis et al. (2006), with DRACULA and emission functions for each vehicle as a function of instantaneous speed and acceleration, Lin et al. (2011) with Dynust and MOVES, Madireddy et al. (2011) with PARAMICS and VERSIT+, and Xie et al. (2012) with PARAMICS and MOVES.

3.3.1.1 Case study coupling traffic and emissions

A coupling between microscopic traffic models and both macroscopic and microscopic emission models was conducted. The results of the two couplings are compared to understand the difference between each coupling. In the first coupling, the dynamic microscopic traffic model, Symuvia, is coupled with an instantaneous emission model, PHEM. PHEM calculates the emission rates of individual vehicles by taking into account the vehicle kinematic parameters with time resolution of 1 s. The second coupling is between the same microscopic traffic model and a macroscopic emission model, CopCETE (CETE Normandie, 2010). In this case, the average speed and number of vehicles on each road segment are obtained from the traffic model. CopCETE is based on the COPERT4 methodology (Ntziachristos et al., 2009) with the same methods and equations but with a mesoscopic approach that considers each road category separately. The simulations were performed for an urban boulevard, Cours Lafayette, and its associated street network in Lyon, France. The network is divided into 84

segments with a total distance of 2.87 km. These different segments include the street intersections and the distinct lanes for passenger cars and buses (Figure 3.3).

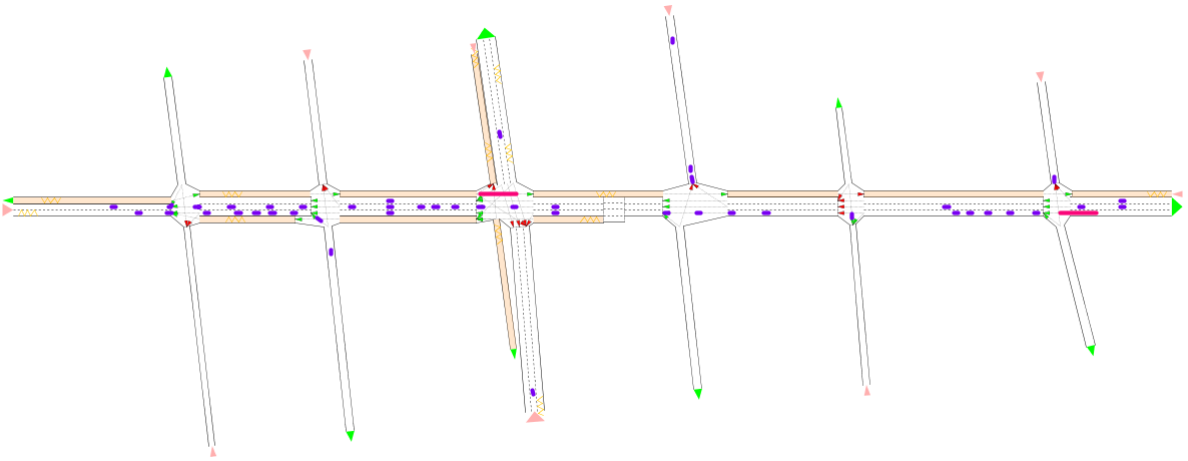

Figure 3.3. Schematic representation of Cours Lafayette; orange lines are bus lanes. The dark blue dots represent individual vehicles, the elongated red dots represent buses.

There are six common pollutants in the two emissions models, which are NO_x, PM_{10}, CO, CO_2, SO_2, and benzene. The exhaust emissions calculated with both model couplings for a 15 min simulation are illustrated in Figure 3.4. For all pollutants except benzene, emissions are greater with the instantaneous emission models i.e., Symuvia-PHEM. The results are in agreement with the study of Chanut and Chevallier (2012) who compared emissions of NO_x, PM_{10}, CO, CO_2, and hydrocarbons (HC) calculated with three emission models, an average-speed model (IMPACT), a traffic-situation model (ARTEMIS), and an instantaneous model (INST). Emissions of NO_x, PM_{10}, CO, and CO_2 were greater with the coupling of the traffic microscopic model (AIMSUN) and the instantaneous emission model (INSTA), but this was not the case for HC. The reason for theses results is that the driving cycle of the average-speed emission model does not represent the actual movement of vehicles, which includes a stop & go behaviour over short distances between intersections. The example of Chanut and Chevallier (2012) (Figure 3.5) shows for a situation of stop & go that the emissions of CO_2 for diesel passenger cars calculated with the average-speed model are 3 times smaller than those of the instantaneous emission model.

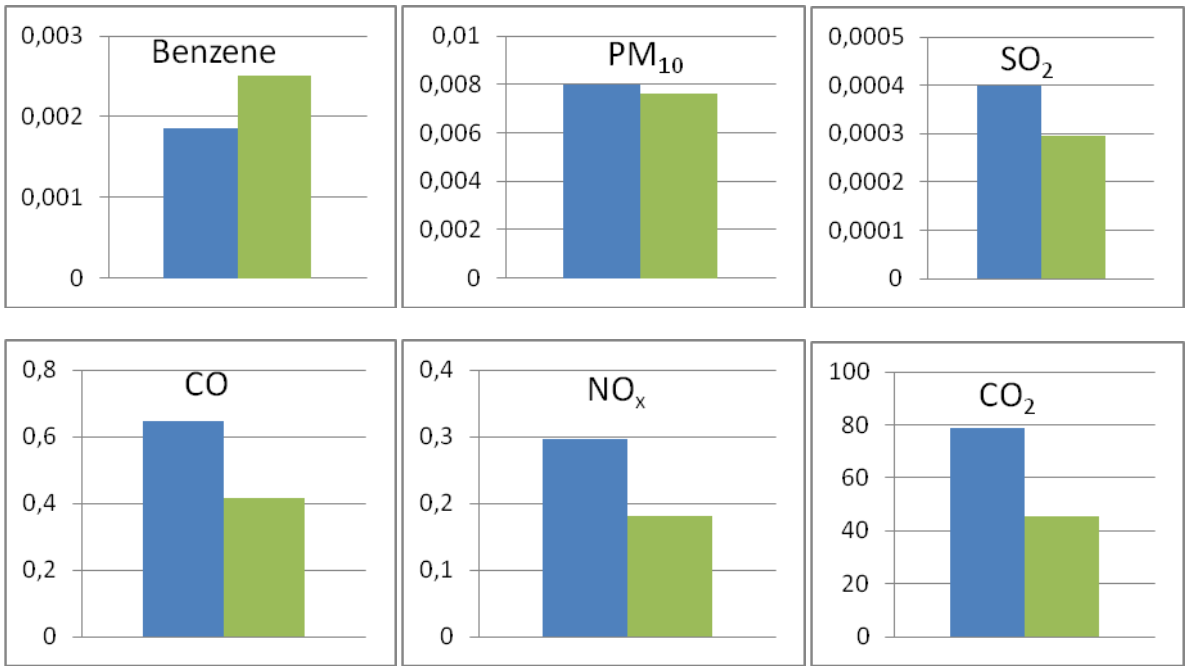

Figure 3.4. Emissions of pollutants (kg/15 min) with a Symuvia simulation for the Cours Lafayette network and the PHEM (blue) and CopCETE (green) emission models.

In our case study, the ratio of the macroscopic and microscopic models are 134%, 96%, 74%, 65%, 61%, 58% for benzene, PM_{10}, SO_2, CO, NO_x, and CO_2, respectively. The fuel consumption ratio is 59%. The emission of benzene depends on cold-start emissions and increases during the warm-up phase (Boulter and Latham, 2009). It is difficult to estimate cold-start emissions for short-time simulations that depend strongly on ambient temperature and the engine conditions. Furthermore, the approaches for estimating cold-start emissions in CopCETE and PHEM are very different. PHEM is based on a heat balance in the engine and the exhaust system; whereas CopCETE uses a method, which is a function of the aggregated value (e.g., average national value of trip length). It should be noted that we tried to match the fleet composition in both models but different definitions of vehicle categories did not allow us to obtain exactly the same fleet compositions.

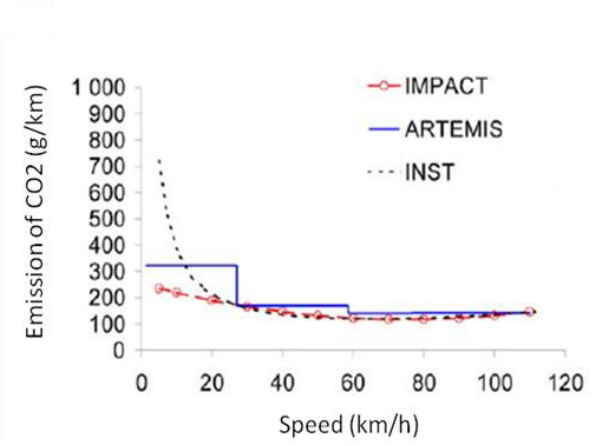

Figure 3.5. Comparison of CO_2 emissions calculated with an average speed model (IMPACT), a traffic-situation model (ARTEMIS) and an instantaneous model (INST) for diesel passenger cars (Source: Chanut and Chevallier, 2012).

The ratio of the emissions calculated with the average-speed model and the instantaneous model for street segments and intersections provides information on the impact of acceleration and deceleration on pollutant emissions. These results (Table 3.5) show that the emission ratio is smaller for intersections than for street segments, which suggests that acceleration in intersections can increase emissions twice as much as in street segments.

Table 3.5. Ratio of pollutant emissions calculated with the CopCETE and PHEM models using a 15-min Symuvia simulation of Cours Lafayette, Lyon, France.

Emission ratio CopCETE/PHEM	Benzene	PM_{10}	SO_2	CO	NO_x	CO_2
Street segment	1.5	1.05	0.82	0.72	0.66	0.64
Intersection	0.65	0.54	0.39	0.32	0.37	0.3

3.3.2 Coupling of emission models and atmospheric models

Understanding vehicle traffic flow and induced emissions alone is not sufficient to predict air pollution in an urban area; hence, an atmospheric dispersion model is needed to predict the temporal and spatial variation of air pollutant concentrations. The major input data necessary for the air quality model are spatially-distributed and temporally-resolved emissions provided by the emission model, meteorological inputs and background concentrations of air pollutants. It is also useful to have input data from a traffic model for dispersion models that account for vehicle-induced turbulence (VIT). The emissions inventory must be compatible with the dispersion model to facilitate data transfer between the two (Lim et al., 2005).

Atmospheric dispersion in urban areas is complex because of street and building geometry effects. CFD modeling techniques provide a detailed representation of the air flow and turbulence, including vehicle-induced turbulence, which is particularly useful in areas with complex geometries such as street canyons and areas with noise barriers. However, the large computational requirements limit their applications to small areas for limited periods. Wang and Zhang, (2009) demonstrated that the results of Gaussian models for atmospheric dispersion of traffic emissions near a road can be better than those of a CFD model without considering VIT and RIT (road-induced turbulence). However, a CFD model with VIT and RIT can be a valuable tool thanks to the rigorous representation of the turbulent mixing mechanisms. The output frequency of instantaneous emission models, which can be on the order of 1 s, can only be taken into account by CFD model. It is, however, possible to average the emission rates over time if one is only interested in concentrations averaged over time. For example, Misra et al. (2013) used hourly average results of microscopic traffic and emission models with a Gaussian model.

The Gaussian models are suitable for local-scale applications and their computational efficiency makes them attractive for applications to large road networks over long time periods. Typically, the input and output frequencies of Gaussian models are 1 h with a receptor resolution or grid size ranging from a few meters to several hundred meters.

Sahlodin et al. (2007) developed a mathematical model that incorporated VIT into a Gaussian dispersion model. Also, the effect of air flow around buildings can be approximated by modifying the dispersion coefficient in the Gaussian equation (Huber, 1991). In the most commonly used models (Gaussian and CFD models), roads are divided into segments which are considered as line (or elongated surface) sources and emissions from vehicles are estimated individually for each road segment. A comparison of air pollutant concentrations obtained from Gaussian and urban CFD models has been conducted by Pullen et al. (2005). Their study shows that the results of the Gaussian puff model are satisfactory in the far field.
Lagrangian and Eulerian models allow one to compute the transport and dispersion of pollutants at a large spatial scale. In the case of Eulerian air quality models, the emissions must be defined for the 3D grid-mesh and for each pollutant. They have been widely applied to simulate air pollution from all sources including roadways. However, they are not able to provide fine spatial resolution near sources. Thus, it is useful to combine regional-scale models such as Eulerian models and local-scale models such as Gaussian models. For example, Beevers et al. (2012) added the urban background concentrations calculated by an Eulerian model CMAQ to roadside concentrations obtained from the ADMS Gaussian model. Karamchandani et al. (2009) and Briant and Seigneur (2013) used a Gaussian puff or plume model, respectively embedded within the Eulerian model Polair3D. This coupling includes the transfer of pollutants between the Gaussian model and the Eulerian model at each time step thereby providing a more accurate representation of air pollutant transport and transformation and leading to better model performance.

One issue with the coupling of an emission model with an air quality model is the time scales involved, because the results of most emission models are not currently valid for short time scales. The output frequency of macroscopic emission models can be adapted to the input requirements of most air quality models, which are on the order of 1 h. To make full use of the advantages of microscopic emission models for simulation with time steps less than 1 h, e.g., on the order of 1 min, one should use CFD models or Gaussian puff models.

3.3.2.1 Case study coupling emission and atmospheric models

This case study corresponds to the atmospheric dispersion and deposition of pollutants emitted from traffic on a freeway in eastern France. Measurements of cadmium (Cd) particulate deposition were conducted by Promeyrat (2001). The measurements were performed at 5, 20, 40, 80, 160, and 320 meters on both side of the freeway in 1997. The A31 freeway segment is located between Metz and Maizières-lès-Metz. Due to difficult access, the measurement sites on each side of the road are distant by about a kilometer but correspond to the same road segment. The traffic data and meteorological conditions were recorded daily.

In this study, we focus on Cd deposition near the freeway in February 1997. The exhaust and non-exhaust emissions were calculated with the average-speed emission model CopCETE. This emission model seemed appropriate because traffic flow on the freeway was at nearly constant speed without congestion and was measured daily. Figure 6 shows the Cd daily

emissions during February. The minimum values of emissions in the time series represent the light traffic on sundays and the maximum emissions are due to heavy traffic on fridays.

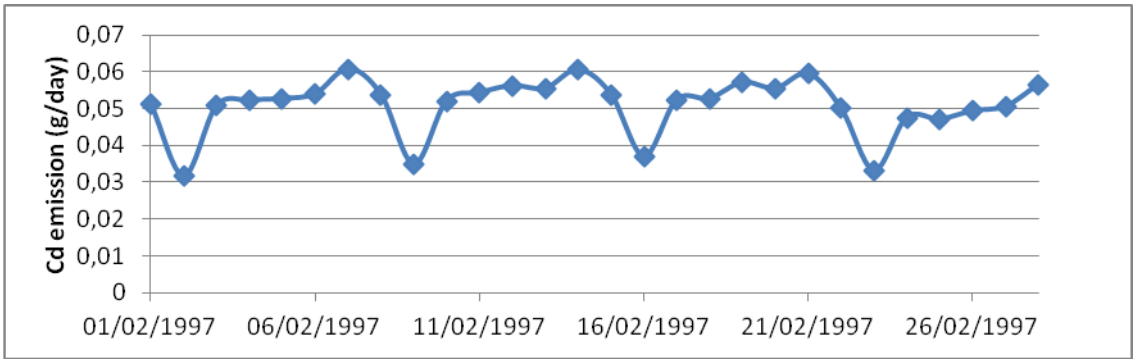

Figure 3.6. Cadmium emissions calculated with CopCETE during February 1997.

Following the calculation of the traffic emissions and the preparation of the other necessary inputs (meteorological data, receptor and source coordinates), the dispersion of pollutants was calculated at the receptor points with the Polyphemus Gaussian plume model (Briant et al., 2011).

Atmospheric deposition was calculated from the pollutant concentrations and compared with the experimental results. Atmospheric deposition occurs via dry processes (i.e., when gas molecules and aerosol particles get into contact with surfaces) and wet processes (i.e., when gases and particles are scavenged by precipitation, mostly by rain). Several studies have experimentally quantified atmospheric deposition of metals near roadways (Viard et al., 2004; Azimi et al., 2005; Sabin et al., 2006; Loubet et al., 2010). These studies show that the deposition fluxes decrease rapidly as the distance increases from the roadway, which is consistent with the spatial gradients observed for atmospheric concentrations.

Theoretical models have been developed for dry deposition (e.g., Zhang et al. (2001), Wesely (2000), Sportisse (2007)) and wet deposition (e.g., Duhanyan and Roustan, 2011).

The dry deposition flux is typically computed using the following formulation:

$$F_{dry}(x,y) = V_d . C(x,y,z_{ref}) \qquad 3.1$$

where V_d is the dry deposition velocity, which is a function of meteorology, land use, and particle size and z_{ref} is the reference height for the pollutant concentration measured or modelled near the surface. The deposition velocities used here were obtained from Roustan (2005). The Cd mass distribution in PM_{10} particles was assumed to be 74% in particles with a diameter less than 1 µm, 10% in particles between 1 and 2.5 µm, and 16% in particles with a diameter between 2.5 and 10 µm. Coarse particles with diameter >10 µm were not considered here. The dry deposition velocities were estimated as a function of an average wind speed (5 m/s) representation of conditions at the site.

Wet deposition was assumed to be homogeneous over the measurement area. The wet deposition scavenging coefficient was calculated following the Andronache (2004) formulation for rural areas.

Figure 3.7 shows the comparison of Cd deposition fluxes modeled and measured on both sides of the freeway. The results are satisfactory on the eastern side of the freeway from 20 m

from the roadside onward. There is same overestimation on the western side between 50 and 200 m from the freeway. The underestimation in close vicinity of the freeway may be due to the fact that particles with diameter greater than 10 µm were not included in the emission estimates. These larges particles, which can be emitted from tyre and brake wear have greater sedimentation velocity than PM_{10} particles and, therefore, deposit rapidly near the roadside.

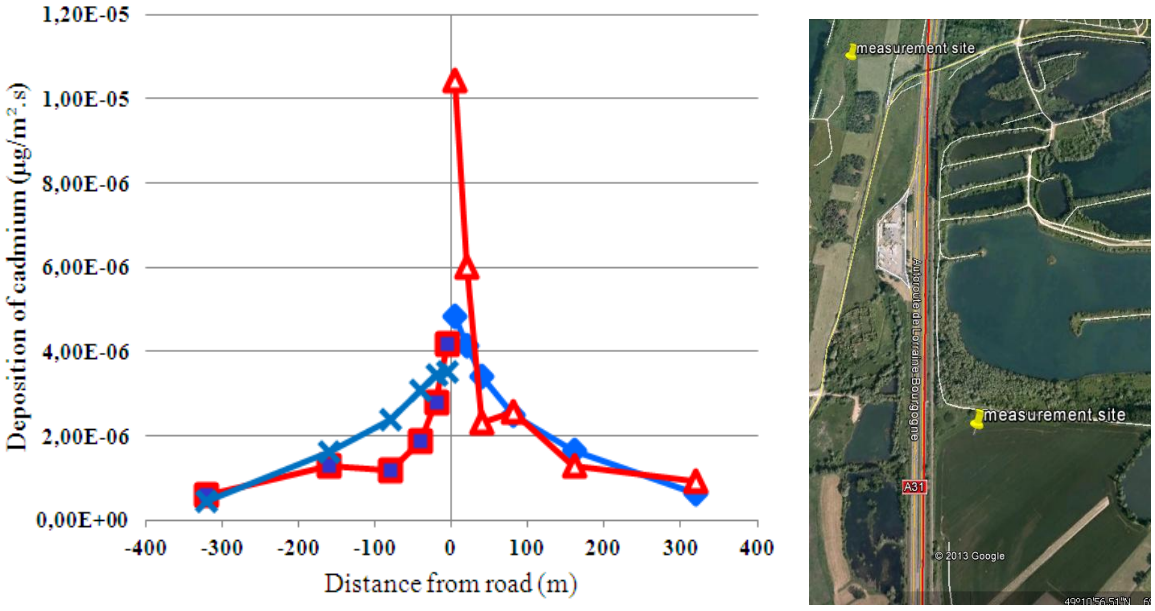

Figure 3.7. Cadmium deposition fluxes modeled (blue) and measured (red) on both sides of the A31 freeway.

3.3.3 Coupling of atmospheric models and stormwater runoff models

The estimation of the traffic impact on water quality is often based on measurements of pollutant concentrations in air and water. However, this method is site-specific and does not allow one to evaluate the impact of traffic at any point of an urban catchment or to estimate water contamination for future road projects. The effect of the atmospheric deposition of pollutants is important to predict water quality when major sources are located near or within a catchment. Therefore, the outputs from air quality models should be used as data inputs for stormwater models. Deposition fluxes of atmospheric pollutants can be estimated for dry and wet deposition as a function of time and location. Deposition near roadways of atmospheric pollutants emitted by traffic is mostly due to dry deposition. Wet deposition scavenges the entire atmospheric column and, therefore, includes background pollutants. Sabin et al. (2005) calculated that in Los Angeles, California, annual wet deposition fluxes were significantly lower than dry deposition fluxes with wet deposition, comprising only 1-10% of the total deposition flux. Nevertheless, air pollution models must estimate both dry deposition to determine pollutant buildup (mass per unit area) during dry periods and washout during rainfall events.

A major scientific stumbling block is that air quality models typically consider only those particles smaller than 10 µm in aerodynamic diameter (e.g., see case study above) because

coarser particles are not subject to air quality regulations, which are driven mainly by inhalation-based health concerns. There is, therefore, a lack of an integrated multi-media environmental approach (Hidy et al., 2014). However, the mass of particles greater than 10 µm is significant and relevant to water quality and should be taken into account (Kakooei and Kakooei, 2007). Although the smaller fraction of particles may have a higher concentrations of some pollutants, the fraction of pollutants contained in particles of larger sizes may not be negligible (Gunawardena et al., 2012). Improving emission models as requested by regulations such as the EU Water Framework Directive and the EU Environmental Quality Standard Directive should be an objective to address multi-media issues.

Several studies coupling air and watershed models at the regional scale already exist (e.g., Burian et al., 2002; Schwede et al., 2009; Vijayaraghavan et al., 2010). These coupled models are able to read a processed gridded output of atmospheric deposition from the air quality model, and calculate average fluxes per unit area. Most of the work conducted so far on the coupling of atmospheric models and stormwater models was done at regional scales for long time periods, such as annual or seasonal budgets of atmospheric pollutant loadings to address environmental issues such as acid or mercury deposition. However, the dynamics of multimedia pollutant transfer is of interest for urban applications. Therefore, there is a real need for the development of a modelling chain that can address both urban air and water quality issues in an integrated fashion. The evaluation of this new modelling chain will need to distinguish between pollutants linked to traffic emissions and other pollutant sources in urban areas.

The main limitation is coupling of spatial scales between air quality and stormwater models. The air quality models provide spatially-distributed deposition fluxes. These fluxes must be used by stormwater models, but it is generally necessary to adapt the spatial scale to the semi-distributed water quality models (Fallah Shorshani et al., 2014). Therefore, the deposition fluxes must be calculated by averaging deposition over each subcatchment. The fully-distributed stormwater models may simulate water quality on the same grid resolution as the air quality model, however, the description of land use may not be detailed enough, because different land use types may be present in each model grid cell. This difficultly can be solved by using high grid resolution.

Finally, the evaluation of integrated air and water quality models remains challenging because of the variety of sources of pollutants in stormwater, which make source attribution difficult and may lead to compensation of errors (Vezzaro et al., 2012).

3.3.3.1 Case study of the effect of air pollution on water quality

This case study addresses the impact of traffic emissions on water quality via atmospheric deposition in an area located in the Paris region. The whole modelling chain has been treated by Fallah Shorshani et al. (2014); here, we focus on the atmosphere/water interface. Therefore, instead of using model outputs from traffic, emission and air quality models, experimental data on pollutant deposition fluxes are used to estimate roadside impacts.

The Grigny catchment is located 20 km south of Paris. The catchment area of 365.7 ha is covered by several municipalities. This area is impacted by two main roads (D310 and D445)

and the A6 highway, having annual average daily traffic volumes of 17,000, 21,000 and 125,300 vehicles per day respectively.

The present study focuses on three trace metals (Cd, Zn, and Pb) emitted from traffic and deposited to the Grigny catchment during 2009 and 2010. The model used to perform the stormwater runoff analysis is SWMM 5 (Rossman, 2010). This model is an open-source modelling software, which is appropriate for this study as it allows rainfall-runoff simulations (quantity and quality) over long periods with short time steps. The water quantity modelling and the flow-rate calibration were performed using a genetic algorithm to maximize the Nash criteria, as described in detail by Petrucci et al. (2013).

The dispersion of atmospheric pollutants is calculated using wind direction data covering two years, 2009 and 2010. The wind rose is based on observations at the nearest station (Orly airport, 8 km from the catchment). The use of the wind rose from a close but different location is appropriate in this case because of the relatively flat terrain and the surrounding land use (i.e., suburban residential area). Total concentrations of Cd, Pb, and Zn are simulated in runoff from the Grigny catchment during 23 months (01/01/2009-01/12/2010) with a 5 min reporting time step. The aim of such a long-term simulation is to determine the effects of traffic on the pollutant levels at the outlet of the catchment within this period. To that end, two cases were studied. The first case takes explicitly into account background deposition and the local pollutant deposition due to the three main roadways of this heavy-traffic area; the latter is spatially variable. The second case uses only a uniform deposition flux corresponding to an averaged urban pollution background typical of low-volume surface roads (<2000 vehicles/day). The study by Wicke et al. (2011) was used to estimate the following background deposition fluxes of Cd, Pb, and Zn: 0.13, 8, and 140 $\mu g\ m^{-2}\ day^{-1}$, respectively.

Water quality simulations include the pollutant buildup during dry periods and washoff during rainfall events. Different mathematical approaches are available to represent the processes governing pollutant accumulation and washoff. The exponential buildup and power washoff equations are used in this study (Hossain et al. 2010). The daily accumulation rates are calculated according to the deposition flux of each pollutant source (i.e., the two roads and the highway), the associated level of traffic, and the wind direction. Pollutant deposition exhibits well-defined linear relationships with traffic volume (Brett and Gavin, 2011). Therefore, the traffic effect can be calculated based on the measurement data of highway A31 with the proper traffic scaling. The spatial distribution of deposition fluxes is estimated for each road or highway based on the wind rose. According to previous work (Azimi et al., 2005; Sabin et al., 2006; Loubet et al., 2010), the daily accumulation rates for each sub-catchment are calculated over areas impacted by road traffic that extend up to about 240 m from the road. Then, traffic emissions for each road impact a fraction of the sub-catchment area based on road location with respect to the sub-catchment and wind direction. The background deposition level was attributed to all sub-catchments. Next, based on those input parameters for stormwater modelling, the pollutant concentrations in water were calculated with SWMM.

The comparison of two simulations (heavy traffic and low-level traffic) shows a significant effect of traffic on water contamination. The results presented in Figure 8 show the relative load of Zn in each sub-catchment for both simulations: i.e., with an explicit description of the contribution of traffic and considering only the effect of a background residential contamination. Some sub-catchments present low pollutant concentrations because they do

not produce any runoff due to a large amount of pervious surface (vegetation-covered areas) in the sub-catchment. Figure 3.8 shows that the traffic emissions can increase the water contaminant concentrations on highly exposed sub-catchments by up to 3 times in comparison with the case without traffic.

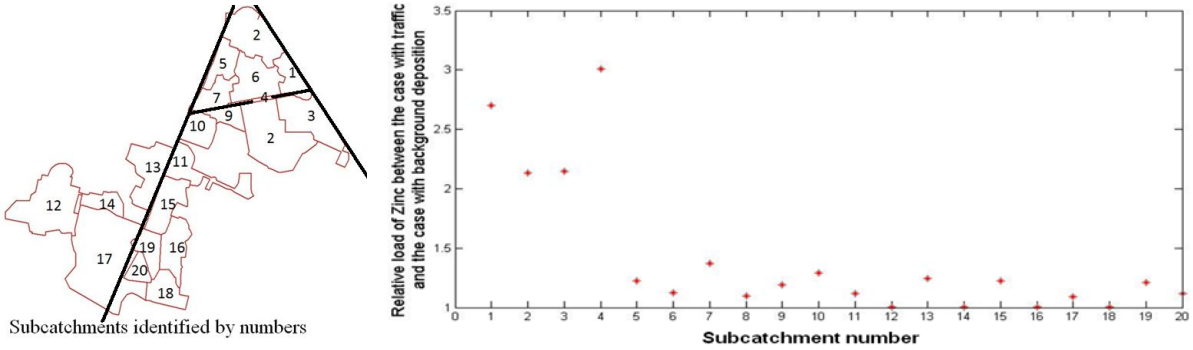

Figure 3.8. Relative load of Zn in each sub-catchment between the case with explicit treatment of traffic on main roads and the case with background deposition only.

The results of Zn concentrations at the outlet between the case with background deposition and with traffic during 6 days are shown in Figure 3.9. The relative variation between daily and period-averaged Zn concentrations was simulated over two years for both cases. The highest concentration peak compared to the average Zn concentration is about twice greater in the case with explicit traffic treatment than in the case with urban background deposition. The highest concentrations of Cd, Pb, and Zn at the outlet are respectively 2.12, 285, and 1758 µg L^{-1}. Cases without traffic reach a maximum of 0.78 µg-Cd-L^{-1}, 47.7 µg-Pb-L^{-1}, and 835 µg-Zn-L^{-1}. These important differences are related to the pollution peaks. The average concentrations over the two-year period (2009-2010) are 0.08 µg-Cd-L^{-1}, 6.33 µg-Pb-L^{-1}, and 79 µg-Zn-L^{-1} with the explicit treatment of traffic. These values in the case without explicit treatment of traffic impact are 0.06 µg-Cd-L^{-1}, 4.0 µg-Pb-L^{-1}, and 70.2 µg-Zn-L^{-1}. These results show that an explicit description of local atmospheric pollution sources such as traffic has a strong impact on pollution peaks observed at the outlet of an urban catchment.

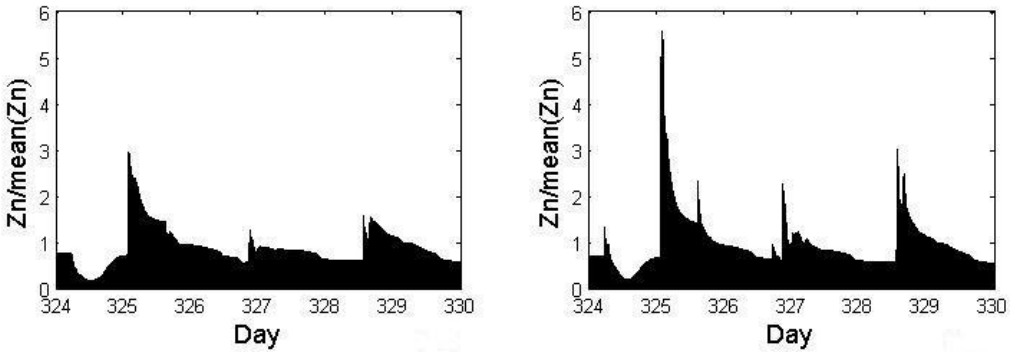

Figure 3.9 . Relative Zn concentration (ratio between daily and period- averaged concentrations of zinc) over 6 days for the case with background deposition (left) and the case with explicit traffic treatment on main roads (right).

3.4 Conclusion and Recommendations

In this study, the various modeling approaches available for traffic, emissions, atmospheric pollution, and stormwater pollution were presented and discussed in terms of their advantages, shortcomings, and compatibility. This review aimed at providing relevant information to facilitate the selection of the most appropriate models to be coupled in order to implement an integrated and efficient modelling chain for the simulation of air and water quality in urban areas. The importance of input and output data, compatibility among models, spatial and temporal scales were discussed. Most available models are based on temporally and spatially averaged input data. These average-based models are useful for many particular problems. However, the use of dynamic models is recommended for some applications and their use is feasible with current computing resources. As examples, we propose below two modelling chains to simulate the environmental impacts of traffic at the local urban scale for both average-based and dynamic models (see Figure 3.10).

1) Regarding the special requirements and level of details needed for a mesoscopic scale such as a city or neighbourhood, the modelling chain may consist of a static traffic model or a macroscopic dynamic model. These models provide the flow and speed of vehicles for an average-speed emission model such as Copert or CopCETE. A Gaussian or street-canyon model will then be appropriate to simulate the atmospheric dispersion of vehicle emissions at the mesoscopic scale. A semi-distributed water quality model can simulate the transfer of pollutants to the wastewater system. If a large number of pollutants and emission phenomena (fuel evaporation and non-exhaust emissions in addition to exhaust emissions) must be treated, such a modelling chain may be needed, because emission factors may not be available for more detailed models (see below).

2) A microscopic modelling chain can be used at a local scale, but only for exhaust emissions, because instantaneous emission models cannot estimate fuel evaporation and non-exhaust particle emissions. These models are able to represent the dynamic phenomena occurring in the traffic flow. The microscopic dynamic (car-following) models require many parameters and such models are data and computation demanding. The microscopic models with macroscopic law models (such as Symuvia) are an alternative because they are well suited for a dynamic representation of urban traffic with manageable data needs. For air quality, the CFD models can be used to calculate the dispersion of vehicle emissions at fine spatio-temporal scales. For water quality, a fully-distributed model can be coupled with a CFD model using compatible spatial grids. However, the limitations of instantaneous emission models do not allow one to treat non-exhaust emissions, which can be an important source of pollutants relevant to water contamination.

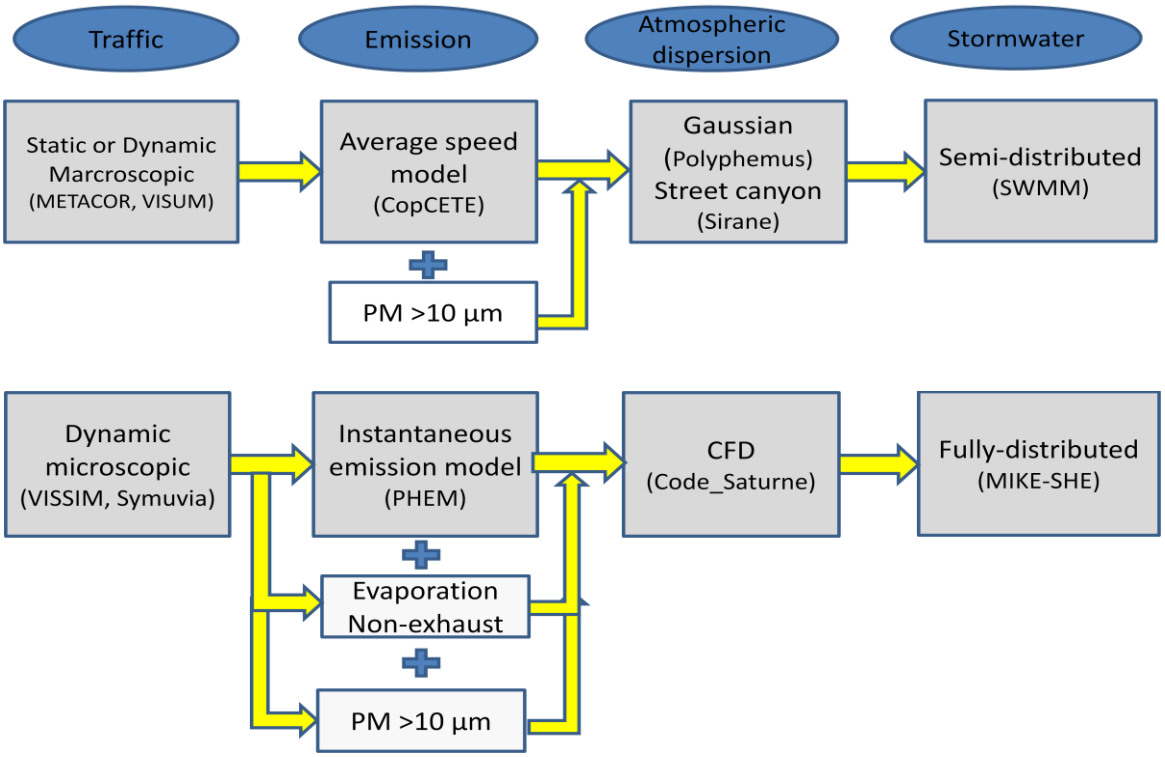

Figure 3.10. Schematic representation of the modelling chains for mesoscopic (top) and microscopic (bottom) scales with examples of models for each component of the modeling chain. Note that the list of models is not exhaustive and that other model choices are possible.

Case studies were provided to explain model integration between traffic, emission, atmospheric dispersion and stormwater quality. These examples underlined the strengths and limitations of the different models in terms of their ability to represent physical processes and demonstrated the importance of the environmental impacts of traffic at the local scale.
In summary, a modelling chain must be able to handle the various aspects enunciated above in a realistic, yet computationally efficient manner. Existing models will, therefore, need to be improved and adapted to address all these issues.

Chapitre 4

4 Modélisation de la pollution atmosphérique liée à la circulation automobile

Deux chaînes de modélisation ont été proposées au chapitre 3, l'une statique avec des pas de temps horaires, la seconde envisageant une approche dynamique. Une évaluation des performances d'une chaîne de modélisation statique pour deux formulations d'un modèle de dispersion atmosphérique est présentée dans ce chapitre. La dispersion des polluants atmosphériques à proximité des sources est généralement simulée de manière satisfaisante avec des modèles Gaussiens en raison de leur bon compromis entre précision de résultats et temps de calcul. Toutefois, la formule de dispersion gaussienne s'applique en aval d'une source en direction du vent et ne peut pas calculer les concentrations de polluants atmosphériques dans des conditions météorologiques calmes avec une direction du vent fluctuante et / ou en amont de la source d'émission. Cependant, de telles conditions doivent être prises en compte lors de calculs d'exposition de la population à proximité des axes routiers et il semble nécessaire d'améliorer la formulation des modèles pour ces conditions particulièrement difficiles à modéliser. Le modèle de panache gaussien a donc été amélioré avec la formulation de Venkatram et al. (2013). Dans cette formulation, le panache de polluants est représenté avec deux termes : un panache Gaussien classique, qui s'étend en aval de la source dans le sens du vent et un panache qui s'étend dans toutes les directions à proximité de la source pour les situations météorologiques calmes (faible vitesse de vent). Ce travail évalue la performance de modèles de panache Gaussien standard et modifié avec des mesures de NO_2, PM_{10}, $PM_{2.5}$, cinq ions inorganiques (Na^+, NO_3^-, K^+, Mg^{2+}, Ca^{2+}) et sept métaux (Co, Cu, Fe, Mn, Pb, Sb, Sn) effectuées près d'une autoroute à Grenoble pendant la période du 11 au 27 septembre 2011. Ces données ont été obtenues dans le cadre des projets MOCOPO du programme PREDIT et PM-DRIVE du programme CORTEA de l'ADEME.

Les émissions du trafic automobile peuvent être calculées en fonction du parc automobile, des nombres de véhicules légers, poids lourds et bus et de leurs vitesses. Le parc automobile local a été défini à partir d'observations vidéo et de comptages de trafic effectués durant le projet MOCoPo (André et al., 2014). Les données de taux d'occupations (un proxy pour la densité du trafic) mesuré sur le tronçon d'autoroute permettent d'estimer l'état de congestion du trafic. En effet, les courbes débit/taux d'occupation permettent de déterminer les taux d'occupation critiques du tronçon qui correspondent au seuil de congestion du trafic. On considère donc que les situations de trafic avec un taux d'occupation supérieur à ce taux

critique sont congestionnées et que la vitesse des véhicules légers est alors considérée comme égale à celle des poids lourds. Pour les situations de trafic non-congestionnées, la vitesse des véhicules légers a été prise comme supérieure de 28 km/h à celle des poids lourds (les résultats sont peu sensibles à cette hypothèse). Les émissions « échappement » et « non-échappement » de NO_2 et PM (PM_{10}, $PM_{2,5}$) ont été calculées avec le modèle d'émissions CopCETE. La remise en suspension de particules par le trafic a été incluse sur la base des résultats d'une analyse de PMF (Positive Matrix Factorization) spécifique au site (Polo, 2013). Les émissions d'autres polluants (métaux et ions inorganiques) ont été estimées grâce aux facteurs d'émission de COPERT pour l'émission non-échappement et des facteurs d'émission d'Amato et al. (2011) pour la resuspension.

Pour les particules, on fait l'hypothèse que la distance limitée (7 m) entre l'autoroute et la station de mesures ne laisse pas suffisamment de temps pour que des transformations chimiques menant à la formation de polluants particulaires secondaires aient lieu. Pour NO_2, il faut tenir compte des réactions rapides entre NO, O_3 et NO_2. On fait donc l'hypothèse de l'état photo-stationnaire de Leighton pour calculer les concentrations de NO_2 à partir des concentrations de NO_x et des concentrations de fond de NO, NO_2 et O_3. Pour les émissions de NO_x, la spéciation a été calculée à partir d'un calcul d'émission spécifique à la composition du parc automobile de MOCOPO et elle est estimée à 26% de NO_2 et 74% de NO.

Les simulations ont été réalisées avec des pas de temps horaires et des pas de temps de 15 minutes ; les résultats sont similaires pour les deux simulations, avec cependant une légère diminution de la corrélation temporelle entre simulation et mesures pour NO_2.

Les performances des modèles standard et modifié sont présentées en termes de résultats statistiques qui incluent corrélation, RMSE, MNE, MNB, NME, et MFE. Les résultats des modèles standard et modifiés ont été comparés à des mesures. Il apparaît que le traitement des conditions météorologiques calmes améliore le coefficient de corrélation et permet de réduire les erreurs de manière significative.

Il apparaît que les modèles sous-estiment les concentrations de particules et de NO_2. Pour PM_{10}, la corrélation entre valeurs mesurées et simulées (modèle modifié) est significative (0,76), mais partiellement influencée pas la concentration de fond. Pour NO_2, la corrélation est faible et suggère que le modèle sous-estime l'influence des émissions du trafic sur le site de mesures. L'effet de la turbulence due au mouvement des véhicules sur le transport horizontal des polluants n'est pas pris en compte dans la formule utilisée pour représenter ce phénomène, ce qui pourrait expliquer la sous-estimation en cas de vent faible. Une autre source d'incertitude est liée aux données d'entrée du calcul, telles que les facteurs d'émission.

Ce chapitre est constitué de Fallah Shorshani et al., (2014) :

> Fallah Shorshani M., Seigneur C., Polo L., Chanut H., Pellan Y., Jaffrezo J.L., Charron A., André M. (2014). Atmospheric dispersion modeling near a roadway under calm meteorological conditions. Submited to Transportation Research Part D.

Abstract

Atmospheric pollutant dispersion near sources is typically simulated by Gaussian models because of their efficient compromise between reasonable accuracy and manageable computational time. However, the standard Gaussian dispersion formula applies downwind of a source under advective conditions with a well-defined wind direction and cannot calculate air pollutant concentrations under calm conditions with fluctuating wind direction and/or upwind of the emission source. Attempts have been made to address atmospheric dispersion under such conditions. This work evaluates the performance of standard and modified Gaussian plume models using measurements of NO_2, PM_{10}, $PM_{2.5}$, five inorganic ions and seven metals conducted near a freeway in Grenoble, France, during 11 - 27 September 2011. The formulation for calm conditions significantly improves model performance. However, it appears that atmospheric dispersion due to vehicle-induced turbulence is still underestimated. Furthermore, model performance is poor for particulate species unless road dust resuspension by traffic is explicitly taken into account.

4.1 Introduction

Studies have shown that populations spending large amounts of time near major roadways have an increased incidence and severity of health problems that may be related to air pollution from roadway traffic (Baldauf et al., 2008). Health effects include reduced and impaired lung function, asthma and other respiratory symptoms, cardiovascular effects, low birth weight, cancer, and premature death (e.g., Garshick et al., 2003; Janssen et al., 2002; Gauderman et al., 2005; Heinrich et al., 2005; McConnell et al., 2006; Pirjola et al., 2006). Therefore, it is essential to estimate population exposure near roadways in support of exposure and epidemiological studies as well as for impact studies of future roadway projects. To that end, one needs to select traffic, emission, and air quality models relevant to the given case study. Traffic models can be classified as static or dynamic models according to spatio-temporal scales. However, in many studies, traffic data are available from measurements that can be used directly as inputs for emission models. Emission models use traffic data (fleet composition, vehicle speed, etc.) and other relevant data (e.g., road gradient, ambient temperature) to estimate traffic-related emissions of air pollutants, which are used as inputs to an atmospheric dispersion model. A variety of atmospheric dispersion models are available to simulate the concentrations of air pollutants as a function of time and space, with different levels of details (Holmes and Morawska 2006; Zannetti 1990; Sportisse 2009). Eulerian and Lagrangian models are typically used for large domains, ranging from urban to global scales. At local scales (i.e., near emission sources), different models are used depending on

topography. Gaussian dispersion models are typically used for cases without obstacles or with obstacles of simple geometry. Street-canyon models may be appropriate for cities with high buildings, although for cases with complex geometries Computational Fluid Dynamics (CFD) models may be required.

In this work, we use a Gaussian dispersion model to simulate air pollutant concentrations near a roadway. Actual traffic data are used as input to estimate air pollutant emissions. Concentrations of pollutants were measured near the roadway for a two-week period. Local meteorological measurements were also available. During that period, wind speeds were mostly low and the prevailing wind direction was such that the measurement site was located mostly upwind of the roadway. Most Gaussian dispersion models are designed for receptors located downwind of the roadway and for conditions with a significant wind speed (Benson, 1989; Zhang and Batterman, 2010; Kerstin et al., 2007). However, conditions with calm meteorological conditions and upwind locations are also relevant to population exposure. Therefore, this study examines the performance of a Gaussian model with and without modification for calm meteorological conditions using the measurements conducted near a roadway. First, the formulation of the atmospheric dispersion model is briefly presented. Then, the field campaign is described. Finally, the model simulation results are presented and discussed.

4.2 Model description

The emission and atmospheric dispersion models must be selected such that they are consistent in terms of level of detail, input requirements, and spatial and temporal resolution. An emission model based on average vehicle speed is appropriate here considering the available traffic data.

Two steady-state models are used here to simulate the atmospheric dispersion of pollutants: a Gaussian plume model for roadway sources (Briant et al., 2011, 2013) and this plume model augmented with a formulation suitable for conditions with light winds (Venkatram et al., 2013).

4.2.1 Gaussian plume formulation for roadway sources

The Gaussian dispersion model used here for the atmospheric dispersion of pollutants emitted from a roadway is that of Briant et al. (2011, 2013). The concentration field is calculated with an equation that minimizes the error when the wind direction is not perpendicular to the roadway:

$$C_p(x,y,z) = \frac{qF(z)}{2\sqrt{2\pi}u\cos\theta\sigma_z(d_{eff})} \times \left[erf(t_1) - erf(t_2)\right] \times \left(\frac{1}{L(x_{wind})+1}\right) + E(x_{wind}, y_{wind}, z) \quad 4.1$$

where, $t_i = \frac{(y - y_i)\cos\theta - x\sin\theta}{\sqrt{2}\sigma_y(d_i)}$; $F(z) = \left(\exp\left(-\frac{(h_s - z)^2}{2\sigma_z^{\,2}} \right) + \exp\left(-\frac{(h_s + z)^2}{2\sigma_z^{\,2}} \right) \right)$;

$d_{eff} = \frac{x}{\cos\theta}$; $d_i = (x - x_i)\cos\theta + (y - y_i)\sin\theta$

C is the pollutant concentration in g m^{-3} at the location of the receptor (*x*, *y*, *z*), x is the distance from the source along the wind direction in m, y and z are the cross-wind distances from the plume centerline in m, x_i and y_i are the coordinates of the source (road segment) extremities, *u* is the wind velocity in m s^{-1}, *q* is the emission rate per unit length of the line source in g m^{-1} s^{-1}, and σ_y and σ_z are the standard deviations representing pollutant dispersion in the cross-wind directions in m. L and E are analytical functions that minimize the error when the wind direction is not perpendicular to the line source. The standard deviations σ_y and σ_z are computed here with the Briggs parameterization (Briggs, 1973). The effective distance d_{eff} is used to compute σ_z and d_i is the distance from each extremity of the line source section in the wind direction used to compute σ_y. This equation applies when the angle θ between the wind direction and the normal to the road segment ranges from 0° to 80°.

When the wind is parallel or nearly parallel (80°≤θ≤90°) to the roadway, the concentration, C, is calculated as a combination between Equation (1) and a numerical solution ($C_{discretized}$) obtained by discretizing the line source as aseries of point source is used:

$$C = (1-\alpha)\, C_p + \alpha\, C_{discretized} \qquad 4.2$$

The coefficient α varies linearly from 0 to 1 when θ vary from 80° to 90°.

This model was successfully evaluated against a reference solution as well as against observations obtained over a large road network in France (Briant et al., 2013). The overall spatial correlations for nitrogen dioxide (NO_2) concentrations measured and modeled at 242 sites were between 0.74 and 0.79, which indicates that the model explains more than half of the spatial variability observed in the monthly-averaged observations. Although the results for spatial variability were satisfactory, the ability of the model to reproduce temporal variability could not be evaluated in this previous work (Briant et al., 2013) because of a lack of hourly-averaged data. However, the temporal correlations between observed and modeled concentrations are typically poor for many models. For example Misra et al. (2013) obtained a correlation of hourly nitrogen oxides (NO_x) simulated concentrations with the Gaussian model AERMOD of 0.35. Hirtl and Baumann-Stanzer (2007) simulated NO_x concentration with the Gaussian model ADMS-Roads. They showed that point-to-point comparisons of measured and modeled concentrations paired in space and time (hourly) usually result in a very weak correlation. A variety of statistical metrics may be used to evaluate model performance. Several studies (Qian and Venkatram. 2011; Venkatram et al., 2013; Chang and Hanna, 2004) used the fraction of the modeled concentrations that are within a factor of two of the observations; this statistical metric is denoted fac2. In this work, we have chosen both the correlation (r) and fac2 to quantify model performance.

4.2.2 Model formulation under light winds

Several studies have been conducted for conditions with low wind speeds (e.g., Cimorelli et al., 2005; Carruthers et al., 1994). It was assumed that when the mean wind speed is below a certain threshold (0.1 m/s), the horizontal plume spread covers 360° (i.e., there is no well-defined wind direction). Venkatram et al. (2013) assumed that the vertical dispersion of the plume is linear with distance and derived the following formula for the contribution of the meandering components of the line source plume as:

$$C_{lw}(x,y,z) = \sqrt{\frac{2}{\pi}} \frac{qF(z)\theta_s}{2\pi u \sigma_z} \quad 4.3$$

where θ_s is the angle subtended by the line source at the receptor.

$$\theta_s = \tan^{-1}\left(\frac{y_2 - y}{x}\right) + \tan^{-1}\left(\frac{y - y_1}{x}\right) \quad 4.4$$

This concentration does not depend on wind direction.

Then, the concentration at a receptor is calculated as the sum of two terms, which represent the advected plume and the random spread of the meandering plume. A coefficient (f_r), which depends on wind speed, defines the relative importance of the advected plume and random spread components.

$$C = C_p(1 - f_r) + C_{lw} f_r \quad 4.5$$

where $f_r = \frac{2\sigma_v^{\,2}}{u_e^{\,2}}$, and u_e is the effective velocity given by $u_e = \sqrt{\left(\sigma_u^{\,2} + \sigma_v^{\,2} + u^2\right)}$; $\sigma_v^{\,2} = u^2 \sinh(\sigma_\theta^{\,2})$; and $\sigma_u^{\,2} = u^2(\cosh(\sigma_\theta^{\,2}) - 1)$ are the standard deviations of the turbulent velocity fluctuations along the mean flow and in the lateral direction, respectively. σ_θ is the measured standard deviation of the horizontal wind direction fluctuations. We used by default σ_θ=72° based on Cirillo and Poli (1992).

4.3 Field study

The traffic, meteorological, and air pollution data used in this study were obtained in the MOCOPO (Measuring and mOdelling traffic COngestion and POllution) project, which covered 4 periods (one in each season) during 2011 near freeway N87 located south of Grenoble in eastern France. Another project (PM-Drive; Particulate Matter, Direct and Indirect On-Road Vehicular Emissions) was conducted in part jointly with MOCOPO for a two-week campaign in September 2011, to obtain measurements of inorganic ions and trace metal concentrations every 4 hours. The main objective of PM-Drive was to understand the chemical composition of PM from vehicle exhaust and non-exhaust emissions as well as their contributions to PM concentrations near roadways. Therefore, we focus here on the data from

11 till 27 September because the data set includes: (1) the classification of all vehicles circulating on freeway N87 according to vehicle categories, age and fuel used as well as pollutant emission regulation (vehicle fleet composition), (2) detailed traffic data relevant to traffic flow, including average vehicle speed and occupancy data (i.e. the fraction of time that the traffic count loop is occupied by a vehicle, a surrogate measurement of traffic density) every 6 min, and (3) air pollutant concentrations and meteorological data every 15 min, and (4) PM concentrations of inorganic ions and trace metal concentrations every 4 hours. Most of these data are available at http://mocopo.ifsttar.fr.

Measurements of gaseous and PM species concentrations were conducted at two sites: the Echirolles site, which is the traffic site of this study and the Les Frenes site, which is the nearest urban background site for the Grenoble area from the Local Air Quality Network. The traffic site is located 7 m from the edge of the freeway, which is characterized by two lanes in each direction and a speed limit of 90 km/h. It carries over 68,000 vehicles daily with a peak hour count of 7,800 vehicles/hour. The background site is located 1 km away from the freeway (Figure 4.1).

Figure 4.1. Geographical location and characteristics of the Echirolles freeway including traffic (green dot), and background (red dot) sites (Source: Google Maps).

The comparison of pollutant concentration measurements at the traffic and background sites determines the impacts due to the freeway traffic.

The near-road site is located 7 m from the roadway without any significant difference in elevation (see Figure 4.2). It is, therefore, representative of maximum population exposure in the vicinity of traffic. Measurements of wind speed and direction (vane anemometer) and temperature were conducted on a 10 m mast. Air pollutant measurements were conducted at about 4 m agl. Nitrogen oxides (NO_x and NO, NO_2 by difference) were measured by chemiluminescence using a 15 min time step. PM_{10} and $PM_{2.5}$ were measured with TEOM instruments with a 15 min time step. In addition, PM_{10} was sampled on quartz filters with a DA80 (30 m^3/h flow) with a 4 hour time step for later chemical analysis of metals, ions, and carbonaceous compounds.

4.2. View of the Echirolles (traffic) measurement site

4.3.1 Traffic data

Given the traffic data and the input requirement of the steady-state atmospheric dispersion model, an emission model based on average vehicle speed was considered appropriate. Therefore, the CopCETE model (CETE Normandie, 2010) of the French Ministry of Ecology was applied for exhaust and non-exhaust emissions. This model calculates vehicle emissions from most emission processes including vehicle exhaust, fuel evaporation, and equipment wear. It treats the road gradient, the length of the road segment, different types of traffic density (urban or rural road), fleet composition, including number of vehicles per categories (passenger, light-duty, and heavy-duty vehicles, buses) and their average speeds. This model uses emission functions from the European COPERT 4 methodology (Ntziachristos et al., 2009). CopCETE is based on the same methods and equations as COPERT 4, but with a mesoscopic approach that allows one to break down a road network into segments.

The traffic was measured with electromagnetic loops (SIREDO) on the segments of the freeway close to the traffic site, in both directions. The electromagnetic loops were used to estimate the average speed of the vehicles averaged over 6 min and total traffic count, regardless of vehicle types or lanes.

The road gradient and length of this freeway segment are 0% and 956 m, respectively. The fleet composition was obtained by image processing of vehicle front registration plates captured by four cameras located over the freeway as part of the MOCOPO project (in both directions). The identification of each vehicle was performed using data from the national registration file and allowed one to determine their detailed specifications (type of vehicle, year of registration, pollutant emission standard). Only 53% of the vehicles were identified because of experimental malfunctions and foreign registration plates. The observed local fleet composition on freeway N87 (André et al., 2014) differs slightly from the national fleet

composition of 2011 (André et al., 2013). Figure 4.3 shows a comparison of the national and local (MOCOPO) fleet compositions presented by fuel categories for passenger cars, Euro standard (exhaust emission regulations, see Kousoulidou et al., 2008) for passenger cars, and vehicle categories. There are more passenger cars compared to the national fleet composition, and the fraction of diesel passenger cars is less than in the national fleet. The Euro 3 cars are the largest number of vehicles in the local data whereas the national fleet shows that Euro 4 cars dominate the fleet; therefore, the local data reflect an older fleet than the national data. The local fleet composition was used here.

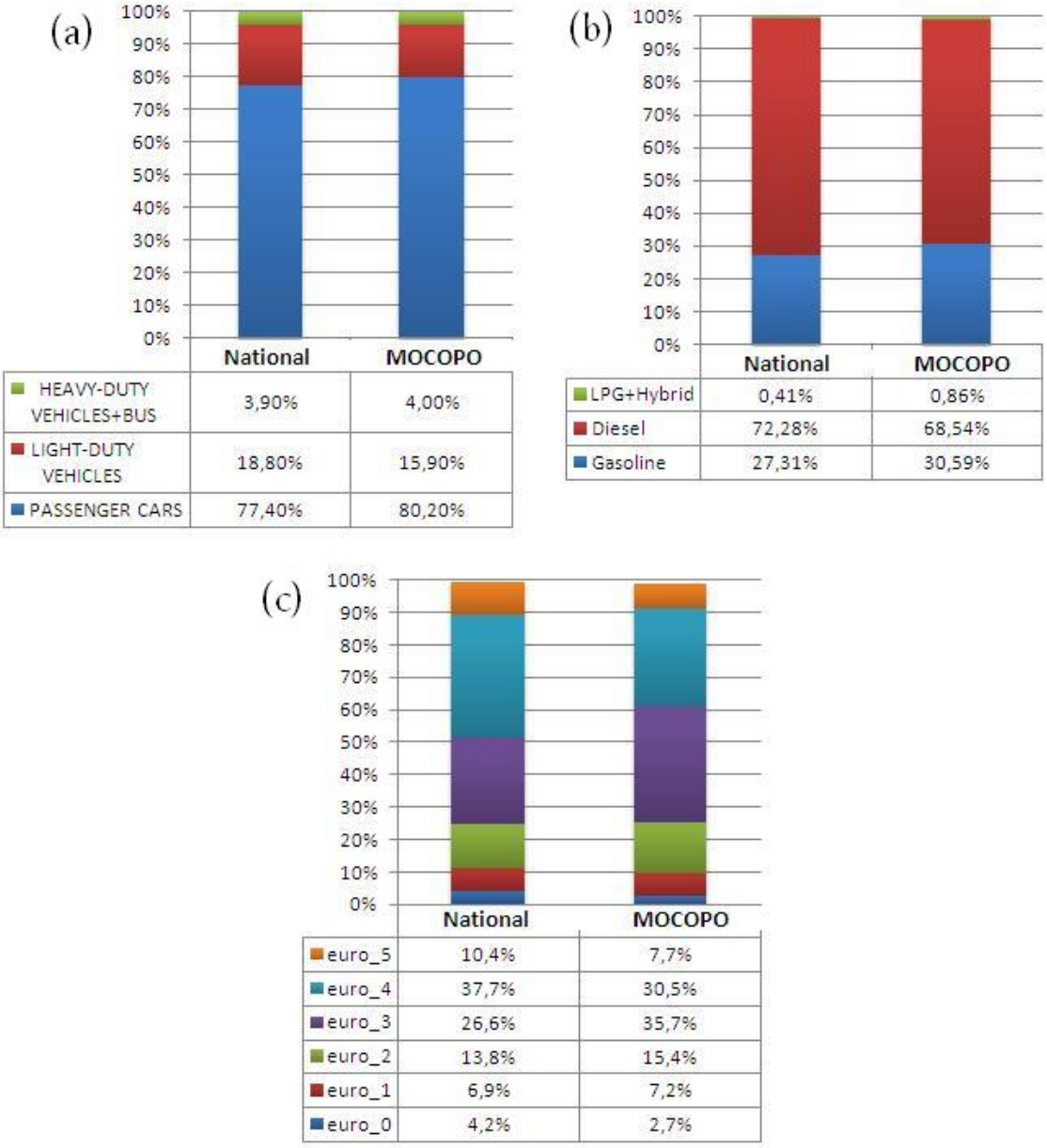

Figure 4.3. Comparison of the national and local (Mocopo) fleet compositions: (a) fuel category, (b) Euro standard category, (c) vehicle type category.

Another parameter required by the CopCETE emission model is the average speed per vehicle category. The traffic data only include the vehicle mean speed and occupancy rates for all the

vehicles. These data are used to estimate the state of congestion. The data depicting traffic flow as a function of occupancy rates are shown in Figure 4.4 for both directions of the N87 freeway next to the traffic site. These data were used to determine the critical occupancy rate corresponding to the threshold of traffic congestion. The critical rate varies from 12% to 14% for both directions (see Figure 4.4). Therefore, we considered that the traffic situations with an occupancy rate over 13% are congested and that the speed of passenger cars is considered equal to that of the heavy-duty vehicles above this threshold. For traffic situations that are not congested, the speed of passenger cars was taken to be 28 km/h greater than the speed of the heavy-duty vehicles (Hugrel and Joumard, 2004). As a sensitivity study, we calculated pollutant emissions with the assumption that the speed of passenger cars is equal to that of heavy-duty vehicles in all traffic situations. The results showed that the emissions of PM_{10} and NO_x increase only by 1% and 5%, respectively, in the latter case. The results presented below use the former case.

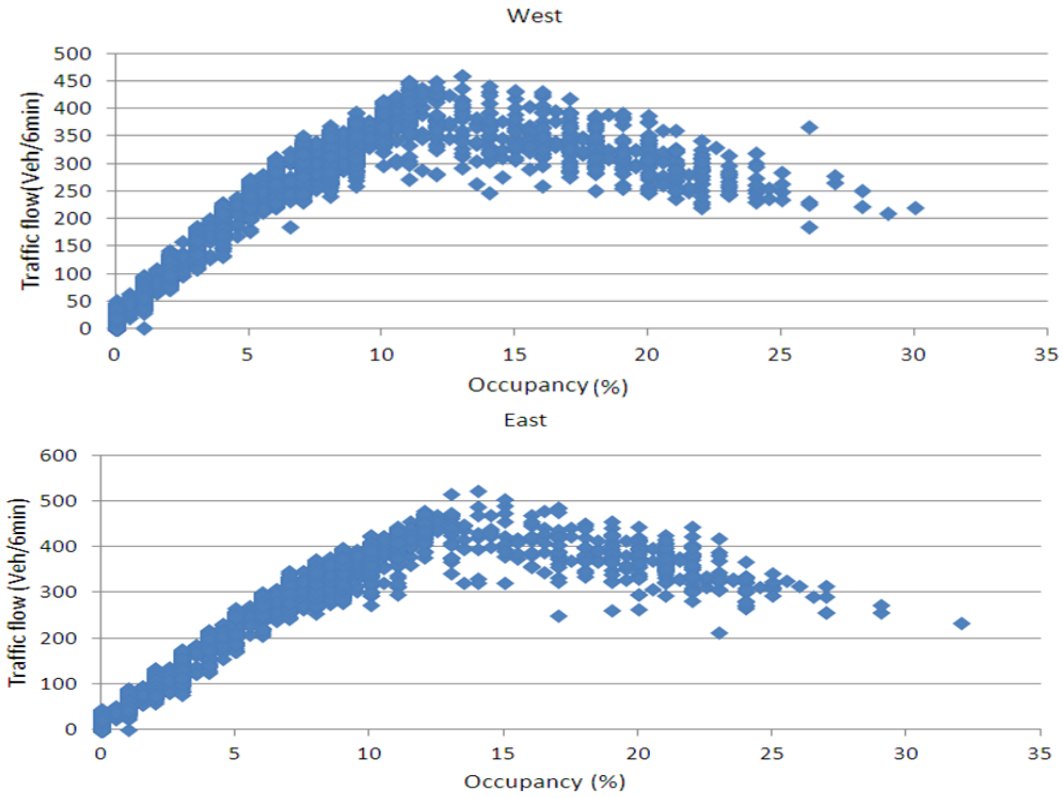

Figure 4.4. Traffic flow (vehicles/6min) versus occupancy data (%) in the east (bottom) and west (top) directions from the Echirolles measurement site. Occupancy can be seen as a surrogate measurement of traffic density (see text).

4.3.2 Emission data

The particulate matter (PM) emissions due to exhaust, tire, break, and clutch wear were calculated with the CopCETE model. Another important source of PM is re-emission of road dust by traffic. Dust resuspension by traffic depends on several factors such as vehicle speed, vehicle fleet composition, and time elapsed since the last rain event. Although algorithms exist to estimate dust resuspension based on such factors (e.g., Pay et al., 2011; Denby et al., 2013), there are still large uncertainties associated with such estimates. Therefore, a simple

approach was used here that takes advantage of a statistical analysis of PM_{10} composition time series conducted by Polo Rehn at the traffic measurements site. Road dust contains particles originating from a wide range of sources. Polo Rehn and co-workers (Polo Rehn, 2013; Polo Rehn et al., 2014) used the PM-DRIVE data collected during the MOCOPO project to estimate the contributions of emission source categories to PM concentrations measured at the traffic site using Positive Matrix Fractorization (PMF). PMF is a principal component analysis method that can identify and quantify the relative contributions of various air pollution sources to ambient concentrations. It is a multivariate analysis based on determination of factors related to source profiles (Paatero and Tapper, 1994; Paatero, 1997). A data matrix (X) is decomposed into two matrices, a matrix of factors of contributions (G) and a matrix of factor profiles (F). In an air quality application, as was conducted by Polo Rehn (2013) at the traffic site in order to discriminate road dust resuspension, non-exhaust and exhaust traffic sources, X is a matrix which contains measured concentrations at distinct times of a series of chemical species (inorganic ions and trace metals), G is the contribution matrix source categories, and F is the matrix characterizing the chemical species profile of each source. The equation is, therefore, written as follows:

$$X = FG + E \tag{4.6}$$

where E is the residual matrix (i.e., the unexplained part of X). It is the difference between the measured concentrations (X) and the concentrations modeled with PMF in the matrix Y = FG:

$$E = X - Y \tag{4.7}$$

The objective function to be minimized as a function of G and F is given by:

$$Q(E) = \sum_{i=1}^{m} \sum_{j=1}^{n} \left(\frac{e_{ij}}{\sigma_{ij}} \right)^2 \tag{4.8}$$

where σ_{ij} represents the uncertainty related to each concentration *i* and each measured species *j*. In this way, the PMF problem is then identified as a minimization of Q(E) with respect to G and F, with the constraint that each element of the matrices G and F is to be non-negative.

PMF was applied to the PM-DRIVE data set to determine the contributions of PM_{10} resuspension versus PM_{10} direct traffic emissions. The EPA PMF v3.0 was used. Polo Rehn (2013, 2014) showed that the contribution of PM_{10} resuspension represents on average over the period 76% of the emissions due to direct exhaust and tire, break, and clutch wear. Dust resuspension by traffic depends on several factors such vehicle speed, vehicle fleet composition, and time elapsed since the last rain event. A simple approach was used here and a model simulation was conducted using a road dust resuspension emission term that was set in 76% of the vehicle emissions. However, dust resuspension was not taken into account during rain events (here on 19 September). The hourly emissions of PM_{10} for cases with and without road dust resuspension are compared in Figure 4.5.

The composition of road dust PM_{10} particles has been measured by Amato et al. (2011) for several metals, anions, and cations. Their study provides relative mean concentrations of major road dust components at three sites Zurich, Switzerland, Barcelona and Girona, Spain (hereafter of Amato (species)). We used the average value among these three sites (Table 1) to estimate the emission rates of these species due to road dust resuspension. Therefore, the total emission rates of PM_{10} species are provided by the following equation:

$$q_{\text{species}} = q_{PM_{10}} \times f_{COPERT}(\text{species}) + q_{roaddust} \times f_{Amato}(\text{species}) \quad 4.9$$

where the first term on the right hand side represents the direct vehicle emissions and the second term represents dust resuspension, q is the emission rate and f is the fraction of each species in PM_{10}. As discussed above, we assumed $q_{roaddust}=0.76\ q_{PM10}$.

Table 4.1. Relative mean concentrations of road dust components averaged over three urban sites (based on Amato et al., 2011) (µg g^{-1}).

Ca^{2+}	K^{+}	Na^{+}	NO_3^{-}	Fe	Mg^{2+}	Co	Cu	Mn	Pb	Sb	Sn
14×10^4	**1.7×10^4**	**0.6×10^4**	**1.7×10^4**	**5.1×10^4**	**1.3×10^4**	**14.7**	**1978**	**580.3**	**207.7**	**194.7**	**243.3**

.

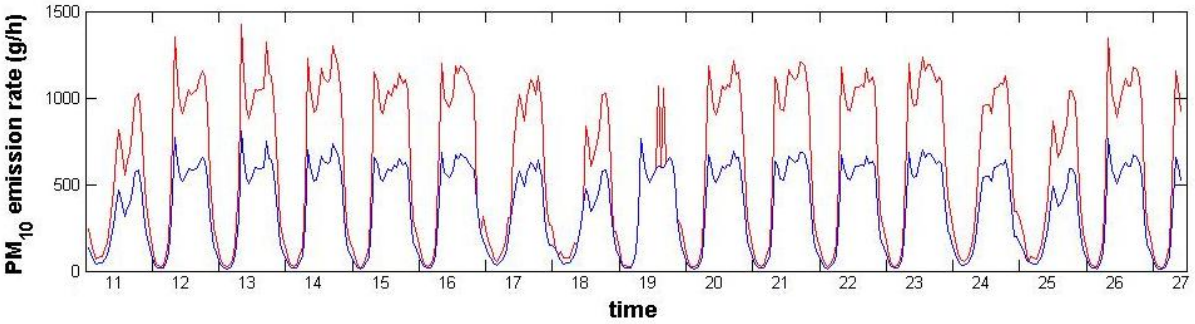

Figure 4.5. Hourly emissions of the N87 freeway segment without resuspension (blue) and with resuspension (red) from 11 to 27 September 2011.

Finally, these data (as presented in Figure 4) were used as input to the atmospheric dispersion model.

4.3.3 Meteorological data

The meteorological data included cloud cover, temperature, wind speed, and wind direction at the traffic site. Meteorological data were used here as hourly and 15 min averaged data. Figure 4.6 shows that the measurement campaign took place during a period characterized by low wind speeds. During 97% of the measurement period, the wind velocity was less than 2 m/s and it was less than 1 m/s 63% of the time. Furthermore, it appears that according to the wind directions, the measurement site is located mostly upwind of the freeway.

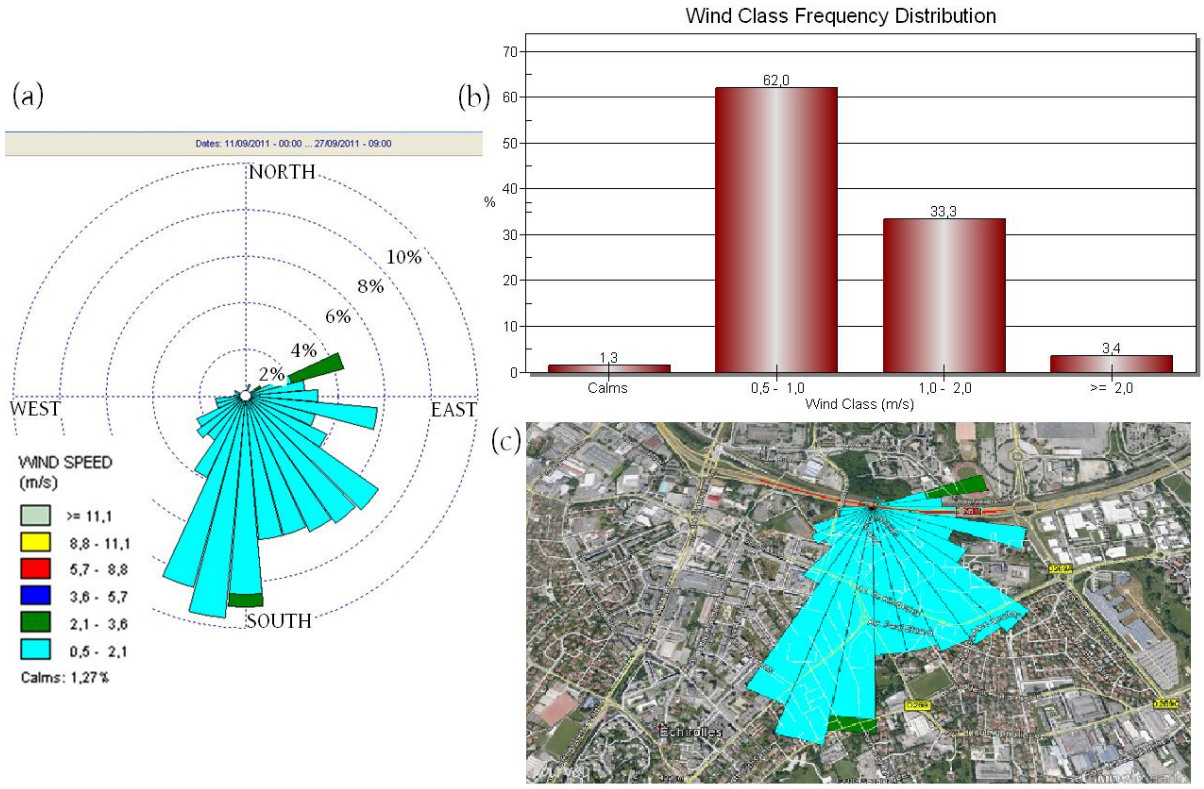

Figure 4.6. Wind data at the traffic monitoring station: (a) wind rose, (b) wind speed frequency distribution, (c) configuration of the wind direction with respect to the N87 freeway segment.

4.3.4 Air quality data

Air quality data from 11 to 27 September 2011 are available for several air pollutants. The concentrations of NO, NO_2, PM_{10}, and $PM_{2.5}$ were measured at high frequencies and were subsequently aggregated as 1-hour averaged values. Particulate species (trace metals and inorganic ions) were measured as 4-hour averaged values from September 19 at 11:30 am till September 23 at 11:30 pm at the background site and from September 14 at 3:30 pm till September 23 at 11:30 pm at the traffic site. This 4-hour temporal resolution was required for proper chemical analysis. It may not capture the full details of traffic flow, but it can distinguish among different traffic situations. These off-line measurements provided detailed chemical characterization of PM_{10}, which was used for instance to estimate the contribution of road dust resuspension (see above).

The PM_{10} analysis (Polo Rehn, 2013) was carried out by ICP-MS for a wide range of elements (Al, As, Ba, Ca, Cd, Ce, Co, Cr, Cs, Cu, Fe, K, La, Li, Mg, Mn, Mo, Na, Ni, Pb, Pd, Pt, Rb, Sb, Sc, Se, Sn, Sr, Ti, Tl, V, Zn, Zr). Only those metals that were detected at both sites were included in the analysis. The other pollutants measured include Cl^-, NO_3^-, SO_4^{2-}, $C_2O_4^{2-}$, Na^+, NH_4^+, K^+, Mg^{2+}, and Ca^{2+}. Ozone (O_3) was also measured at the background site and was used to account for NO_x/O_3 chemistry.

4.4 Results

The pollutants simulated in this study are NO_2, PM_{10}, $PM_{2.5}$, Na^+, NO_3^-, K^+, Mg^{2+}, Ca^{2+}, Co, Cu, Fe, Mn, Pb, Sb, and Sn based on data at both the background and traffic sites and emission factors availability. For example, emission factors for SO_4^{2-} and NH_4^+ were not available for road dust resuspension. The simulations were conducted with hourly input and output data and comparison with actual measurements was made for hourly and 4 hr averages depending on data availability.

Chemical transformations leading to secondary particulate pollutants can be ignored here because of the close distance between the freeway and the measurement site, and particles were therefore assumed to be chemically inert. Thus, the concentrations of PM and particulate species at the traffic site were calculated as the sum of the background concentration measured at the background site and the traffic contribution obtained with Equations (4.5) and (4.9). For NO_2, the rapid reactions between NO, NO_2 and O_3 were taken into account. The Leighton steady-state relationship was used to calculate the NO_2 concentrations from the NO_x concentration at the traffic site and the concentrations of NO, NO_2 and O_3 at the background site (e.g., Briant et al., 2013). We considered a fraction of 26% of NO_2 and 74% of NO for NO_x traffic emissions based on the fleet composition of the N87 freeway and the COPERT 4 data.

Two simulations were conducted: one with the standard Gaussian plume model (Eq. 4.1) referred to as the standard model, and one with the Gaussian plume model modified with the option to account for conditions with light winds (Eq. 4.5). They are compared here to evaluate the effect of the light wind algorithm. They were performed for PM_{10}, $PM_{2.5}$, a selection of PM_{10} chemical species, and NO_2.

Figure 4.7 shows simulated and measured concentrations of PM_{10}. The simulation follows the temporal evolution of the measurements; however, some observed peaks are not reproduced by the simulations (for example on 12, 21, and 27 September at 9 am, and 26 September at 8 am).

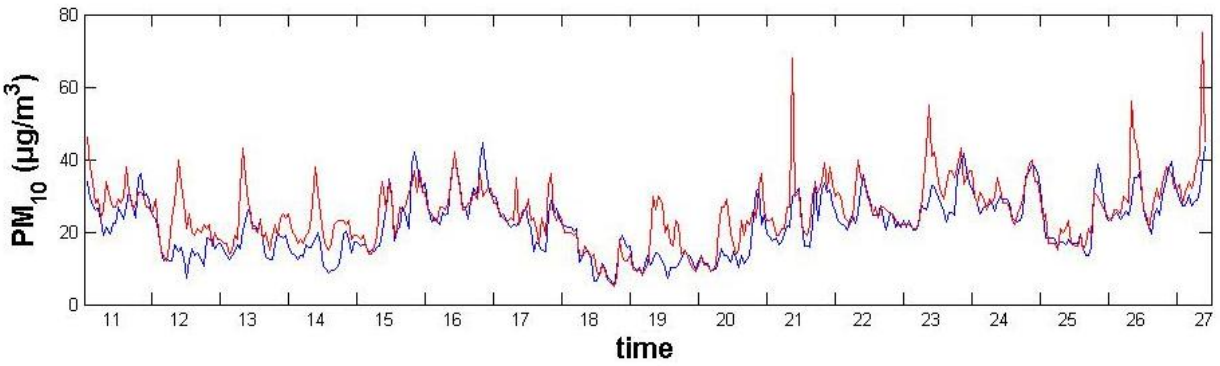

Figure 4.7. Comparison of PM_{10} hourly concentrations measured (red) and simulated with the calm option (blue) at the traffic site.

The performance of the models is presented in Table 4.2 in terms of statistical results, which include the Root Mean Square Error (RMSE), the Mean Normalized Error (MNE), the Mean Normalized Bias (MNB), the Normalized Mean Error (NME), and the Mean Fractional Error (MFE) (see Yu et al., 2006, for definition of the metrics). The model underestimates the concentrations of PM_{10} and $PM_{2.5}$. For PM_{10}, the correlation between measured and simulated values is satisfactory (r= 0.76; n= 394) and, therefore explains more than half of the observed variability (r^2>0.5). Similar results are obtained for $PM_{2.5}$. When comparing the results of the modified model with those from the standard model, which neglects the impacts of light winds under calm conditions, it appears that the treatment of calm conditions leads to a significant improvement in the correlation of PM_{10} from 0.48 to 0.76. Similar results are obtained for $PM_{2.5}$ with an improvement from 0.41 to 0.72 in the correlation coefficient. The comparison of the two models for PM_{10} shows that RMSE, MNE, MNB, NME, and MFE decrease by 40%, 29%, 0%, 28%, and 27%, respectively when adding the option for calm winds. The corresponding decreases for $PM_{2.5}$ are 40%, 32%, 8%, 30%, and 26%. These significant decreases of the errors for the modified model highlight the importance of the calm wind algorithm to better simulate pollutant concentrations under such conditions.

It is of interest to investigate whether the location of the measurement site with respect to the road, downwind or upwind, has a significant effect on model performance and/or the effect of the incorporation of the light wind parameterization (i.e., Eq. 4.5 vs Eq. 4.1). The same performance statistics are, therefore, presented in Table 3 for the two subsets of the sampling data corresponding to the location of the measurement site with respect to the road (i.e., downwind subset and upwind subset). The statistics show better model performance for PM_{10} and $PM_{2.5}$ with the modified model (Eq. 4.5) compared to the standard model (Eq. 4.1) whether the measurement site is upwind or downwind of the road.

For the cases where the site is downwind of the road, the improvement in model performance is due in part to the overestimation of the PM concentrations by the standard model; incorporating the light wind parameterization lowers the modeled concentrations since the emissions are then dispersed in all directions rather than only downwind. If the standard model had underestimated the measured concentrations, model performance would have deteriorated in terms of bias and error. This appears for the downwind NO_2 concentrations for which the model overestimation is less than that for PM (ratio of the average modeled and measured values of 1.23 for NO_2, compared to 1.44 for PM_{10} and 1.49 for $PM_{2.5}$) and the performance of the modified model is better than that of the standard model only for correlation and RMSE.

For the cases where the site is upwind of the road (about 90% of the cases), the improvement in model performance due to the parameterization of light wind conditions is expected since the standard model consistently underestimates and, consequently, model performance improves for all three pollutants and all statistics. One notes that although the decrease in model error and bias is significant in all cases, the improvement in the correlation is slight for the upwind cases.

Wind speeds were low during this study with a wind speed less than 1.5 m/s 84% of the time and less than 1 m/s more than 60% of the time. Therefore, no clear trend appears in terms of model performance as a function of wind speed (using thresholds of 1 and 1.5 m/s); the standard model overestimates at all wind speeds when the measurement site is downwind of the road and underestimates at all wind speed when it is upwind. Correlation between modeled and measured concentrations improves with the modified model at all wind speeds, except for NO_2, where a decrease in the correlation coefficient from about 0.5 to 0.25 occurs for wind speeds above 1 m/s when the site is upwind of the road. Nevertheless, a slight improvement in correlation from 0.41 to 0.44 occurs when all upwind cases are considered.

The categorization of model performance as a function of atmospheric stability was investigated for correlation between measured and modeled concentrations using three main categories in order to have sufficient cases in each category: unstable conditions (classes A and B), slightly unstable and neutral conditions (classes C and D) and stable conditions (classes E and F). The standard model showed for the three pollutants (i.e., PM_{10}, $PM_{2.5}$, and NO_2) better correlations (about 0.8 or greater) for slightly unstable and neutral conditions and worse correlations (less than 0.4) for unstable conditions. The modified model does not show such clear trends although better correlations are obtained either for slightly unstable and neutral conditions or for stable conditions.

Table 4.2. Statistical performance for NO_2, PM_{10}, and $PM_{2.5}$ concentrations for the standard model (Eq. 4.1) and the model modified for calm conditions (Eq. 4.5).

	Average measured value (μgm^{-3})	Average estimated value (μgm^{-3})	Correlation (r)	RMSE (μgm^{-3})	MNE	MNB	NME	MFE
PM_{10} (Eq. 4.5)	25.2	21.9	0.76	6.8	0.17	-0.12	0.18	0.19
PM_{10} (Eq. 4.1)		21.4	0.48	11.2	0.24	-0.12	0.25	0.26
$PM_{2.5}$ (Eq. 4.5)	19.9	17.1	0.72	5.6	0.17	-0.11	0.19	0.2
$PM_{2.5}$ (Eq. 4.1)		16.6	0.41	9.4	0.25	-0.13	0.27	0.27
NO_2 (Eq. 4.5)	51.2	31.8	0.44	28.4	0.4	-0.35	0.43	0.56
NO_2 (Eq. 4.1)		27	0.23	34.3	0.52	-0.4	0.55	0.72

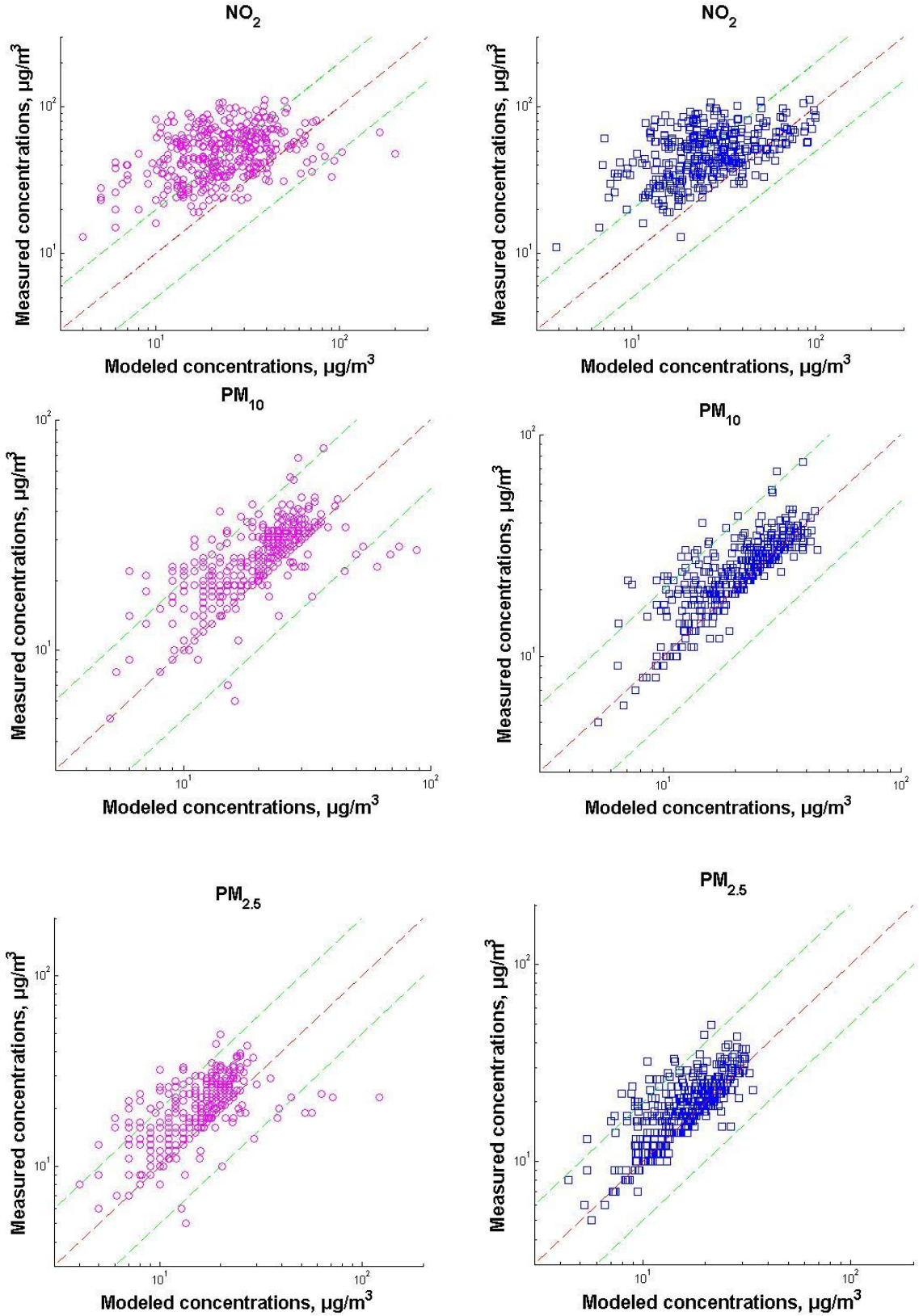

Figure 4.8. Comparison of concentrations of the standard model (pink, left side) and the model modified for calm conditions (blue, right side) with measured concentrations of NO_2, PM_{10}, and $PM_{2.5}$.

4.3. Statistical performance for NO_2, PM_{10}, and $PM_{2.5}$ concentrations for the standard model (Eq. 4.1) and the model modified for calm conditions (Eq. 4.5) as a function of wind direction: measurement site located downwind of the road (top) and upwind of the road (bottom).

	Number of samples	Average measured value (μg m^{-3})	Average modeled value (μg m^{-3})	Correlation coefficient	RMSE (μg m^{-3})	MNE	MNB	NME	MFE
Downwind of the road									
PM_{10} (Eq. 4.5)	42	21.7	17.4	0.74	6.6	0.18	-0.16	0.21	0.22
PM_{10} (Eq. 4.1)			31.2	0.43	24.7	0.58	0.44	0.59	0.37
$PM_{2.5}$ (Eq. 4.5)	42	17.3	14.3	0.70	5.4	0.19	-0.14	0.21	0.23
$PM_{2.5}$ (Eq. 4.1)			25.8	0.46	20.7	0.59	0.48	0.61	0.37
NO_2 (Eq. 4.5)	37	45.1	20.8	0.38	29.2	0.50	-0.50	0.54	0.72
NO_2 (Eq. 4.1)			55.6	0.27	38.5	0.51	0.27	0.53	0.39
Upwind of the road									
PM_{10} (Eq. 4.5)	352	25.6	22.2	0.77	6.8	0.16	-0.12	0.17	0.19
PM_{10} (Eq. 4.1)			20.2	0.73	8.2	0.20	-0.20	0.22	0.25
$PM_{2.5}$ (Eq. 4.5)	352	20.3	17.4	0.72	5.7	0.17	-0.12	0.19	0.20
$PM_{2.5}$ (Eq. 4.1)			15.6	0.68	7.0	0.21	-0.20	0.24	0.26
NO_2 (Eq. 4.5)	318	51.9	33.0	0.43	28.3	0.39	-0.34	0.42	0.54
NO_2 (Eq. 4.1)			23.7	0.41	33.8	0.52	-0.52	0.55	0.76

The performance of both models is poorer for the simulation of NO_2 concentrations. The standard model significantly underestimates the NO_2 concentrations with performance showing a correlation of 0.44 and a mean normalized error of 40-50%. Although performance is still poorer than those obtained for PM_{10} and $PM_{2.5}$, the modified model improves this performance.

The PM_{10}, $PM_{2.5}$, and NO_2 concentrations were also simulated at a fine temporal resolution (15 min) using the modified model. The average concentrations are similar to those of the 1 hr simulation for PM_{10} and $PM_{2.5}$ but the average NO_2 concentration decreases to 21.2 μg m^{-3} with this finer time resolution. The correlations for PM_{10}, $PM_{2.5}$, and NO_2 decrease to 0.71, 0.66, and 0.39, respectively. Therefore, a finer temporal resolution does not improve model performance as it becomes increasingly difficult to match the time series of the observed concentrations.

NO_2 concentrations near a freeway are strongly influenced by local NO_x traffic emissions because of the rapid chemical transformations of NO to NO_2, while the contribution of the background air is less important than it is for PM concentrations. Therefore, the results obtained for NO_2 are more representative of model performance than the results for PM_{10} and $PM_{2.5}$, which depend more strongly on background pollution. Our results indicate that pollutant dispersion near a roadway under calm conditions is difficult to simulate, although the option for light wind conditions improves performance significantly (for example, the correlation coefficient nearly doubles). However, it appears necessary to further improve the model formulation for these conditions.

Figure 4.9 illustrates for 15 species the ratio of the average concentration for the whole period near the freeway at the traffic site and the same concentration at the background site. The ratios are presented for the measured and simulated concentrations. The pollutants are presented from left to right in terms of decreasing measured ratio, i.e., the species concentrations impacted most by traffic are to the left.

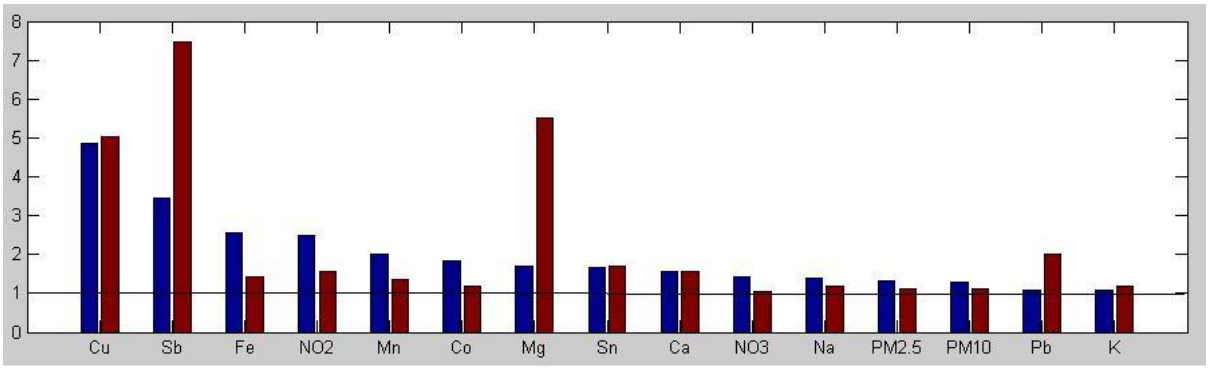

Figure 4.9. Ratio of the concentrations at the traffic and background sites: measured values (blue) and modeled values (red).

The measured and modeled concentrations of anions, cations, and metals averaged over the measurement period at the traffic site are presented in Table 4.4 along with the modified model performance statistics. Scatter plots are presented in Figure 4.10 for each pollutant. Cu and Sb show the greatest impact of traffic emissions and the lowest correlation (<11%) between measurement and simulation. The model overestimates the measured value, which may be due to inappropriate emission factors. Other pollutants that are overestimated are Mg^{2+} and Pb. Their non-exhaust emission factors are based on data obtained between 1983 and 2007. They are likely to overestimate current Pb emissions because of reductions in Pb non-exhaust emissions in recent years. For example, Hjortenkrans et al. (2007) showed that Pb emissions from brake linings in Stockholm, Sweden, were reduced from 560 kg/year in 1993 to 35 kg/year in 2005. Except for Co, the other pollutants show satisfactory correlation coefficients (greater than 69%) with the modified model. However, model performance is more meaningful for those species that include a significant traffic contribution (see Figure 4.9). The emission factors of Amato et al. were used here as generic emission factors. Better results would be obtained if the site-specific emission profile obtained by Polo (2013) for road dust were used, since that profile was derived from the traffic site measurements ; however, such a model performance evaluation would less meaningful because it would use as input the

same emission profile as seen in the observations. Better correlations are obtained with the model that considers calm conditions than with the standard model.

Table 4.4. Statistical performance for inorganic ions and trace metals for the model modified for calm conditions. The correlation is also presented for the standard model.

Pollutants / statistical criterion	Ca^{2+}	K^{+}	Na^{+}	NO_3^{-}	Mg^{2+}	Co	Cu	Fe	Mn	Pb	Sb	Sn
Average measured value (μgm^{-3})	420	74	85	565	17	0.26	49.6	1371	15.6	5.9	4.75	15.2
Average estimated value (μgm^{-3})	378	81.9	73.4	409	55.3	0.17	51.3	765	10.5	11.1	10.3	15.5
Correlation (Eq. 4.5)	0.78	0.84	0.69	0.8	0.05	0.57	0.11	0.93	0.82	0.36	0.1	0.97
Correlation (Eq. 4.1)	0.52	0.55	0.29	0.78	0.01	0.2	0.3	0.51	0.67	0.11	-0.3	0.68
RMSE (μgm^{-3})	167	19.7	34.3	235	64	0.1	49.5	881	8.7	7.8	10.5	6.34
MNE	0.44	0.2	0.22	0.26	2.58	0.38	0.87	0.4	0.4	1.25	1.75	0.55
MNB	-0.02	0.12	-0.1	-0.2	2.56	-0.3	0.43	-0.4	-0.3	1.24	1.57	0.19
NME	0.33	0.18	0.24	0.29	2.29	0.39	0.7	0.45	0.39	0.9	1.41	0.31
MFE	0.45	0.17	0.24	0.33	0.78	0.53	0.65	0.57	0.5	0.58	0.72	0.49

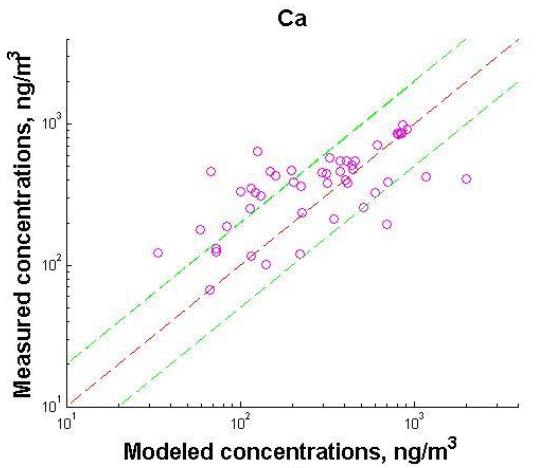
Ca
Measured concentrations, ng/m3
Modeled concentrations, ng/m3

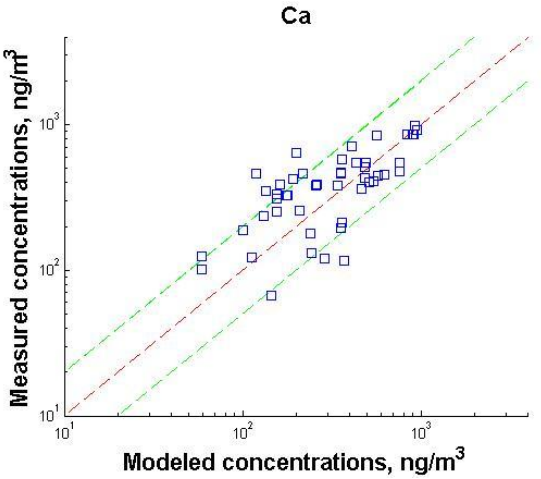
Ca
Measured concentrations, ng/m3
Modeled concentrations, ng/m3

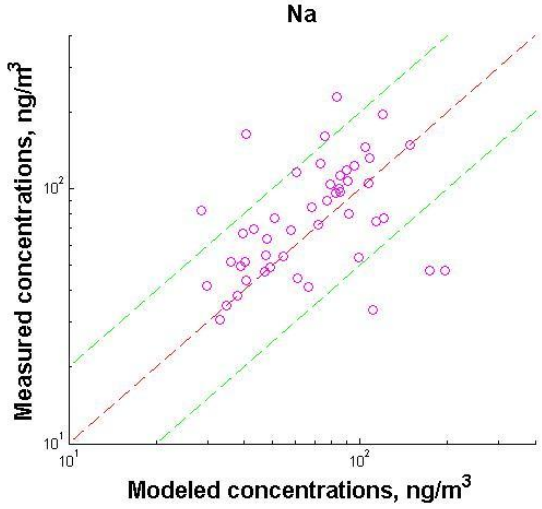
Na
Measured concentrations, ng/m3
Modeled concentrations, ng/m3

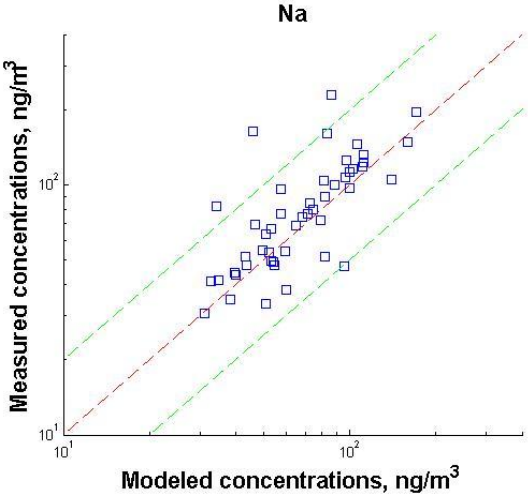
Na
Measured concentrations, ng/m3
Modeled concentrations, ng/m3

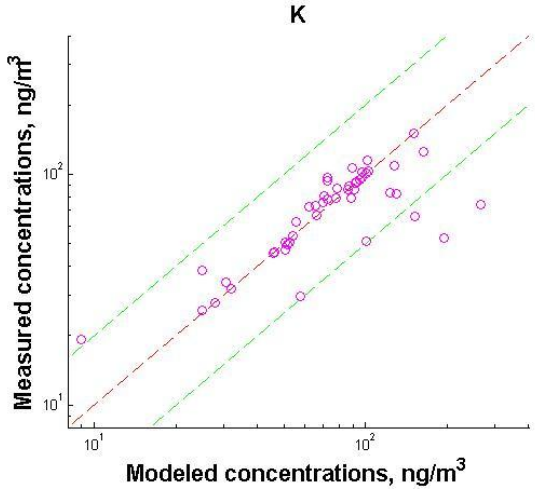
K
Measured concentrations, ng/m3
Modeled concentrations, ng/m3

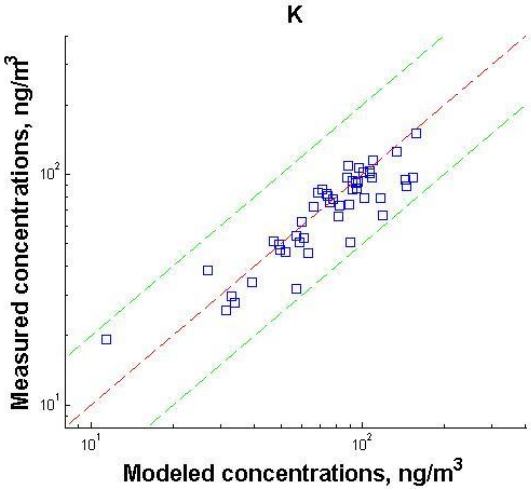
K
Measured concentrations, ng/m3
Modeled concentrations, ng/m3

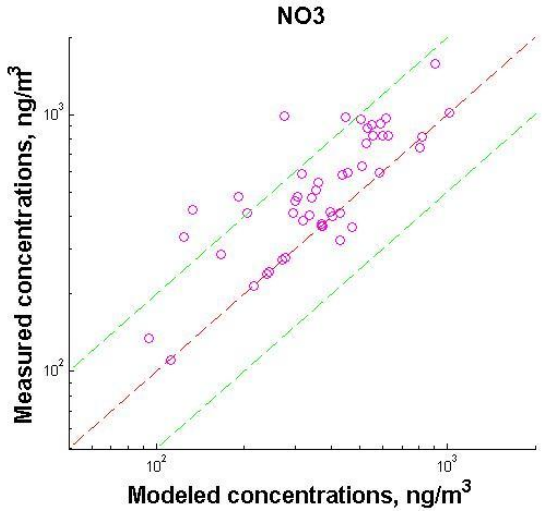
NO3
Measured concentrations, ng/m3
Modeled concentrations, ng/m3

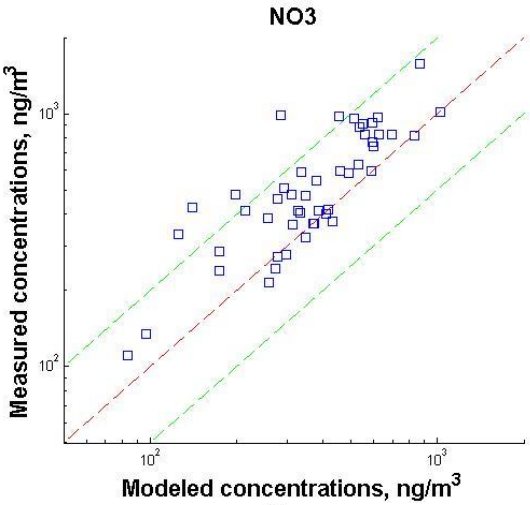
NO3
Measured concentrations, ng/m3
Modeled concentrations, ng/m3

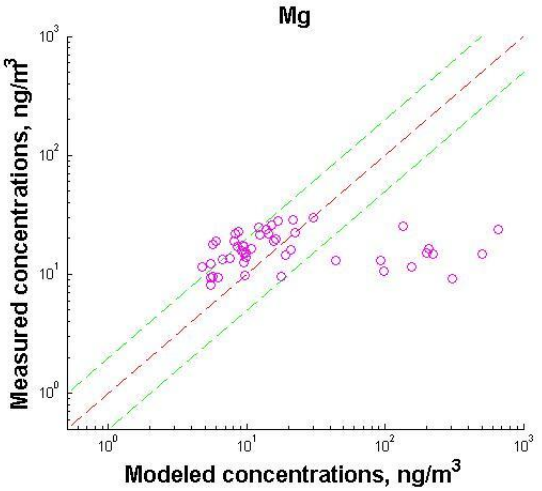
Mg
Measured concentrations, ng/m3
Modeled concentrations, ng/m3

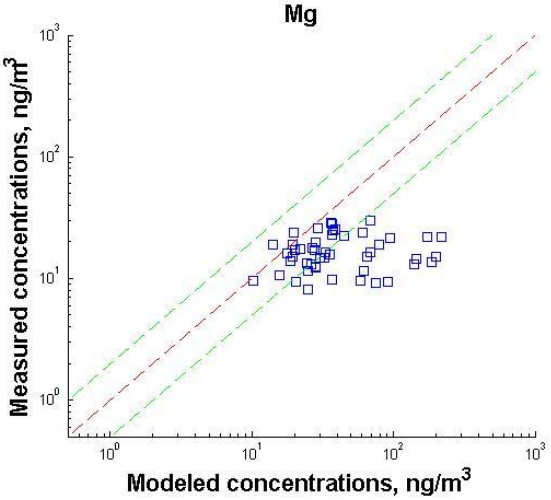
Mg
Measured concentrations, ng/m3
Modeled concentrations, ng/m3

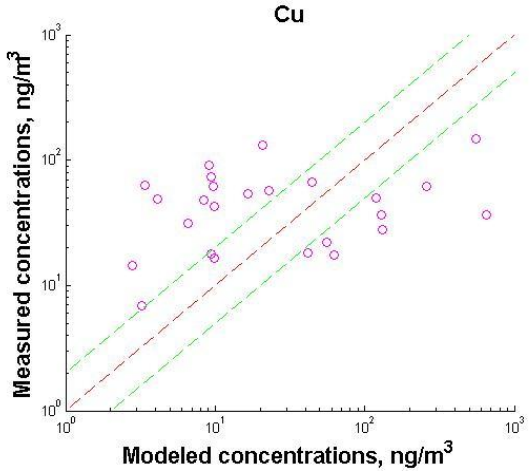
Cu
Measured concentrations, ng/m3
Modeled concentrations, ng/m3

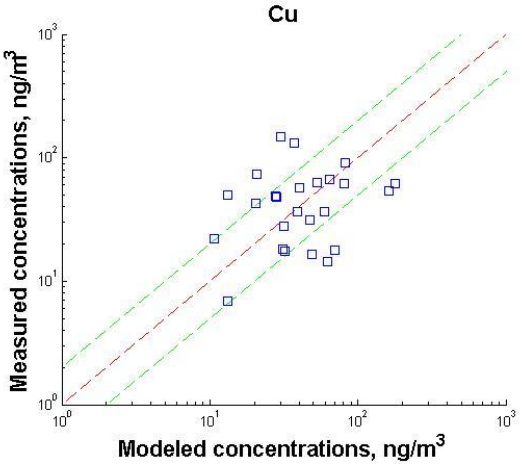
Cu
Measured concentrations, ng/m3
Modeled concentrations, ng/m3

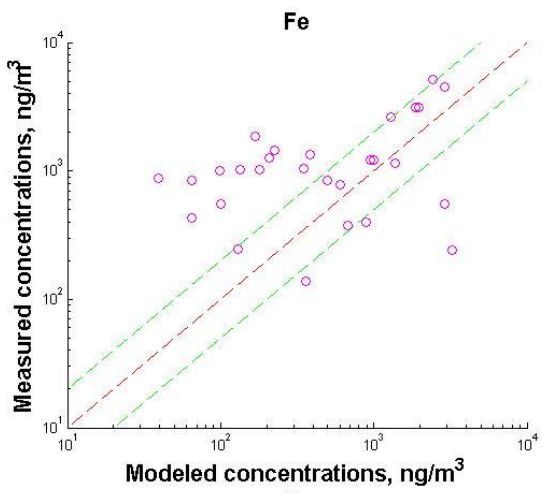
Fe
Measured concentrations, ng/m3
Modeled concentrations, ng/m3

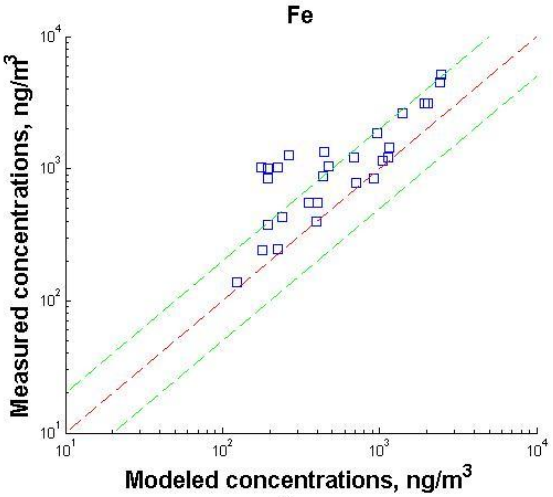
Fe
Measured concentrations, ng/m3
Modeled concentrations, ng/m3

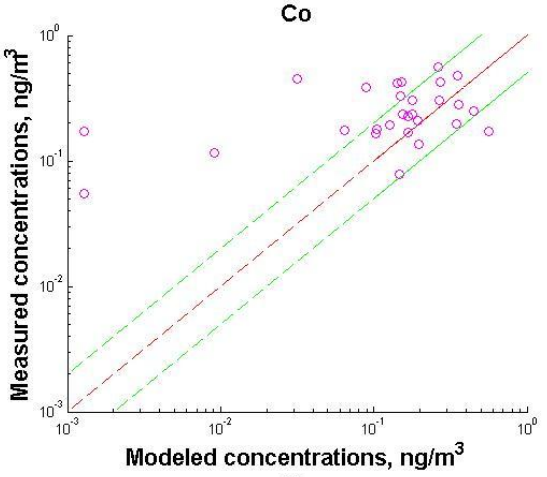
Co
Measured concentrations, ng/m3
Modeled concentrations, ng/m3

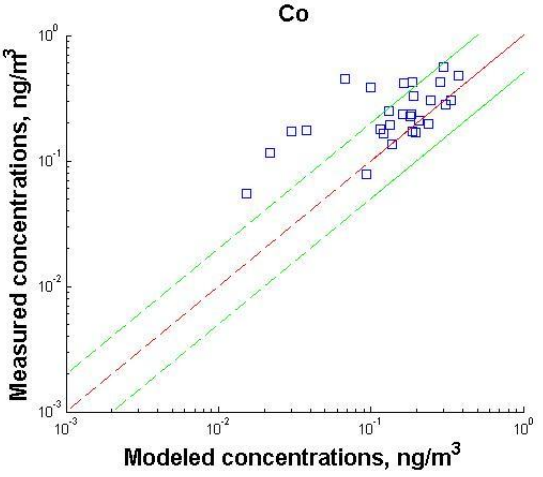
Co
Measured concentrations, ng/m3
Modeled concentrations, ng/m3

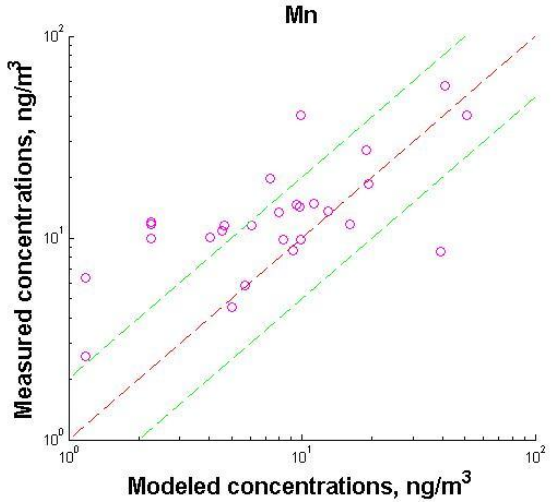
Mn
Measured concentrations, ng/m3
Modeled concentrations, ng/m3

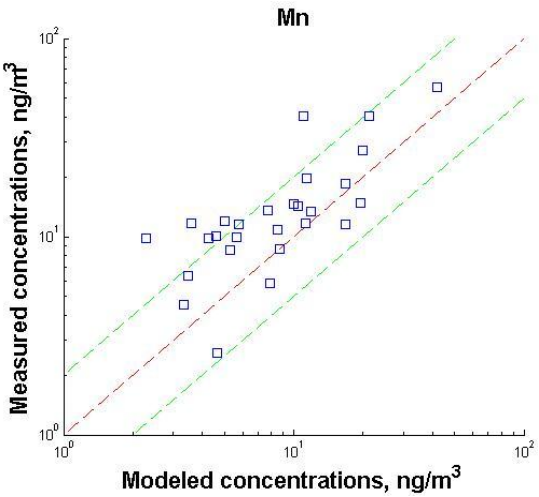
Mn
Measured concentrations, ng/m3
Modeled concentrations, ng/m3

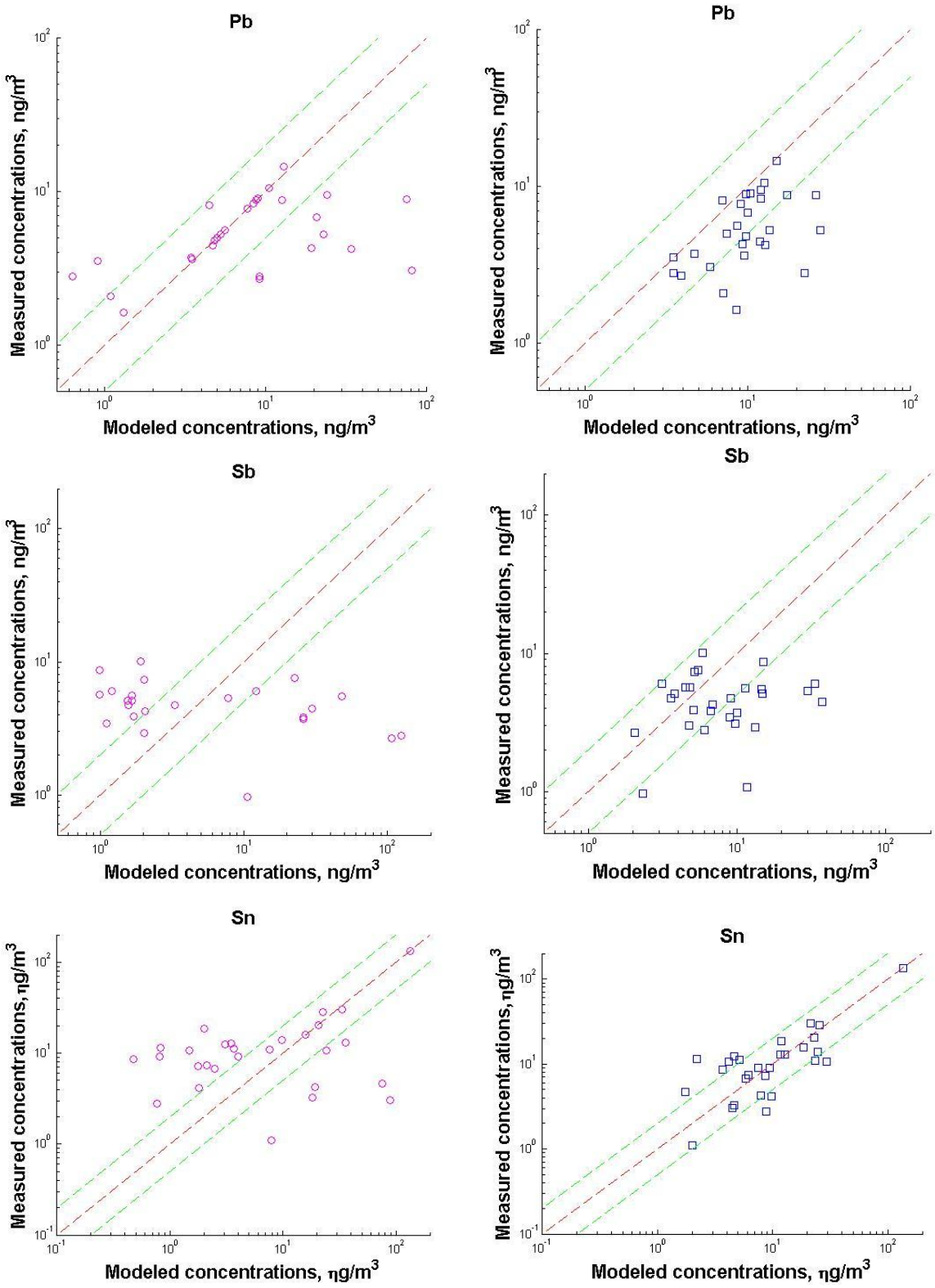

Figure 4.10. Comparison of concentrations modeled with the standard model (pink circles, left side) and with the modified model (blue squares, right side) with measured concentrations at the traffic site for inorganic ions and trace metals.

According to Chang and Hanna (2004), a "good" model would be expected to have about 50% of the predictions within a factor of two (fac2) of the observations, a relative mean bias (RMB) within ±30%, and a relative scatter (RS) of about a factor of two or three. These

values, which are provided in Table 4, confirm that the “modified model” can be considered as a "good" model for predictions of PM_{10}, $PM_{2.5}$, Na^+, NO_3^-, K^+, Ca^{2+}, Cu, and Sn concentrations. However, these criteria are not met for predictions of NO_2, Mg^{2+}, Co, Fe, Mn, Pb, and Sb.

Table 4.5. Performance indicators of the model modified for calm condition.

	PM_{10}	$PM_{2.5}$	NO_2	Ca^{2+}	K^+	Na^+	NO_3^-	Mg^{2+}	Co	Cu	Fe	Mn	Pb	Sb	Sn
RMB	-0,14	-0,15	-0,61	-0,1	0,1	-0,15	-0,32	1,06	-0,4	0,03	-0,6	-0,39	0,61	0,74	0,02
RS	0,85	0,85	0,48	0,84	1,1	0,89	0,73	2,53	0,58	1,02	0,53	0,66	1,88	1,82	0,97
fac2	0,95	0,94	0,45	0,75	1	0,92	0,9	0,42	0,71	0,56	0,68	0,74	0,57	0,54	0,64

The consideration of vehicle turbulence effects during stable atmospheric conditions may improve the model. Several studies have proposed modifications of the vertical dispersion coefficient as a function of vehicle-induced turbulence (VIT) (Eskridge and Rao, 1986; Kastener et al., 2000; Di Sabatino et al., 2003; Baumer et al., 2005). An empirical model (Kastner-Klein et al., 2000) was applied here to account for the effects of VIT based on the hourly velocity, density, frontal area and drag coefficients of the vehicles. This formulation did not lead to significant effect of VIT on pollutant dispersion and, therefore, on model performance. Parameterizations of VIT mostly affect the vertical dispersion of the air pollutants, but do not reflect the possible impact on horizontal transport under calm conditions. Further work appears warranted to improve VIT parameterizations under such challenging conditions. CFD modeling (e.g., Wang and Zhang, 2009) may provide useful insights in that regard.

4.5 Conclusion

In this study, we estimated the atmospheric dispersion of pollutant emitted by vehicles near a freeway under calm meteorological situations. To that end, an average-speed emission model was applied to estimate vehicle emissions with local traffic data. In addition, PM resuspension by traffic was included based on results of a site-specific PMF analysis. The concentrations of NO_2, PM_{10}, $PM_{2.5}$, Na^+, NO_3^-, K^+, Mg^{2+}, Ca^{2+}, Co, Cu, Fe, Mn, Pb, Sb and Sn were simulated and compared with observations at a receptor site located 7 m from the freeway. The standard Gaussian plume model was modified to account for calm conditions. In this modified formulation, the plume of pollutants from the freeway includes two terms: a classic Gaussian plume, which extends from the freeway downstream in the direction of the wind, and a plume extending in all directions close to the road. The results of the modified and standard models were compared to measurements and showed that the treatment of calm conditions improves the correlation coefficient significantly and reduces the errors. However, it appears necessary to further develop this formulation, a possible way being to better represent the effect of VIT on the horizontal transport of pollutants under such calm conditions. Another area for improvement is a better characterization of the various emission factors, for both direct and indirect (dust resuspension) sources.

Chapitre 5

5 Modélisation de l'impact du trafic sur la qualité des eaux de ruissellement urbaines

Ce chapitre est consacré à l'élaboration des données d'entrée nécessaires au modèle de qualité de l'eau et à la simulation de la propagation des polluants des eaux de ruissellement en milieu urbain. Les données essentielles sont les données météorologiques et les caractéristiques du bassin versant (en particulier l'occupation du sol) pour la simulation quantitative de l'eau, l'accumulation et le lessivage superficiel des polluants en vue de la modélisation de la qualité de l'eau. Dans ce chapitre, on présente trois méthodes différentes pour modéliser l'impact du trafic sur la qualité des eaux de ruissellement.

La première méthode utilise des données expérimentales de dépôts atmosphériques liés au trafic à proximité d'une route. Cette partie a été publiée dans des actes d'un congrès international : Fallah Shorshani M., Bonhomme C., Petrucci G., André M., Seigneur C. (2012) Road traffic impact on water quality in an urban catchment (Grigny, France), *9th International Joint IWA/IAHR Conference on Urban Drainage Modelling*, Belgrade, Serbie (Annexe C).

La deuxième méthode est basée sur l'utilisation d'un modèle « boîte » qui calcule les concentrations de polluants et les dépôts atmosphériques. Cette partie a été publiée dans une revue internationale avec comité de lecture : Petrucci G., Gromaire M. C., Fallah Shorshani M., Chebbo G. (2014). Non-point source pollution of urban stormwater runoff: a methodology for primary sources' analysis, *Environmental Science and Pollution Research*. doi:10.1007/s11356-014-2845-4 (available online) (Annexe D).

La troisième méthode crée une chaîne de modélisation complète qui inclut les modèles de trafic, d'émissions, de qualité de l'air et de qualité de l'eau. Cette chaîne de modélisation est évaluée avec des données expérimentales du bassin versant de Grigny en banlieue parisienne. Cette partie a été publiée dans une revue internationale avec comité de lecture : Fallah Shorshani M., Bonhomme C., Petrucci G., André M., Seigneur C. (2014). Road traffic impact on urban water quality: a step toward integrated traffic, air and stormwater modeling, *Environmental Science and Pollution Research*, Volume 21, Numéro 8, Pages 5297-5310.

5.1 Couplage basé sur les données expérimentales de dépôts atmosphériques

Cette étude estime l'effet de l'impact du trafic sur les eaux de ruissellement du bassin versant de Grigny en région parisienne, pendant les années 2009 et 2010. On ne réalise pas ici une chaîne de modélisation complète, car nous utilisons directement des données expérimentales de flux de dépôts de polluants atmosphérique (Promeyrat, 2001) au lieu de simuler ces dépôts atmosphériques. L'étude se concentre sur certaines contaminations des eaux de ruissellement induites par le trafic comme celles liées au cadmium (Cd), plomb (Pb) et zinc (Zn). Le bassin versant de Grigny est divisé en 20 sous-bassins versants. Chaque sous-bassin versant est supposé être constitué de quatre catégories de milieux (espaces verts ou végétalisés, toitures, routes, et autres surfaces) pour tenir compte de la variabilité d'occupation des sols. La situation géographique, la division du bassin versant et la rose des vents sont présentées en Figure 5.1.

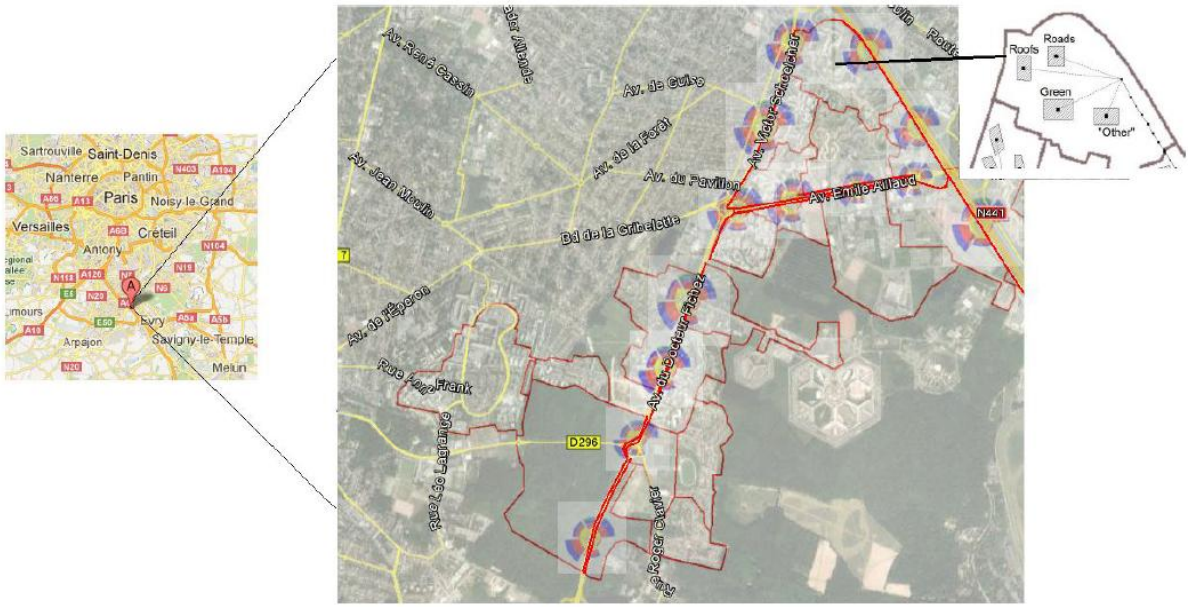

Figure 5.1. Situation géographique et détails du bassin versant de Grigny.

Le modèle utilisé pour la simulation de la quantité et de la qualité de l'eau est SWMM 5 (Rossman, 2010). La modélisation et la calibration de la quantité de l'eau ont été réalisées par Petrucci et al. (2013). Les simulations de la qualité de l'eau comprennent l'accumulation de polluants pendant les périodes sèches et leur lessivage au cours des événements de précipitation. Différentes approches mathématiques sont disponibles pour représenter les processus qui régissent l'accumulation de polluants et leur lessivage. Une approche exponentielle est utilisée ici pour l'accumulation. Dans cette équation, l'accumulation de polluants (masse par unité de surface) dépend du taux d'accumulation quotidien (masse par unité de surface et par jour), le nombre de jours secs antécédents (jours) et le coefficient

d'enlèvement (1/jour) qui est disponible dans la littérature scientifique selon le mode d'occupation de sol (Liu et al., 2010). Les taux d'accumulation quotidiens sont calculés selon le flux de dépôt de chaque source de polluant en fonction du niveau de trafic et de la direction du vent. Le dépôt de polluant suit une relation linéaire avec le volume de trafic (Brett et al., 2011). Le taux d'accumulation quotidienne peut donc être calculé selon le volume de trafic et en fonction de la rose des vents. D'après des travaux précédent sur les zones d'impact du trafic routier en bordure de route (Sabin et al., 2006 ; Loubet et al., 2010), les taux d'accumulation quotidienne pour chaque sous-bassin versant ont été calculés sur des zones impactées par la circulation routière qui s'étendent jusqu'à 240 m de la route. Chaque route impacte donc une fraction du sous-bassin versant en fonction de sa localisation par rapport au sous-bassin versant et selon la direction du vent. Les autres parties du sous-bassin versant sont supposées être impactées seulement par les dépôts de fond. Pour les zones en bordure de route (< 240 m), le flux de dépôt atmosphérique est calculé en utilisant ces données expérimentales de Promeyrat (2001), qui ont été obtenues sur un autre site et qui sont donc pondérées par le rapport des débits de trafic estimés pour ces différentes sites. La charge de lessivage des polluants est proportionnelle à une fonction du débit d'eau (mm/h) qui dépend d'un coefficient d'ajustement, au coefficient de lessivage et à l'accumulation de polluants. La simulation de la qualité de l'eau peut alors être réalisée à l'aide de ces paramètres et de données d'entrée par le modèle SWMM. Une analyse de sensibilité pour tous les coefficients du modèle d'accumulation et de lessivage a aussi été effectuée.

La comparaison des deux cas avec et sans trafic local confirme un effet significatif de la circulation automobile sur la contamination de l'eau. Les concentrations maximales de Cd, Pb, et Zn à l'exutoire sont respectivement 2,12; 284,6; et 1758 µg L^{-1} (Figure 5.2.a). Ces valeurs pour le cas sans trafic (impacté seulement par les dépôts de fond) sont respectivement 0,78 µg-Cd-L^{-1}, 47,72 µg-Pb-L^{-1}, et 835,17 µg-Zn-L^{-1} (Figure 5.2.b). Les concentrations moyennes dues au trafic et à la concentration de fond sur une période de deux ans (2009-2010) sont 0,08 µg-Cd-L^{-1}, 6,33 µg-Pb-L^{-1}, et 79 µg-Zn-L^{-1}. Dans le cas où on ne prend pas explicitement en compte l'impact du trafic, ces valeurs sont 0,06 µg-Cd-L^{-1}, 4,01 µg-Pb-L^{-1}, et 70 µg-Zn-L^{-1}. Compte-tenu de l'incertitude des paramètres du modèle, ces résultats sont réalistes et comparables aux mesures effectuées par Sabin et al. (2005) à Los Angeles, qui donnent des concentrations annuelles mesurées moyennes (± écarts-types) de 160 ± 130 µg-Zn-L^{-1} et 12 ± 10 µg-Pb-L^{-1}.

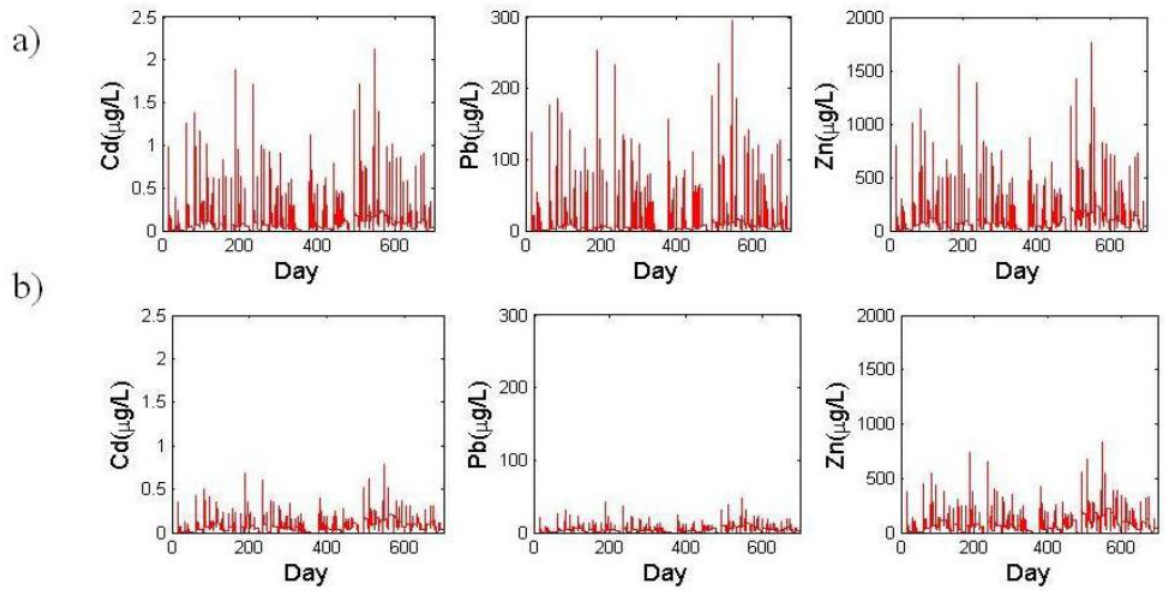

Figure 5.2. Concentrations de métaux lourds (mg / L) à l'exutoire du bassin versant de Grigny : a) avec prise en compte du trafic local et b) dues seulement aux dépôts de fond moyens en zone urbaine.

Les concentrations de zinc au moment de pics de pollution dans différents sous-bassins versants sont illustrées en Figure 5.3. Les zones les plus polluées (> 800 µg-Zn-L^{-1}) sont les sous-bassins versants imperméables près de l'autoroute très fréquentée et les sous-bassins versants influencés par les deux routes principales. Les zones les moins polluées contiennent des sous-bassins versants situés loin des routes et les grands sous-bassins versants ayant une faible fraction de la surface impactée par le trafic.

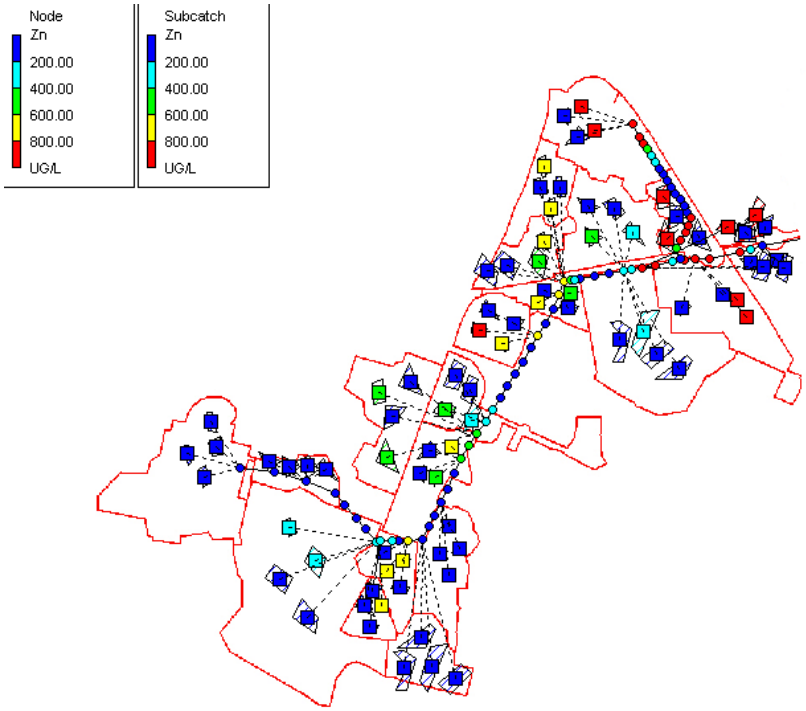

Figure 5.3. Répartition spatiale de la concentration de zinc (µg/L) issue des dépôts atmosphériques au pic de pollution, 06h30, 07/03/2010.

Ces résultats montrent que les concentrations de polluants dans les eaux de ruissellement peuvent être trois fois plus élevées pour certaines zones géographiques si on utilise une description explicite du trafic. Par conséquent, une connaissance exhaustive de la répartition spatiale des routes avec un volume important de trafic est importante pour prévoir correctement la qualité de l'eau dans les zones modélisées.

5.2 Estimation des dépôts atmosphériques à l'aide d'un modèle boîte

La méthode précédente a utilisé des données expérimentales de dépôts atmosphériques pour estimer l'accumulation des polluants sur les bassins versants. Ici, les dépôts atmosphériques sont calculés avec un modèle boîte. Les résultats sont également évalués avec des mesures effectuées sur un bassin versant en région parisienne (Sucy-en-Brie). Cette approche suppose que les concentrations atmosphériques et les dépôts sont spatialement uniformes sur le domaine de l'étude. Celui-ci est défini comme un volume parallélépipédique couvrant le bassin versant. La hauteur de la boîte s'étend en altitude jusqu'à 1000 m de la surface pendant la journée et est limitée à 50 m pendant la nuit à cause de la stabilité atmosphérique qui réduit le mélange vertical dans la couche limite atmosphérique. Ce modèle suppose également que la dynamique de l'écoulement est dominée par l'advection plutôt que par la convection (Bénarie, 1967). Les concentrations et le flux de dépôt peuvent être calculés pour chaque pas de temps (1 h) par les équations suivantes:

$$C = \frac{E}{\sqrt{LW}\,hu} \tag{5.1}$$

$$F_d = V_d.C \tag{5.2}$$

où C est la concentration (g/m^3), E est l'émission (g/s), L et W sont la longueur et la largeur (m) du bassin versant, h est la hauteur (m) de la couche de mélange, u est la vitesse du vent (m/s), F_d est le flux de dépôt, et V_d est la vitesse de dépôt, définie en fonction des conditions météorologiques et de la taille des particules. On suppose que la distribution en taille des PM_{10} inclut 74% de particules de diamètre inférieur à 1 µm, 10% de particules entre 1 et 2,5 µm, et 16% de particules avec un diamètre entre 2,5 et 10 µm. Les vitesses de dépôt des particules dans ces trois gammes de taille pour une vitesse de vent moyenne de 5 m/s sont respectivement de 0,2, 0,4 et 4 cm/s, selon Roustan (2005).

Les données d'entrée nécessaires au modèle sont les concentrations de fond des polluants, les données météorologiques, et les émissions provenant du trafic et du chauffage domestique. Les concentrations de fond ont été obtenues à partir de mesures effectuées dans la région parisienne (Ayrault et al., 2010; INERIS, 2000). Les valeurs des concentrations de fond sont 18,4, 6,3, 45,8, et 1,61 ng/m^3 pour Cu, Pb, Zn et HAP, respectivement. Ces concentrations de fond sont spatialement uniformes sur le domaine de l'étude et constantes dans le temps. Les données météorologiques sont basées sur des observations à la station la plus proche (aéroport

d'Orly, à 10 km du bassin versant). L'utilisation de ces données est appropriée dans ce cas, en raison d'un terrain relativement plat.

Les émissions des véhicules sont estimées à partir de données de trafic et de facteurs d'émission. Les facteurs d'émission des métaux lourds sont définis d'après les résultats expérimentaux de Sternbeck et al. (2002). Pour les HAP, nous avons utilisé le modèle CopCETE (voir plus haut). Les émissions de chauffage domestique ont été estimées par Petrucci et al. (2014).

Le modèle calcule le dépôt annuel moyen par hectare. Les résultats ont été comparés avec les dépôts moyens atmosphériques mesurés sur le bassin versant, qui comprennent huit mesures effectuées entre 2011 et 2013 par Gasperi et al. (2013), ainsi qu'une estimation des dépôts dans un bassin versant voisin (Créteil) en 2001/2002 (Azimi et al., 2003, 2005). Pour les trois métaux, et en particulier Pb, les données de Créteil sont plus élevées que les mesures effectuées à Sucy-en-Brie et que les résultats de la modélisation. Ceci est probablement dû à la densité plus élevée, au trafic et à l'industrialisation du bassin versant de Créteil par rapport au bassin versant de Sucy-en-Brie, et aussi à la réduction progressive des émissions dans la dernière décennie à cause des réglementations. Par exemple, les émissions de Pb ont fortement diminué à cause de l'élimination de ce métal des essences et de ses usages actuellement plus limités dans les pièces des véhicules. Le modèle utilise les facteurs émission qui surestiment probablement les émissions actuelles de Pb et donne donc des résultats plus élevés que les valeurs mesurés sur le bassin versant. Les résultats des autres métaux sont assez satisfaisants par rapport aux mesures. En revanche, le modèle surestime les HAP. Le bon accord entre les données de Créteil et les mesures de Sucy-en-Brie suggère que les résultats de la modélisation ne sont pas fiables pour les HAP.

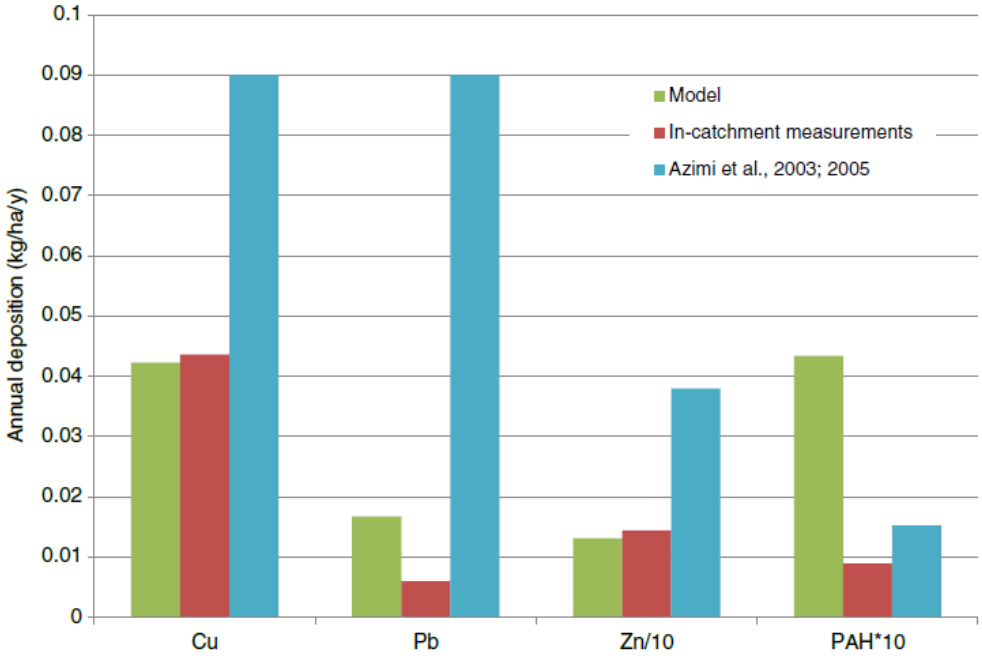

Figure 5.4. Les estimations des dépôts atmosphériques annuels sur le bassin versant de Sucy-en-Brie (Petrucci et al., 2014).

Ce modèle boîte est relativement simple et n'est donc pas capable de décrire précisément les processus de dispersion et de dépôt des métaux lourds et des HAP. Il est cependant utile pour fournir des estimations moyennes sur une période assez longue.

5.3 Chaîne de modélisation

Cette partie est consacrée au développement d'une chaîne de modélisation complète avec couplages des modèles de trafic, d'émission de polluants, de dispersion et de dépôts atmosphérique, et de contamination des eaux de ruissellement. Cette étude se concentre sur la mise en œuvre d'une chaîne de modélisation sur un bassin versant suburbain (Grigny) en région parisienne pendant la période du 2 avril au 3 mai 2012. Les polluants des eaux de ruissellement étudiés sont le cadmium (Cd), le plomb (Pb) et le zinc (Zn). Ces métaux peuvent être émis par le trafic routier.

Les volumes horaires de trafic sont déterminés à partir de comptage sur l'autoroute et une modélisation par modèle statique de VISUM pour les routes nationales. La circulation locale sur la zone résidentielle a été traitée comme une source spatialement uniforme dans le bassin versant en utilisant le nombre de véhicules immatriculés et le nombre de travailleurs qui vivent dans le domaine d'étude. Avec des données horaires de trafic, les émissions à l'échappement de ces trois métaux lourds ont été estimées par le modèle basé sur la vitesse moyenne (CopCETE). Les émissions non-échappement ont été calculées avec la méthode de COPERT4 pour l'usure des pneus et des freins. En revanche, l'usure de la chaussée n'a pas été prise en compte en raison d'un manque de données. Une grande partie de ces émissions est constituée de particules grossières qui ne restent pas longtemps dans l'air en raison de leurs sédimentations, mais celles-ci sont une source importante de contaminations des eaux de ruissellement. La contribution de l'usure des chaussées est particulièrement importante quand on s'intéresse à la contamination des eaux en HAP, mais elle est moindre pour l'étude des métaux. Par conséquent, les émissions de particules supérieures à 10 µm de diamètre aérodynamique doivent être prises en compte dans les inventaires d'émission. La dispersion atmosphérique des polluants a été calculée avec le modèle de dispersion Gaussien pour les sources linéiques de la plateforme de modélisation Polyphemus (Briant et al., 2011, 2013). Le modèle Polyphemus utilise une nouvelle approche pour réduire l'erreur de calcul lorsque la direction du vent n'est pas perpendiculaire à la route. Les concentrations des polluants dues à l'autoroute et aux routes nationales sont calculées sur des grilles rectangulaires constituées de récepteurs espacés de 50 m et spécifiques à chaque sous-bassin versant. La contribution de la circulation sur les rues résidentielles a été simulée en utilisant une approche de modèle boîte (voir ci-dessus), en supposant une dispersion atmosphérique uniforme des polluants sur le bassin versant. Le dépôt sec à chaque point récepteur a été estimé en fonction de la concentration du polluant et de sa vitesse de dépôt. En revanche, le dépôt humide est considéré spatialement homogène sur le bassin versant.

La simulation de la qualité de l'eau nécessite une simulation de la quantité d'eau parce que les concentrations de polluants dépendent du flux d'écoulement simulé. Le modèle utilisé pour effectuer l'analyse des eaux de ruissellement est SWMM 5 (Rossman 2010). La modélisation

de la quantité d'eau pour le bassin versant de Grigny est réalisée en utilisant des données topographiques et des données sur l'occupation des sols. Elle est complétée par une calibration avec un algorithme génétique (Petrucci et al., 2013). Les simulations de qualité de l'eau comprennent l'accumulation de polluants pendant les périodes sèches et leur lessivage lors des événements pluvieux. Dans cette étude, l'accumulation est obtenue à partir de dépôts atmosphériques calculés avec les modèles de dispersion et de dépôts atmosphériques. Le lessivage peut ensuite être déterminé en fonction de l'accumulation des polluants, de l'intensité de la pluie et de paramétrisations (voir plus haut) qui dépendent de l'occupation des sols.

Dans ce cadre, trois simulations ont été réalisées : (1) une simulation du modèle Gaussien, avec toutes les sources d'émissions (trafic local et concentrations de fond), (2) une simulation sans aucune émission du trafic local, avec seulement les concentrations de fond, (3) une simulation du modèle boîte (voir partie précédente) avec toutes les émissions du trafic local et les concentrations de fond.

La comparaison entre la simulation avec le modèle Gaussien et les mesures expérimentales montrent que pour les taux moyens de débits massiques la valeur simulée représente 77% de la valeur mesurée pour Zn, 100% pour Cd et 211% pour Pb, ce qui démontre un impact significatif des polluants atmosphériques sur la qualité de l'eau. Le Zn provient de la corrosion des matériaux de construction, ce qui peut expliquer le fait que les concentrations simulée sont plus faibles que les concentrations mesurées car cette source n'est pas prise en compte dans le modèle. On a utilisé les facteurs émission de COPERT référencés entre 1983 et 2005 mais, actuellement, l'essence ne comporte plus de Pb en Europe et les émissions de Pb « non-échappement » ont aussi été réduites. Les résultats simulés de Pb surestiment donc fortement les mesures. Cependant, le Pb reste encore une source importante de contamination de l'eau (Gromaire et al. 2011).

La comparaison des simulations 1 (avec trafic local) et 2 (sans trafic local) montre que l'effet maximum de la concentration de fond de polluants est inférieur à 10%. La contribution du trafic local est donc dominante parce que (1) les émissions du trafic sont à proximité du sol et, par conséquent, disponibles pour le dépôt sec et (2) la présence de particules d'un diamètre supérieur à 10 µm de l'usure des équipements du véhicule (c'est-à-dire des particules avec de grandes vitesses de dépôt) produit des dépôts secs importants à proximité des routes.

Le rapport des résultats de la simulation 3 (émissions moyennées spatialement) sur ceux de la simulation 1 (émissions du trafic distribuées spatialement) montre des écarts des taux moyens des débits massiques calculés par les modèles en moyenne pour tous les événements de pluie de 24% pour Zn, 41% pour Cd et 34% pour Pb. Cela signifie qu'un modèle boîte réduit l'impact des sources de trafic local sur les concentrations des contaminations des eaux à l'exutoire du bassin versant de manière significative à cause d'une dilution exagérée des émissions du trafic dans la couche de mélange atmosphérique. Par conséquent, les différences entre les concentrations de métaux émis par le trafic obtenues avec ces deux simulations montrent qu'il est essentiel d'avoir une représentation spatiale correcte des sources d'émissions locales.

Abstract

Methods for simulating air pollution due to road traffic and the associated effects on stormwater runoff quality in an urban environment are examined with particular emphasis on the integration of the various simulation models into a consistent modelling chain. To that end, the models for traffic, pollutant emissions, atmospheric dispersion and deposition, and stormwater contamination are reviewed. The present study focuses on the implementation of a modelling chain for an actual urban case study, which is the contamination of water runoff by cadmium (Cd), lead (Pb), and zinc (Zn) in the Grigny urban catchment near Paris, France. First, traffic emissions are calculated with traffic inputs using the COPERT4 methodology. Next, the atmospheric dispersion of pollutants is simulated with the Polyphemus line source model and pollutant deposition fluxes in different subcatchment areas are calculated. Finally, the SWMM water quantity and quality model is used to estimate the concentrations of pollutants in stormwater runoff. The simulation results are compared to mass flow rates and concentrations of Cd, Pb, and Zn measured at the catchment outlet. The contribution of local traffic to stormwater contamination is estimated to be significant for Pb and, to a lesser extent, for Zn and Cd; however, Pb is most likely overestimated due to outdated emissions factors. The results demonstrate the importance of treating distributed traffic emissions from major roadways explicitly since the impact of these sources on concentrations in the catchment outlet is underestimated when those traffic emissions are spatially averaged over the catchment area.

5.3.1 Introduction

Traffic is a major source of pollution in cities and near highways. Therefore, it is essential to assess the impact of road traffic on air and stormwater pollution. To that end, numerical modelling is needed to estimate the contribution of on-road vehicles to pollutant concentrations in air and water and to provide the basis for the design of efficient emission reduction strategies. Models have been developed to address the various components of this environmental system: traffic, emissions, atmospheric pollution, and stormwater pollution. Current traffic models can predict the position and kinematic parameters of the vehicles with various levels of detail. Emission models can estimate the amount of different pollutants emitted by vehicles, albeit with some uncertainty (Smit et al., 2010). The dispersion of pollutants in the atmosphere can be simulated using atmospheric dispersion models available for application at a variety of spatial scales and with different levels of detail (Holmes et al. 2006; Zannetti 1990; Sportisse 2009). A fraction of the air pollutants deposits to surfaces by dry and wet processes. These pollutants may then be entrained by the water runoff during rainfall events, which can be simulated by hydrologic models. If models have been developed, applied and, to some extent, evaluated for each of those components, the integration of all those components to simulate the impact of road traffic on air and water pollution has been very limited to date.

Some modelling systems linking traffic flow, emissions of air pollutants and air quality modelling tools have been developed (e.g., Lim et al. 2005; Schmidt and Schäfer 1998; Hatzopoulou 2010). Although a large amount of work has been conducted to link atmospheric pollution to surface water contamination at regional and global scales for environmental

issues such as acid deposition, mercury contamination and nutrients inputs causing eutrophization of water bodies, little attention has been paid to linking air and water pollution in urban areas. Since similar pollutants (e.g., polycyclic aromatic hydrocarbons (PAHs), metals) are regulated for air and water quality, it seems essential to treat air and water contamination jointly when addressing the environmental impacts of major sources of those pollutants. For example, it has been estimated that 57-100% of the trace metal load on urban surfaces is impacted by atmospheric deposition in the Los Angeles basin (Sabin et al., 2005). Traffic exhaust emissions are a major source of atmospheric pollution in urban areas, and in addition, tyre, brake, and road wear lead to the release of particulate pollutants, which are transported by stormwater runoff (Ken, 2013). To date, the link between traffic emissions, atmospheric deposition and the contamination of water runoff in urban areas has not been treated yet in a comprehensive manner.

In this work, we address a new area in the field of urban modelling by developing a new modelling method that integrates different models simulating traffic, emissions, air pollution and stormwater pollution in order to predict the level of contamination of surface waters at the scale of an urban district. The existing methods for modelling each component are presented first and the levels of detail needed for specific applications are briefly discussed. Interfaces are developed here for pollutant emissions due to on-road traffic, mass transfer between the atmosphere and surfaces, and mass transfer of deposited pollutants to stormwater runoff. This method is evaluated for the Grigny catchment near Paris, France, by a comparison of model simulations with measurements of metal concentrations at the catchment outlet. The contribution of local traffic emissions to those metal concentrations is estimated and compared to background deposition. Furthermore, the sensitivity of the modelling results to the treatment of traffic in the modelling chain (spatially-distributed versus spatially-averaged) is investigated.

5.3.2 Overview of models

The different types of models typically used are summarized below for each component (traffic, emissions, air quality and water quality).

5.3.2.1 Traffic models

Three major classes of traffic models can be identified in order of increasing complexity:

1. Static models rely on population data and predict average traffic volumes in different areas of a road network. They give vehicle fluxes on each link of the road network. These models are highly simplified, but are useful to describe the road traffic (flow and speed) over large spatial scales, such as an entire metropolitan area.

2. Aggregated dynamic models provide an explicit representation of traffic congestion by describing the temporal evolution of traffic states over a simplified network (via spatial aggregation). A typical application is the evaluation of the level of congestion, which can be used to manage traffic flow.

3. Dynamic models describe the temporal variations of traffic conditions in order to determine the positions and kinematic parameters of vehicles in a road network. Dynamic models can be classified into two main categories according to different aspects of traffic

flow operations. The macroscopic models use an aggregate representation of vehicles and continuous traffic flow; they are characterized by variables such as traffic flow and vehicle density. The microscopic models consider the time-space behaviour of individual drivers in relationship with the presence of vehicles in their proximity.

5.3.2.2 *Emission models*

The usual approaches for estimating the emissions associated with road traffic can be classified according to the input data, the scale of the study, and the type of pollutants being considered. These approaches can be distinguished in order of increasing complexity as follows:

1. Models relying on fuel sale data
2. Models relying on annual average traffic volumes per vehicle categories
3. Models relying on average speed of traffic
4. Models relying on traffic situations
5. Models relying on traffic-related variables
6. Models providing emissions from various driving cycle variables
7. Models relying on speed chronology, also known as instantaneous emission models

Models of categories 1 and 2 can be used for large-scale emission inventories (e.g., national level inventories). Models of categories 3 and 4 provide more accurate information and cover the major emission processes and most pollutants from a single road up to an entire city. Models of category 5 require traffic flow variables for each road and category 6 is defined by individual vehicle movement data. These two categories of models are restricted to specific conditions and a limited number of pollutants. Models of category 7 represent explicitly the vehicle emission behaviour by relating emission rates to vehicle operation (engine power, speed, and acceleration) during a series of short time steps. They only address a limited number of pollutants (typically regulated gaseous pollutants) from vehicle exhaust.

5.3.2.3 *Air pollution models*

Air pollution models (also referred to as air quality models or atmospheric chemical-transport models) calculate atmospheric pollutant concentrations from inputs (emissions, meteorology, terrain, initial and boundary conditions) and mathematical representations of the physico-chemical processes governing the temporal evolution and spatial distribution of the pollutant concentrations. The different approaches available are the following (Zannetti, 1990; Jacobson, 2005; Seinfeld and Pandis, 2006; Sportisse, 2009):

1. Eulerian models: These models can handle all emission sources over domains ranging from an urban area to the entire globe. Eulerian models consider a three-dimensional (3D) array of volume elements, each of homogeneous properties for the variables of interest (e.g., air pollutant concentrations, meteorological variables) and calculate the flow of those variables among those volume elements. All atmospheric processes can be modeled in Eulerian models (emissions, transport, transformations, and deposition). The outputs consist of the values of the variables (e.g., concentrations, deposition fluxes) as a function of time and location.

2. Lagrangian trajectory models: In a Lagrangian trajectory model, air masses are advected and pollutants are dispersed along mean wind trajectories. They are computationally less demanding than Eulerian models, but, unlike Eulerian models, Lagrangian models are typically limited to the simulation of a few sources.

3. Plume-in-grid models: A plume-in-grid model combines the advantages of Eulerian models (large domain and multiple sources) and Lagrangian models (fine resolution near the sources); these models simulate selected sources using a Lagrangian model imbedded within the 3D Eulerian model and all other sources are treated by the Eulerian model.

4. Gaussian dispersion models: Gaussian dispersion models are widely used to calculate pollutant concentrations downwind from a few selected sources in the absence of major obstacles to atmospheric transport. Stationary atmospheric conditions are assumed in the Gaussian plume dispersion formulation and, as a result, the impact of a source can be represented by a Gaussian plume model only over limited distances from the source (at most 50 km). When atmospheric conditions are variable, the atmospheric plume may be approximated by releasing distinct puffs from the source at successive intervals of time; the puffs may then follow different air mass trajectories.

5. Street-canyon models: For situations where the atmospheric dispersion of pollutants is constrained by obstacles such as buildings, street-canyon models must be used; they use parameterizations to approximate the effect of those obstacles on the atmospheric flow and pollutant dispersion.

6. CFD (Computational Fluid Dynamics) models: CFD models provide detailed representations of the atmospheric flow and some also treat the physics and chemistry of air pollutant transformations. However, they are limited to local applications such as the impact of a single pollution source in complex terrain or in a built environment, where the flow characteristics are complex. These models provide accurate representations of the atmospheric flow but are computationally demanding.

The selection of an air quality model for a specific application depends mostly on the spatial scale and source types being considered. The concentrations of air pollutants can be simulated over large domains, ranging from urban to global scales, by Eulerian and Lagrangian models. At local scales, Gaussian dispersion models, street-canyon models or CFD models are typically used. Plume-in-grid models can cover all spatial scales.

5.3.2.4 Stormwater models

The models of urban hydrology may be classified in terms of their functionality, accessibility, water quantity and quality components included in the model and their temporal and spatial scales (Zoppou, 2001; Elliot et al., 2007). In terms of spatial distribution, hydrological models may be categorized as follows:

1. Lumped: A lumped model is based on spatial averaging of the input parameters over the catchment. Therefore, these models provide only outputs at the outlet of the catchment without an explicit consideration of spatial variability.
2. Semi-distributed: Semi-distributed models take into account the variability of land use and inflow into the drainage network by dividing a catchment into several

subcatchments. Therefore, the spatial resolution is related to the size and number of subcatchments.

3. Fully-distributed: A fully-distributed model represents the surface water flow by using physical laws over a gridded domain. They include spatial and temporal variability (such as soil properties, land use, etc.) according to the grid size.

5.3.3 Model Integration

The main building blocks of a modelling chain of the environmental impacts of road traffic are (1) the overall structure of the modelling chain, which should include traffic, emissions, air pollution, and water quality models (Figure 5.5) and (2) the interfaces linking the output from a model to the input of the next model. The selection of the models and these integrations are briefly discussed below.

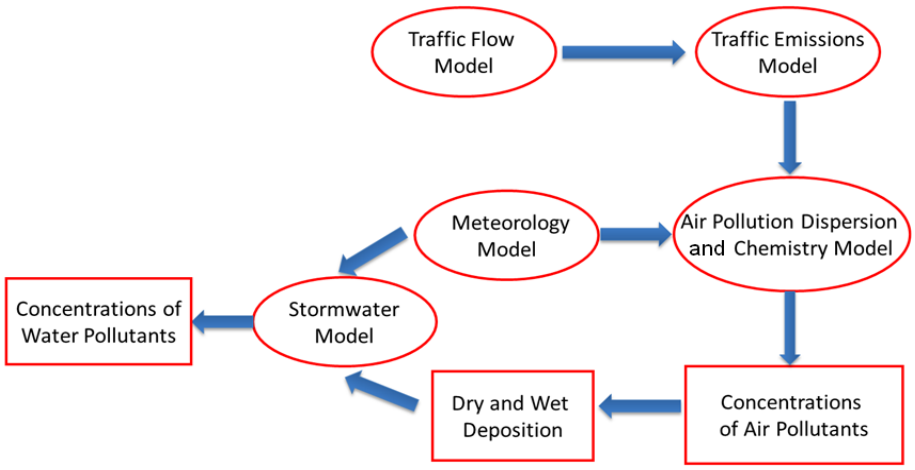

Figure 5.5. Schematic representation of the modelling chain (components are represented with ellipses) with expected input and output data (represented with boxes).

The selection of the models must be conducted in such a way that there is consistency among the level of detail, spatial and temporal resolutions, and input requirements of the various models of the modelling chain. The use of a dynamic traffic model will be of little use if the emission model is based on average vehicle speed. Similarly, an air quality model with a 50 km horizontal grid size will be inappropriate to investigate the impacts of local sources on an urban catchment. Once models that are internally consistent have been selected, the development of their interfaces will be mostly straightforward, because the inputs and outputs of the models should be compatible. There may, however, be some need for adapting the transfer of variables from one model to the next, because the original use intended for a model may differ from that considered in the modelling chain. For example, a traffic model designed to investigate congestion scenarios will differentiate among heavy-duty vehicles, light-duty vehicles, and passenger vehicles. Its use for an environmental impact study will require additional information on the types of vehicles present in each category, for example, diesel versus spark-ignition vehicles, as well as the vehicle original year (which defines the associated emission control characteristics and, therefore, pollutant emission rates).

In the case study presented below, we investigate the contribution of local road traffic to the contamination of stormwater runoff in an urban catchment. Since we are interested in the impact of traffic on major roads with relatively smooth traffic conditions, a static traffic model (category 1 in section 5.3.2.1) may be sufficient, because the impact of acceleration and deceleration on pollutant emissions may not be as critical as it would be, for example, at a major intersection. Then, an emission model based on vehicle speed would be appropriate (category 3 in section 5.3.2.2). Because we are focussing on the impacts of local traffic, it is important to resolve the atmospheric concentrations and deposition fluxes of pollutants at a fine spatial scale near the roadways. Gaussian models for line sources are appropriate for this type of air pollution impact study (category 4 in section 5.3.2.3). Finally, the water quantity and quality model must be consistent with the output of the atmospheric model and the objective of the study (contamination of stormwater at the catchment outlet). Thus, a semi-distributed model (category 2 in section 5.3.2.4) will provide some level of detail in terms of subcatchment variability, without imposing unneeded computational and input data burden on the study. Clearly, other choices could be made and the user's judgment is an important part of the construction of a modelling chain. We present in the following section the specific models selected for the study of the Grigny urban catchment and the results of the model simulations.

5.3.4 Case Study: Design, Methodology, and Results

The objective of this study is to simulate the impact of road traffic on stormwater contamination, to compare the modelling results to available measurements, and to investigate the sensitivity of those results to the level of detail of traffic air pollutant emissions. The present study focuses on three metals emitted by road traffic: cadmium (Cd), lead (Pb), and zinc (Zn). The Grigny catchment is located 20 km south of Paris in a suburban area. The catchment area is 451 ha, covered by several municipalities and divided into 32 subcatchments according to the topography and the structure of the drainage system. The geographical location and division of the catchment are presented in Figure 5.6. The models, available data and results are presented sequentially for each component (traffic, emissions, atmospheric pollution, stormwater contamination).

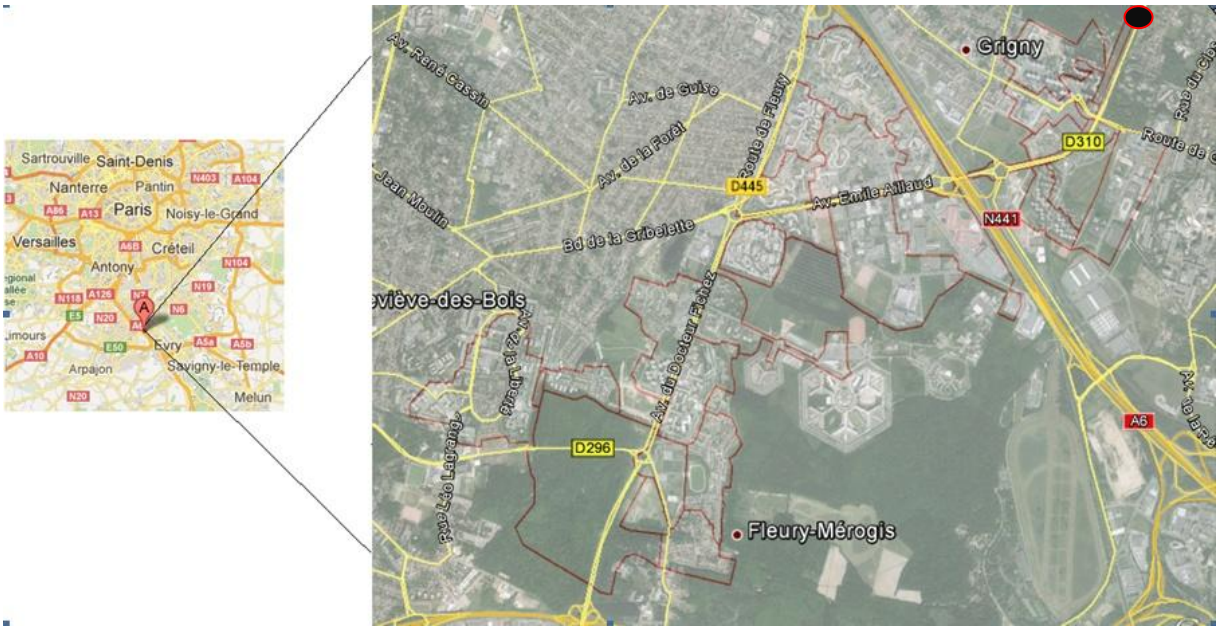

Figure 5.6. Geographical location and characteristics of the Grigny catchment including major roads (in yellow), outlet (black circle), and subcatchment boundaries (in red). (Source: Google Maps)

Traffic

The Grigny catchment is impacted by four main roads (D310, D296, N441, and D445) and the A6 freeway. Based on traffic variability and road direction, these roads were divided into eleven sections assumed to be of uniform traffic flow, speed, and fleet composition.

Annual average hourly traffic volumes on the A6 freeway were obtained from traffic count equipment operated by the French Ministry of Ecology, Sustainable Development, and Energy. Traffic volumes of the other main roads were simulated using the VISUM traffic model by the Regional Department of Transportation and Planning (DRIEA) (Figure 5.7). Their hourly traffic volumes were assumed to follow the hourly distribution of the A6 freeway traffic observations.

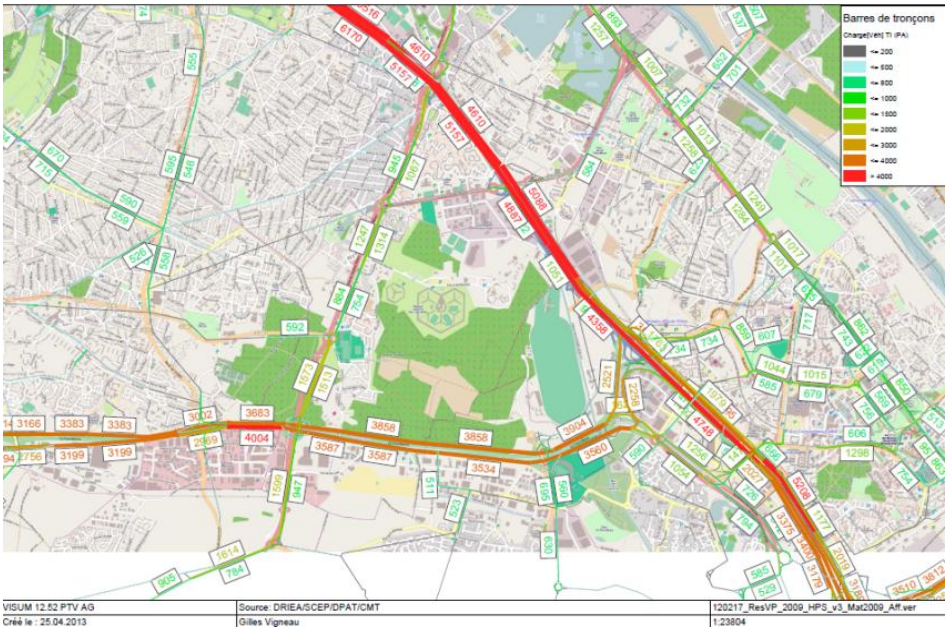

Figure 5.7. Peak hour traffic volumes in the Grigny catchment area (source: DRIEA).

The local traffic flow on residential streets was treated as a uniform area source based on the number of workers who live and commute out of the Grigny catchment area and the number of vehicles registered in the area. Such data were obtained from the French National Institute for Statistics and Economic Studies (INSEE). Traffic flow on residential streets accounts for 1% of total traffic in the study area.

Traffic emissions

Since the traffic output data are hourly, pollutant emissions could be estimated by an average-speed based model. For this purpose, the CopCETE model of the French Ministry of Ecology was used for exhaust emissions. It is based on the COPERT4 methodology (Ntziachristos et al. 2009). This model calculates vehicle emissions from most processes including vehicle exhaust, fuel evaporation, and equipment wear depending on road gradient, length of road, different types of traffic density (urban or rural road), fleet composition, number of vehicles per categories (passenger, light-duty, and heavy-duty vehicles, buses) and their average speeds. The fleet composition was assumed to be the same as the urban fleet composition for surface roads and main roads and a typical freeway fleet composition for the A6 freeway (Hugrel et al., 2004). Road dust contains particles derived from a wide range of sources. They can be classified into 4 categories: 1) vehicle sources (exhaust particles, tyre, break and clutch wear), 2) roadway sources (road surface wear, corrosion of crash barrier), 3) non-transport sources (e.g., industrial and commercial activities, vegetative detritus), 4) atmospheric deposition derived from the above sources in other areas. Legret and Pagotto (1999) found road dust to be heavily polluted by Pb, Cu, Cd, and Zn, originating from traffic. Currently, because of emission control regulations, exhaust emissions from road traffic have been reduced, but non-exhaust emissions from road vehicles are still largely unabated (Thorpe and Harrison 2008). For example, the ban of leaded gasoline significantly decreased Pb emissions from vehicles. In this study, non-exhaust emissions were calculated with the COPERT4

methodology for road vehicle tyre and brake wear, but road surface wear was not included due to a lack of data. A significant fraction of metals emitted by equipment wear may be present in coarse particles; therefore, emissions of particles greater than 10 µm in aerodynamic diameter are taken into account in the emission inventory used here. Another source of uncertainly is that re-emission of road dust by traffic was not taken into account; although this process may account for a significant fraction of atmospheric particulate matter (PM) in urban areas (e.g., Pay et al., 2011), it is still poorly characterized and, therefore, highly uncertain. An example of output from the emission model is provided in Figure 5.8.

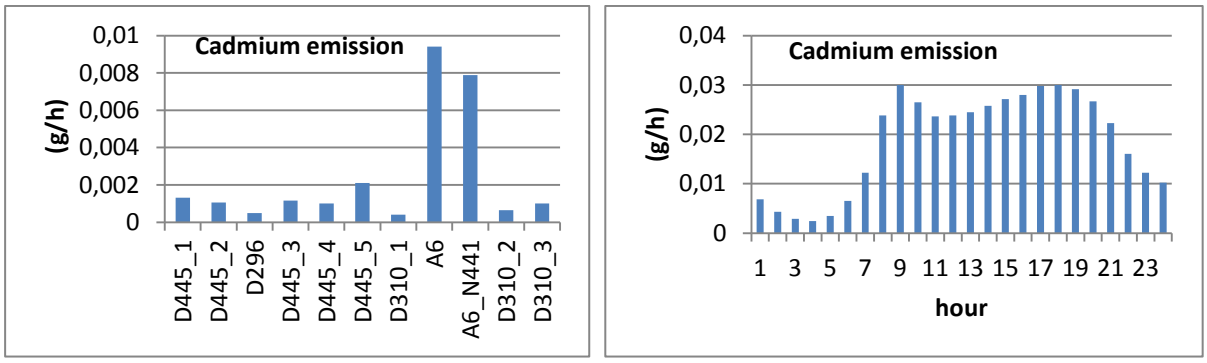

Figure 5.8.Cd emissions (g/h) for each road section at 10 am (left) and hourly profile of daily Cd emissions due to road traffic in the modelled area (right).

Atmospheric dispersion

The dispersion of atmospheric pollutants was calculated using the Polyphemus Gaussian dispersion model for a line source (Briant et al., 2011, 2013). The Gaussian dispersion formulation for a line source is exact to simulate emissions from road traffic when the wind is perpendicular to the line source and approximations are needed for other wind directions. The Polyphemus model uses a novel method to reduce the calculation error when the wind direction is not perpendicular to the road.

The model was used to simulate pollutant dispersion from major roadways in the catchment for the period from 2 April to 3 May 2012. The dataset used contains the following:

1. The coordinates of 4 roads and 1 freeway divided into 11 sections representing a total of 10 km of linear road length.

2. The Cd, Zn, and Pb hourly emission rates associated with traffic for each one of the 11 sections computed with the CopCETE emission model for exhaust emissions and the COPERT4 database for non-exhaust emissions.

3. The receptor locations; the overall receptor grid consists of several rectangular grids of 50 m spacing assigned to each one of the subcatchments.

4. Meteorological data required by the Polyphemus Gaussian model, which include wind speed and direction and cloud coverage. Meteorological variables are based on observations at the nearest measurement station (Orly airport, 8 km from the catchment). The use of the wind speed and direction from a close but different location is appropriate in this case because of the relatively flat terrain.

Figure 5.9 shows the modelled Zn concentrations (µg/m^3) at ground level on 5 April at 9 am. Only the concentrations located within the catchment are shown. These values correspond solely to traffic emissions, i.e., without background atmospheric concentrations. The concentrations decrease when the distance of the receptor from the road increases. The concentration at each point varies in time depending on traffic and meteorology.

In addition to the emissions associated with traffic from the major roadways, the contribution of emissions associated with local traffic on residential streets and that of background concentrations were also taken into account. The contribution of traffic flow on residential streets was simulated using a box model approach, which implies that those emissions are spatially uniform over the study area. We assumed that advection processes are more important than convection for air pollutant dispersion; therefore, the atmospheric concentrations associated with those emissions are inversely proportional to the wind speed (Benarie, 1967).

Background concentrations were obtained from measurements conducted by Ayrault et al. (2010) near Paris. The average urban background total suspended particulate (TSP) values are 0.393, 15.37 and 45.8 ng/m^3 for Cd, Pb, and Zn, respectively. These background concentrations were assumed to be spatially uniform over the study area and constant in time.

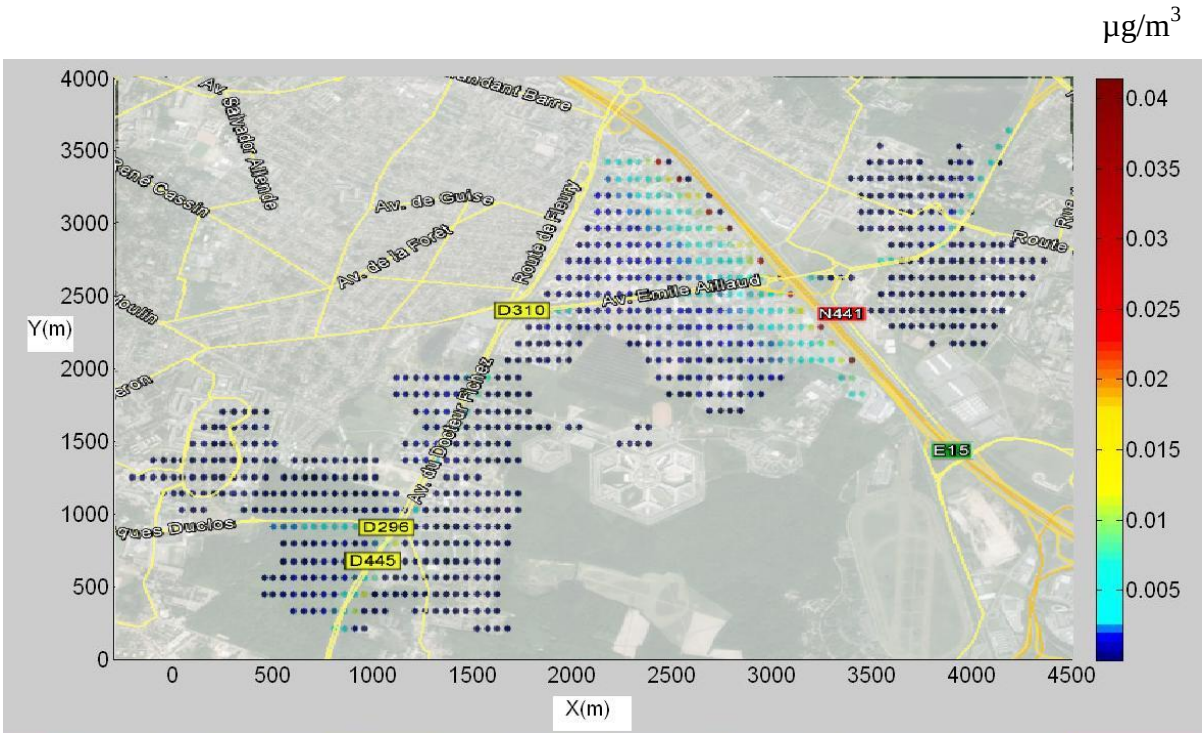

Figure 5.9. Zn concentrations (µg/m^3) due to traffic on major roads over the Grigny catchment on 5 April at 9 am on a receptor grid (m) corresponding to the urban catchment. The southwestern origin is at 48° 39’ 41’’ N, 2° 20’ 02’’ E.

Atmospheric deposition

Atmospheric deposition occurs via dry processes (i.e., when gas molecules and aerosol particles get into contact with surfaces) and wet processes (i.e., when gases and particles are scavenged by precipitation, mostly by rain). Several studies have experimentally quantified atmospheric deposition of metals near roadways (Viard et al., (2004); Azimi et al., (2005);

Sabin et al., (2006); Loubet et al., (2010)). These studies show that deposition fluxes decrease rapidly as the distance from the roadway increases, which is consistent with the spatial gradient observed for atmospheric concentrations. Theoretical models have been developed for dry deposition (e.g., Zhang et al. (2001), Wesely (2007), Sportisse (2007)) and wet deposition (e.g., Duhanyan and Roustan, 2011). The model formulations presented below follow those of standard theoretical models.

The dry deposition flux is typically computed using the following formulation:

$$F_{dry}(x,y) = V_d.C(x,y,z) \qquad 5.3$$

where V_d is the dry deposition velocity, which is a function of meteorology, land use, and particle size. The deposition velocities used here were obtained from Roustan (2005). The size distribution of PM_{10} mass in the atmospheric background was assumed to be 74% in particles with a diameter less than 1 µm, 10% in particles between 1 and 2.5 µm, and 16% in particles with a diameter between 2.5 and 10 µm. The size distribution of particles from traffic emissions consists of 58% of particles with a diameter less than 1 µm, 8% of particles between 1 and 2.5 µm, 13% of particles between 2.5 and 10 µm, and 21% of particles greater than 10 µm. The coarse particles (>10 µm) results mostly from non-exhaust processes. The selected values for the dry deposition velocities of particles in these four size ranges were 0.2, 0.4, 4 and 20 cm/s, respectively. The subcatchments were assumed to have approximately the same land use. The effect of meteorology on dry deposition velocities was not taken into account here and time-average values were used.

Pollutant buildup on the subcatchment surfaces is calculated according to the dry deposition flux of each pollutant source (i.e., local traffic, background concentration, traffic on the roads and the freeway), the associated level of traffic and the meteorological situation. 1784 virtual receptors separated by a distance of 50 m from each other and covering the whole catchment were selected (Figure 5.8). The average deposition over all receptors located in each subcatchment determines the buildup for each hour.

Wet deposition was assumed to be homogeneous over the catchment. The atmosphere over the catchment was assumed to be a well-mixed box with a height of 1000 m corresponding to a typical mixing height. The following formulation then applies.

$$F_{wet} = \frac{E_{total}.\Lambda}{\sqrt{S}.u} \qquad 5.4$$

where, E, S, u and Λ are the total emission of the pollutant within the domain, the surface of the catchment, the wind speed, and the wet deposition scavenging coefficient, respectively. Λ was calculated following the Andronache (2004) formulation for urban areas.

$$\Lambda = 6.67\times10^{-5} I^{0.7} \qquad 5.5$$

where I is the rain intensity (mm/h). The average pollutant concentration in rainfall can be calculated as the wet deposition flux divided by the precipitation amount over the rain event.

Water quality

The water quality simulation requires a satisfactory water quantity simulation because pollutant concentrations are highly dependent on the simulated flow rate. The model used to perform the stormwater runoff analysis is SWMM 5 (Rossman, 2010). This model is an open-source modelling software, well adapted to this investigation as it allows rainfall-runoff simulations (quantity and quality) over long periods with short time steps (2 min in this case). The water quantity modelling for the Grigny catchment is performed using land use and topography data, and is completed by a calibration with a genetic algorithm. The performance of the model is evaluated by the Nash-Sutcliffe criterion. Details on the model, its setup for the Grigny catchment and the calibration procedure followed are presented by Petrucci *et al.* (2013).

Water data availability and treatments

Continuous measurements of flow rate and turbidity were conducted by SIVOA (Syndicat mixte de la Vallée de l'Orge Aval) at the outlet of the Grigny catchment and are available for the whole year 2012. In this study, 14 rainfall events were selected from 2 April to 3 May 2012.

Continuous measurements were complemented by chemical analyses on several rainfall events. An automatic sampler measured the different metal concentrations (Cd, Zn, and Pb) of 6 distinct samples of a rainfall event occurring on 5 November 2012 (Tableau 5.1). For this rainfall event, the Cd concentration was below the quantification threshold for 4 measurements out of 6.

Tableau 5.1. Table 1. Metal concentrations on 5 November 2012 (SIVOA)

Time	Total Suspended Solid (TSS) (mg/l)	Cd* (µg/l)	Zn (mg/l)	Pb (µg/l)
17 h 44	210	<1	0,24	20,28
18 h 02	103	<1	0,21	14,57
19 h 02	223	1,08	0,26	24,83
20 h 02	191	1,04	0,18	18,58
21 h 02	126	<1	0,12	10,45
23 h 02	66	<1	0,1	9,61

(*). Half the quantification limit (i.e., 0.5 µg/l) was used when Cd concentrations were below the quantification limit.

The "observed" continuous metal concentrations were re-constructed over the period by calculating the total suspended solids (TSS) concentration using the TSS-turbidity relation and the ratio between TSS and metal concentrations obtained by the available samples. The averages of these ratios are 5.14×10^{-6}, 0.11×10^{-3} and 1.29×10^{-3} µg/l for Cd, Pb, and Zn,

respectively. These ratios were used to calculate continuous metal concentrations at the outlet of the catchment.

Water quantity was simulated for 14 rainfall events. Half of the rainfall events (from 2 to 19 April) were used to calibrate the model and half (from 20 April to 3 May) were used for the model validation. Figure 5.10 compares the simulated flows with continuous measurements. The Nash values are 0.6772 and 0.6063 for calibration and validation, respectively.

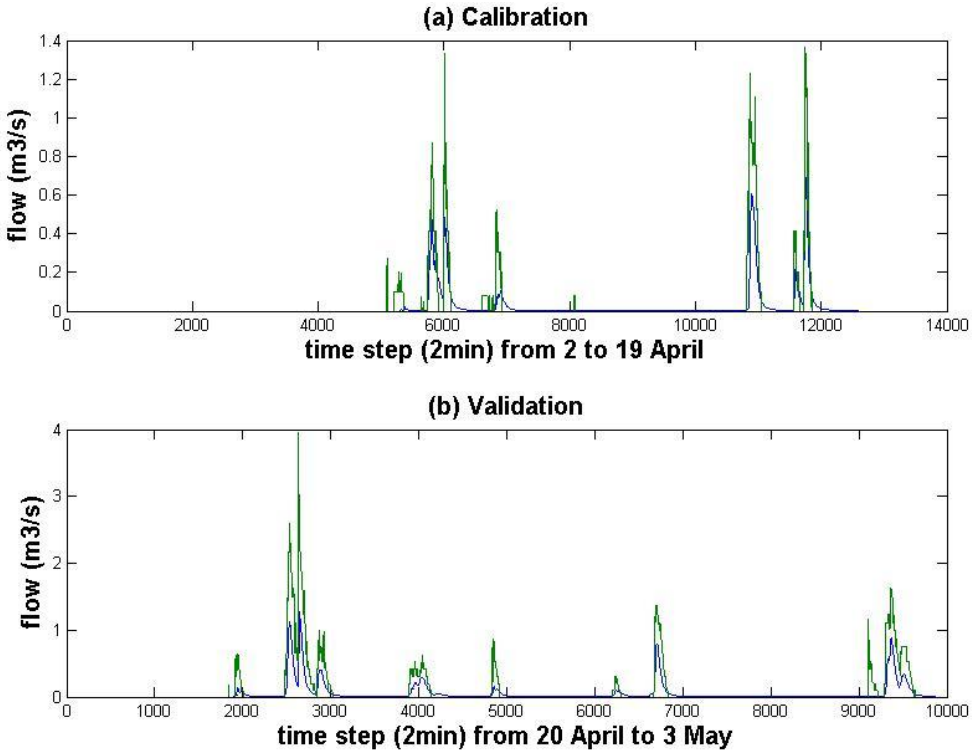

Figure 5.10. Comparison between simulation (blue line) and measurements (green line) results from 2 to 19 April (top, calibration) and from 20 April to 3 May (bottom, validation) at the outlet.

Water quality modelling

Usually water quality simulations include the pollutant buildup during dry periods and washoff during rainfall events. Different mathematical approaches are available to represent the processes governing pollutant accumulation and washoff. In this study, the buildup is obtained from the atmospheric deposition calculations and the power washoff equation can be written as follows:

$$W = E_1 q^{E_2} B \qquad 5.6$$

where, W is the washoff load (mass per hour), E_1 is the washoff coefficient, E_2 is the washoff exponent, q is the runoff rate per unit area (mm/hour) and B is the available mass of buildup. Thus, the pollutant washoff load is proportional to the product of runoff raised to some power and to the amount of available pollutants.

The washoff parameters, E_1 and E_2 depend on land use (Cheah 2009). On the basis of the available literature and without further information on the catchment, the chosen values for the parameters are constant average value: E_1=0.1, E_2=1.5.

Three model simulations were conducted:

(1) a reference model simulation including all emission sources and the background atmospheric concentrations, based on the model configuration described above

(2) a model simulation without any traffic emissions from the study area but including background atmospheric concentrations

(3) a model simulation with traffic emissions, but with emissions for traffic on major roadways treated as spatially-averaged over the study domain, which is defined as the smallest rectangular area covering the catchment and extending up to 1000 m from the surface (i.e., within the atmospheric mixing layer).

The results of the reference simulation can be compared to measured concentrations at the catchment outlet. A comparison between the first and second simulations allows us to investigate the contribution of local traffic within the catchment area to stormwater contamination. A comparison between the first and third simulations provides a quantitative assessment of the uncertainty associated with a spatially-averaged treatment of all emissions within the study area compared to the reference simulation where the emissions associated with major roadways are treated explicitly (i.e., spatially distributed).

Comparison of model simulation with measurements

The results presented in Figure 5.11 show the comparison of metal mass flow rates (µg/s) between the simulation and the measurements. The rainfall event of 24 April was excluded because the flow rate was not estimated correctly. The average ratios of modeled and measured mass flow rates are 77% for Zn, 100% for Cd, and 211% for Pb. These ratios vary among the fourteen rain events and range from 9 to 106% for Zn, from 11 to 150% for Cd, and from 24 to 296% for Pb. These results show that the impact of atmospheric deposition of Zn, Cd and Pb on water contamination is considerable. Zn originates from the corrosion of building materials, which can explain the fact that the simulation concentrations underestimate the measurements (Gromaire et al. 2011). Unleaded gasoline is now used in Europe, and Pb due non-exhaust emissions has also been reduced, but it still remains an important source of water contamination (Gromaire et al. 2011). In this study, the COPERT4 non-exhaust emission factor for Pb was used. Because this emission factor includes data between 1983 and 2007, it is likely to overestimate current Pb emissions because of reductions in Pb non-exhaust emissions in recent years. For example Hjortenkrans et al. (2007), showed that Pb emissions from brake linings in Stockholm (Sweden) were reduced from 560 kg/year in 1993 to 35 kg/year in 2005. The results for Cd should be taken with caution because two-thirds of the measurements were below the quantification limit and using half the quantification limit may over- or underestimate the actual contamination.

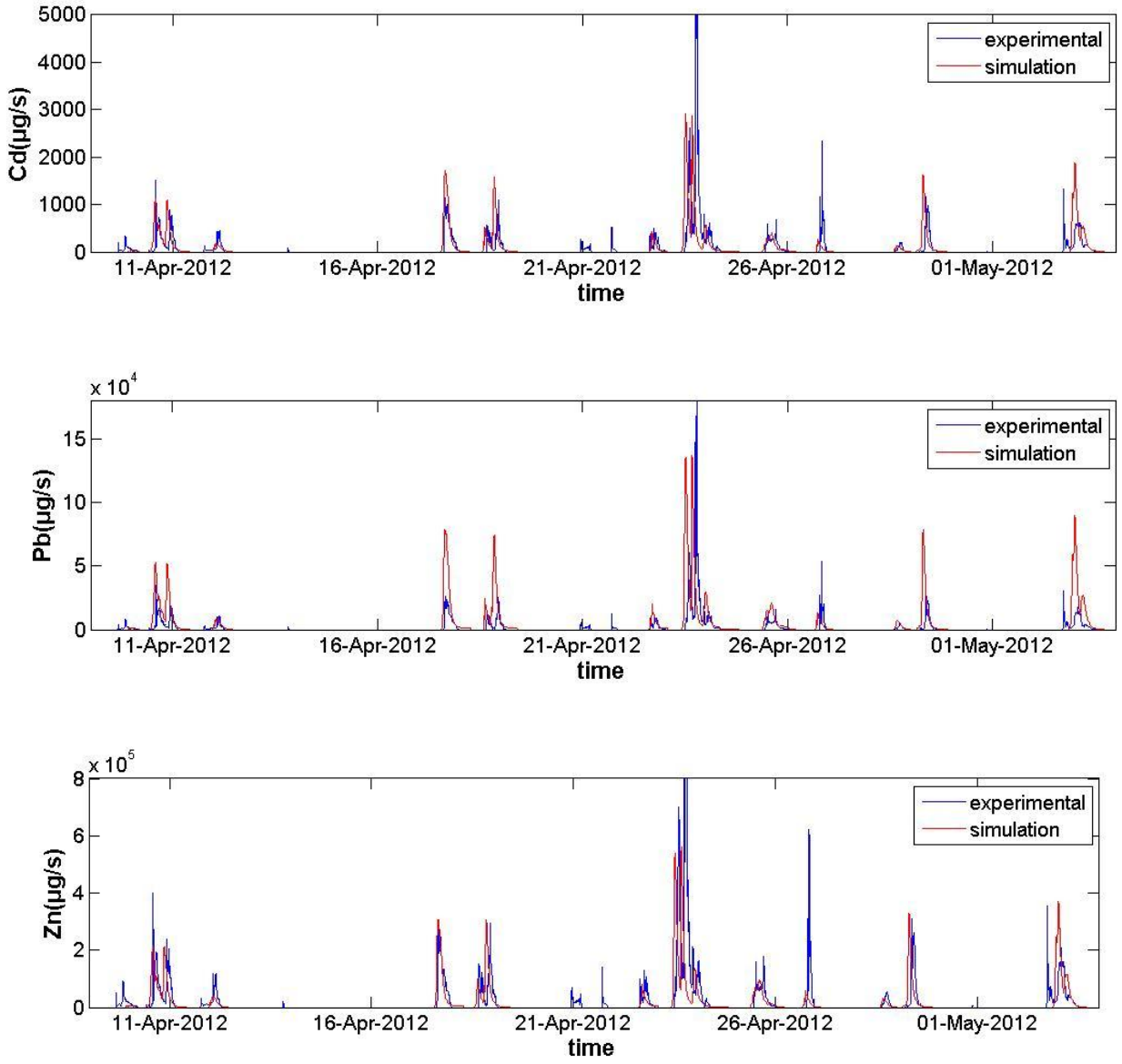

Figure 5.11.Metal mass flow rates (µg/s) at the outlet of the Grigny catchment: simulation results with an explicit treatment of traffic (in red) and experimental results (in blue). The rainfall event of 24 April was excluded (see text).

Impact of road traffic in the study area

The comparisons between the simulations with and without considering local traffic within the study area are presented in Figure 5.12. The comparison of these two cases (with and without traffic) demonstrates a significant effect of local traffic on Cd, Pb and Zn mass flow rates. The background contribution is 4% of the Zn concentrations on average (calculated as the average of the contributions for each rain event), with a range of 2 to 6% among the fourteen rain events. For Pb, the background contribution in stormwater is 6%, with a range of 3% to 8% among rain events. For Cd, the background contributes 7% in stormwater, with a range of 4% to 10% among rain events. The traffic contribution is dominant because (1) traffic emissions are close to the ground and, therefore, available for dry deposition and (2)

the presence of particles with diameters greater than 10 µm from vehicle equipment wear (i.e., with large dry deposition velocities) leads to significant dry deposition near the roadways.

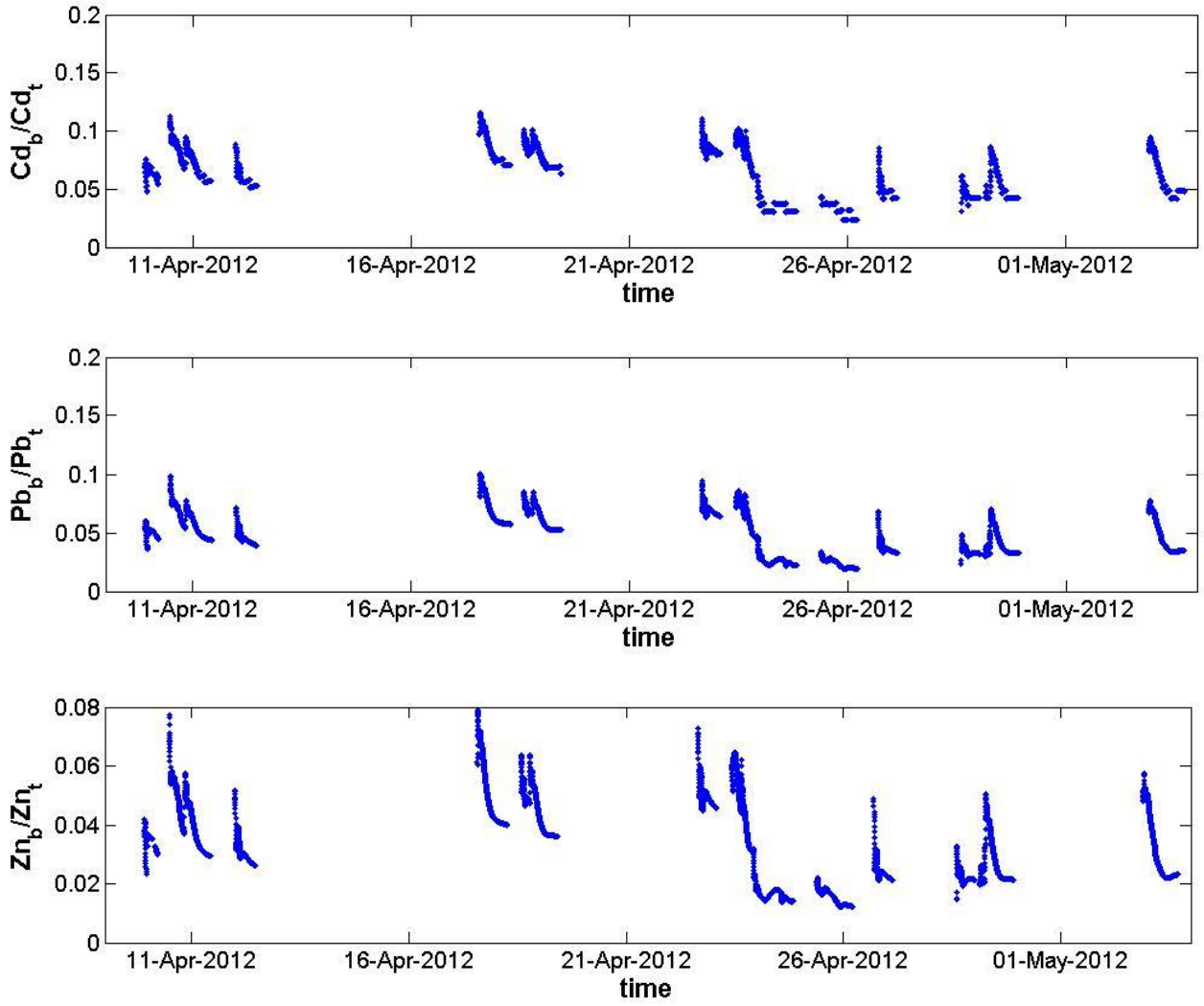

Figure 5.12. Cd, Pb, and Zn mass flow rate ratios between the case with an explicit treatment of local traffic ($metal_t$) and without local traffic ($metal_b$) in the study area at the outlet of the Grigny catchment. Only the average background atmospheric concentration was used in the second simulation.

Effect of the spatial representation of traffic on major roadways

The metal concentrations in runoff were simulated by using two different representations of the emissions associated with traffic on major roadways: in the reference simulation, four roadways and one freeway were represented explicitly, In the other simulation, the emissions from those major roadways were treated as those from residential streets, that is, they were spatially averaged and treated uniformly over the study area covering the catchment and their emissions were spatially distributed within a volume covering the study area with a height of 1000 m. This comparison provides, therefore, important information on the benefits of using an explicit representation of the emissions from major road traffic.

Figure 5.13 shows the temporal variation of the concentrations simulated with those two model configurations. The average ratios of the mass flow rates calculated by those two models (spatially-averaged / spatially-distributed) averaged over all rain events are 24% for Zn, 41% for Cd, and 34% for Pb. These ratios vary among the fourteen rain events and range from 11% to 38% for Zn, from 21 to 58% for Cd, and from 16 to 50% for Pb. The spatially-averaged results are low compared to those of the spatially-distributed model, because of the dilution of the traffic emissions within the atmospheric mixing layer over the study area. It means that averaging emissions with a box model leads to reduced impact of local traffic sources that have a strong impact on concentrations at the catchment outlet. Therefore, the differences in concentrations of metals emitted by traffic between the two simulations demonstrate that it is essential to have a correct spatial representation of those local emission sources.

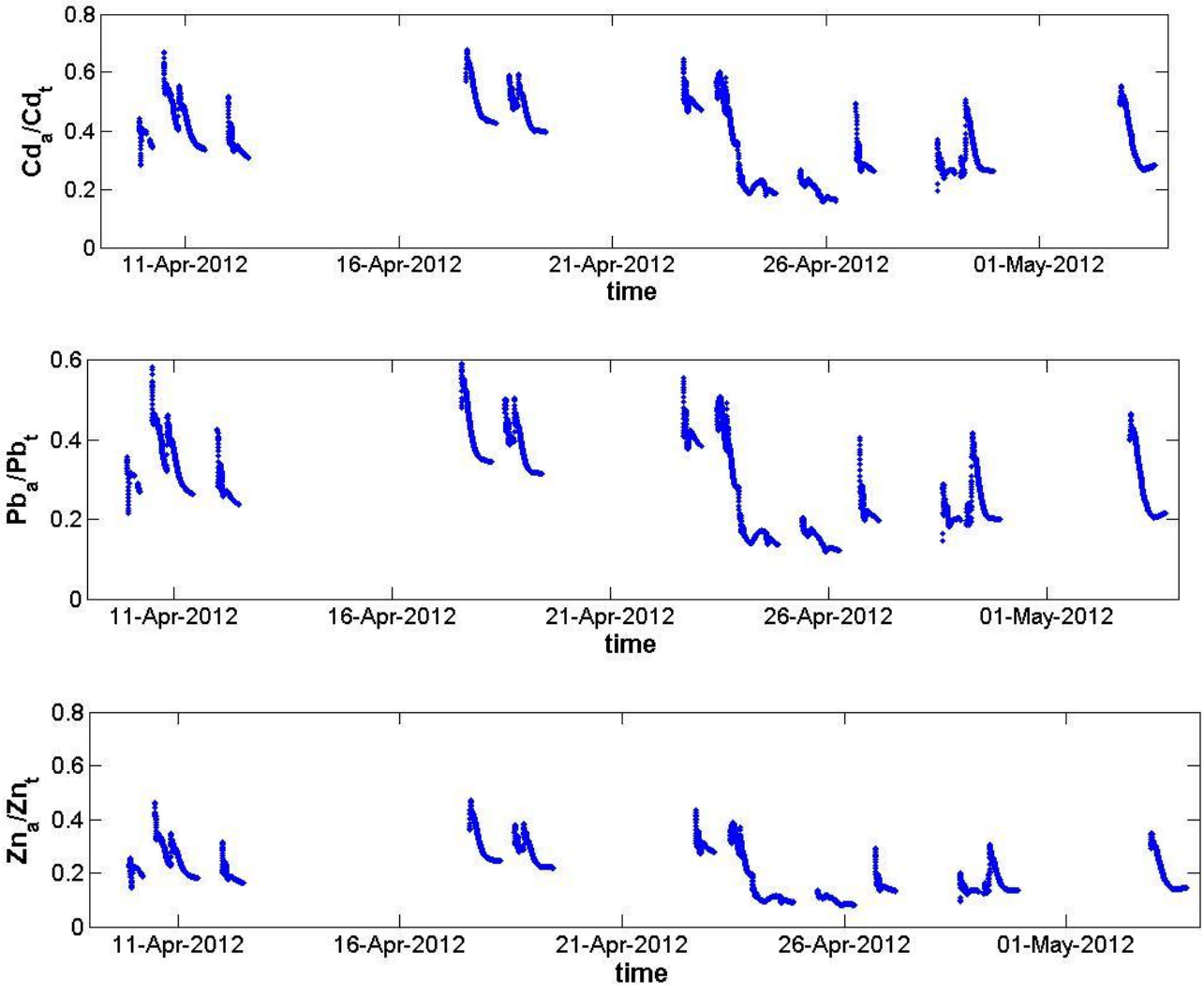

Figure 5.13. Ratios of Cd, Pb and Zn mass flow rates at the outlet of the Grigny catchment with spatially-distributed ($metal_t$) and spatially-averaged ($metal_a$) traffic emissions.

5.3.5 Discussion

This first step into air and water integrated quality modelling shows some limitations that should be overcome in the next few years to make these integrated models more reliable to predict contaminant concentrations in urban waters. First of all, the major drawback of this integrated model chain comes from the different modelling bricks themselves.

In order to simulate the environmental impacts of traffic at the local urban scale, it was necessary to choose the most appropriate modelling tools in terms of computational efficiency, which is a very important point when several models have to be coupled to constitute a modelling chain. Moreover, a major scientific stumbling block is that air quality models typically consider only those particles smaller than 10 µm in aerodynamic diameter (PM_{10}) since coarser particles are not regulated. This consideration is inherited from public health concerns and is related to the fact that only PM_{10} and fine particles affect human health. However, the mass of particles greater than 10 µm is significant and is relevant to water quality. Accordingly, it should be taken into account because particles of diameter above 10 µm are measured with the turbidimeter. Here, we took into account those coarse particles emitted by vehicle equipment wear; however, we did not account for road wear nor the re-suspension of road dust. Clearly, uncertainties are associated with every component of the modelling chain and some of those are discussed below.

For example, the most widely used air pollution models for calculating the dispersion of vehicle emissions at local scales are Gaussian dispersion models. However, in a densely built environment, the Gaussian dispersion assumption no longer applies and street-canyon models or CFD models may be more suitable. A comparison between Gaussian dispersion models and more detailed ones as part of a similar modelling chain is an interesting perspective. Furthermore, the background air pollution was treated here in a simple manner, using spatially uniform and temporally constant values in a box model. A plume-in-grid approach would provide a more comprehensive multi-scale modelling approach to better characterize this urban background in future studies.

Further, in an air-water modelling approach, the emission models must be able to estimate the main water pollutants such as total suspended solids (TSS), polycyclic aromatic hydrocarbons (PAH), and heavy metals (e.g., Pb, Zn, Cd, and Cu). It is a very restrictive need for emission models because most of them do not include these pollutants (in particular instantaneous models). Moreover, to consider a large number of pollutants and emission phenomena (e.g., including fuel evaporation and non-exhaust particle emissions), the microscopic emission models, which only treat a few pollutants emitted from the vehicle exhaust, have to be complemented with aggregated emission models such as COPERT4. However, those aggregated models pertain to large temporal scales, thereby leading to a discrepancy in the estimation of traffic emissions at very fine temporal scales.

At last, water quality can be well described by semi-distributed models such as SWMM, but the approach by subcatchments, adapted to hydrologic considerations, is not necessarily suited for coupling with the air component. The resolution used for the Grigny catchment (average subcatchment size) is about 200 m, coarser than that of the output from the deposition model. A fully-distributed hydrologic model would offer the advantage of explicitly taking into account distributed land uses and road surface characteristics at a higher

resolution, in addition to rainfall characteristics at the scales of the resolution of the atmospheric receptors. Therefore, future work may use a fully distributed model for surface water flow and water quality modelling coupled to a hydraulic model for the urban drainage network.

The second major source of uncertainties in this integrated modelling approach is the lack of data covering the different components of this modelling chain.

For example, to assess the relationship between turbidity and metal concentrations, it would be necessary to consider more measurements of metal concentrations in water at the outlet of the catchment. In fact, the relations between turbidity, TSS and metal concentrations are not simple (Hannouche at al. 2011; Wust et al. 1994). These relations may depend, for instance, on pH, which was not measured for the samples available in this study. Therefore it would be necessary to obtain different samples in different seasons to confirm these results.

Another source of uncertainty in this modelling chain is the estimation of atmospheric deposition fluxes, both wet and dry, because those are strongly dependent on the particle size distributions. In particular, the dry deposition velocity still remains difficult to estimate as a function of particle size, atmospheric conditions and surface types (Roustan 2005). As this velocity may vary by an order of magnitude or more depending on the particle size, the influence on the simulated water concentrations is surely very high and further work is needed to determine more accurately this parameter accounting for particle size distributions and for the distribution of metals between the different sizes of particles.

5.3.6 Conclusion

In this study, we developed, applied, and discussed a modelling chain linking road traffic emissions to air and stormwater concentrations. Different models for traffic, emission, atmospheric dispersion and stormwater flow and contamination were presented. This brief review provided the context needed for the selection of the most appropriate models to be coupled in order to implement an integrated and efficient modelling system for a simulation of air and water quality in urban areas. This approach was tested on a urban catchment in the Paris region.

The effect of traffic impact in the Grigny catchment located in a southern suburb of Paris was studied from 2 April to 3 May 2012. The simulated Zn, Pb, and Cd concentrations in pollution peaks are commensurate with experimental results at the outlet, thereby suggesting the important contribution of atmospheric deposition to stormwater contamination in urban areas. Comparison of metal loading from atmospheric deposition under two hypotheses (with and without local traffic) indicates an important contribution of local traffic to Cd, Pb and Zn in urban catchments. Furthermore, an explicit representation of major roadways in the catchment area was shown to have a significant effect on simulated mass flow rates and concentrations.

Through this process, we observed several limitations in the simulation of all phenomena (traffic, emission, atmospheric dispersion and stormwater). The main challenges are associated with the consistency between inputs and outputs of the different models constituting the modelling chain, especially the available data, the scale of the problem and its complexity.

The method developed in this work appears very promising in the context of water quality modelling. Currently, pollutant loads are usually calculated from urban land use. Here, the atmospheric loads near heavy-traffic areas appear to be major contributions. Therefore, the traditional approach may need to be reconsidered depending on the configuration of major roadways within the catchment area. These encouraging results may be useful to test different urban scenarios at the time of the design and planning of new urban areas.

To that end, experimental data are needed to calibrate and /or evaluate the different components of the modelling chain. Although reasonable agreements were obtained here between model simulations results and measurements at the catchment outlet, more work is needed to refine this modelling approach and evaluate it over different settings. Furthermore, this work highlights the importance of developing interdisciplinary research programmes with strong interactions between modelling and experimental studies.

Chapitre 6

6 Conclusion et perspectives

6.1 Conclusion

L'objectif de cette thèse a été de mettre au point une chaîne de modélisation qui permette de quantifier les impacts environnementaux du trafic routier sur la pollution atmosphérique et au-delà, sur la pollution des eaux de ruissellement, en prenant en compte le trafic, les émissions des véhicules, les processus de transport et de transformation atmosphériques, les dépôts atmosphériques sur les bassins versants et les processus de lessivage et de transport par les eaux de ruissellement. Ces travaux ont permis d'améliorer nos connaissances, d'identifier les limites et les précautions nécessaires à la réalisation de cette chaîne, ainsi que de souligner la nécessité de données expérimentales robustes pour la validation de ces chaînes de modélisation.

La première partie de la thèse a permis de réaliser un état de l'art complet et détaillé des outils de modélisation des différents phénomènes (trafic, émissions, transferts atmosphériques et hydrologiques) pertinents pour notre problématique. Des classifications des modèles ont été proposées afin de faciliter la sélection des modèles les plus appropriés pour être utilisés conjointement dans un système de modélisation intégré, pertinent et efficace. Nous avons souligné les points forts, les limites, les lacunes et les incertitudes des différents modèles en fonction de leur précision pour la représentation physique des processus étudiés. L'importance des données d'entrée, leur disponibilité, représentativité, précision et pertinence et la cohérence entre les sorties d'un modèle et les entrées du modèle suivant ont été discutées car ces questions affectent la sélection des modèles pour leur intégration dans une chaîne de modélisation. Cet état de l'art s'est révélé particulièrement complexe car de nature pluridisciplinaire et portant sur des objets hétéroclites. Différents couplages de modèles existants ont été présentés pour chaque échelle spatio-temporelle. Par ailleurs, deux chaînes de modélisation, l'une statique et horaire, la seconde envisageant une approche dynamique ont été proposées.

La deuxième partie de la thèse a consisté à développer des outils automatisés d'interfaçage entre les différents modèles (certains résultats ont été présentés au chapitre 3, afin d'illustrer par des exemples concrets la première partie). En raison du caractère peu modulaire de ces outils, il n'est généralement pas possible de réaliser leur intégration dans une chaîne intégrée. Ce sont donc des outils automatisés d'interfaçage (créant les données nécessaires aux modèles suivants) qui ont été développés. Ces chaînes de modèles ont ensuite été testées sur différents cas d'étude :

1- Couplage trafic / émissions avec la simulation du trafic sur une zone urbaine (Cours Lafayette, Lyon) utilisant un modèle dynamique de trafic (Symuvia) en lien avec des modèles d'émissions instantané (PHEM) et agrégé (CopCETE). La comparaison des résultats de ces deux couplages montre une forte différence d'émissions calculées pour des conditions de circulation à vitesse faible (<10 km/h), ce qui comprend à 50% des véhicules dans cette étude.

2- Couplage émission / qualité de l'air et dépôts atmosphériques sur l'autoroute A31, Metz. Les facteurs d'émission moyennés de COPERT4 ont été utilisés. Ce couplage a permis d'évaluer le modèle de panache gaussien pour les impacts à proximité d'une autoroute. Les résultats montrent une sous-estimation des dépôts de cadmium pour des distances inférieures à 20 m de l'autoroute. Au-delà de cette distance, les résultats du modèle sont satisfaisants. La sous-estimation à proximité de l'autoroute peut être due au fait que les particules grossières non-prises en compte dans les estimations des émissions pourraient contribuer significativement aux dépôts.

3- Couplage trafic / émission / qualité de l'air, en bordure d'une autoroute à Grenoble. Le modèle de panache gaussien a été modifié pour mieux simuler la dispersion de polluants atmosphériques liés au trafic routier pour des conditions de vent faible. Ce modèle a été évalué avec des mesures effectuées en bordure de l'autoroute pour plusieurs polluants. Le traitement des conditions météorologiques calmes améliore significativement le coefficient de corrélation entre concentrations mesurées et simulées (par exemple le coefficient de corrélation de $PM_{2,5}$ croît de 0,41 à 0,72) et permet aussi de réduire les erreurs. La resuspension des particules par le trafic routier contribue fortement aux concentrations de particules. Dans cette étude, la remise en suspension des particules a été incluse sur la base des résultats d'une analyse des sources de polluants effectuée par Polo (2013). Si les résultats sont satisfaisants pour les particules (PM_{10}, $PM_{2.5}$ et certains métaux), le modèle sous-estime les concentrations de NO_2. Comme les concentrations de NO_2 sont moins influencées par les concentrations de fond que celles des particules, ces résultats suggèrent que des améliorations doivent encore être apportées au modèle pour ces conditions météorologiques particulièrement difficiles à simuler en bordure de route (effet de la turbulence induite par le trafic par exemple).

4- Couplage émissions / pollution atmosphérique (modèle boîte) pour un quartier suburbain (Sucy-en-Brie). Ce modèle relativement simple a été développé pour fournir des dépôts atmosphériques moyens sur une période assez longue, qui peuvent être utilisés comme des données d'entrée à un modèle d'eaux de ruissellement. Le modèle fait l'hypothèse d'une dispersion homogène des polluants sur le bassin versant. Les résultats du modèle sont en accord avec les mesures de dépôts des métaux lourds mais peu fiables pour les HAP. La surestimation des HAP peut être due aux facteurs d'émission et / ou à des vitesses de dépôt incorrectes.

5- Couplage dépôts atmosphériques / qualité des eaux de ruissellement pour un bassin versant suburbain. Cette étude a consisté à développer un modèle de calcul de dépôts en fonction du trafic et à simuler avec SWMM la propagation des polluants dans les sous-bassins versants sur une zone expérimentale de Grigny (2009-2010). Cette simulation a montré que les

concentrations simulées de polluants (Cd, Pb et Zn) dans l'eau sont respectivement trois fois, six fois et deux fois plus élevées quand une description explicite de la distribution spatiale du trafic est utilisée.

6- Une chaîne de modélisation complète avec couplages trafic / émissions /qualité de l'air et qualité des eaux de ruissellement pour un bassin versant suburbain (Grigny, avril 2012). Cette chaîne permet de simuler la plupart des processus d'émission, y compris les particules grossières de diamètre supérieur à 10 µm qui ne sont généralement pas prises en compte dans les modèles atmosphériques. Deux simulations distinctes ont été réalisées, l'une avec un modèle boîte et l'autre avec un modèle de panache gaussien. La comparaison entre les deux simulations a montré que le modèle boîte sous-estime considérablement l'impact des sources de trafic local sur les concentrations des polluants dans l'eau à l'exutoire du bassin versant. La comparaison entre la simulation avec le modèle Gaussien et les mesures expérimentales à l'exutoire du bassin versant montrent que, pour les taux moyens de débits massiques, la valeur simulée représente 77% de la valeur mesurée pour Zn, ce qui démontre un impact significatif des polluants atmosphériques sur la qualité de l'eau.

A travers ces différents cas d'étude, ces travaux ont permis d'identifier les enjeux associés à l'intégration de modèles pour le calcul de la pollution de l'air et des eaux de ruissellement due au trafic routier. Par ailleurs, ils fournissent une base solide pour le développement futur de modèles numériques intégrés de la pollution urbaine.

6.2 Perspectives

Les travaux effectués lors de cette thèse ont permis l'élaboration de différentes chaînes de modélisation et leur application à différents cas d'études. Néanmoins, des améliorations de ces chaînes de modélisation et de leur couplage semblent souhaitables, de même que d'autres configurations s'appuyant sur d'autres modèles pour envisager d'autres cas d'application de simulation de la qualité de l'air et de l'eau.

Il a été mentionné que la plupart des modèles disponibles sont basés sur des données d'entrée moyennées. Ces modèles relativement agrégés présentent des limites pour de nombreux problèmes particuliers (par exemple les concentrations des polluants à proximité des routes tel que sur les trottoirs). Dans cette étude, le couplage entre un modèle de trafic dynamique et un modèle d'émissions instantanées a été effectué. Les résultats de ce couplage pourraient alimenter un modèle CFD (RANS ou LES) afin de simuler la qualité de l'air à des échelles spatio-temporelles fines. De même, les modèles distribués de la qualité de l'eau avec un maillage compatible avec celui du modèle CFD pourraient être alimentés avec les dépôts issus du modèle CFD. Des problèmes associés à de tels couplages sont dus au manque de facteurs d'émission pour les polluants importants pour l'eau (par exemple les émissions non-échappement de particules). L'utilisation de modèles dynamiques serait préférable pour ces applications et leur utilisation est possible avec les ressources informatiques actuelles mais une amélioration du modèle d'émissions instantanées sera nécessaire pour considérer la qualité de l'eau avec une chaîne de modélisation dynamique car ces modèles d'émissions sont

actuellement limités à quelques polluants atmosphériques et quelques processus d'émissions (principalement échappement).

Les couplages effectués dans ce cadre ont été appliqués à la pollution en bordure de routes sans prise en compte des obstacles et des bâtiments. Pour un milieu urbain, la prise en compte des infrastructures urbaines (bâtiments) dans les simulations de dispersion de polluants est souvent nécessaire. Les modèles de panache gaussiens considèrent généralement un domaine d'étude plat, par conséquent des modèles qui tiennent compte de l'impact des bâtiments sur la dispersion des polluants sont nécessaires.

Dans cette thèse, la dispersion atmosphérique des polluants émis par le trafic prend en compte l'effet de la turbulence due aux véhicules avec la formulation de Kastner-Klein et al. (2000). Cette formulation influence peu la concentration des polluants dans des conditions de vent faible où la turbulence due aux véhicules pourrait être prédominante. De nouvelles formulations plus réalistes devraient donc être développées.

La chaîne de modélisation peut être intégrée dans un algorithme d'optimisation de la qualité de l'air et de la qualité de l'eau. En effet, les données associées aux différents scénarios de trafic pourraient être utilisées dans la chaîne de modélisation pour simuler la qualité de l'air et la qualité de l'eau. Ces résultats peuvent ensuite être comparés avec les valeurs réglementaires des concentrations de polluants et en optimisant des différents paramètres mis en jeu (le trafic, ses émissions, mais aussi par exemple l'ajout de barrières anti-bruits), de nouveaux scénarios peuvent être définis afin de re-modéliser les concentrations des polluants jusqu'à ce qu'un accord avec les réglementations soit atteint.

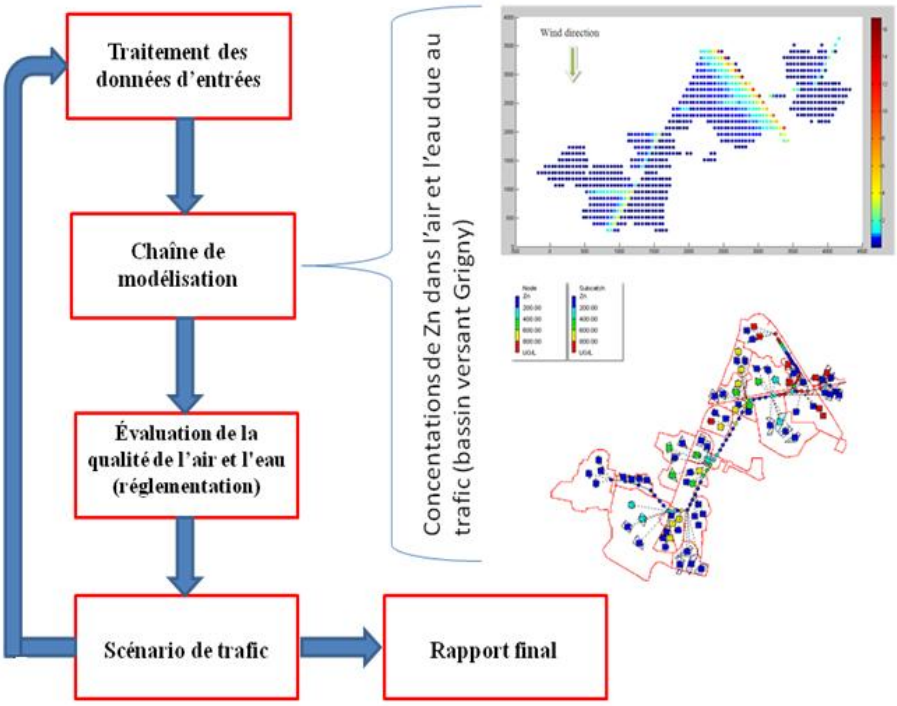

Figure 6.1. Algorithme d'optimisation de la qualité de l'air et de l'eau

7 Référence

Amato, F., Pandolfi, M., Moreno, T., Furger, M., Pey, J. Alastuey, A., Bukowiecki, N,. Prevot, A.S.H,. Baltensperger, U., Querol, X. (2011). Sources and variability of inhalable road dust particles in three European cities. Atmospheric Environment 45, 6777-6787.

An, X., Hou, Q., Li, N., Zhai, S., 2013. Assessment of human exposure level to PM10 in China. Atmos. Environ. 70, 376–386.

André, M., Fantozzi, C., Adra, N. (2006). Development of an approach for estimating the pollutant emissions from road transport at a street level. Commission Européenne. Bron, INRETS, LTE0628, 149 p.

André, M., Roche, A. L., Bourcier, L. (2012). *Statistiques de parcs et trafic pour le calcul des émissions de polluants des transports routiers*. Bron, France.

André, M., Fallah Shorshani, M., Berger, C., Montenon, A., & Brutti-Mairesse, E. (2012). *Evaluation des PDU - problématique du calcul des émissions de polluants du trafic*.

André, M., Roche, A.L., Bourcier L. (2013). Statistiques de parcs et trafic pour le calcul des émissions de polluants des transports routiers pour la France. In French. Rapport IFSTTAR LTE, Bron (France), 132pp.

André, M., Chanut, H., Pasquier, A., Pellet, C., Montenon, A., (2014). Modélisation et estimation des émissions de polluants du trafic routier. Rapport 7.1, Projet MOCoPo (Mesure et mOdélisation de la COngestion et de la Pollution), In French, Contrat n° 2010 MT CVS 121.

Andronache, C., (2004). Estimates of sulfate aerosol wet scavenging coefficient for locations in the Eastern United States. Atmos. Environ. 38, 795–804.

Ayrault S, A Senhou, M. Moskura, A Gaudry (2010) Atmospheric trace element concentrations in total suspended particles near Paris, France. Atmos. Environ. 44, 3700-3707.

Azimi S, Ludwig A, Thévenot DR, Colin J-L. (2003). Trace metal determination in total atmospheric deposition in rural and urban areas. Sci Total Environ 308:247–256.

Azimi, S., Rocher, V., Garnaud, S., Varrault, G., and Thevenot D.R. (2005). Decrease of atmospheric deposition of heavy metals in an urban area from 1994 to 2002 (Paris, France). Chemosphere, 61, 645-651.

Baklanov, A., Schlünzen, K., Suppan, P., Baldasano, J., Brunner, D., Aksoyoglu, S., Zhang, Y. et al. (2014). Online coupled regional meteorology chemistry models in Europe: current status and prospects. Atmospheric Chemistry and Physics, 14(1), 317-398.

Baldauf, R., Thoma E., Hays, M., Shores, R., Kinsey, J., Gullett, B., Kimbrough, S,. Isakov, V., Long T., Snow, R., Khlystov, A., Weinstein, J., Chen, FL., Seila, R., Olson, D.,Gilmour, I., Cho, SH., Watkins, N., Rowley, P., Bang. J. (2008). Traffic and meteorological impacts on near-road air quality: summary of methods and trends from the Raleigh Near-Road Study. J Air Waste Manag Assoc. 58(7), 865-78.

Barceló, J., and Casas, J. (2005). Dynamic network simulation with AIMSUN. In Simulation approaches in transportation analysis (pp. 57-98). Springer US.

Barth, M., Malcolm,C., Scora, G. (2001b). Integration a comprehensive modal emission model into ATMIS. Transportation modeling framworks institute of transportation studies. Research report UCB-ITS-PRR-2001-19.

Barth, M., An, F., Younglove, T., Scora, G., Levine, C., Ross, M., Wenzel, T. (2000). Comprehensive modal emission model (CMEM), version 2.0 User's Guide. University of California, Riverside, USA.

Bäumer, D., Vogel, B., Fiedler, F. (2005). A new parameterisation of motorway-induced turbulence and its application in a numerical model. Atmospheric Environment, 39(31), 5750-5759.

Beevers, D,. Kitwiroon, N,. Williams, M,. Carslaw, D. (2012). One way coupling of CMAQ and a road source dispersion model for fine scale air pollution predictions. Atmospheric Environment, 59, 47-58.

Beck, M.B,. (1987). Water quality modelling: a review of the analysis of uncertainty Water Resour. Res., 23 (1987), pp. 1393–1442.

Bell, M. L., Davis, D. L. (2001). Reassessment of the lethal London fog of 1952: novel indicators of acute and chronic consequences of acute exposure to air pollution. *Environmental health perspectives*, *109*(Suppl 3), 389.

Benarie M (1967) The simple Box Model revisited. Atmos. Environ., 12, 1929-1930.

Benson, P.E. (1989). CALINE4 – A Dispersion Model for Predicting Air Pollution Concentration near Roadways. Office of transportation laboratory, California department of transportation, Sacramento, CA.

Bessagnet, B., Menut, L., Curci, G., Hodzic, A., Guillaume, B., Liousse, C., Moukhtar, S., Pun, B., Seigneur, C. Schulz, M. (2009). Regional modeling of carbonaceous aerosols over Europe - focus on secondary organic aerosols. J. Atmos. Chem., 61:175-202.

Boriboonsomsin, K., and Barth, M. (2008). Impacts of freeway high-occupancy vehicle lane configuration on vehicle emissions. Transportation Research Part D: Transport and Environment, 13(2), 112-125.

Boulter, P.G.(2007). Non-exhaust particulate matter emission from road traffic. TRL Report PRR231. TRL Limited, Wokingham.

Boulter, P. G., and Latham, S. (2009). Emission factors 2009: Report 4-a review of methodologies for modeling cold-start emissions.

Boxill, S.A, and Yu, L. (2000). An evaluation of traffic simulation models for supporting ITS development. Center for transportation training and research texas southern university Report No.SWUTC/00/167602-1.

Brett, S. D., and Gavin, F. B. (2011). Spatial distribution of bulk atmospheric deposition of heavy metals in metropolitan Sydney, Australia. Water Air Soil Pollution, (214),147–162.

Briant, R., and Seigneur, C. (2013). Multi-scale modeling of roadway air quality impacts: Development and evaluation of a Plume-in-Grid model. Atmospheric Environment, 68, 162-173.

Briant, R., I. Korsakissok, C. Seigneur, (2011). An improved line source model for air pollutant dispersion from roadway traffic, Atmos. Environ., 45, 4099-4107.

Briant, R., Seigneur, C., Gadrat, M., Bugajny, C. (2013). Evaluation of roadway Gaussian plume models with large-scale measurement campaigns. Geoscientific Model Development, 6, 445–446.

Briggs, G. (1973). Diffusion estimation for small emissions. Report NOAA n. 79, Oak Ridge, TN (U.S.A.).

Burian, S. J., McPherson, T. N., Brown, M. J., Streit, G. E., Turin, H. J. (2002). Modeling the effects of air quality policy changes on water quality in urban areas, Environ. Model. Assess., 7, 179–190.

Byun, D.. and Ching, J. (1999). Science algorithms of the EPA models-3 community multiscale air quality (CMAQ) modeling system. EPA/600/R-99/030. US Environmental Protection Agency, Washington, DC, United States.

Cappiello, A., Chabini, I., Nam, E., Abou-Zeid, M., and Lue, A. (2002). A Statistical Model of Vehicle Emissions and Fuel Consumption. IEEE ITSC 2002 Paper, (Number 107).

Carruthers, D., Holroyd, R., Hunt, J., Weng, W., Robins, A., Apsley, D., Thompson, D., Smith, F., (1994). UK-ADMS: a new approach to modeling dispersion in the earth's atmospheric boundary layer. Journal of Wind Engineering and Industrial Aerodynamics, 52, 139–153.

CETE Normandie Centre, and DADT Département aménagement durable des territoires. (2010). User guide of COPCETE v3.

Chang, J., and Hanna, S. (2004). Air quality model performance evaluation. Meteorol. Atmos. Phys. 87, 167-196.

Chanut, S., Chevallier, E. (2012). Estimating the atmospheric impacts of traffic management projects: application of theoretical models to concrete cases, Recherche Transports Sécurité, 011-0018-4.

Cheah, (2009). Kinematic wave modelling of surface runoff quantity and quality for small urban catchments in Sydney. Thesis of university of New South Wales.

Chen, K, and Yu, L. (2007). Microscopic traffic-emission simulation and case study for evaluation of traffic control strategies, J Transpn Sys Eng & IT, 2007, 7(1), 93−100.

Chevallier, E. (2005). A microscopic modelling framwork for estimating emission from traffic management policier. Report Master of science of the University of London.

Chevallier, E., Leclercq, L., (2008). Macroscopic investigation of microscopic merging models at unsignalized intersections. In Transportation Research Board, Washington DC.

Chevallier, E., Leclercq, L., (2008b). A microscopic dualregime model for single-lane roundabouts. Submitted in Journal of Transportation Engineering.

Choudrie, S.L., Brown, L., Miln, R., Murrells, T.P., Thidtlethwaite, G., Watterson, J D. Jackson, J. (2008). UK greenhouse gas inventory, 1990 to 2006. AEA Technology, Harwell, Oxfordshire.

Cimorelli, A.J., Perry, S.G., Venkatram, A., Weil, J.C., Paine, R.J., Wilson, R.B., Lee, R.F., Peters, W.D., Brode, R.W., (2005). AERMOD: a dispersion model for industrial source applications. Part I: general model formulation and boundary layer characterization. Applied Meteorology 44, 682–693.

Cirillo, M.C., Poli, A.A., (1992). An intercomparison of semi-empirical diffusion models under low wind speed, stable conditions. Atmospheric Environment A. General Topics 26, 765–774.

Csanady, G. (1973). Turbulent diffusion in the environment. reidel publishing company, Dordrecht, Netherlands.

Daganzo, C.F. (1980). Optimal sampling strategies for statistical models with discrete dependent variables. Transportation Science 14, 324–345.

Daganzo, C.F. (2007). Urban gridlock: Macroscopic modeling and mitigation approaches, Transportation Research part B (41), 49-62.

Davis, N., Lents, J., Osses, M., Nikkila, N., Barth, M. (2005). Part 3: Developing countries: development and application of an international vehicle emissions model. Transportation Research Record: Journal of the Transportation Research Board, 1939(1), 155-165.

Declercq, C., Pascal, M., Chanel, O., Corso, M., Ung, A., Pascal, L., Blanchard, M., Larrieu, S., Medina, S., (2012). Impact sanitaire de la pollution atmosphérique dans neuf villes françaises. Résultats du projet Aphekom.

Deletraz, G. (2002): Géographie des risques environnementaux liés aux transports routiers en montagne - Incidence des émissions d'oxydes d'azote en vallée d'Aspe et de Biriatou (Pyrénées). Thèse de l'Université de Pau et des Pays de l'Adour, Pau, France, 564p.

Di Sabatino, S., Kastner-Klein, P., Berkowicz, R., Britter, R. E., Fedorovich, E. (2003). The modelling of turbulence from traffic in urban dispersion models Part I: theoretical considerations. Environmental Fluid Mechanics, 3(2), 129-143.

Diakaki, C., and Papageorgiou, M., (1996). Integrated modelling and control of corridor traffic networks using the METACOR modelling tool. Dynamic systems and simulation laboratory, Technical university of Crete. Internal Report No. 8. Chania, Greece, p. 41.

Dotto, C.B.S., Kleidorfer, M., Deletic, A., Fletcher, T.D., McCarthy, D.T., Rauch, W. (2010). Stormwater quality models: performance and sensitivity analysis. Water Sci. Technol. 62, 837e843.

Dotto, C.B.S., Mannina, G., Kleidorfer, M., Vezzaro, L., Henrichs, M., McCarthy, D.T., Freni, G., Deletic, A. (2012). Comparison of different uncertainty techniques in urban stormwater quantity and quality modeling. Volume 46, Issue 8, Pages 2545–2558.

Draxler, R. R., and Hess, G. D. (1998). An overview of the HYSPLIT_4 modelling system for trajectories. Australian Meteorological Magazine, 47(4).

Duhanyan, N., Roustan, Y. (2011). Below-cloud scavenging by rain of atmospheric gases and particulates atmospheric environment, Volume 45, Issue 39, P 7201-7217.

Eichhorn, J., and Kniffka, A. (2010). The numerical flow model MISKAM: State of development and evaluation of the basic version. Meteorologische Zeitschrift,19(1), 81-90.

Elliott, A.H., Trowsdale, S.A. (2007). A review of models for low impact urban stormwater drainage. Environmental Modelling & Software 22, 394-405

El-Tabach, E., I. Tchiguirinskaia and Schertzer D. (2010). Multi-Hydro: a spatially distributed model to assess and manage runoff processes in peri-urban watersheds. Water Science and Technology (under review).

ENVIRON. (2011). User's Guide, comprehensive air quality model with extensions (CAMx), version 5.40. Available online : http ://www.camx.com.

Eskridge, R. and Rao, S. (1986). Turbulent diffusion behind vehicles: Experimentally determined turbulence mixing parameters. Atmos. Environ., 20 5,851-860.

Fallah Shorshani M., Bonhomme C., Petrucci G., André M., Seigneur C. (2012) Road traffic impact on water quality in an urban catchment (Grigny, France), *9th International Joint IWA/IAHR Conference on Urban Drainage Modelling*, Belgrade, Serbie.

Fallah Shorshani M., Seigneur C., Polo L., Chanut H., Pellan Y., Jaffrezo J.L., Charron A., André M. (2014). Atmospheric dispersion modeling near a roadway under calm meteorological conditions. Submited to Transportation Research Part D.

Fallah Shorshani M., André M., Bonhomme C., Seigneur C. (2014). Modelling chain for the effect of road traffic on air and water quality: Techniques, current status and future prospects. Submited to Environmental Modelling & Software.

Fallah Shorshani M., Bonhomme C., Petrucci G., André M., Seigneur C. (2014). Road traffic impact on urban water quality: a step toward integrated traffic, air and stormwater modeling, *Environmental Science and Pollution Research*, Volume 21, Numéro 8, Pages 5297-5310.

Fellendorf.M., Vortisch,P (2011).Validation of the microscopic traffic flow model VISSIM in different real-world situations, Preprint CD CD-ROM of 80th annual meeting, transport research board, Washington.

Fellendorf, Martin, K. Nokel, and Norbert Handke. (2000). VISUM-online-traffic management for the EXPO 2000 based on a traffic model. Proceeding of the 7th world congress on intelligent system.

Fellendorf,. M., Vortisch. P., (2010), Microscopic Traffic Flow Simulator VISSIM. International Series in Operations Research & Management Science Volume 145, pp 63-93.

Freni, G., Mannina, G., Viviani, G. (2009). Urban runoff modeling uncertainty: comparison among Bayesian and pseudo- Bayesian methods. Environ. Modell. Softw. 24, 1100-1111.

Freni, G., Mannina. G., Viviani, G. (2011). Assessment of data and parameter uncertainties in integrated water-quality model. Water Science & Technology 1913 9 63.99

Frey, H. C. (2007). Quantification of uncertainty in emission factors and inventories. In 16th Annual International conference emission inventories: Integration, Analysis, and Communications, Raleigh, NC.

Garshick, E., Laden, F., Hart, J.E., Caron, A. (2003). Residence near a major road and respiratory symptoms in U.S. Veterans; Epidemiol. 14, 728-736.

Gasperi J, Sebastian C, Ruban V, Delamain M, Percot S, Wiest L, Mirande C, Caupos E, Demare D, Diallo Kessoo M, Saad M, Schwartz JJ, Dubois P, Fratta C, Wolff H, Moilleron R, Chebbo G, Cren C, MilletM, Barraud S, GromaireMC (2013). Micropollutants in urban stormwater: occurrence, concentrations, and atmospheric contributions for a wide range of contaminants in three French catchments. Environmental Science and Pollution ResearchGauderman, W.J., Avol, E., Lurmann, F., Kuenzli, N., Gilliland, F., Peters, J., McConnell, R. Childhood. (2005). Asthma and Exposure to Traffic and Nitrogen Dioxide; Epidemiol., 16, 737-743.

Godlewski, E., Raviart, P.A. (1991) Hyperbolic systems of conservation laws. Paris: Ellipses SMAI, 252p.

Goliff, W. S., Stockwell, W. R., Lawson, C. V. (2013). The regional atmospheric chemistry mechanism, version 2. Atmospheric Environment, 68, 174-185.

Gousseau, P., Blocken, B., Stathopoulos, T., Van Heijst, G. J. F. (2011). CFD simulation of near-field pollutant dispersion on a high-resolution grid: a case study by LES and RANS for a building group in downtown Montreal.Atmospheric Environment, 45(2), 428-438.

Graff, A. (2002). The new German regulatory model–a Lagrangian particle dispersion model. In 8th international conference on harmonisation within atmospheric dispersion modelling for regulatory purposes (pp. 14-17).

Grell, G., Peckham, S., Schmitz, R., McKeen, S., Frost, G., Skamarock, W. Eder, B. (2005). Fully coupled 'online' chemistry in the WRF model. Atmos. Env., 39:6957-6976.

Gromaire MC, Robert-sainte P, Bressy A, Saad M, De Gouvello B, Chebbo G, (2011) Zn and Pb emissions from roofing materials - modelling and mass balance attempt at the scale of a small urban catchment. Source: Water Sci. Technol., 63, 2590-2597

Gunawardena, J., Egodawatta, P., Ayoko, G.A., Goonetilleke, A. (2012). Atmospheric deposition as a source of heavy metals in urban stormwater. Atmospheric Environment, S1352-2310(12)01130-2

Hanna, S. R., J. C. Chang, and M. E. Fernau. (1998). Monte Carlo estimates of uncertainties in predictions by a photochemical grid model (UAM-IV) due to uncertainties in input variables, Atmos. Environ., 32, 3619–3628.

Hanna, S. R., Z. Lu, H. C. Frey, N. Wheeler, J. Vukovich, S. Arunachalam, M. Fernau, and D. A. Hansen (2001). Uncertainties in predicted ozone concentrations due to input uncertainties for the UAM-V photochemical grid model applied to the July 1995 OTAG domain, Atmos. Environ., 35, 891–903.

Hannouche A, Chebbo G, Ruban G, Tassin B, Lemaire BJ, Jonnais C, (2011) Relationship between turbidity and total suspended solids concentration within a combined sewer system. Source: Water Sci. Technol., 64, 2445-2452.

Hatzopoulou, M. and E.J. Miller. (2010). Linking an activity-based travel demand model traffic emission and dispersion models: Transport's contribution to air pollution in Toronto. Transport and Environment. Volume 16, Issue 6, P. 316-325.

HBEFA, (2010). Handbook Emission Factors for Road Transport. Tech. rep., INFRAS, HBEFA 3.1 URL:. http://www. hbefa. net/e/index. html.

Hertel, O. and Berkowicz, R. (1989a). Modelling NO2 concentrations in a street canyon. DMU Luft A-131, page 31p.

Hertel, O. and Berkowicz, R. (1989b). Modelling pollution from traffic in a street canyon. Evaluation of data and model development. DMU Luft A-129, page 77p.

Hertel, O. and Berkowicz, R. (1989c). Operational street pollution model (OSPM). evaluation of the model on data from st. Olavs street in Oslo. DMU Luft A-135.

Heinrich, J., Topp, R., Gehring, U., Thefeld, W. (2005). Traffic at residential address, respiratory health, and atopy in adults: the national german health survey 1998; Environ. Res., 98, 240-249.

Hidy, GM., Brook, J. R., Demerjian, K. L., Molina, L. T., Pennell, W. T., Scheffe, R. D. (Eds.). (2011). Technical challenges of multipollutant air quality management. New York: Springer, 553pp.

Hirschmann.K, M. Zallinger, M. Fellendorf, S. Hausberger. (2010). A New Method to Calculate Emissions with Simulated Traffic Conditions, Annual Conference on Intelligent Transportation Systems,13th International IEEE.

Hirtl, M. and Baumann-Stanzer, K. (2007). Evaluation of two dispersion models (ADMS-Roads and LASAT) applied to street canyons in Stockholm, London and Berlin. Atmospheric Environment, 41, 5959-5971.

Hjortenkrans, D. S., Bergbäck, B. G., Häggerud, A. V. (2007). Metal emissions from brake linings and tires: case studies of Stockholm, Sweden 1995/1998 and 2005. Environ. Sci. Technol., 41, 5224-5230.

Holmes, N.S., Morawska, L. (2006). A review of dispersion modelling and its application to the dispersion of particles: An overview of different dispersion models available. Atmospheric Environment 40, 5902–5928.

Hossain, I., Imteaz, M., Gato-Trinidad, S., Shanableh, A. (2010). Development of a catchment water quality model for continuous simulations of pollutants build-up and wash-off. International Journal of Civil and Environmental Engineering, 2(4), 210-217.

Houghton, J.T., Meira Filho, L.G., Lim, B., Treanton, K., mamaty, I., Bonduki, I., Griggs, D.J. and Callender, B.A., (1996). Revised IPCC Guidelines for national greenhouse gas inventories. Refrence manuel, vol. 3, by http://www.ipcc-nggip.iges.or.jp/public/gl/invs6.htm.

Huber, A. H. (1991). Wind tunnel and Gaussian plume modeling of building wake dispersion. Atmospheric Environment. Part A. General Topics, 25(7), 1237-1249.

Hugrel C, Joumard R, (2004) French fleet composition (1970-2025). Report: LTE n°0420, 2004, IFSTTAR, Bron, France. http://www.inrets.fr/ur/lte/publi-autresactions/notedesynthese/hugrel-dossier/Rapport1.pdf

INERIS (2000) Hydrocarbures Aromatiques Polycycliques dans l'air ambient (HAP). PAH in ambient air. In French. Report. Institut National de l'Environnement Industriel et des Risques (INERIS), Laboratoire central de surveillance de la qualité de l'air.

Jacobson, C.R. (2011). Identification and quantification of the hydrological impacts of imperviousness in urban catchments: A review Journal of Environmental Management 92,1438-1448.

Janssen, N.A.H., van Vliet, P.H.N., Aarts, F., Harssema, H., Brunekreef, B. (2002). Assessment of exposure to traffic related air pollution of children attending schools near motorways; Atmos. Environ., 35, 3875-3884.

Kakooei, H., Kakooei, A.A. (2007). Measurement of PM10, PM2.5 and TSP Particle 24 Concentrations in Teharan Uran. Journal of Applied Sciences 7(20), 3081-3085.

Kanso, A., Gromaire, M.C., Gaume, E., Tassin, B., Chebbo, G., (2003). Bayesian approach for the calibration of models: application to an urban stormwater pollution model. Water Sci. Technol. 47, 77e84.

Kanso, A., Chebbo, G., Tassin, B. (2004). Application of MCMC–GSA model calibration method to urban runoff quality modelling. Journal of Reliability Engineering & System Safety 32 (3), 56–68.

Karamchandani, P., L. Santos, I. Sykes, Y.Zhang, C. Tonne., C. Seigneur. (2000). Development and evaluation of a state-of-the-science reactive plume model, Environ. Sci. Technol., 34, 870-880.

Karamchandani, P., Lohman, K. Seigneur, C. (2009). Using a sub-grid scale modeling approach to simulate the transport and fate of toxic air pollutants. Environ. Fluid Mechanics, 9:59-71.

Karamchandani, P., Vijayaraghavan, K. Yarwood, G. (2011). Sub-grid scale plume modeling. Atmosphere, 2:389-406.

Kastner-Klein, P., Berkowicz, R., Plate, E. J. (2000). Modelling of vehicle-induced turbulence in air pollution studies for streets. International Journal of Environment and Pollution, 14, 496-507.

Ken M.U, Kreider M.L, Panko M.J, (2013) Comparison of tire and road wear particle concentrations in sediment for watersheds in France, Japan, and the United States by quantitative pyrolysis GC/MS Analysis. Environ. Sci. Technol., in press, doi:10.1021/es400871j.

Kerstin L. Kenty, Noreen D. Poor, Keith G. Kronmiller, William McClenny, Clark King, Thomas Atkeson, Scott W. Campbell, (2007). Application of CALINE4 to roadside NO/NO2 transformations, Atmospheric Environment, Volume 41, Pages 4270-4280,

Kim, Y., Seigneur, C., Duclaux, O. (2014). Development of a plume-in-grid model for industrial point and volume sources: application to power plant and refinery sources in the Paris region. Geoscientific Model Development, 7(2), 569-585.

Kouridis, C., Gkatzoflias, D., Kioutsioukis, J., Ntziachristos, L., Pastorello,C., Dilara, P., (2010). Uncertainty estimates and guidance for road transport emission calculations, European Union, ISBN 978-92-79-15307-5.

Kousoulidou, M., Ntziachristos, L., Mellios, G., Samaras, Z. (2008). Road-transport emission projections to 2020 in European urban environments.Atmospheric Environment, 42(32), 7465-7475.

Laval, J., Leclercq, L., (2008). Microscopic modeling of the relaxation phenomenon using a macroscopic lane-changing model. Transportation Research Part B, 42 (6), 511-522.

Le Tertre, A., Henschel, S., Atkinson, R. W., Analitis, A., Zeka, A., Katsouyanni, K., Medina, S. (2014). Impact of legislative changes to reduce the sulphur content in fuels in Europe on daily mortality in 20 European cities: an analysis of data from the Aphekom project. *Air Quality, Atmosphere & Health*, 1-9.

Leclercq, L., Laval, J., (2007). A multiclass car-following rule based on the LWR model. In Traffic and Granular Flow, Paris.

Leclercq, L., Laval, J., Chevallier, E., (2007). The Lagrangian coordinates and what it means for first order traffic flow models. In Allsop, RE., Bell, MGH., Heydecker, BG. (Ed.), ISTTT, 735-753.

Leclercq, L., Laval, J., Chevallier, E. (2007). The Lagrangian coordinates and what it means for first order traffic flow models. Proceedings of the 17th International Symposium on Transportation and Traffic Theory, Ed.: Allsop, R.E., Bell, M.G.H., Heydecker, B.G., Elsevier, London, 735-753.

Leclercq, L., & Bécarie, C. (2012). A meso LWR model designed for network applications. In Transportation Research Board 91th Annual Meeting (Vol. 118, p. 238).

Legret, M., C. Pagotto (1999). Evaluation of pollutant loadings in the runoff waters from a major rural highway, Sci. Total Environ., 235, 143-150.

Leonard, D.R., Power, P., Taylor. N.B. (1989). CONTRAM: structure of the model, Transportation research laboratory, Crowthorn.

Lighthill, M. J., and Whitham, G. B. (1955). On kinematic waves. II. A theory of traffic flow on long crowded roads. Proceedings of the Royal Society of London. Series A. Mathematical and Physical Sciences, 229(1178), 317-345.

Lim. L.L, Susan J. Hughes, Emma E. Hellawell. (2005). Integrated decision support system for urban air quality assessment, Environmental Modelling & Software 20 947-954.

Lin, J., Yi-Chang Chiu, Song Bai, Vallamsundar, S. (2011). TRB 90 th Annual Meeting #137, January 23.

Lindblom, E., Madsen, H., Mikkelsen, P.S., (2007). Comparative uncertainty analysis of copper loads in stormwater systems using GLUE and grey-box modeling. Water Sci. Technol. 56, 11e18.

Liu, R. (2005). The DRACULA dynamic network microsimulation model. In simulation approaches in transportation analysis (pp. 23-56). Springer US.

Liu A., Egodawatta P., Kjolby M.J. and Goonetilleke A. (2010). Development of pollutant build-up parameters for MIKE URBAN for Southeast Queensland, Australia. *In Proceedings of the International MIKE by DHI Conference*.

Loubet, B., Aubry, C., Dugay, F., Petit, C., Missonnier, J., Remy, E., Honore, C., Feiz, A.A., Blondeau, C,. Cordeau, E., Mauclair, C,. Durand, B,. De Biasi, L., Kaufmann, A,. AMPE, C,. Hibault, C., Cellier, P. (2010). Concentrations and deposition of pollutants in the vicinity of a highway near Paris. Final report, Programme PRIMEQUAL 2 / PREDIT, Paris, France.

Madireddy, M., De Coensel, B., Can, A., Degraeuwe, B., Beusen, B., De Vlieger, I., Botteldooren, D. (2011). Assessment of the impact of speed limit reduction and traffic signal coordination on vehicle emissions using an integrated approach. Transportation research part D: transport and environment,16(7), 504-508.

Mallet, V., Quélo, D., Sportisse, B., Ahmed de Biasi, M., Debry, E., Korsakissok, I., Wu, L., Roustan, Y., Sartelet, K., Tombette, M. et Foudhil, H. (2007). Technical Note: The air quality modeling system Polyphemus. Atmos. Chem. Phys., 7(20):5479-5487.

Mannina, G., Freni, G., Viviani, S., Sægrov, L. S. Hafskjold. (2006). Integrated urban water modelling with uncertainty analysis. Water Sci. Technol. 54(6–7), 379–386.

Matzoros. A (1990). Results from a model of road traffic air pollution, featuring junction effects and vehicle operating modes Traffic Engineering and Control, 31 (1), pp. 24–35.

McConnell, R., Berhane, K., Yao, L., Jerrett, M., Lurmann, F., Gilliland, F., Kuenzli, N., Gauderman, J., Avol, E., Thomas, D., Peters, J. (2006). Traffic, susceptibility, and childhood asthma; Environ. Health Perspect. 114, 766-772.

Milliez, M. and Carissimo, B. (2007). Numerical simulations of flow and pollutant dispersion in an idealized urban area, for different meteorological conditions. Boundary-Layer Meteor., 122(2):321-342.

Misra, A., Roorda, M.G., MacLean, H.l., (2013). An integrated modelling approach to estimate urban traffic emissions. Atmospheric Environment 73, 81-91.

Nam, E.K, Gierczak C A, Bulter J W. (2003), Acomparison of real-world and modeled emission under condition of variable driver aggressiveness. Ford Scientific Research Laboratory, MI 48121-2053.

Namdeo.A, G.Mitchell, R. Dixon (2002). TEMMS: an integrated package for modelling and mapping urban traffic emissions and air quality. Environmental Modelling & Software 17,179–190.

Noland, R.B, Quddus.M (2006). Flow improvement and vehicle emission:effet of trip generation and emission control technology. Transportation Research:Part D,vol, 11.PP1-14.

Ntziachristos L, Gkatzoflias D, Kouridis C, Samaras, Z, (2009). COPERT: a European road transport emission inventory model. In information technologies in environmental engineering, I.N. Athanassialis et al., eds., 491–504, Environmental Science and Engineering, Springer-Verlag Berlin Heidelberg.

Obropta, C., J.S. Kardos. (2007). Review of urban stormwater quality models: Deterministic, stochastic, and hybrid approaches. Journal of the American Water Resources Association. Vol.43, No.6.

Ortuzar, J. D., Willumsen, L. G. (2011). Modelling transport, 4th. Edition. Chichester: John Wiley, Sons Ltd.

Panis. L, Broekx. S, Liu.R. (2006). Modelling instantaneous traffic emission and the influence of traffic speed limits, Science of the Total Environment 371, 270–285

Park J.Y, Noland R.B., Polak J.W. (2001). A Microscopic model of air pollutant concentration : comparison of simulated results with measured and macroscopic estimates, paper presented at the 80th Annual Meeting of the Transportation Research Board, Washington, DC.

Park, D., Roesner, L.A. (2012). Evaluation of pollutant loads from stormwater BMPsto receiving water using load frequency curveswith uncertainty analysis.Volume 46, Issue 20, 15, Pages 6881–6890.

Paatero, P., (1997). Least squares formulation of robust non-negative factor analysis. Chemom. Intell. Lab. Syst. 37, 23–35.

Paatero, P., Tapper, U., (1994). Positive matrix factorization: A non-negative factor model with optimal utilization of error estimates of data values. Environmetrics 5, 111–126.

Patnaik, G., and Boris, J. (2010). FAST3D-CT: an LES model for urban Aerodynamics Model. In *Proceedings: International Symposium on Computational Wind Engineering*.

Pay, M.T, P. Jiménez-Guerrero, J.M. Baldasano (2011) Implementation of resuspension from paved roads for the improvement of CALIOPE air quality system in Spain, Atmos. Environ. 45, 802-807.

Petrucci G, Rioust E, Deroubaix J-F., Tassin B. (2013). Do stormwater source control policies deliver the right hydrologic outcomes? J. Hydrology, 485, 188-200.

Petrucci G., Gromaire M. C., Fallah Shorshani M., Chebbo G. (2014). Non-point source pollution of urban stormwater runoff: a methodology for primary sources' analysis, *Environmental Science and Pollution Research*. doi:10.1007/s11356-014-2845-4 (available online).

Pirjola, L., Paasonen, P., Pfeiffer, D., Hussein, T., Hameri, K., Koskentalo, T., Virtanen, A., Ronkko, T., Keskinen, J., Pakkanen, T.A., Hillamo, R.E. (2006). Dispersion of particles and trace gases nearby a city highway: mobile laboratory measurements in Finland; Atmos. Environ., 40, 867-879.

Pitt, R., Voorhees, J. (2002). SLAMM, the source loading and management model. Wet-weather flow in the urban watershed: technology and management, 103-139.

Polo Rehn L. (2013). Caractérisation et impacts des émissions de polluants du transport routier : apports méthodologiques et cas d'études en Rhône-Alpes, in France http://tel.archives-ouvertes.fr/tel-00876623.

Polo Rehn, L., Waked, A., Charron, A., Piot, C., Besombes, J. L., Marchand, N., Guillaud, G., Favez, O., Jaffrezo, J. L. (2014). Estimation de la contribution des émissions véhiculaires à l'échappement et hors échappement aux teneurs atmosphériques en PM10 par Positive Matrix Factorization (PMF). Poll Atmos., 221, *2268-3798*.

Promeyrat S. (2001). Contribution à l'étude de la pollution atmosphérique autoroutière – caractérisation des flux de deposition de la contamination métallique de l'environnement de proximité (The contribution of case study of highway air pollution- characterization of metallic contamination flow). Ph.D. thesis, University of Metz, France.

Pullen, J., Boris, J.P.,Young, T., Patnaik, G., Iselin, J. (2005). A comparison of contaminant plume statistics from a Gaussian puff and urban CFD model for two large cities. Atmospheric Environment 39, 1049–1068.

Pun, B. K., and Seigneur, C. (2001). Sensitivity of particulate matter nitrate formation to precursor emissions in the California San Joaquin Valley.Environmental science & technology, 35(14), 2979-2987.

Quadstone. (2002). PARAMICS V4.0 User Guide and Reference Manuals, Quadstone limited, Edinburgh, U.K., Lee, D-H. PARAMICS simulations at the California ATMIS testbed: A benchmark analysis. Proceedings of

the 6th International conference on the applications of advanced technologies in transportation engineering.

Qian, W., and Venkatram, A. (2011). Performance of steady-state dispersion models under low wind-speed conditions. Boundary-layer meteorology, 138, 475-491.

Refshaard, J. C., Storm, B., Singh, V. P. (1995). MIKE SHE. Computer models of watershed hydrology., 809-846.

Richards, P. I. (1956). Shock waves on the highway. Operations research, 4(1), 42-51.

Rodriguez F., Andrieu H., Morena F. (2008). A distributed hydrological model for urbanized areas. Model development and application to urban catchments. Journal of Hydrology 351:268-287.

Rossman, L. A. (2010). Storm water management model user's manual, version 5.0. National Risk Management Research Laboratory, Office of Research and Development, US Environmental Protection Agency.

Roustan. Y, (2005). Modélisation de la dispersion atmospherique du mercure, du plomb et du cadmium l'échelle européenne. Ph.D. thesis, École Nationale des Ponts et Chaussées, France. 167pp.

Russell, A., and R. Dennis (2000). NARSTO critical review of photochemical. models and modeling, Atmos. Environ., 34, 2234– 2283.

Sabin L.D., Lim J.H., Stolzenbach K.D., Winer A.M. and Schiff K.C. (2005). Contribution of trace metals from atmospheric deposition to stormwater runoff in a small impervious urban catchment. Water Research, (39), 3929–3937

Sabin L.D, Lim J.H, Venezia M.T, Winer A.M, Schiff K.C, and Stolzenbach K.D. (2006). Dry deposition and resuspension of particle-associated metals near a freeway in Los Angeles. Atmos. Environ, 40, 7528-7538.

Sahlodin, A. M., Sotudeh-Gharebagh, R., Zhu, Y. (2007). Modeling of dispersion near roadways based on the vehicle-induced turbulence concept.*Atmospheric Environment*, *41*(1), 92-102.

Sartelet, K., Debry, E., Fahey, K., Roustan, Y., Tombette, M. Sportisse, B. (2007). Simulation of aerosols and related species over Europe with the Polyphemus system. part I : model-to-data comparison for 2001. Atmos. Env., 41:6116-6131.

Schmidt, M., Schäfer, R.P. (1998). An integrated simulation system for traffic induced air pollution. Environmental modelling & software 13, 295-303.

Schwede, D. B., Dennis, R. L., Bitz, M. A. (2009). The watershed deposition tool: A tool for incorporating atmospheric deposition in water-quality analyses, J. Amer. Water Res. Assoc.,45, 973–985.

Seigneur, C., Wu, X. A., Constantinou, E., Gillespie, P., Bergstrom, R. W., Sykes, I., Venkatram, A., Karamchandani, P. (1997). Formulation of a second-generation reactive plume and visibility model. Journal of the Air & Waste Management Association, 47(2), 176-184.

Seinfeld, J.H and S.N. Pandis (2006) Atmospheric Chemistry and Physics: From Air Pollution to Climate Change, 2nd edition, John Wiley & Sons.

Sharan, M., Anil Kumar Y., M. P. Singh, (1996). Plume dispersion simulation in low-wind conditions using coupled plume segment and gaussian puff approaches. J. Appl. Meteor., 35, 1625–1631.

Singh, V., & Murty Bhallamudi, S. (1998). Conjunctive surface-subsurface modeling of overland flow. *Advances in Water Resources*, *21*(7), 567-579.

Smit R. (2006). An examination of congestion in road traffic emission models and their application to urban road networks, Phd Report.

Smit, R., Smokers, R., Rabé, E. (2007). A new modelling approach for road traffic emissions: VERSIT+. Transportation research part D: transport and environment, 12(6), 414-422.

Smit R., Brown A.L. and Chan Y.C. (2008). Do air pollution emissions and fuel consumption models for roadways, include the effects of congestion in the roadway traffic flow? *Environmental Modelling & Software*, (23), 1262–1270

Smit R, Ntziachristos L, Boulter paul,. (2010) Validation of road vehicle and traffic emission models – A Review and meta-analysis. . Atmos. Environ., 44, 2943–2953.

Soulhac, L., Salizzoni, P., Cierco, F.-X. Perkins, R. (2011). The model SIRANE for atmospheric urban pollutant dispersion ; part I, presentation of the model. Atmos. Env., 45:7379-7395.

Soulhac, L., Salizzoni, P., Mejean, P., Didier, D. Rios, I. (2012). The model SIRANE for atmospheric urban pollutant dispersion ; part II, validation of the model on a real case study. Atmos. Env., 49:320-357.

Sportisse, B. (2007). A review of parameterizations for modelling dry deposition and scavenging of radionuclides. Atmospheric Environment, 41, 2683-2698.

Sportisse, B (2009) Fundamentals in Air Pollution: From Processes to Modeling, Springer.

Stevanovic A, Stevanovic .J, Zhang .K, Batterman .K. (2009). Optimizing traffic control to reduce fuel consumption and vehicular emissions, Vol 2128, 105-113.

Stohl, A., Hittenberger, M. Wotawa, G. (1998). Validation of the lagrangian particle dispersion model FLEXPART against large-scale tracer experiment data. Atmos. Env., 32:4245-4264.

Sternbeck J, Sjodin A, Andréasson K. (2002). Metal emission from road traffic and the influence of resuspension—results from two tunnel studies. Atmos Environ 36:4735–4744.

Sun, N., Hong, B., Hall. H., (2013). Assessment of the SWMM model uncertainties within the generalized likelihood uncertainty estimation (GLUE) framework for a high-resolution urban sewershed, Hydrol. Process. DOI: 10.1002/hyp.9869.

Tate, J., Bell, M. C., Liu, R. (2005). The application of an integrated traffic microsimulation and instantaneous emission model to study the temporal and spatial variations in vehicular emissions at the local-scale. In Proceedings of the 14th International Symposium on Transport and Air Pollution.

Thomson, D.J., Manning, A.J. (2001). Along-wind dispersion in light wind conditions. Boundary-Layer Meteorology 98 (2), 341–358.

Thorpe A, and Harrison R.M (2008) Sources and properties of non-exhaust particulate matter from road traffic: A review. Sci. .Total Environ., 400, 270-282.

U.S. EPA (U.S. Environmental Protection Agency) (1994). User's guide to MOBILES (Mobile Source Emission Factor Model) Report # EPA-AA-AQAB-94-O1Office of air and radiation & office of mobile Sources, Ann Arbor, Michigan.

Vassilios, A. Tsihrintzis. Hamid, A. (1997). Modeling and management of urban stormwater runoff quality: A review water resources management 11: 137–164, 1997. 137.

Venkatram, A. et Horst, T. (2006). Approximating dispersion from a finite line source. Atmos. Env., 40:2401-2408.

Venkatram, A., M. Snyder, V. Isakov, (2013). Modeling the impact of roadway emissions in light wind, stable and transition conditions, Transportation Res. D, 24, 110-119.

Vezzaro, L., Ledin, A., Mikkelsen, P.S. (2012). Integrated modelling of Priority Pollutants in stormwater systems, Physics and Chemistry of the Earth, Parts A/B/C Volumes 42–44, 42–51

Vijayaraghavan.K, J. Herr, S.Y. Chen, E. Knipping. (2010). Linkage between an advanced air quality model and a mechanistic watershed model, Geosci. Model Dev. Discuss., 3, 1503–1548.

Viard, B., Pihan F., Promeyrat S. and Pihan J.C. (2004). Integrated assessment of heavy metal (Pb, Zn, Cd) highway pollution: bioaccumulation in soil, Graminaceae and land snails. Chemosphere, (55), 1349-1359.

Vlachokostas, C., Chourdakis, E., Michalidou, A.V., Moussiopoulos, N., Kelessis, A., Petrakakis, M., (2012). Establishing relationships between chemical health stressors in urban traffic environments: Prediction of toluene concentration levels in European cities. Atmos. Environ. 55, 299–310.

Wang, Y.J., Zhang, K.M. (2009). Modeling near-road air quality using a computational fluid dynamics model, CFD-VIT-RIT. Environ. Sci. Technol. 43 (20), pp 7778–7783.

Wesely M.L and Hicks B.B. (2000). A review of the current status of knowledge on dry deposition, Atmos. Environ., 34, 2261-2281.

Wicke D., Cochrane T.A. and O'Sullivan A.D. (2011). Atmospheric deposition and storm induced runoff of heavy metals from different impermeable urban surfaces. J. Environ. Monit, (1), 209-16.

Willems, P. (2008). Quantification and relative comparison of different types of uncertainties in sewer water quality modeling. Water Res. 42, 539e3551.

Wust W, Kern U, Herramanner R, (1994) Streer wash-off behaviour of heavy-metals, polyaromatic hydrocarbons and nitrophenols. Sci. Total Environ., 147, 457-463.

Xia.L Y.Shao. (2005). Modelling of traffic flow and air pollution emission with application to Hong Kong Island Volume 20, 9, 1175-1188.

Xie, Y., Chowdhury, M., Bhavsar, P., Zhou, Y. (2012). An integrated modeling approach for facilitating emission estimation of alternative fueled vehicles. Transport and Environment, 17, 15-20.

Yim, S.H.L., Barrett, S.R.H. (2012). Public Health Impacts of Combustion Emissions in the United Kingdom. Env. Sci Technol 46, 4291–4296.

Yu, S., Eder, B., Dennis, R., Chu, S.H., Schwartz, S. E. (2006). New unbiased symmetric metrics for evaluation of air quality models, Atmos. Sci. Lett., 7, 26–34.

Yuan, C., Ng, E., & Norford, L. K. (2014). Improving air quality in high-density cities by understanding the relationship between air pollutant dispersion and urban morphologies. Building and Environment, 71, 245-258.

Zallinger, M., Tate, J., Hausberger, S. (2008). An instantaneous emission model for the passenger car fleet, Proceeding of 16th International Conference, Transport and Air Pollution, Graz.

Zannetti P, (1990). Air pollution modelling: Theories, computational methods, and available software, Computational Mechanics Publications.

Zegeye.K, B. De Schutter, J. Hellendoorn, E.A. Breuness. (2010). Integrated macroscopic traffic flow and emission model based on METANET and VT-micro, Delft university of technology, Technical report 09-01.

Zhang, Y. (2008). Online-coupled meteorology and chemistry models: history, current status, and outlook. *Atmospheric Chemistry and Physics*, *8*(11), 2895-2932.

Zhang, K. and Batterman, S., (2010). Near-road air pollutant concentrations of CO and PM2.5: A comparison of MOBILE6.2/CALINE4 and generalized additive models, Atmospheric Environment, 44, 1740-1748,

Zhang, Y., Bocquet, M., Mallet, V., Seigneur, C. and Baklanov, A. (2012). Real-time air quality forecasting, part I : History, techniques, and current status. Atmos. Env., 60:632-655.

Zhang L, S. Gong, J. Padro, L. Barrie. (2001). A size-segregated particle dry deposition scheme for an atmospheric aerosol module. Atmos. Environ. 35, 549-560.

Zgheib, S., (2009). Flux et sources des polluants prioritaires dans les eaux urbaines en lien avec l'usage du territoire, Ecole Nationale des Ponts et Chaussées, Paris, France (2009) 349 p.

Zmirou, D., S. Gauvin, I. Pin, I. Momas, F. Sahraoui, et al. (2004). Traffic related air pollution and incidence of childhood asthma: results of the Vesta case-control study, J. Epidemiology Community Health, 58, 18-23.

Zoppou, C., (2001). Review of urban storm water models. Environmental Modelling and Software 16, 195-231.

8 Annexe

Annexe A : Le Modèle COPERT

COPERT (Computer Programme to calculate Emissions from Road Transport) est un outil disponible sur internet (http://www.emisia.com/copert/), dont la méthode est principalement explicitée dans la méthodologie européenne d'inventaire (Guidebook, documents EMEP/EEA 2009 a, b, et c) qui distingue les émissions à l'échappement, les émissions par évaporation de carburant, par usure de pneumatiques et des freins, et par abrasion de la route.

COPERT4 (2007, mise à jour 2011 v4.9) s'appuie sur des mesures d'émission sur cycles d'essai représentatifs et concerne l'ensemble des polluants atmosphériques des différentes catégories de véhicules routiers. Il permet de réaliser un inventaire agrégé d'émission agrégé sur un territoire, en distinguant les milieux « urbain », « rural » et « autoroute », à partir des véhicules x kilomètres selon ces milieux et des vitesses de circulation représentatives, et calcule :

- les émissions à chaud pour les véhicules légers (voitures, véhicules utilitaires légers, 2-roues) et lourds (camions, autobus et autocars) ;
- les surémissions à froid pour les véhicules légers ;
- les surémissions liées à la pente et au chargement pour les véhicules lourds ;
- les corrections liées aux améliorations des carburants ;
- les corrections liées au vieillissement des catalyseurs et leur maintenance ;
- les émissions par évaporation des véhicules légers (essence) ;
- l'émission non échappement (usure des freins et pneumatiques seulement).

Tous les calculs de la méthodologie COPERT4 sont accessibles et paramétrables (surémissions à froid, évaporations, corrections liées aux spécificités des carburants, corrections liées à l'ancienneté et l'entretien des véhicules).

Les véhicules sont subdivisés en 242 types (63 VP, 14 VUL, 99 PL, 46 bus, 20 deux roues) selon le carburant utilisé, la taille du moteur ou le poids du véhicule, la technologie et les réglementations portant sur les émissions.

Les émissions totales sont calculées par sommation sur les catégories détaillées de véhicules, des différents phénomènes d'émissions (échappement de moteur chaud et froid, et évaporation), chacun résultant de produits de facteurs d'émission par une donnée d'activité (par exemple, véhicules-km). Les émissions non échappement ne sont pas toujours comptabilisées. Les émissions du véhicule dépendant fortement des conditions de circulation (et de fonctionnement du moteur), on différentie également les émissions en zones urbaine, rurale et autoroute.

$$E_{total} = E_{chaud} + E_{froid} + E_{évaporation}$$

$$E_{total} = E_{Urbain} + E_{rural} + E_{autoroute}$$

Émission à chaud

L'émission à chaud dépend de la distance parcourue par chaque type de véhicule, de sa vitesse (ou le type de route), son âge (dégradation), la taille du moteur ou le poids du véhicule. Pour une période de temps (heure, jour, an) et un type de véhicule, elle s'exprime comme suit :

$$\text{Emission [g]} = \text{FE [g/km]} \times \text{N [veh]} \times \text{Km [km/veh]}$$

- FE facteur ou fonction spécifique d'émission (fonction de la vitesse de circulation)
- N nombre des véhicules
- km kilométrage (annuel) par véhicule

Par conséquent, la formule est applicable pour le calcul des émissions à chaud des polluants des groupes 1 et 3 (voir Tableau 8.2 et 8.3).

$$E_{chaud\ ;i,k,r} = N_k \times M_{k,r} \times e_{chaud\ ;i,k,r}$$

avec

- $E_{chaud\ ;i,k,r}$ émission à chaud de polluant i, produit dans la période concernée par véhicule de technologie k sur la route de type r (ou milieu urbain, rural, autoroute),
- N_k nombre de véhicules ayant technologie k,
- $M_{k,r}$ kilométrage des véhicules de technologie k [km/veh] sur la route de type r,
- $e_{chaud\ ;i,k,r}$ facteur spécifique d'émission [g/km] pour le polluant i, technologie k, route r.

Cette formule est également utilisée pour calculer la consommation de carburant.

Les fonctions d'émissions variant fortement selon la vitesse des véhicules, on considérera des vitesses moyennes représentatives pour chaque type de route (urbain-20 km/h, rural-60 km/h et autoroute-100 km/h), ou alternativement des distributions de vitesses. Ces fonctions sont de la forme générale suivante :

$$EF = (a+c\times V+e\times V^2)/(1+b\times V+d\times V^2)$$

où les coefficients a, b, c, d, e ont été déterminés par régression sur les données expérimentales d'émission et les caractéristiques des cycles de conduite.

Tableau 8.1. Coefficients des fonctions d'émission de Copert4

Pollutant	Emission Standard	Engine capacity	Speed Range (km/h)	R^2	a	b	c	d	e
CO	Euro 1	All capacities	10−130	0.87	1.12E+01	1.29E-01	-1.02E-01	-9.47E-04	6.77E-04
	Euro 2	All capacities	10−130	0.97	6.05E+01	3.50E+00	1.52E-01	-2.52E-02	-1.68E-04
	Euro 3	All capacities	10−130	0.97	7.17E+01	3.54E+01	1.14E+01	-2.48E-01	
	Euro 4	All capacities	10−130	0.93	1.36E-01	-1.41E-02	-8.91E-04	4.99E-05	
HC	Euro 1	All capacities	10−130	0.82	1.35E+00	1.78E-01	-6.77E-03	-1.27E-03	
	Euro 2	All capacities	10−130	0.95	4.11E+06	1.66E+06	-1.45E+04	-1.03E+04	
	Euro 3	All capacities	10−130	0.88	5.57E-02	3.65E-02	-1.10E-03	-1.88E-04	1.25E-05
	Euro 4	All capacities	10−130	0.10	1.18E-02		-3.47E-05		8.84E-07
NO_x	Euro 1	All capacities	10−130	0.86	5.25E-01		-1.00E-02		9.36E-05
	Euro 2	All capacities	10−130	0.52	2.84E-01	-2.34E-02	-8.69E-03	4.43E-04	1.14E-04
	Euro 3	All capacities	10−130	0.80	9.29E-02	-1.22E-02	-1.49E-03	3.97E-05	6.53E-06
	Euro 4	All capacities	10−130	0.71	1.06E-01		-1.58E-03		7.10E-06

Surémission à froid

Cette surémission n'affecte que les milieux urbain et rural, les véhicules particuliers et utilitaires légers, et ne varie pas avec l'âge du véhicule. Pour un polluant donné, l'équation s'écrit :

$$E_{froid,j,V} = \beta \text{ x } E_{chaud,j,Vurbain} \text{ x } (e_{surémission,j} - 1)$$

avec :

- $E_{froid,j,V}$ = surémission à froid pour les véhicules de type j circulant à la vitesse V
- β = fraction des kilomètres parcourus à froid par les véhicules de type j (dépend de la température ambiante et de la distance moyenne du déplacement)
- $E_{froid,j,V}$ = surémission à froid pour le véhicule de type j circulant à la vitesse V
- $e_{surémission,j}$ = coefficient de surémission à froid pour le véhicule de type j (dépend aussi de la température ambiante)
- $E_{chaud,j,Vurbain}$= émission à chaud pour le véhicule j circulant à la vitesse V_{urbain}
- V_{urbain}= vitesse de circulation en milieu urbain (valeur unique pour l'ensemble du réseau dans COPERT, < à 50km/h)
-

Émissions par évaporation

L'émission (véhicules essence seulement) est fonction de la cylindrée, des volumes du réservoir et du dispositif de piégeage (canister ou filtre à charbon) des vapeurs de carburant, des conditions de températures et des caractéristiques du carburant (volatilité). Le calcul distingue 3 facteurs d'émission selon l'équation suivante :

$$E_{Voc} = \sum_s D_s \times \sum_j N_j \times \left(HS_j + e_{d,j} + RL_j \right)$$

avec,

- E_{VOC} = l'émission de COV par évaporation sur une période (année, etc.)
- D_s = le nombre de jours pour lesquels le facteur d'émission saisonnier doit être appliqué
- N_j = le nombre de véhicules à essence de type j

et les facteurs d'émission par évaporation :

- HS_j = la moyenne quotidienne des évaporations après arrêt moteur chaud du véhicule de catégorie j [g/jour], fonction du nombre de trajets journalier
- $e_{d,j}$ = la moyenne des évaporations journalières dues aux variations de température ambiante pour le véhicule de type j en stationnement [g/jour]
- RL_j = la moyenne quotidienne des évaporations du véhicule j en marche [g/jour].

Les facteurs d'émissions sont fonctions du type de véhicule, de la saison, de la température, de la taille de l'absorbeur de vapeur du carburant, de la taille du moteur et de la pression de vapeur saturante.

$$HS_j = x \{c [p\ e_{s,hot,c} + (1 - p)\ e_{s,warm,c}] + (1 - c)\ e_{s,hot,fi}\}$$

$$RL_j = x \{c [p\ e_{r,hot,c} + (1 - p)\ e_{r,warm,c}] + (1 - c)\ e_{r,hot,fi}\}$$

Ces facteurs d'émissions sont donnés dans le Guidebook (EMEP/EEA)

Tableau 4. Facteurs d'émission par évaporation des véhicules particuliers

	summer		winter		summer		winter		summer		winter	
T. variation (°C)	20−35	10−25	0−15	-5−10	20−35	10−25	0−15	-5−10	20−35	10−25	0−15	-5−10
Fuel DVPE (kPa)	60	70	90	90	60	70	90	90	60	70	90	90
	Gasoline passenger cars < 1.4 l — uncontrolled				Gasoline passenger cars 1.4–2.0 l — uncontrolled				Gasoline passenger cars > 2.0 l — uncontrolled			
e_d (g/day)	3.90	2.35	1.74	1.24	4.58	2.76	2.04	1.45	5.59	3.36	2.49	1.77
$e_{s,hot,fi}$ (g/proced.)	0.10	0.07	0.04	0.04	0.10	0.07	0.04	0.04	0.10	0.07	0.04	0.04
$e_{s,warm,c}$ (g/proced.)	8.48	5.09	3.75	2.63	10.01	6.01	4.42	3.10	12.29	7.38	5.43	3.80
$e_{s,hot,c}$ (g/proced.)	11.93	7.16	5.27	3.69	14.08	8.45	6.22	4.36	17.31	10.39	7.65	5.35
$e_{r,hot,fi}$ (g/trip)	0.13	0.08	0.06	0.04	0.13	0.08	0.06	0.04	0.13	0.08	0.06	0.04
$e_{r,warm,c}$ (g/trip)	1.84	1.11	0.81	0.53	2.15	1.30	0.95	0.67	2.62	1.58	1.15	0.81
$e_{r,hot,c}$ (g/trip)	10.05	6.03	4.44	3.11	11.85	7.12	5.24	3.67	14.56	8.74	6.43	4.50

Les émissions non échappement de particules

Les particules (PM) sont produites à la suite de l'interaction entre les pneus d'un véhicule et la surface de la route, et également lorsque les freins sont appliqués pour ralentir le véhicule. Dans les deux cas, la génération de forces de cisaillement par le mouvement est le principal mécanisme de production de particules. Un mécanisme secondaire consiste à l'évaporation du matériau de surface aux hautes températures.

Deux méthodes sont proposées dans le Guidebook 2009, mais COPERT en utilise une troisième non explicitée. La première méthode exprime l'émission en fonction du nombre de

véhicules de différentes catégories, le kilométrage moyen pendant une durée définie et le facteur spécifique d'émission de véhicule de type j pour chaque polluant i.

$$TE = \sum_j N_j \times M_j \times EF_{i,j}$$

La deuxième méthode considère aussi les facteurs de fraction de masse (TSP) qui peuvent être attribués à une classe de taille de particule et un facteur de correction de la vitesse moyenne (S_s).

$$TE = \sum_j N_j \times M_j \times EF_{TSP,i,j} \times f_{s,i} \times S_s(V)$$

Données d'entrées

Les données d'entrées demandées sont :

- pour chacun des 242 types de véhicule (selon technologie, carburant, taille et réglementation pollution),
    - Les nombres de véhicules, kilométrages annuels [km/an] et totaux cumulés [km],
    - La distribution du kilométrage annuel selon les milieux urbain, rural et autoroute,
    - La vitesse de circulation selon ces milieux (avec cependant des limites basses 10km/h pour les véhicules légers, 12 km/h pour les véhicules lourds, et bus
    - La taille du réservoir et de l'absorbeur
    - Le type d'injection
- Les températures (max/min) et la tension de vapeur mensuelles,
- Les spécifications des différents carburants (teneurs en métaux lourds, soufre, HC, OC mg/kg)
- Les distances moyennes de déplacement et nombres de trajets journaliers
- Pour les véhicules lourds, l'indication de la pente de la route (-6 à +6% par pas de 2%) et du chargement (0, 50 ou 100% en poids)
- L'affectation de l'évaporation selon les milieux urbain/rural/autoroute.

Résultats de Copert

Les résultats du modèle COPERT couvrent la plupart des phénomènes d'émission (échappement, évaporation, non-échappement) et des polluants importants. Les résultats sont complétement déclinés par type d'émission (chaud, froid, évaporation, climatisation, non-échappement), par milieu (urbain/rural/autoroute) et pour tous les types de véhicules. Seules les spéciations de COV et de HAP / POP ne sont pas détaillées par types de véhicule et d'émission.

Limites de la méthode et de l'outil COPERT

Principalement adapté pour le calcul à échelles macroscopiques (agglomération, région, pays, heure, journée, année), l'approche COPERT est très largement utilisée par les États pour les inventaires nationaux d'émission de polluants, et également pour des estimations et études d'impact à échelles régionales ou d'agglomération.

Cependant, les facteurs d'émission, basés sur la vitesse moyenne et des cycles de conduite représentatifs, ne tiennent pas compte de la dynamique des conditions de circulation (accélérations, arrêts, etc.) qui peut cependant avoir un impact sur les émissions. De même, la donnée de la mesure (à échelle d'un cycle d'essai équivalent d'un trajet) qui permet leur élaboration, n'autorise guère des analyses à des échelles plus fines que plusieurs minutes ou plusieurs centaines de mètres.

De fait, l'approche n'est pas vraiment appropriée pour des calculs à échelles plus locales (rue, tronçons) ou fine d'un point de vue temporel, ni pour une approche par tronçons de voies, si ceux-ci sont envisagés à des échelles relativement microscopiques, et l'outil COPERT propose un cadre d'analyse agrégé et macroscopique en 3 milieux urbain / rural / autoroute (sans spatialisation et à échelle annuelle), non adaptée pour une analyse détaillée d'un réseau routier par exemple.

Pour ces raisons, de nombreux outils sont développés à partir de la méthode COPERT / Guidebook, pour des applications locales et intégrant généralement de nombreuses hypothèses nationales (parcs automobiles, données de météo, longueur des trajets, etc.).

Polluants

Les polluants peuvent également se diviser en quatre catégories en fonction des différentes techniques de calcul par le modèle d'émission.

- Groupe 1 : les polluants pour lesquels des fonctions d'émission ont été établies à partir de nombreuses mesures sur banc d'essai. Les émissions sont donc approchées en tenant compte des conditions de circulation (le plus souvent la vitesse moyenne) et/ou de fonctionnement du moteur (régime et couple moteur pour les véhicules lourds, température, voire charge). Ce groupe inclut notamment les COV ou HC totaux, et également la consommation de carburant, dont seront dérivées les émissions de polluants des autres groupes.

Tableau 8.2. Polluants connus selon les vitesses et conditions de fonctionnement (groupe 1)

Pollutant	**Equivalent**
Carbon monoxide (CO)	Given as CO
Nitrogen oxides (NO_x: NO and NO_2)	Given as NO_2 equivalent
Volatile organic compounds (VOCs)	Given as $CH_{1.85}$ equivalent (also given as HC in emission standards)
Methane (CH_4)	Given as CH_4
Non-methane VOCs (NMVOCs)	Given as VOCs (or HC) minus CH_4
Nitrous oxide (N_2O)	Given as N_2O
Ammonia (NH_3)	Given as NH_3
Particulate matter (PM)	The mass of particles collected on a fliter kept leblow 52°C during diluted exhaust sampling. This corresponds to $PM_{2.5}$. Coarse exhaust PM (i.e.>2.5 µm diameter) is considered to be negligible, hence PM=$PM_{2.5}$.
PM number and surface area	Given as particle number and particle active surface per kilometre, respectively

- Groupe 2 : les polluants pour lesquels peu de données existent (métaux) ou pour lesquels la conversion est immédiate (SO_2, CO_2). Les émissions sont estimées à partir de la consommation de carburant. Ce sont notamment tous les métaux (issus des carburants, des lubrifiants et de l'usure interne du moteur), ainsi que le contenu en CO_2 (Tableau 8.3).

Tableau 8.3. Polluants calculés à partir des consommations de carburant (groupe 2)

Pollutant	**Equivalent**
Carbon dioxide (CO_2)	Given as CO_2
Sulphur dioxide (SO_2)	Given as SO_2
Lead (Pb)	Given as Pb
Cadmium (Cd)	Given as Cd
Chromium (Cr)	Given as Cr
Copper (Cu)	Given as Cu
Nickel (Ni)	Given as Ni
Selenium (Se)	Given as Se
Zinc (Zn)	Given as Zn

- Groupe 3 : les polluants pour lesquels peu de données existent, et pour lesquels les émissions ne sont généralement pas connues selon les conditions de fonctionnement ou de circulation, mais seulement par grande famille de véhicules et de carburants (Tableau 8.4).

Tableau 8.4. Polluants HAP et POP donnés sous forme de spéciations (groupe 3)

Pollutant	**Equivalent**
Polycyclic aromatic hydrocarbons (PAHs) and persistent organic pollutants (POPs)	Detailed speciation, including indeno(1,2,3-cd) purene, benzo(k)fluoranthene, benzo(b)fluoranthene, benzo(g,h,i)perylene, fluoranthene, benzo(a)pyrene
Polychlorinated dibenzo dioxins (PCDDs) and polychlorinated dibenzo furans (PCDFs)	Given as dioxins and furans respectively

- Groupe 4 : les COV individuels ou par famille, qui sont estimés selon une spéciation i.e. leur proportion respective dans l'ensemble des COV non méthaniques. Bien que les COV totaux soient approchés selon les conditions de fonctionnement et les catégories détaillées des véhicules, les composés individuels ou familles de COV ne devraient pas être évalués de manière aussi détaillée car on dispose de très peu de spéciations (par grande famille de véhicule et de carburant, sans distinction des conditions opératoires).

Tableau 8.5. Polluants COV donnés sous forme de spéciation (composition) (groupe 4)

Pollutant	**Equivalent**
Alkanes (C_nH_{2n+2}):	Given in alkanes speciation
Alkenes (C_nH_{2n}):	Given in alkenes speciation
Alkynes (C_nH_{2n-2}):	Given in alkynes speciation
Aldehydes ($C_nH_{2n}O$)	Given in aldehydes speciation
Ketones ($C_nH_{2n}O$)	Given in ketones speciation
Cycloalkanes (C_nH_{2n})	Given as cycloalkanes
Aromatic compounds	Given in aromatics speciation

Annexe B : Les polluants pris en compte dans le logiciel COPCETE

Polluant	Chaud	Froid	Evaporation	Hors échap.
Dioxyde de carbone CO_2	**X**	**X**		
Oxydes d'azotes NO_x	**X**	**X**		
Monoxyde de carbone CO	**X**	**X**		
Dioxyde de soufre SO_2	**X**	**X**		
Particules diesel et essence PM	**X**	**X**		**X**[(1)]
Composés organiques Volatiles COV	**X**	**X**	**X**	
Méthane CH_4	**X**	**X**		
Spéciation COV non méthanique				
- benzène	**X**	**X**	**X**	
- formaldéhyde	**X**	**X**		
- acétaldéhyde	**X**	**X**		
- acroléine	**X**	**X**		
- 1,3-butadiène	**X**	**X**		
HAP				
- total des 6 HAP les plus cancérigènes[(2)]	**X**			
- benzo(a)pyrène	**X**			
Métaux lourds				
- Plomb Pb	**X**	**X**		
- Cadmium Cd	**X**	**X**		**X**
- Cuivre Cu	**X**	**X**		
- Chrome Cr				**X**
- Nickel Ni	**X**	**X**		
- Sélénium Se	**X**	**X**		
- Zinc Zn	**X**	**X**		
- Baryum Ba				**X**
- Arsenic As				**X**
Protoxyde d'azote N_2O	**X**	**X**		
Ammoniac NH3	**X**	**X**		

Annexe C

Fallah Shorshani M., Bonhomme C., Petrucci G., André M., Seigneur C. (2012) Road traffic impact on water quality in an urban catchment (Grigny, France), *9th International Joint IWA/IAHR Conference on Urban Drainage Modelling*, Belgrade, Serbie.

Road traffic impact on water quality in an urban catchment (Grigny, France): a step towards integrated traffic, air and stormwater modelling

Masoud Fallah Shorshani[1,2,3], Céline Bonhomme[1], Guido Petrucci[1], Michel André[3], Christian Seigneur[2],

[1] LEESU, École des Ponts ParisTech, Université Paris-Est
[2] CEREA, Joint Laboratory École des Ponts ParisTech/EDF R&D, Université Paris-Est
[3] IFSTTAR Institut Français des Sciences et Technologies des Transports, de l'Aménagement et des Réseaux.

masoud.fallah@ifsttar.fr, celineb@leesu.enpc.fr, guido.petrucci@leesu.enpc.fr, michel.andre@ifsttar.fr, seigneur@cerea.enpc.fr,

ABSTRACT

Methods for simulating air quality due to vehicles and the associated effects on stormwater runoff quality in an urban environment and their coupling are examined. To achieve this aim, the models (traffic, emission, atmospheric dispersion, and stormwater) must be carefully selected according to the special requirements and the level of details needed for the integrated system. The present study focuses on the interface between the air quality and stormwater models. The development of this interface raises questions concerning the processes treated to represent mass transfer between the atmosphere and stormwater. Moreover, other pollutant sources are added to road pollutants in an urban context: the evaluation of this new modelling chain with observations needs to distinguish between pollutants linked to traffic emissions and other pollutants. To assess the contamination of water runoff induced by traffic, concentrations of cadmium (Cd), lead (Pb), and zinc (Zn) in the Grigny catchment in France were simulated using typical pollutant deposition fluxes measured at roadside. The highest simulated concentrations of Cd, Pb, and Zn at the outlet were 2.12, 284.61, and 1757 µg L^{-1} respectively. These results show that pollutant concentrations are increased up to three times with an explicit description of road contaminant sources. Therefore, an exhaustive knowledge of the spatial distribution of roads with heavy traffic is important to predict water quality in urban areas.

Keywords

Integrated modelling; Stormwater; Traffic; Emissions; Air pollution; Runoff.

INTRODUCTION

Traffic is a major source of pollution in cities and near highways. Thus, the modelling of air and stormwater quality due to vehicles and of the presence of contaminants is, therefore, essential to control road traffic impact on the environment. Today, traffic models can predict the position and kinematic parameters of the vehicles and emission models can estimate the amount of different

pollutants emitted by vehicles, albeit with some uncertainty. Then, the dispersion of pollutants in the atmosphere can be simulated using atmospheric dispersion models. A fraction of the air pollutants deposits to the ground by dry and wet processes. These pollutants may be entrained by the water runoff during rainfall events, which may be simulated by hydrologic models. The main building blocks of such a simulation framework are (1) the models and (2) the interfaces which transfer the output from a model to the input for the next model, as shown in Figure 1. The types of model for each phenomenon (traffic, emissions, air quality and water quality) are presented below with increasing accuracy and complexity.

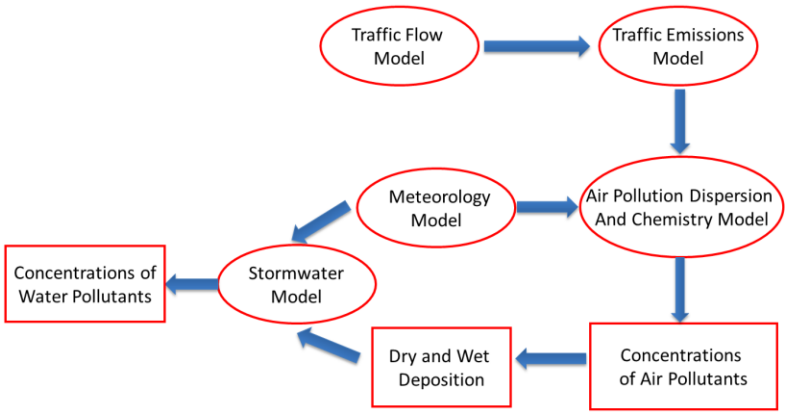

Figure 8.1. Schematic representation of the modelling chain (components are represented with ellipses) with expected input and output data (represented with boxes).

Three major classes of traffic models can be identified (Table 1):

1. Static models rely on localization of population and average traffic volumes in different areas of a network and are used mainly to study vehicles fluxes over large spatial and temporal scales.

2. Aggregated dynamic models can keep an explicit representation of congestion by describing the temporal evolution of traffic states of a simplified network (spatial aggregation).

3. Dynamic models describe the temporal variations of traffic conditions in order to determine the impact of individual vehicle movement.

Table 8.6. Traffic models

Models		**Field study**	**Results**	**Example**
Static		Large-scale	Average quantity of vehicles	DAVISUM MARS
Aggregated dynamic		Several neighborhoods	Average speed, congestion	THOMSON DAGANZO
Dynamic	Macroscopic	Local scale Highway	Density & speed of vehicles	SYAMUT CORFLO METACOR
	Mesoscopic	A few streets	Vehicle's trajectory	CONTRAM DYNAMART FASTLAN
	Microscopic	Urban network	Position, speed, acceleration per second	SYMUVIA VISSIM PARAMICS

The usual approaches for estimating the associated emissions can be classified according to the input data, the scale of the study and the type of pollutants being considered. These approaches can be distinguished as follows:

8. Models relying on fuel sales data (e.g., AGO)
9. Models relying on annual average traffic volumes per vehicle categories (e.g., HUGREL)
10. Models relying on average speed of traffic (e.g., COPERT)
11. Models implying a particular traffic situation. (e.g., HBEFA)
12. Models implying traffic-related variables (e.g., TEE)
13. Models providing the emissions from various driving cycle variables. (e.g., VERSIT+)
14. Models relying on speed chronology or instantaneous models (e.g., PHEM)

Models of categories 1 and 2 can be used for large-scale emission inventories (national). Models of categories 3 and 4 are more reliable, and cover the major emission processes and most pollutants from a single road up to a city. Models of category 5 require traffic flow variables for each road and category 6 is defined by individual vehicle movement data. Both models are restricted to specific conditions and pollutants. Models of category 7 represent explicitly the vehicle emission behaviour by relating emission rates to vehicle operation (engine power, speed, and acceleration) during a series of short time steps.

For model integration, the input requirements of the emission models have to be linked with the outputs of the traffic models. A traffic model must be chosen according to its capacity to produce the inputs for the emission model (Smit et al., 2008). Thus, integrated chains of models can be considered according to three main types (or levels) of application:

1. Macroscopic: Static models simply calculate the traffic volume, mean travelling speed and the number of vehicles needed by the emission models of categories 1 and 2. Average speed emission models of categories 3 and 4 can be coupled with static models or aggregated dynamic traffic models, which provide the average speed or the level of congestion. Macroscopic traffic flow and emission models are used for large-scale road networks.

2. Mesoscopic: Emissions can be modeled more accurately with both vehicle speed and acceleration as input parameters. Macroscopic traffic models of categories 1 and 2 do not provide the acceleration as do microscopic models (i.e., category 3), but it is possible to assess such kinematic characteristics through an intermediate sub-model at a given speed range and according to other parameters (Cappiello et al., 2002; Zegeye et al., 2010).

3. Microscopic: Emission rates for vehicle operation during a series of short time steps can be predicted by coupling microscopic traffic models with instantaneous emission models. The essential advantages of such approaches are the prediction of individual vehicle emission behaviour in real time. The validity of such tools and chain of models at a microscopic level has however to be demonstrated.

A coupling between emission and air quality models is necessary to predict the temporal and spatial variability of urban air quality and to calculate the pollutant deposition fluxes. The major input data necessary for the air quality model are spatially-distributed and temporally-resolved emissions provided by the emission model, meteorological inputs, boundary conditions, and land-use data. In the

case of Eulerian air quality models, the emissions must be defined for the 3D grid-mesh and for each pollutant. In the case of models used to assess near-source impacts (e.g., Gaussian dispersion models and CFD (Computational fluid dynamics) models), roads are considered as line (or elongated surface) sources and emissions induced by vehicles are estimated individually for each road segment. Atmospheric pollutants are introduced to the stormwater runoff by dry and wet deposition. These processes can be described in air quality models by several algorithms (Sportisse, 2007).

The hydrological models may be classified in terms of their functionality, accessibility, water quantity and quality components included in the model and their temporal and spatial scales (Zoppou, 2001; Elliot et al., 2007). In terms of spatial distribution, hydrological models may be categorized in "lumped", "semi-distributed" or "fully distributed". Lumped models are based on spatial averaging of the input parameters over the catchment: these models consider time variability but not spatial variability. "Semi-distributed" models take into account spatial variability over the catchments through hydrological units (sub-catchments), whereas "fully distributed" models include explicitly spatial variability: information such as soil properties and land use are averaged over a model mesh.

a. Study Design and Methodology

This study estimated and tested the effect of traffic impacts in the Paris region. The whole modelling chain is not performed here as we focus mainly on the atmosphere/water interface. Therefore, instead of using model outputs from traffic, emission and air quality modelling, experimental data on pollutant deposition fluxes are used to estimate roadside impacts.

The present study focuses on major metallic road pollutants (Cd, Zn, and Pb) emitted from traffic and observed in the Grigny catchment, during years 2009 and 2010. The model used to perform the stormwater runoff analysis is SWMM 5 (Rossman, 2010). This model is an open-source modelling software, well adapted to this investigation as it allows rainfall-runoff simulations (quantity and quality) over long periods with short time steps. The water quantity part of the model of the Grigny catchment was developed by Petrucci et al. (2012).

The Grigny catchment is located 20 km south of Paris. The catchment area is 365.7 ha, covered by several municipalities. This area is impacted by two main roads (D310 and D445) and the A6 highway, respectively having annual average daily traffic volumes of 17,000, 21,000 and 125,300 vehicles per day.

The Grigny catchment is divided into 20 sub-catchments. Each sub-catchment is further divided to reflect the variability of land use according to four land-cover types. Therefore, for each "real" sub-catchment, four "model" sub-catchments corresponding to green, roof, road, and "other" areas are defined. The geographical location and division of the catchment are presented in Figure 2. The model parameters that could not be defined according to physical measurements were calibrated and validated on a two-month long flow rate time series recorded at the outlet. The flow-rate calibration was performed using a genetic algorithm to maximize the Nash criteria, as described in details by Petrucci et al. (2012).

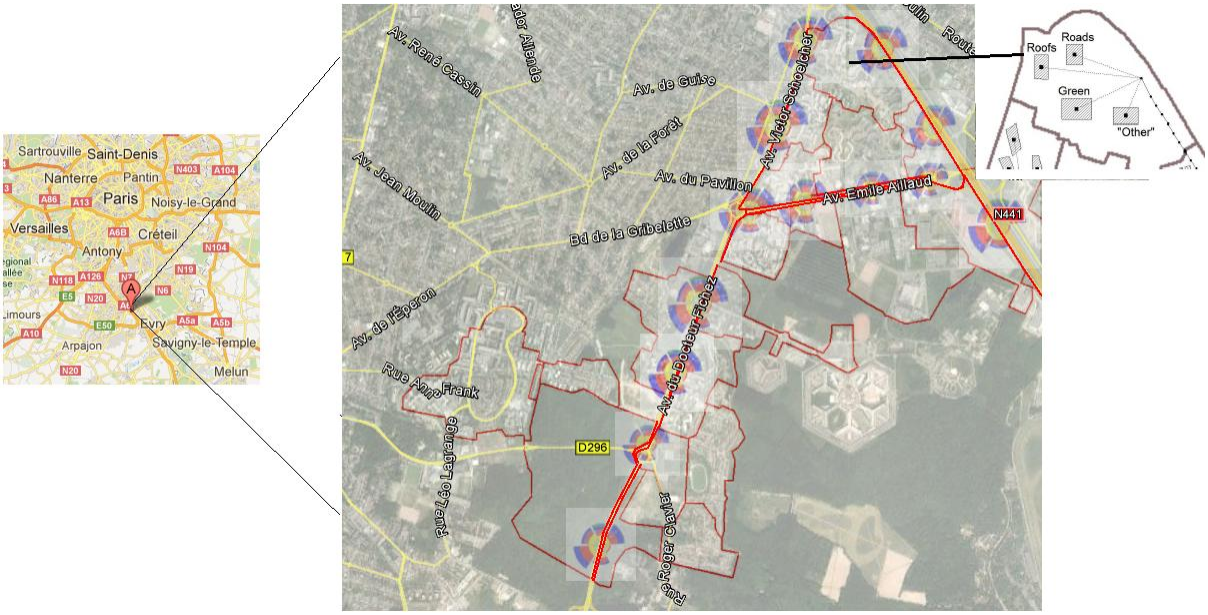

Figure 8.2. Geographical location and details of the Grigny catchment.

The dispersion of atmospheric pollutants is calculated using wind direction data covering two years, 2009 and 2010. The wind rose is based on observations at the nearest station (Orly airport, 8 km from the catchment). The use of the wind rose from a close but different location is appropriate in this case because of the relatively flat terrain and the surrounding urbanization (i.e., residential area). Considering the road network geometry, a wind rose with six directions represents the transport and dispersion of pollutants effectively, as shown in Figure 3. Total concentrations of Cd, Pb, and Zn are simulated in runoff from the Grigny catchment during 23 months (01/01/2009-01/12/2010) with a 5 min reporting time step. The aim of such a long-term simulation is to determine the effects of traffic on the pollutant levels at the outlet of the catchment within this period. For this purpose, two cases are studied. The first case takes explicitly into account background deposition and the local pollutant deposition due to the three main roadways of this heavy-traffic area, which is spatially variable. The second case uses only a uniform deposition flux corresponding to an averaged urban pollution background typical of low-volume surface roads (<2000 vehicles/day). The study by Wicke et al., (2011) is used for the following background deposition fluxes of Cd, Pb, and Zn: 0.13, 8, and 140 µg m^{-2} day^{-1} respectively.

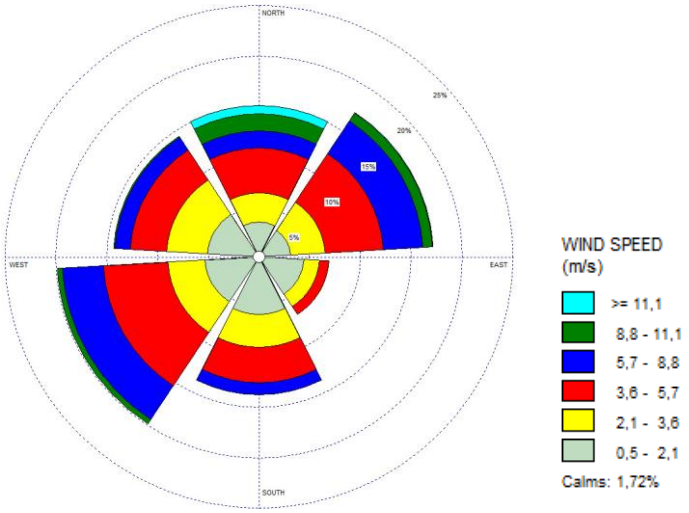

Figure 8.3. The wind rose for the Orly airport station calculated from 2009 and 2010 data by the WRPLOT software.

b. Atmospheric deposition

Several studies have experimentally quantified atmospheric deposition of metals near roadways. In France, Promeyrat measured in 2001 the deposition of three metals (Pb, Cd, and Zn) on both side of the A31 highway (France) along transects with sampling points ranging from 1 to 320 m. The average traffic on this highway is about 60,000 vehicles per day. The results were summarized by Viard et al. (2004). In the Paris metropolitan area, the study of Azimi et al. (2005) quantified the deposition of four metals (Pb, Cd, Zn, and Cu). These measurements include deposition due to road traffic emissions and other sources (incinerator, airport, and power plant). The traffic volume was that of highway A86. More recently, the PPTA project was conducted by Loubet et al. (2010) to quantify deposition of several metals (Fe, Cu, Pd, Pb, and Zn) along highway A6 in the south of Paris, with 6 sites ranging from 4 to 284 m. The volume of traffic is on the order of 80,000 vehicles per day. In the USA, Sabin et al. (2006) measured the deposition of several metals (Cr, Cu, Ni, Pb, and Zn) along highway I-405 in Los Angeles, California at distances ranging from 10 to 450 m. The traffic on this highway is on the order of 3000,000 vehicles per day. Our modelling is based on deposition flux measurements near highway A31 (France) by Promeyrat (2001), because that study provides the most complete and consistent data base for a French setting. The mean deposition fluxes of pollutants from data on both sides of the highway are shown in Table 2.

Table 8.7. Daily load (µg m^{-2} day^{-1}) of heavy metals (Cd, Zn, and Pb) used in this study (based on Promeyrat, 2001).

Pollutant /Distance (m)	10	20	30	60	120	average
Cd	1,88	1,08	0,49	0,27	0,21	0,40
Zn	992	321	80	512	142	277
Pb	404	192	119	80	7	71

c. Modelling

Water quality simulations include the pollutants buildup during dry periods and washoff during rainfall events. Different mathematical approaches are available to represent the processes governing pollutant accumulation and washoff. The exponential buildup and power washoff equations can be written as follow:

$$B = \frac{A}{C_1}\left(1 - e^{-C_1 t}\right) \quad (1)$$

$$W = E_1 q^{E_2} B \quad (2)$$

where B is the pollutant buildup (mass per unit area), A is the daily accumulation rate (mass per unit area per day), t is the number of antecedent dry days (days) and C_1 is the removal coefficient (1/day), which represents the removal of pollutants from surfaces by various mechanisms such as wind, traffic, street sweeping, biological and chemical degradation, except stormwater washoff (Liu et al., 2010). The pollutant washoff load is proportional to the product of runoff raised to some power and to the amount of available pollutants (Eq. 2), where, W is the washoff load (mass per hour), E_1 is the washoff coefficient, E_2 is the washoff exponent, and q is the runoff rate per unit area (mm/hour).

In order to define the buildup and washoff parameters, coefficients C_1, E_1, and E_2 are chosen from previous studies according to different land uses. The value of the removal coefficient (C_1=0.01- 0.05) was calculated for residential land-use by Liu et al. (2010). Reported values related to the washoff coefficient (E_1) range from 0.0013 to 0.11. The exponent (E_2) was found to range from 1.0 to 2.0 according to various experimental studies (Cheah, 2009). On the basis of the available literature and without further information on the catchment, the chosen values for the parameters are C_1=0.01, E_1=0.1, E_2=1.5.

The daily accumulation rates (A) are calculated according to the deposition flux of each pollutant source (i.e., the two roads and the highway), the associated level of traffic and the wind direction. The pollutant deposition exhibits well-defined linear relationships with traffic volume (Brett et al., 2011). Therefore, the traffic effect can be calculated based on the measurement data of highway A31 with the proper traffic scaling. With regards to the wind rose, deposition fluxes are estimated for each road or highway. According to previous work (see above), the daily accumulation rates for each sub-catchment are calculated over areas impacted by road traffic that extend up to 240 m from the road. Then, each road affected a fraction of the sub-catchment area based on road location with respect to the sub-catchment and wind direction. The background deposition level was attributed to the remaining area of the sub-catchment. Next, based on those input parameters for stormwater modelling, the variation of water quality was calculated with SWMM.

d. Sensitivity analysis

A sensitivity analysis was conducted to determine the influence of the three parameters discussed above (C_1, E_1, E_2) on simulated peak and average concentrations at the outlet. The sensitivity can be represented by the relative sensitivity coefficient (S) defined as:

$$S = \left| \left(\frac{x}{y} \right) \left(\frac{y_2 - y_1}{x_2 - x_1} \right) \right| \quad (3)$$

where x is the default value of the parameter and y is the corresponding output value. x_1, x_2 are the extreme values of the parameter range and y_1 y_2 are the corresponding output values. The greater the S value is, the more sensitive to a specific parameter the model output. The analysis was realized for the removal coefficient ($C_{1,min}$=$C_{1,default}$=0.01; $C_{1,max}$=0.05), washoff coefficient ($E_{1,min}$=0.01; $E_{1,default}$=0.1; $E_{1,max}$=0.3), and for the washoff exponent ($E_{2,min}$=1; $E_{2,default}$=1.5; $E_{2,max}$=2). The sensitivity coefficients for each pollutant are presented in Table 3.

Table 8.8. Sensitivity analysis

Parameters/ Sensitivity coefficient	C_1(removal coefficient)		E_1(washoff coefficient)		E_2(washoff exponent)	
concentration	Peak	Mean	Peak	Mean	Peak	Mean
S_{Zn}	0.50	0.4276	0.48	0.0954	2.49	2.2411
S_{Cd}	0.50	0.4297	0.48	0.0951	2.44	2.2232
S_{Pb}	0.48	0.4416	0.45	0.0953	2.29	2.1442

For all parameters, the peak concentration output is more sensitive to parameter fluctuations than the average pollutant concentration. Moreover, the washoff exponent E_2 is the most influent parameter on

model outputs and the sensitivity analysis enables to evaluate error bars on model outputs due to parameter uncertainties (in particular E_2).

RESULTS

The comparison of two cases (heavy traffic and without traffic) confirms a significant effect of traffic on water contamination. The highest concentrations of Cd, Pb, and Zn at the outlet are respectively 2.12, 284.61, and 1757.93 µg L^{-1} (Fig. 4a). Cases without traffic reach a maximum of 0.78 µg-Cd-L^{-1}, 47.72 µg-Pb-L^{-1}, and 835.17 µg-Zn-L^{-1} (Fig. 4b). These important differences are related to the pollution peak. Otherwise, 0.08 µg-Cd-L^{-1}, 6.33 µg-Pb-L^{-1}, and 79 µg-Zn-L^{-1} are the averaged concentrations due to traffic over two years (2009-2010). These values in the case without taking explicitly into account the traffic impact are 0.06 µg-Cd-L^{-1}, 4.01 µg-Pb-L^{-1}, and 70.19 µg-Zn-L^{-1}. Regarding the sensitivity analyses, the variability of outputs caused by the uncertainties in the model parameters, the results remain in accordance with measurements by Sabin et al. (2005). In these measurement the annual mean concentrations ± standard errors are 160±130 µg-Zn-L^{-1} and 12±10 µg-Pb-L^{-1} for a small urban catchment. The SWMM simulation results are consistent with these observations as these measurements fall within the range of the mean and maximum values. Accounting for wet deposition would increase slightly the SWMM concentrations; however, total deposition is dominated by dry deposition near roadways.

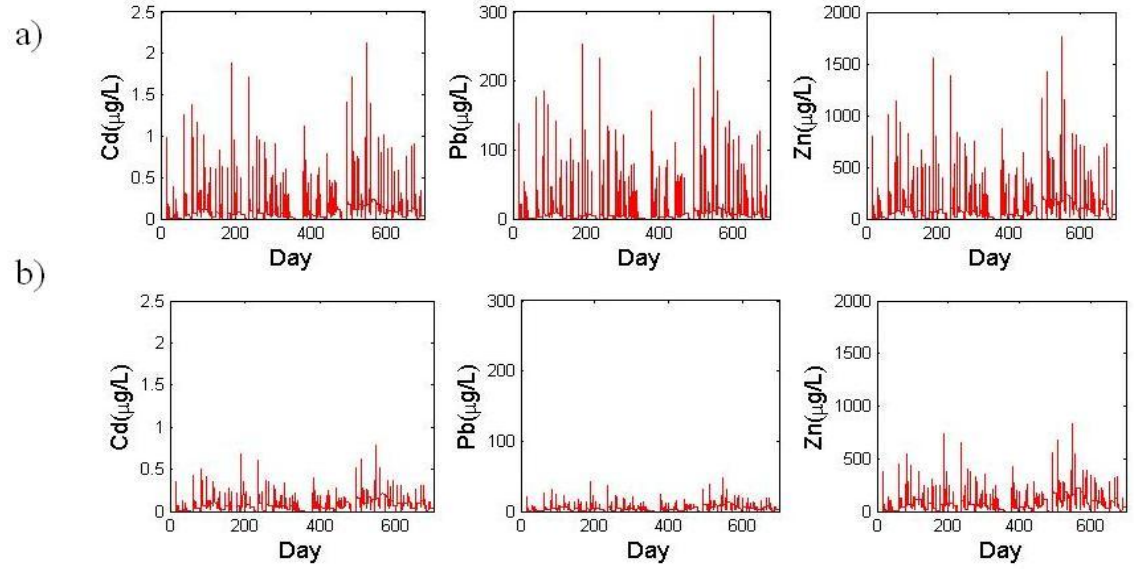

Figure 8.4. Heavy metal concentrations (µg/L) at the outlet of the Grigny catchment a) with an explicit consideration of traffic and b) due to an average background deposition typical of urban areas.

Comparison of metal concentrations related to the sub-catchment locations revealed different traffic impacts on sub-catchments near roads and highways. At the time of pollution peak, total Zn concentrations are shown in Figure 5 for all sub-catchments and nodes. The most polluted areas (>800 µg-Zn-L^{-1}) include the impervious sub-catchment near highway A6 having a traffic volume of 125,300 vehicles per day and sub-catchments impacted by both main roads. The least polluted zone contains sub-catchments located far from roads and the biggest sub-catchment with a small surface fraction impacted by traffic. In addition, bulk water contaminations in pervious areas like green space are negligible, even when they are located at the roadside.

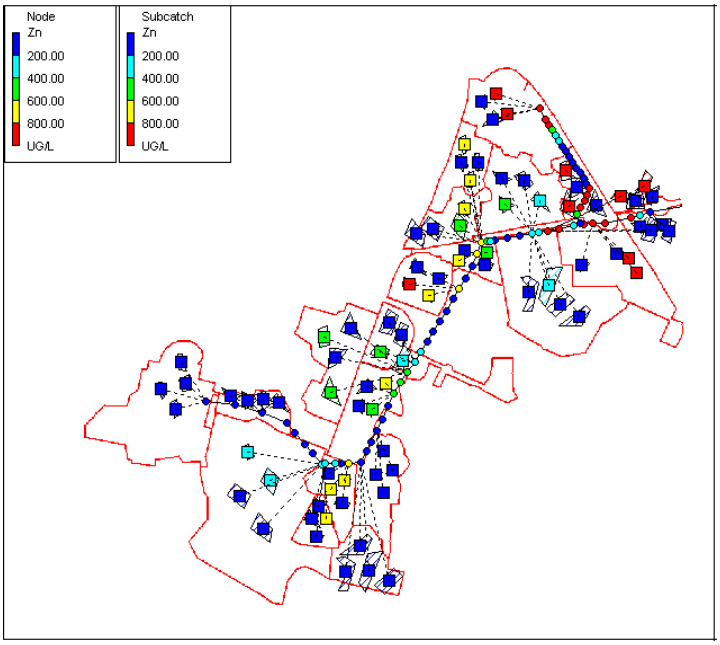

Figure 8.5. Spatial distribution of Zinc concentration (µg/L) from atmospheric deposition at pollution peak, 6:30 07/03/2010.

The results presented in Figure 6 show the relative load of Zn from each sub-catchment in both conditions: with an explicit description of the contribution of traffic or considering only the effect of a background residential contamination. Some sub-catchments present low pollutant concentrations because they do not produce any runoff due to a large amount of pervious surface (green space) in the sub-catchment. Figure 6 shows that the traffic effect can increase the water contaminant concentrations on highly exposed sub-catchments by up to 3 times in comparison with the case without traffic.

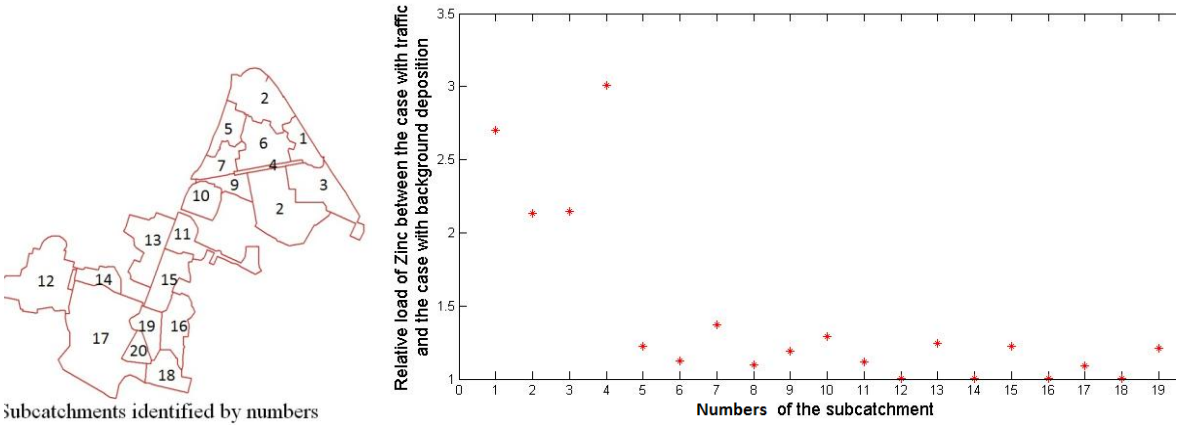

Figure 8.6. Relative load of Zn from each sub-catchment between the case with traffic on main roads and the case with background deposition.

The results of Zn concentrations at the outlet between the case with background deposition and with traffic during 6 days are shown in Figure 7. The relative variation between daily Zn concentration and average concentrations over two years were simulated. The highest concentration peak compared to the average Zn concentration is 2 times greater in the case with traffic than in the case with background deposition. This result shows that an explicit description of local atmospheric pollution

sources such as traffic has a strong impact on pollution peaks observed at the outlet of an urban catchment.

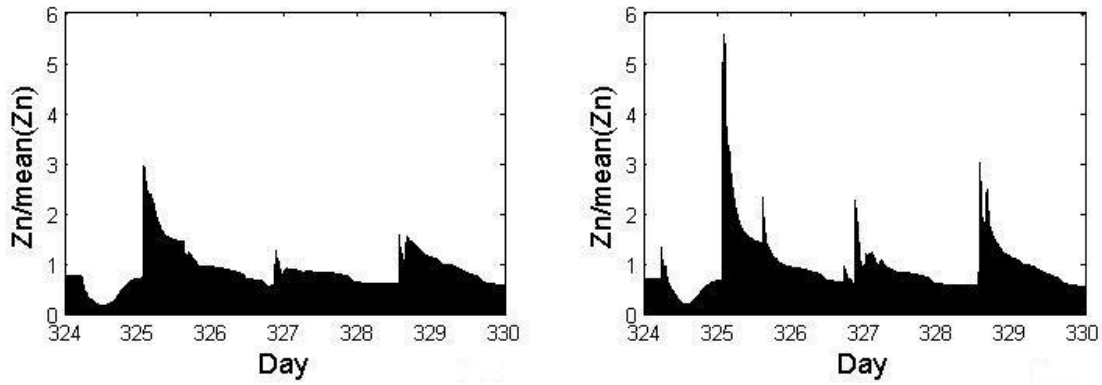

Figure 8.7. Relative Zinc concentration (ratio between daily concentration of Zinc and average concentration) over 6 days for the case with background deposition (left) and the case with traffic on main roads (right).

DISCUSSION

One major limitation of this study is that the variation of traffic volume in urban areas (e.g., hourly variability) was not considered. This problem will be solved next by the implementation of an integrated modelling chain, which simulates traffic situation up to atmospheric deposition. Such a modelling chain will estimate the pollutant concentrations in stormwater according to the temporal variability of traffic, which is not possible with long-term averaged measurements.

As the atmospheric deposition potentially accounts for 57-100% of the trace metal load on urban surfaces, traffic is a major source of atmospheric pollution (Sabin et al., 2005). In order to simulate the environmental impacts of traffic at the local urban scale, the first step is to choose the most appropriate tools in terms of relative scales. The most appropriate air pollution models for calculating the dispersion of vehicle pollutant emissions at local scales are mostly Gaussian dispersion models. In order to account for the atmospheric urban background as well (essential for wet deposition), it is planned to use a plume-in-grid model, which combines an Eulerian model and an imbedded line-source Gaussian model.

Nevertheless, a major scientific stumbling block is that air quality models typically consider only those particles smaller than 10 µm in aerodynamic diameter. However, the mass of particles greater than 10 µm is significant and is relevant to water quality and should be taken into account. Therefore, the selected emission models must be able to estimate the main water pollutants such as suspended solids (SS), polycyclic aromatic hydrocarbons (PAH), and heavy metals (e.g., Pb, Zn, Cd, and Cu). Moreover, to consider a large number of pollutants and emission phenomena (e.g., including fuel evaporation and non-exhaust particle emissions), the microscopic emission models have to be completed with aggregated emission models such as ARTEMIS and COPERT.

At last, the water quality can be modelled either by semi-distributed models such as SWMM, but this modelling has the drawback to consider only homogeneous sub-catchments. A fully distributed model would offer the advantage of explicitly taking into account distributed land uses, road surface characteristics at a high resolution, in addition to rainfall characteristics at different scales. Therefore, future work may use a fully distributed model for surface water flow and water quality modelling (for example, the model TREX) coupled to the well-know SWMM model for the urban drainage network.

CONCLUSION

In this study, different models for traffic, emission, dispersion and stormwater were presented. This review aims at making easier the selection of the most appropriate models to be coupled in order to implement an integrated and efficient modelling system for a simulation of air and water quality in urban areas.

Nevertheless, there are several limitations for the simulation of all phenomena (traffic, emission, dispersion and stormwater). The main challenges are associated with the importance of inputs and outputs of the different models constituting the modelling chain, especially the available data, the scale of the problem and its complexity.

Moreover, the effect of traffic impact in the Grigny catchment located in a southern suburb of Paris was considered in combination with experimental deposition flux data during 2009 and 2010. The water quality analysis showed that the maximum concentration of heavy metals can reach 2.12 µg-Cd-L^{-1}, 284.61 µg-Pb-L^{-1}, and 1757.93 µg-Zn-L^{-1} at the outlet. Comparison of metal loading from atmospheric deposition under two hypotheses (with and without considering explicitly the influence of traffic) indicates an important contribution of main road traffic to stormwater runoff in urban catchments. These encouraging results may be useful to test different urban planning scenarios at the time of the designing and building of new urban areas.

Finally, the method that is developed in this work is quite new in the context of water quality modelling. In fact, pollutant loads are usually calculated from urban land use. Here the atmospheric loads near heavy-traffic areas are shown to be major contributions and the traditional approach only considering land use is put into question.

Acknowledgements

The authors thank the "Ville numérique" and "OPUR" programs for their financial support and SIVOA for providing the data on the catchment.

REFERENCES

Azimi S., Rocher V., Garnaud S., Varrault G. and Thevenot D.R. (2005). Decrease of atmospheric deposition of heavy meatls in an urban area from 1994 to 2002 (Paris, France). *Chemosphere,* (61), 645-651.

Brett S. Davis. and Gavin F. Birch (2011). Spatial Distribution of Bulk Atmospheric Deposition of Heavy Metals in Metropolitan Sydney, Australia. *Water Air Soil Pollution, (*214),147–162.

Cappiello A., Chabini I., Nam E., Abou-Zeid M. and Lue A. (2002). A Statistical Model of Vehicle Emissions and Fuel Consumption. *IEEE ITSC* 2002 Paper, (Number 107).

Cheah (2009). Kinematic Wave Modelling of Surface Runoff uantity and Quality for Small Urban Catchments in Sydney. *Thesis of University of New South Wales.*

Elliott A.H. and Trowsdale S.A. (2007). A review of models for low impact urban stormwater drainage. *Environmental Modelling & Software,* (22), 394-405

Liu A., Egodawatta P., Kjolby M.J. and Goonetilleke A. (2010). Development of pollutant build-up parameters for MIKE URBAN for Southeast Queensland, Australia. *In Proceedings of the International MIKE by DHI Conference*.

Loubet et al. (2010). Concentrations and deposition of pollutants in the vicinity of a highway near Paris. final report, *Programme PRIMEQUAL* 2 / PREDIT.

Petrucci G., Rioust E., Deroubaix J.F. and Tassin B. (2012). Do stormwater source control policies deliver the right hydrologic outcomes? *Journal of Hydrology*. Available online 18 juin 2012, ISSN 0022-1694, 10.1016

Promeyrat S. (2001). Contribution à l'étude de la pollution atmosphérique autoroutière – caractérisation des flux de deposition de la contamination métallique de l'environnement de proximité (The contribution of case study of highway air pollution- characterization of metallic contamination flow). *Ph.D. thesis, University of Metz*, France.

Rossman L. (2010). Storm water management model user's manual version 5.0. report no. epa/600/r-05/040. Technical report, U.S. EPA National Risk Management Research Laboratory, Cincinnati, OH. http://www.epa.gov/nrmrl/wswrd/wq/models/swmm/epaswmm5_user_manual.pdf accessed 8 June 2011.

Sabin L.D., Lim J.H., Stolzenbach K.D., Winer A.M. and Schiff K.C. (2005). Contribution of trace metals from atmospheric deposition to stormwater runoff in a small impervious urban catchment. *Water Research*, (39), 3929–3937

Sabin L.D., Lim J.H., Venezia M.T., Winer A.M., Schiff K.C. and Stolzenbach K.D. (2006). Dry deposition and resuspension of particle-associated metals near a freeway in Los Angeles. *Atmos. Environ*, (40), 7528-7538.

Smit R., Brown A.L. and Chan Y.C. (2008). Do air pollution emissions and fuel consumption models for roadways, include the effects of congestion in the roadway traffic flow? *Environmental Modelling & Software*, (23), 1262–1270

Sportisse, B., (2007). A review of parameterizations for modelling dry deposition and scavenging of radionuclides. *Atmospheric Environment*, (41), 2683-2698.

Viard, B., Pihan F., Promeyrat S. and Pihan J.C. (2004). Integrated assessment of heavy metal (Pb, Zn, Cd) highway pollution: bioaccumulation in soil, Graminaceae and land snails. *Chemosphere*, (55), 1349-1359.

Wicke D., Cochrane T.A. and O'Sullivan A.D. (2011). Atmospheric deposition and storm induced runoff of heavy metals from different impermeable urban surfaces. *J. Environ. Monit*, (1), 209-16.

Zegeye K., De Schutter B., Hellendoorn J. and Breuness E.A.(2010). Integrated macroscopic traffic flow and emission model based on METANET and VT-micro. *Delft University of Technology, Technical report 09-01*

Zoppou C., (2001). Review of urban storm water models. *Environmental Modelling and Software* (16), 195-231.

Annexe D

Petrucci G., Gromaire M. C., Fallah Shorshani M., Chebbo G. (2014). Non-point source pollution of urban stormwater runoff: a methodology for primary sources' analysis, *Environmental Science and Pollution Research*. doi:10.1007/s11356-014-2845-4 (available online).

Non-point source pollution of urban stormwater runoff: a methodology for source analysis.

Guido Petrucci[a,b,*], Marie-Christine Gromaire[a], Masoud Fallah Shorshani[a,c,d], Ghassan Chebbo[a]

[a] Université Paris-Est. Laboratoire Environnement Eau Systèmes Urbains (UMR MA102), UPEC, UPEMLV, ENPC, AgroParisTech. 6-8 av. Blaise Pascal, 77455 Champs sur Marne cedex 2, France

[b] Vrije Universiteit Brussel (VUB), Earth System Sciences (ESSc), Brussels, Belgium

[c] Université Paris-Est. CEREA, Joint Laboratory École des Ponts ParisTech/EDF R&D

[d] IFSTTAR, Institut Français des Sciences et Technologies des Transports, de l'Aménagement et des Réseaux

* Corresponding author: guido.petrucci@vub.ac.be ; Earth System Sciences (ESSC), Dept. of Analytical, Environmental and Geo-Chemistry (AMGC), Vrije Universiteit Brussel (VUB) Pleinlaan, 2 - 1050 Brussels – Belgium; Tel: 0032 (0)2 629 33 93

Abstract

The characterization and control of runoff pollution from non-point sources in urban areas is a major issue for the protection of aquatic environments. We propose a methodology to quantify the sources of pollutants in an urban catchment and to analyze the associated uncertainties. After describing the methodology we illustrate it through an application to the sources of Cu, Pb, Zn and PAH from a residential catchment (228 ha) in the Paris region. In this application we suggest several procedures that can be applied for the analysis of other pollutants in different catchments, including an estimation of the total extent of roof accessories (gutters and downspouts, watertight joints and valleys) in a catchment. These accessories result as the major source of Pb and as an important source of Zn in the example catchment, while activity-related sources (traffic, heating) are dominant for Cu (brake pad wear) and PAH (tire wear, atmospheric deposition).

Keywords: substance flow analysis; uncertainty estimation; non-point source pollution; urban runoff; metals; PAH.

1. Introduction

Non-point pollution of urban runoff is considered an important cause of degradation of aquatic environments and ecosystems since several decades (e.g. Deutsch and Desbordes 1981). The interest for this type of water pollution is still increasing because of the evolutions in the regulatory framework for micropollutants. In the context of the European Water Framework Directive (2000), in order to protect aquatic ecosystems it is essential to mitigate

diffuse urban pollution sources. Analyses of the sources and fluxes of pollutants, often gathered under the name of "substance flow analyses" (SFA; Brunner and Rechberger 2003; Hansen and Lassen 2002), have flourished in recent years. They provide a global insight of the flows of pollutants emitted by urban areas to stormwater and/or to the receiving water body (Terekhanova et al. 2012). The main purposes of SFA are both scientific and operational: they include environmental impact assessments, prioritization of the sources for research (which sources are the less known and the most relevant to investigate) and policy-making (which sources are the most important to mitigate). Some SFA focused on downstream impact assessment detail extensively the flows of pollutants through the urban and drainage systems (e.g. combined sewer overflows, treatment plants, sludge; Benedetti et al. 2006; Rule et al. 2006). However, these SFA are often simplistic in the estimation of the sources of pollution, recurring sometimes to an aggregated approach based on the average pollutants concentration in runoff from each land-use (see the review by Göbel et al. 2007). The main disadvantage of this approach is that it reduces the capability to understand which processes and sources are actually responsible of the pollutant load. For example, it is unable to distinguish if pollution of roof runoff is mainly emitted by roof materials or comes from atmospheric deposition. As a consequence, this approach is unable to predict any change, for instance, in building materials or in fuel composition and it is not adapted to source control of non-point emissions (Cui et al. 2010). To overcome this issue, some researches focused particularly on the sources of pollutants in order to provide insight on the relative weight of each source on the global urban flow of pollutants (Bjorklund 2010; Chèvre et al. 2011; Davis et al. 2001).

The main difficulty in this kind of studies is constituted by the multiplicity of factors influencing the different sources and emissions. In a "calculation chain" aiming at quantifying the substance flows, at each step some concentrations, ratios, etc. have to be estimated. Many of these factors are difficult to quantify or even completely unknown. It is necessary to use "reasonable assumptions" on the numbers to be estimated recurring to literature and experience (Davis et al. 2001; Westerlund 2001). This pragmatic solution allows overcoming the lack of information associated with sources estimations but raises the issue of the uncertainty of the flows quantified. Because of the lack of information, but also of the spatial and temporal variability of the processes involved, estimations of pollution sources and fluxes are highly uncertain (Benedetti et al. 2006). A correct estimation of uncertainty is even harder than the estimation of sources and fluxes themselves: information on uncertainty and variability are even less available than information on the source magnitude. A further difficulty is that data, information and calculation procedures involved in SFA are highly heterogeneous. Thus, it is in general impossible to define a single, formal procedure of uncertainty estimation able to cover all the situations occurring in the analysis. Procedures currently used involve sensitivity analyses to a selected set of parameters, but the scope of these analyses is generally limited because the variability of parameters is often poorly determined (Chèvre et al. 2011; Hansen and Lassen 2002; Tangsubkul et al. 2005).

In this study we propose a detailed approach (section 2) to quantify and distinguish pollution sources as much as possible. This approach includes a procedure to systematically quantify

uncertainty: the procedure allows to pragmatically treat most of the cases occurring in a source analysis taking advantage of all the available information. In section 3 we apply the general approach to the specific case of the emissions of copper (Cu), lead (Pb), zinc (Zn) and polycyclic aromatic hydrocarbons (PAH) from a residential catchment in the Paris region. The case study illustrates the application of the proposed procedure, especially for uncertainty estimation. It also includes the presentation of a sampling method for the estimation of metal emissions from roof linear and point elements (rain gutters and downspouts, watertight joints), often neglected in similar researches.

2. General methodology

2.1 Non-point sources of urban runoff contaminants

Non-point sources of contaminants can be grouped in three main types (activity-related, land-cover related, behavior-related) plus atmospheric deposition. The latter could be operationally treated as a source but strictly speaking it is not one: contaminants from atmospheric deposition are produced from other sources inside or outside the catchment. A synthesis is presented in Fig. 1 and in the following paragraphs. This discussion is intended to provide a framework and a starting point for applications, presenting the major sources that should generally be considered in any source analysis.

The first step of the analysis is to determine which sources are potentially relevant for the specific pollutant(s) of interest in the specific catchment(s) considered. This operation can be helped by a general framework like the one proposed here but has to be adapted on a case-by-case basis. In particular the analyst has to combine two types of information: on one side, the general framework and the literature on the specific pollutant(s) of interest must be used to prepare a list of the potential sources; on the other side, the analysis of the catchment(s) characteristics is necessary to orient the research by excluding irrelevant sources or by suggesting the presence of specific ones. For example the focus in what follows is on chronic sources, while some temporary or accidental sources like construction sites or fires can be relevant in specific cases.

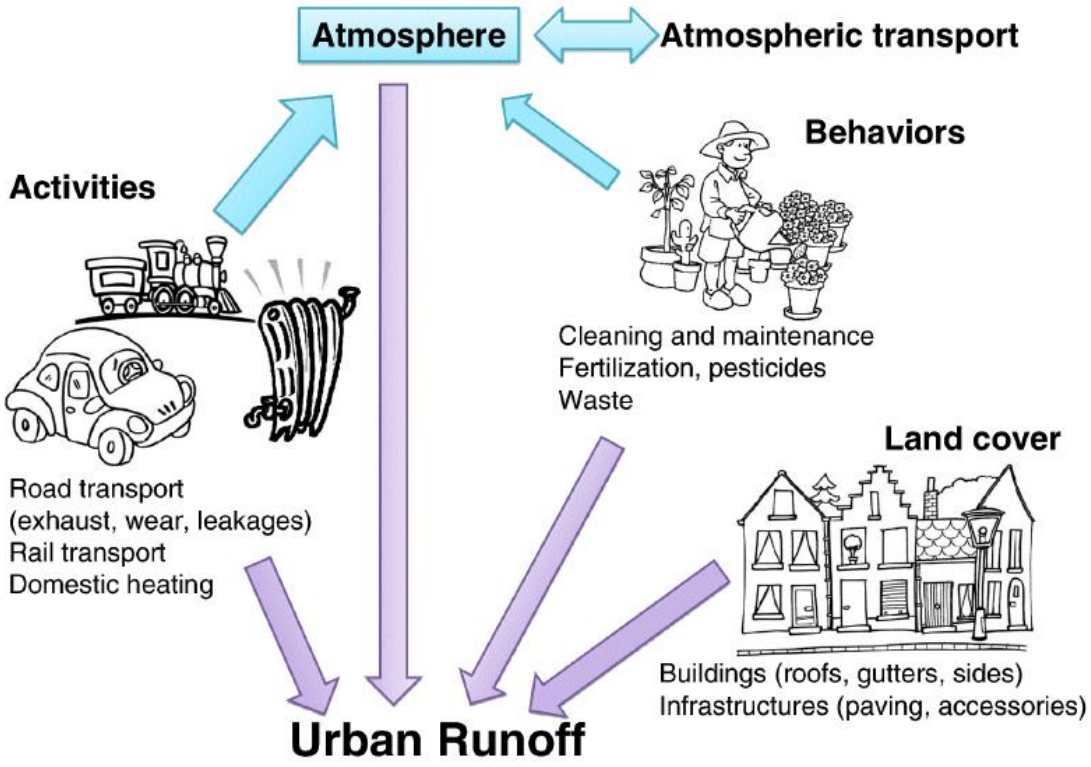

Fig. 1 Non-point chronic sources of runoff pollution in urban catchments

2.1.1 Activity-related sources

Road transport emissions are generally well-documented. However, because of their primary relevance for air pollution, studies are mainly focused on emission of gas and small-size particles (i.e. diameter <10 µm), more subject to atmospheric transportation than coarser particles (Fallah Shorshani et al. 2013). Much information and several models are consequently available for exhaust emission while less are available for non-exhaust emission (Thorpe and Harrison 2008). For water pollution the contribution of the latter can be relevant (Legret 2001; van Bohemen and Janssen van de Laak 2003). Non-exhaust emissions include brake wear (Westerlund 2001; Hjortenkrans et al. 2007), tire wear (Wik and Dave 2009) and road wear (Kennedy and Gadd 2003). These sources depend on parameters like the vehicles distribution (e.g. heavy duty vehicles or cars) and on other specific conditions, like the extended use of winter tires in cold climates. Another source correlated with road transport is leakage of car fluids like motor and brake oil: while the composition of these fluids can be easily found or determined, their potential as a pollutant source is poorly characterized (Göbel et al. 2007; Bjorklund 2010). Other sources can exist for specific pollutants: for example, bisphenol A can be present in the inner layers of car coating, and can eventually be emitted to runoff water (ANSES 2011; Lamprea-Bretaudeau and Gromaire 2014).

Railway transport is also a poorly documented but potentially important source of metals and PAHs (Malawska and Wilkomirski 2001). Domestic heating, like traffic exhaust, is more documented as a source of pollution in terms of air quality than in terms of urban runoff (e.g.

Fenger 1999; Schauer et al. 2003). In general coal and wood are considered the more pollutant fuels, although their use in most urban areas in developed countries is decreasing (Maruejols et al. 2011; EIA 2013).

2.1.2 Land-cover related sources

Land-covers can represent sources of pollutants depending on the building and infrastructure materials exposed to water runoff. Roof materials are the most studied and their emission patterns are available for some pollutants (e.g. Robert-Sainte et al. 2009; Van Metre and Mahler 2003). Upscaling to the catchment are however uncommon. Roof accessories (rain gutters and downspout, watertight joints and valleys) are a less studied source, even if evidences of their relevance exist (Gromaire-Mertz et al. 1999). Building sides are poorly studied because of the small quantity of runoff they produce but some research is available for specific materials and pollutants (Burkhardt et al. 2011; Davis et al. 2001). Infrastructure materials include paving (usually concrete or asphalt; Drapper et al. 2000; Gilbert and Clausen 2006) and accessories, like train and tramway catenaries, guardrails, urban lights, road panels and markings. Catenaries and guardrails are considered significant metal sources (Legret and Pagotto 1999; Chèvre et al. 2011), while lights and panels are less relevant because of the small surface exposed to runoff (van Bohemen and Janssen van de Laak 2003; Westerlund 2007).

2.1.3 Behavior-related sources

The emission of some pollutants depends more on individual, collective or institutional behaviors than on land cover or activities. It is the case for biocides, pesticides, fertilizers and other chemicals used for maintenance in urban areas (Blanchoud et al. 2004; Botta et al. 2012; Van de Voorde et al. 2011; Wittmer et al. 2010). The assessment of these sources of pollution is particularly difficult: factors like local traditions, practices and regulations, social and economic conditions, can be determinant.

2.1.4 Atmospheric deposition

Part of the pollutants emitted in the catchment can pass in the atmospheric compartment. There, pollutants from each source are mixed; part is transported outside the catchment; external contributions can enter the catchment. Finally, a fraction of the pollutants in the air compartment can pass to urban runoff either by deposition on the catchment surfaces and wash-off (dry deposition), or by capture in rain drops (wet deposition). This set of processes makes difficult to distinguish, inside atmospheric deposition, among sources and between local and external contributions. However, the cumulate atmospheric flux of pollutants can be quantified by deposition measurements or by modeling (Azimi et al. 2003; 2005; Davis and Birch 2010; van der Swaluw 2011; Lamprea et al. 2012). Some model-based research on atmospheric deposition has also addressed the question of distinguishing specific sources (Ying 2009; Fallah Shorshani et al. 2013).

2.2 Estimation structure

After identifying the sources relevant for a specific application, the next step is their quantification. As in most SFA (Hansen and Lassen 2002) a mass-balance approach constitutes the starting point. The total annual emission for the pollutant *p*, TE_p (kg/y), can be estimated as the sum of the emissions $E_{p,s}$ (kg/y) from each source *s*:

$$TE_p = \sum_s E_{p,s} \qquad \text{(eq. 1)}$$

Then, for each source, emissions can be expressed, in general, as the product of the source extent e_s, its pollutant content, concentration or specific emission $C_{p,s}$ and an efficiency $\eta_{p,s}$:

$$E_{p,s} = e_s \cdot C_{p,s} \cdot \eta_{p,s} \qquad \text{(eq. 2)}$$

According to the source and the available data the meaning and units of these factors vary, and eq. 2 can be rearranged. For instance, for brake pad wear, e_s can represent the total traffic volume in the catchment ((km·vehicles)/y) multiplied by the mean wear (kg/(km·vehicles)), $C_{p,s}$ the concentration of *p* in brake pads (kg/kg), $\eta_{p,s}$ the fraction of wear product passing to the ground multiplied by the fraction of deposition passing to stormwater. $\eta_{p,s}$ can also include degradation processes, according to the pollutant. For the emission of Zn by zinc roofs, e_s can represent the total surface of zinc roofs (m^2) and $C_{p,s}$ the specific emissions of Zn per unit of rainfall ($kg/(m^2 \cdot mm_{rainfall})$) multiplied by the average yearly rainfall (mm). Further examples are given in section 3.1.

It should be noted that the procedure of defining, source by source, the factors of eq. 2 is one of the most delicate points of the whole procedure, demanding to find a compromise between level of detail and data availability. As a general rule, the estimation of each factor can be further decomposed in simpler estimations, and this until it is possible to provide a value for each elementary parameter using one of four methods: i) direct measurements; ii) literature data; iii) modeling; iv) researcher experience. There is no general ranking among the methods except for iv), that should be usually considered a last resort. For example, the estimation of the annual traffic volume in the catchment can be decomposed in the estimation of daily traffic volumes for each road segment, which can be measured, modeled or estimated more easily than the aggregated value.

This analytical approach allows an iterative refining of estimations: initial gross estimation procedures for each source can provide a first prioritization. Then, for the most relevant sources, the estimation can be improved using more sophisticated procedures.

2.3 Uncertainty estimation

Uncertainty in source quantification can be extremely high. Estimations, as well as measurements, of the single factors described above can span over several orders of magnitude (e.g. Mansson et al. 2008; Morf et al. 2008; Cu content in brake pads in section 3.1.1). However, when several sources are aggregated on sufficiently large catchments, uncertainties are partially compensated (Benedetti et al. 2006; Sommer et al. 2008). This

effect is due to the averaging of a multitude of single local processes: if the emission of a specific car on a specific trip can be extremely variable (e.g. depending on temperature, driving and road conditions, etc.), the total emission of thousands of cars over thousands of trips is much more stable.

In several existing SFA uncertainties are estimated globally on aggregated values resulting from complex physical processes. This estimation is very difficult, often resulting in simplistic assumptions: all the parameters have the same variability (Tangsubkul et al. 2005) or they are equally distributed with the same standard variation (Chèvre et al. 2011). This approach is unable to account for the high uncertainty on single factors and for the stabilizing effect of aggregation. To partially solve this issue it is possible to decompose the global uncertainty estimation in a series of elementary estimations. Instead of directly estimating the uncertainty of total traffic emissions, the estimation is done for single car emissions and for the traffic volume, then the two uncertainties are combined. This procedure is equivalent to that proposed in section 2.2 and can be realized in parallel: for each elementary parameter used in the calculation the uncertainty is systematically assessed. When the parameters are combined to provide global estimations of sources, their uncertainty is propagated to obtain the global uncertainty estimation. This procedure reduces the difficulties associated with aggregated uncertainty estimations and explicitly takes into account the aggregation of individual sources. Furthermore, it provides a complete view of the uncertainties: it makes available not only the uncertainty for global results but also for each source and for intermediate calculation steps. It is thus possible to identify the most important sources of uncertainty. The procedure requires methods to systematically assess parameters uncertainty (section 2.3.1) and a method to propagate it (section 2.3.2).

2.3.1 Uncertainty estimation for elementary parameters

From section 2.2, the quantification of each source is decomposed in the estimation of a series of elementary parameters. For each parameter, we consider that the estimated value corresponds to the mean value μ, and that its uncertainty is described by the standard deviation σ. Because the parameters represent different quantities and have different units, for the sake of comparability we suggest to use the coefficient of variation C_v:

$$C_v = \sigma / \mu \qquad \text{(eq. 3)}$$

The information provided by μ and σ is the same than that of μ and C_v, and passing from one notation to the other is straightforward. To evaluate C_v for each parameter, different methods should be used according to how the parameter itself has been estimated and to the available information.

Estimation from data (method 1)

If a sample of measurements of a given parameter is available, the easiest procedure is to estimate its mean and standard deviation from the sample, using classical estimators like the sample mean and sample standard deviation. More complex analyses can also be performed, when available data suggest specific distributions of the parameter.

Estimation from intervals (method 2)

Often it is not possible to reconstruct the distribution of a parameter, but it is possible to define a variability range. It is often the case for literature reviews, where min and max values can be defined but the lack of information on single measurements or methodological differences prevent any formal statistical treatment. Literature reviews provide also information about the range confidence: if many studies are available and coherent there is a high probability that the actual value falls within the range; on the contrary, if few studies exist and show high variability the actual value can easily fall outside the range. To make the most of this knowledge we suggest a qualitative procedure.

We consider the range *[a,b]* as the confidence interval for the parameter *X*, centrally distributed. The mean value of *X* is $\mu_X=(a+b)/2$.The relation between *[a,b]*, the confidence level γ and σ is:

$$\gamma = P(a < X < b) = P(\mu - \alpha(\gamma)\sigma < X < \mu + \alpha(\gamma)\sigma) \qquad \text{(eq. 4)}$$

where α(γ) is a coefficient depending on γ and on the distribution. Thus:

$$\mu + \alpha(\gamma)\sigma = b \quad \Rightarrow \quad \alpha(\gamma)\sigma = b - \mu = b - (a+b)/2 \quad \Rightarrow \quad \sigma = \frac{b-a}{2\alpha(\gamma)} \qquad \text{(eq. 5)}$$

If we assume a normal distribution of *X*, we have to determine qualitatively the confidence level γ of the range and calculate α(γ) from tables (e.g. Table 1) in order to obtain an estimation of σ.

γ	α(γ)
38 %	0.5
68 %	1
87 %	1.5
95 %	2

Table 1 Sample values of α(γ) for a normal distribution

In most cases, the assumption of a normal distribution is reasonable: in particular, when estimating average values it is possible to consider than their distribution tends to normality. However, if available data suggest a different distribution, the same procedure can be used with some adaptation: for a non-normal centered distribution values of α(γ) should be changed, while for a non-centered distribution also eq. 4 and 5 should be adapted.

Conceptual estimation (method 3)

The two preceding methods cover most of the possible situations that can occur in a SFA. For example, if a parameter is estimated through a deterministic model providing a single output value, two options are available to evaluate the associated uncertainty. The first option is to use Montecarlo methods to obtain a distribution of the output and then apply method 1 (e.g.

Chèvre et al. 2011). The second option is to model two "extreme" scenarios providing a minimalist and a maximalist estimation of the parameter and then apply method 2. However, as well as researcher experience can be used for parameter estimation, it can also be necessary to assess the uncertainty (Morf et al. 2007). In this case, the estimation should be as justified as possible.

2.3.2 Uncertainty propagation

As in other SFA (Tangsubkul et al. 2005; Kwonpongsagoon et al. 2007; Cencic and Rechberger 2008), we adopt the approach of propagating uncertainty through first order linearization (JCGM 2008): for a function *f(x,y)*,

$$\sigma_f^2 \approx \left|\frac{\partial f}{\partial x}\right|^2 \sigma_x^2 + \left|\frac{\partial f}{\partial y}\right|^2 \sigma_y^2 + 2\frac{\partial f}{\partial x}\frac{\partial f}{\partial y}\mathrm{cov}_{xy} \qquad \text{(eq. 6)}$$

If uncertainty is given for all elementary parameters, eq. 6 can be applied to all calculations up to emission estimations (eq. 2) and aggregation (eq. 1). As an example, assuming independence among variables, uncertainty calculation for eq. 1 and 2 are, respectively:

$$\sigma_{TE_p}^2 = \sum_s \sigma_{E_{p,s}}^2 \qquad \text{(eq.7)}$$

$$\sigma_{E_{p,s}}^2 = {C_{p,s}}^2 \cdot {\eta_{p,s}}^2 \cdot \sigma_{e_s}^2 + {e_s}^2 \cdot {\eta_{p,s}}^2 \cdot \sigma_{C_{p,s}}^2 + {e_s}^2 \cdot {C_{p,s}}^2 \cdot \sigma_{\eta_{p,s}}^2 \qquad \text{(eq.8)}$$

In most cases it is reasonable and practical to assume the independence among parameters and neglect the covariance term: for highly uncertain parameters the covariance term can be assumed small compared with variance terms and assessing it would require, if and when possible, a supplementary complexity of the estimation procedure. Because of this difficulty in estimating covariance, in the cases where independence is clearly a non acceptable hypothesis, it can be necessary to find alternative solutions to estimate aggregated uncertainty: an example is provided in section 3.1.1.

3 Specific methodology

In this section the proposed general methodology is illustrated through an application. We focus on the emissions of Cu, Pb, Zn and PAH from an urban catchment in the Paris region. Despite the specificity of the example, many points discussed here are of more general interest: the concentrations and emission factors presented can be used for other applications on the same pollutants and methods to calculate source extent (traffic volume, area and length of roof surfaces and accessories) can be useful to study other pollutants having the same sources.

The studied catchment covers part of the city of Sucy-en-Brie, 15 km south-east of Paris, France. The catchment area is 228 ha, impervious cover is 21% and the population is about 5200 inhabitants. Land-use is mainly residential, with 97% of buildings represented by detached houses. Transportation is mainly provided by a few main roads and a network of service and collecting roads. Even if a train station is at the catchment border, no railways or tramways are present inside the catchment. Available data include cartographic data on roads and buildings (BD TOPO® database; IGN 2009), satellite images, traffic data on major roads (Val-de-Marne 2010) and meteorological data at the Orly airport (10 km west of the catchment).

Potential sources of PAH are road transport and domestic heating, through atmospheric deposition. For Cu, Pb and Zn, the potential sources are road transport (non-exhaust emissions), roof materials and accessories (metallic gutters and downspout, watertight joints and valleys). Infrastructure materials, because of the absence on the catchment of major roads or motorways, can be neglected. The scheme of the estimation is presented in Fig. 2.

In Figure 2, losses are indicated starting from the "Deposition on urban surfaces" compartment. They represent the accumulation of pollutants on the catchment and their degradation. We can neglect these losses because the pollutants considered are slowly or not degraded and we can assume that there is no net accumulation on urban surfaces from one year to another. Other losses like the fraction of emitted pollutants that does not deposit on urban surfaces are however taken into account in the estimation of the different sources.

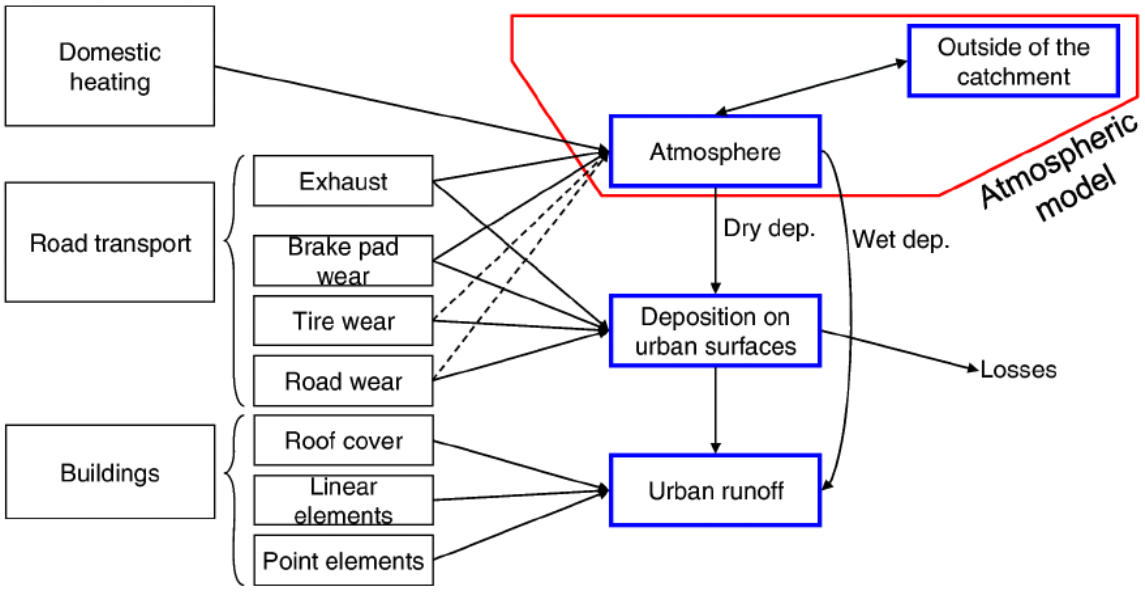

Fig. 2 Scheme of the considered sources. Dotted lines indicates negligible fluxes

3.1 Emissions estimation

3.1.1 Activities: road transport and domestic heating

Part of the activity-related emissions take a direct and short path to deposition on the ground and runoff, while another part passes from the atmospheric compartment and is mixed with contributions from outside the catchment (section 2.1). To quantify these two parts, we adopt different methods: for the first we apply, for each source, the procedure described in section 2.2 (eq. 2); for the second, we recur to an atmospheric model.

To estimate the direct emissions from road traffic we need to estimate the specific emissions for each pollutant and source, the efficiency (i.e. the fraction of emissions passing to stormwater) and the source extent, in this case the annual traffic volume.

Specific emissions and efficiencies

Specific emissions and efficiencies are obtained by a literature review, and their uncertainties are determined through the construction of confidence intervals (method 2). We present a detailed example of this procedure for brake pad wear, while for the other sources we specify only the references and results: detailed numbers are provided in the supplementary material.

Brake pad wear

Composition of brake pads is extremely variable (Thorpe and Harrison 2008). An extended set of measurements (Hjortenkrans et al. 2007) indicates that between 1998 and 2007 average metal concentrations were considerably reduced, suggesting that antecedent measurements are no more up to date. Data sources include a review from Thorpe and Harrison (2008), comprising data from 1991 to 2003; measurements (Pagotto 1999; von Uexkull et al. 2005) and an adaptation of data from Hjortenkrans et al. (2007) to the Hungarian case (Budai and Clement 2011). For Cu an analysis of Denier van der Gon et al. (2007) is also available. A synthesis is presented in Table 2.

ppm=mg/kg	Cu	Pb	Zn
Pagotto (1999)	142,138	3,873	*21,765*
Thorpe and Harrison (2008)	117,006	59,501	94,013
von Uexküll et al. (2005)	*13,525*		
Denier van der Gon et al. (2007)	*75,000*		
Hjortenkrans et al. (2007)	*110,013*	*463*	*36,640*
Budai and Clement (2011)	130,122	*129*	*24,984*

Table 2 Summary of the available estimations of the metal content of brake pads. In bold, the figures included in the selected intervals

According to observations and hypotheses from Hjortenkrans et al. (2007) it is possible to realize an average estimation for the French car pool. Hjortenkrans et al. observe that the main differences in composition occur between "branded brake pads" (i.e. original or agreed replacements) and "independent brake pads" (i.e. from independent suppliers). Because of EU legislation, in recent years independent suppliers have acquired a large and growing share of the replacements market (Autorité de la concurrence 2012), allowing to assume that all new vehicles (<5 years) use branded brake pads while old cars use independent ones (Westerlund 2001; Hjortenkrans et al. 2007). According to data from the French ministry of the environment the share of vehicles with less than 5 years is 32.7%. This value and the average concentrations provided by Hjortenkrans et al. (2007) provide a content estimation for Cu: 42614 mg/kg; Pb: 625 mg/kg; Zn: 13627 mg/kg.

For Cu we select an interval of [13000 ppm, 110000 ppm], comprising the estimations of von Uexkull et al. (2005), Denier van der Gon et al. (2007), Hjortenkrans et al. (2007) and our weighted average. We exclude the estimations of Budai and Clement (2011) and others too old (Pagotto 1999; Thorpe and Harrison 2008). The interval encompasses all the most relevant estimations and we attribute to it a confidence level of 87% (α =1.5). For Pb we select an interval of [130 ppm, 630 ppm] comprising all the recent estimations. Because European norms regulate Pb content in brake pads this interval is more representative than that for Cu and we attribute to it a confidence level of 95% (α =2). For Zn we select an interval of [13000 ppm, 37000 ppm] comprising all the estimations but that of Thorpe and Harrison (2008) which is based on old data. As for Cu we attribute to the interval a confidence level of 87% (α =1.5). A summary is presented in Table 3, with C_v calculated according to method 2.

Table 3 presents also the estimations of the specific wear of brake pads and of the fraction of wear depositing to the ground. Specific brake pad wear (mg/(km·v)) was estimated using data from Abu-Allaban et al. (2003); Budai and Clement (2001); Legret (2001); Pagotto (1999); Sörme and Lagerkvist (2002); Westerlund (2001). For both cars and heavy duty vehicles (HDV) values in literature are coherent, but for cars more data are available. Thus we attributed a higher confidence level to the interval for cars. The fraction of pad wear passing to the ground was estimated from Budai and Clement (2001); Garg et al. (2000); Hulskotte et al. (2007); Sanders et al. (2003); Sörme and Lagerkvist (2002). The coherence of the different estimations suggested a high level of confidence.

Table 3 Pollutant content and wear of brake pads.

		Units	Min	Max	γ	α	μ	σ	**Cv**
Content	Cu	ppm	13000	110000	87%	1.5	**61500**	32333	**53%**
	Pb	ppm	130	630	95%	2	**380**	125	**33%**
	Zn	ppm	13000	37000	87%	1.5	**25000**	8000	**32%**
Wear	Cars	mg/(km*v)	16	33	95%	2	**25**	4	**17%**
	HDV	mg/(km*v)	47	80	87%	1.5	**64**	11	**17%**
Fraction to the soil		%	20	60	87%	1.5	**40**	13	**33%**

Tire and road wear; exhaust emissions

Except for Zn, tires have a small content of metals but can be a significant source of PAH. Literature reflects this proportion with more studies on the PAH content (Takada et al. 1990; Legret 2001; Kennedy and Gadd 2003; Boonyatumanond et al. 2007; Sadiktsis et al. 2012) than on metals (Legret and Pagotto 1999; Kennedy and Gadd 2003; Hjortenkrans et al. 2007). European regulations limited the content of PAH in tires produced after the 1st of January 2010. Because of the time necessary for the regulation to have significant effects on the emissions and of the absence of more recent data, we use in this study values from the preceding period. It is however urgent to update the assessment of PAH content in the actual European car pools. Recent studies on tire specific wear (Aatmeeyata 2010; Wik and Dave 2009) provide consistent figures, while the fraction of deposit to the ground is more uncertain (Budai and Clement 2011; Legret and Pagotto 1999; Wik and Dave 2009).

Few references are available on metal and PAH content of road materials (Lindgren 1998; Legret 2001; Sörme and Lagerkvist 2002). For this reason, the estimations used are highly uncertain. Specific wear is particularly studied in northern countries, where the common use of studded tires produces a road wear up to 100 times higher than for non-studded ones (Kupiainen 2007; Sörme and Lagerkvist 2002; WEAREM 2010). In other countries, available references are Legret (2001) and Luhana et al. (2004). To estimate the fraction of deposition to the ground we use the same coefficients used for tire wear, because particles size is similar (Sörme and Lagerkvist 2002).

Exhaust emissions are considered a major source for PAH and a minor one for metals (Legret 2001; Sörme and Lagerkvist 2002; Wang et al. 2003). In Europe exhaust emissions strongly decreased in the last decade as a consequence of EURO regulations. A recent, extended measurement campaign for PAH emissions taking into account EURO regulations was realized by Joumard et al. (2007). We performed a weighted aggregation of data from Joumard et al. (2007) according to French vehicles pool (www.insee.fr/fr/themes/tableau.asp?reg_id=0&ref_id=NATTEF13629). Consumption values are obtained by actualized French official statistics (DGEMP 2006). Engine oil contains a relevant fraction of Zn, even if its consumption is low (Davis et al. 2001; DGEMP 2006; Sörme and Lagerkvist 2002). Fraction to the ground has been discussed by Sörme and Lagerkvist (2002) and Yang et al. (1999).

Extended data and a summary of the values used are presented in Tables 1 to 4 of the supplementary material.

Traffic volume estimation

To estimate the annual traffic volume two methods are applied. Direct measurements are available for major roads (4.4 km, 13% of the total road length of the catchment). Daily traffic ranges between 5512 and 11418 vehicles per day (v/d) and heavy duty fractions between 2.2% and 4.9%. We consider these values accurate, and assume an uncertainty of 5% (method 3).

For smaller roads (30.5 km), we adopt a procedure based on average European values suggested by WG-AEN (2006). Average values of daily traffic (v/d) are provided for four road categories: small main roads, collecting roads, service roads, dead-end roads. To classify each road of the catchment in one of these four categories we adapt the road classification present in the BD TOPO database: in this database roads are grouped in 5 levels according to their importance (1=motorway, 5=path). In the catchment, only roads of level 3, 4 and 5 are present and measurements are available for all the roads 3 and for some roads 4. Roads needing to be classified in the four categories of WG-AEN are thus some roads of level 4 and all the roads of level 5. We classify roads of level 4 without measurements as "small main roads". Roads of level 5 connecting two roads 3 or 4 are classified as "collecting roads", those connecting at most one road 3 or 4 as "service roads", those non connecting two roads as "dead-end roads". Because of the low accuracy of this procedure, we consider the results affected by an uncertainty of 30% on each road (method 3). Results are summarized in Table 4.

Table 4 Summary of traffic volume estimation

BD TOPO level	Data / class	Daily traffic (v/d)	Heavy duty fraction	Total length (km)
3	Data available	5512 - 11418	2.2% - 4.9%	4,425
4	Small main roads	2000	1,0%	3,657
	Collecting roads	1000	0,5%	10,558
5	Service roads	500	-	10,922
	Dead-end roads	250	-	5,400

Aggregation of traffic loads on the whole catchment is realized by multiplying, for each road, its length and the attributed traffic load, and by summing for all the roads of the catchment. This aggregation results in $21.52 \cdot 10^6$ km·v/y for cars (58% from measurements, 42% from estimations) and $0.36 \cdot 10^6$ km·v/y for heavy duty vehicles (87% from measurements, 13% from estimations). Reported to inhabitants, the result is about 4200 km·v/y per person. Data from USIRF (French road industries union, www.usirf.fr) allow to estimate a French average for 2009 of 5620 km·v/y per person excluding motorways. Our result is of the same order of magnitude, even if smaller of 35%: this is coherent with the abundance of public transportation in the Paris region in comparison with French average.

To calculate uncertainty of the total traffic load T, eq. 6 is applied for the sum of individual traffic estimations t_i. With the assumption of independence:

$$T = \sum_i t_i; \quad c_{v,T} = \frac{\sqrt{\sigma_T^2}}{\sqrt{T^2}} = \frac{\sqrt{\sum_i \sigma_{t_i}^2}}{\sqrt{\left(\sum_i t_i\right)^2}} = \frac{\sqrt{\sum_i t_i^2 c_{v,t_i}^2}}{\sqrt{\left(\sum_i t_i\right)^2}} \qquad \text{(eq. 9)}$$

The uncertainty of traffic load on single roads ($c_{v,ti}$) ranges in our estimations between 5% and 30% but the aggregation of the uncertainty for the total traffic volume ($c_{v,T}$) results in 1.5%.

This small value illustrates the compensation in upscaling discussed in section 2.3. However, this result represents a minimal value, under the hypothesis that single road estimations are uncorrelated. For the specific procedure used, where a single value is assigned to many roads, this hypothesis is clearly unacceptable. The covariance term cannot be neglected and the variance of total traffic becomes:

$$\sigma_T^2 = \sum_i \sigma_{t_i}^2 + 2 \sum_{1 \le i < j \le n} \mathrm{cov}_{t_i t_j} \qquad \text{(eq. 10)}$$

We can estimate a maximum value for the covariance terms recurring to a property of covariance:

$$\left|\mathrm{cov}_{xy}\right| \le \sqrt{\sigma_x^2 \sigma_y^2} \quad \Rightarrow \quad c_{v,T} \le \frac{\sqrt{\sum_i \sigma_{t_i}^2 + 2 \sum_{1 \le i < j \le n} \sqrt{\sigma_{t_i}^2 \sigma_{t_j}^2}}}{T} \qquad \text{(eq. 11)}$$

This calculation provides a maximal value of uncertainty of 15.6%. Considering that most of the estimated traffic comes from independent measurements this value of uncertainty constitutes a significant overestimation. For precaution we assume in further calculations a value close to this maximum: 10%.

Atmospheric deposition

To estimate deposition on urban surfaces we used an atmospheric model. Among available models (Fallahshorshani et al. 2012) we adopted a "box model". This approach assumes that atmospheric concentration and deposition are spatially uniform above the study area, which is defined as the rectangular area covering the catchment and extending up to 1000 m from the surface during the day and 50 m during the night because of atmospheric stability (i.e. within the atmospheric mixing layer). For each time step of 1 hour the concentration C of each pollutant is calculated as the sum of a background concentration and of the catchment emissions divided by the study area volume, and multiplied by a coefficient inversely proportional to wind velocity in order to describe advection processes (de Leeuw et al. 2002). The deposition flux F_d is then estimated using the following formulation:

$$F_d(x, y) = V_d \cdot C(x, y, z = 0) \qquad \text{(eq. 12)}$$

where V_d is the deposition velocity, which is mainly a function of meteorology and particle size. Because in this application time distribution of deposition is not necessary, the effect of meteorology on deposition velocities is not taken into account and time-average values are used. Particle distribution and corresponding deposition velocities are obtained from Roustan (2005): size distribution of PM_{10} emissions is assumed to be 74% in particles with a diameter less than 1 µm, 10% in particles between 1 and 2.5 µm, and 16% in particles with a diameter between 2.5 and 10 µm. Deposition velocities of particles in these three size ranges are respectively of 0.2, 0.4 and 4 cm/s. This relatively simple model is unable to precisely

describe transport and deposition processes but it is adapted to provide average estimations over long periods of time (i.e. one year; Fallahshorshani et al. 2012).

Catchment specific inputs to the model are: atmospheric background concentrations of pollutants, meteorological data, emissions from traffic and domestic heating. Background concentrations were obtained from measurements conducted in the Paris region (Ayrault et al. 2010; INERIS 2000). The average urban background total suspended particulate (TSP) values are 18.4, 6.3, 45.8 and 1.61 ng/m^3 for Cu, Pb, Zn and PAH respectively. These concentrations were assumed to be spatially uniform over the study area and constant in time. Meteorological data were available at the Orly airport, 10 km from Sucy.

Traffic emissions are estimated by traffic data and emission factors. It is important to notice that emission factors for atmospheric models are not necessarily the same as those calculated for ground deposition, because of the differences in the relevant particles size. It is therefore better to use, in this context, specific emission factors. For metals, we used experimental results (Sternbeck 2002). For PAH we applied the CopCETE model, an adaptation to the French context of the European widely used COPERT4 model (http://www.emisia.com/copert/General.html).

Domestic heating emissions were estimated on the basis of data from the French Institute of Statistics (INSEE), providing information of the different energy sources used in each city. For Sucy-en-Brie, 47% of houses and apartments use gas, 20% heating oil, 26% electricity, 7% other fuels. Considering average energy consumption data for France and emission factors corresponding to the different sources (CITEPA 2012), it is possible to estimate annual emissions. It should be noticed that INSEE data concern only the main heating source per house: as a result, wood combustion is never mentioned in the statistics, while it can be present as a complementary, seasonal source of energy.

The model output is the average annual deposition per hectare. To assess the validity of the results, we compared them to other data (Fig. 3): the average atmospheric deposition measured in the catchment, based on eight measurements between 2011 and 2013 (Gasperi et al., 2013) and the estimation of annual deposition in Créteil, a nearby catchment, in 2001/2002 (Azimi et al. 2003; 2005). For the three metals, and particularly Pb, data from Créteil are higher than both the model and the in-catchment measurements: this is probably due to the higher density, traffic and industrialization of the Créteil area as compared with Sucy and to the progressive reduction of emissions in the last decade as a consequence of regulations. Because metal emission factors used in the model date from 2002, the last consideration can explain the result provided by the model for Pb, higher than what estimated by direct measurements. For the other metals there is a good match between the model and direct measurements. For PAH, however, the model estimation is almost five times higher than local measurements: in this case the good match between local and Créteil data suggests that the model is overestimating the annual deposition. An alternative explanation is that measurements of deposition, generally realized in high places, underestimate pollutants emitted locally in low places like traffic-emitted PAH. As a consequence of these considerations, we use the model results for Cu and Zn with an uncertainty of 20% (method

3). For Pb we use direct measurements with an uncertainty of 40% (method 1). For PAH we construct an interval between measurements and model and we attribute to it a confidence level of 68% (method 2). We obtain an average value of 2.6 g/(ha·y), with C_v=66%. To estimate annual loads to stormwater runoff, we assume that deposition on pervious areas is infiltrated to the soils and only impervious areas contribute.

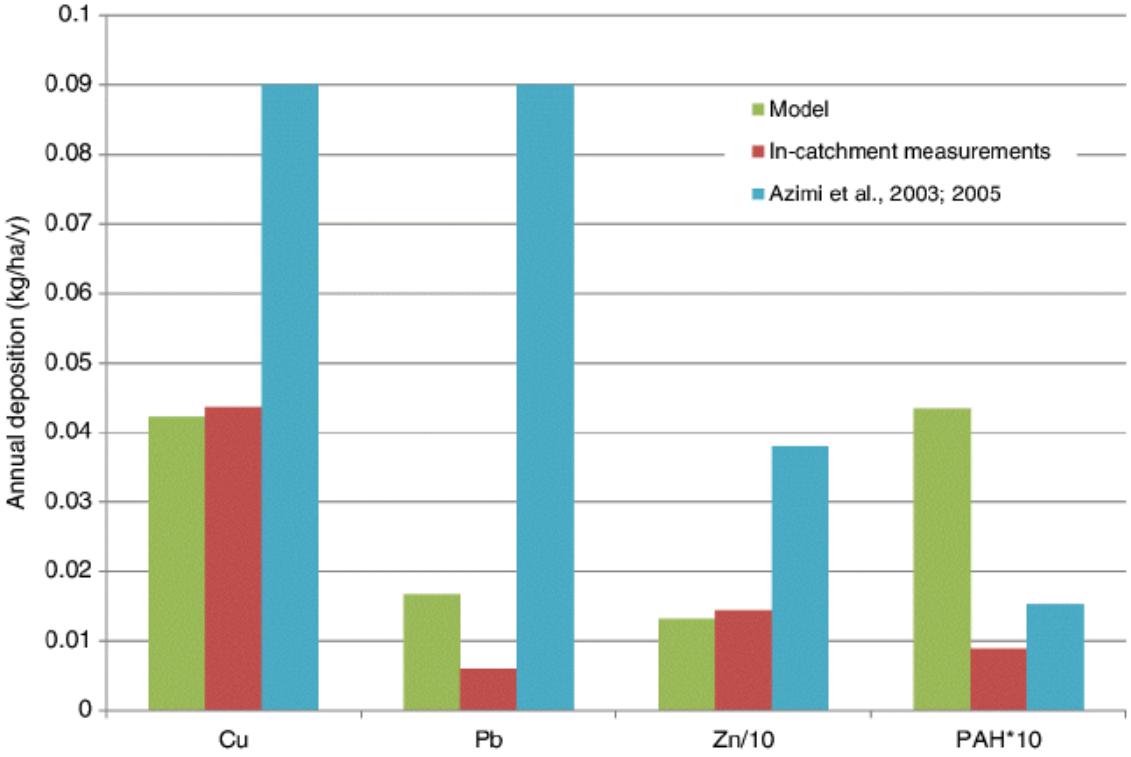

Fig. 3 Estimations of annual atmospheric deposition

3.1.2 Land-cover: emission from buildings

Roof materials and accessories are a significant source of metals. Zinc panels are directly used as roof material as well as galvanized steel (zinc-coated); zinc is also one of the most current materials for linear and point accessories: rain gutters, downspouts, valleys and joints. Copper is used for rain gutters and downspouts. Lead is commonly present in watertight joints and valleys. To estimate specific emissions we used measurements by Robert-Sainte et al. (2009). To quantify sources extent we adopted two procedures considering the catchment features. Roof materials in Sucy are mainly tiles: to identify the few metallic roofs we proceeded to a systematic inventory and classification based on aerial images. For linear and point accessories, invisible in aerial images, we adopted a sampling approach for detached housing which is the most common building type in the catchment. The sample used consisted in 88 houses corresponding to 4% of the total population, as suggested by Sellami et al. (2013). For each house of the sample we visually identified the materials and estimated the length and area of linear and point accessories. We validated the identification by demanding

independent classifications from two researchers expert in building materials. Results were then extrapolated to the whole catchment.

Specific emissions

Robert-Sainte et al. (2009) realized a substantial database on emissions from metal roof materials. This database includes more than one year of measurements on two different sites equipped with different metal surfaces of different ages. Starting from this database, we aggregated data for different materials: roof cover in zinc and galvanized steel (high emissions of zinc) and other metals (like aluminum, coated steel, etc. characterized by low emissions); lead point accessories; gutters in zinc and copper. For each category we computed the distribution of the specific emissions per mm of rainfall and the associated uncertainty (method 1, supplementary materials Table 5). To pass to specific emissions per year we considered an average yearly rainfall of 693 mm.

Roof materials

The systematic identification of roofs from aerial images provided a classification in 8 categories: tiles (78.2% of total surface); concrete or gravel-covered flat roofs (9.3%); fibrocement (1.2%); steel (non-galvanized, 1.4%); zinc (0.8%); non-identified metal (2.2%); mixed with metal (3.3%); mixed without metal (3.6%). Thus, high emitting surfaces cover between 0.8% (zinc roofs) and 6.3% (zinc + non-identified metals + mixed with metal). Low emitting surfaces (other metals) cover between 1.4% (non-galvanized steel) and 6.9% (+ non-identified metals + mixed with metal). Attributing to these intervals a confidence level of 95% we obtain the values reported in Table 5.

Table 5 Roof material surfaces.

	Min	Max	Min area (m^2)	Max area (m^2)	μ (m^2)	C_v
Low-emission surfaces	1.4 %	6.9 %	4,734	23,421	14,077	33 %
High-emission surfaces	0.8 %	6.3 %	2,723	21,409	12,066	39 %

Linear accessories (gutters and downspouts)

For each building in the sample we measured the length of rain gutters on aerial images. Because gutters are normally invisible on these images the estimation was based on the roof structure and particularly on the number and length of the eaves. This procedure is relatively precise for simple roofs because the definition of the available images ranged between 30 and 50 cm. However it can be difficult to apply for complex roof structures. Height and number of downspouts were estimated through visual recognition and measurement on the part of the roof visible from the street, and then extrapolated to the rest of the building according to the roof structure. Height estimation is reasonably precise because it is based on comparisons with standard architectural elements like floors, doors and windows. The most uncertain estimation is the extrapolation to the invisible part of the building. For a small building, having one downspout visible in the front, one or two can be reasonably present in the rear. If

we assume that one is present, the maximal error is 33% (estimation is 1/3 less than reality). Thus we consider an uncertainty in these estimations of about 30%.

Extrapolation to the whole population was based on a regression (R^2=0.58) between the total length of linear accessories and the area of the building (from the BD TOPO database). This regression was applied to estimate the length of linear accessories for each building in the catchment. The result is a total length of linear elements over the catchment of 93.5 km. Similarly to what observed for traffic estimation, this aggregation of highly uncertain individual values results in a small uncertainty on the total length over the catchment: 0.7% for a 30% uncertainty in single buildings. Total uncertainty is poorly sensitive to single estimations: increasing the uncertainty in single building estimations to 100%, the global uncertainty grows only to 2.3%. Even considering correlation maximum uncertainty is 3.5%. This low sensitivity suggests that errors in measurements and regression on single buildings are acceptable. Moreover in the present case estimations are based on a significant local sample and not on literature average values as for traffic. Thus, instead of assuming a value of uncertainty close to the maximum, we decide to use an average value of 1.4%.

Material classification was realized through two independent visual classifications operated by expert researchers. Each resulted in one distribution. We compared the two distributions by a test of comparison of proportions (Saporta 1990). The hypothesis that the proportions are different is always rejected but because of the size of the sample the test is significant only for zinc and PVC. The average distribution is given in Table 6. The uncertainty of each proportion *f* is quantified by the variance estimator:

$$\mathrm{var}(\hat{f}) = (1-\frac{n}{N})\frac{\hat{f}(1-\hat{f})}{n-1} \qquad \text{(eq. 13)}$$

where n is the number of cases observed, N the size of the population, $\hat{f}$ the proportion of the observed cases on the sample. The total length for each material is the product of f and the total length of linear elements in the catchment.

Table 6 Material classification for linear accessories.

	f	σ	Total length (m)	C_v
Zinc	58.7 %	5.6 %	54,882	10 %
PVC	26.1 %	5.0 %	24,426	19 %
Copper	3.2 %	2.0 %	3,016	63 %
Zinc and PVC	8.7 %	3.2 %	8,142	37 %
Not identified	1.9 %	1.6 %	1,809	81 %
Aluminum	1.0 %	1.1 %	905	116 %
Cast iron	0.3 %	0.6 %	302	201 %

Point accessories (watertight joints)

On the same sample used for linear accessories we estimated the surface and material of watertight joints and valleys. Procedure for classification and surface estimation are the same. Extrapolation to invisible parts of buildings is supported by aerial images: for instance, if lead joints of 0.2 m² are present for each visible skylight of a building and two more invisible skylights are observed on aerial images, a supplementary lead surface of 0.4 m² is attributed to the building.

Considering the results, it was impossible to find a satisfactory regression or a single distribution fitting the watertight surfaces in lead as in the case of linear elements. Thus, we adopted a supplementary classification: among the sample we distinguished buildings without lead elements (49%), buildings having less than 1 m² of lead (39%, C_v =14% using eq. 13) and buildings having more than 1 m² (12%, C_v=31%). For the last two categories we computed the average surface of lead per building (0.33 m² and 2.81 m² respectively, C_v = 72% and 59%). Then we computed the total lead surface as the weighted average of the population, resulting in 1026 m² (C_v= 52%). A similar analysis for zinc point accessories resulted in 904 m² (C_v= 57%).

Outlet estimation

In order to check the validity of the results, we compared them with measurements at the outlet. Gasperi et al. (2013) realized a set of measurements of pollutant concentrations at the outlet of the Sucy catchment between 2011 and 2013. To obtain an estimation of the annual flow of each pollutant its average measured concentration was multiplied by an estimation of annual runoff, computed as the product of average rainfall and impervious area.

4 Results and discussion

The results of the estimations are presented in Table 7 and Fig. 4: the table presents emissions per ha of impervious surface (48 ha), while the figure depicts relative contributions of each source and total catchment emissions. In the figure are also represented the estimated flows at the outlet for comparison.

Table 7 Results: estimations of specific emissions by sources. Values are in the format: $\mu \pm \sigma(C_v)$

			Cu (g/(ha·year))	Pb (g/(ha·year))	Zn (g/(ha·year))	PAH (mg/(ha·year))
Activities	Atmospheric deposition		42.2±8.4 (20 %)	6.0±2.4 (40 %)	130.7±26.1 (20 %)	2,610.4±1,722.9 (66 %)
	Road transport (direct emissions)	Brake pad wear	287.5±187.6 (65 %)	1.8±0.9 (50 %)	116.9±58.1 (50 %)	0
		Tire wear	0.3±0.2 (85 %)	0.4±0.3 (64 %)	557.9±209.8 (38 %)	3,719.6±2,057.9 (55 %)
		Road wear	0.1±0.1 (88 %)	0.0±0.0 (108 %)	0.1±0.0 (48 %)	7.0±7.5 (108 %)
		Exhaust	1.7±1.4 (83 %)	2.6±2.1 (83 %)	12.0±10.7 (89 %)	269.0±287.8 (107 %)
Land cover	Buildings	Roof cover	0.4±0.4 (119 %)	0.3±0.4 (160 %)	942.4±527.8 (56 %)	0
		Linear elements	34.7±23.9 (69 %)	2.4±2.0 (83 %)	895.8±385.2 (43 %)	0
		Point elements	0.2±0.5 (244 %)	222.1±148.8 (67 %)	72.9±49.6 (68 %)	0
	TOTAL		367.0±189.3 (52 %)	235.5±148.8 (63 %)	2,728.7±707.6 (26 %)	6,606.0±2,809.9 (43 %)

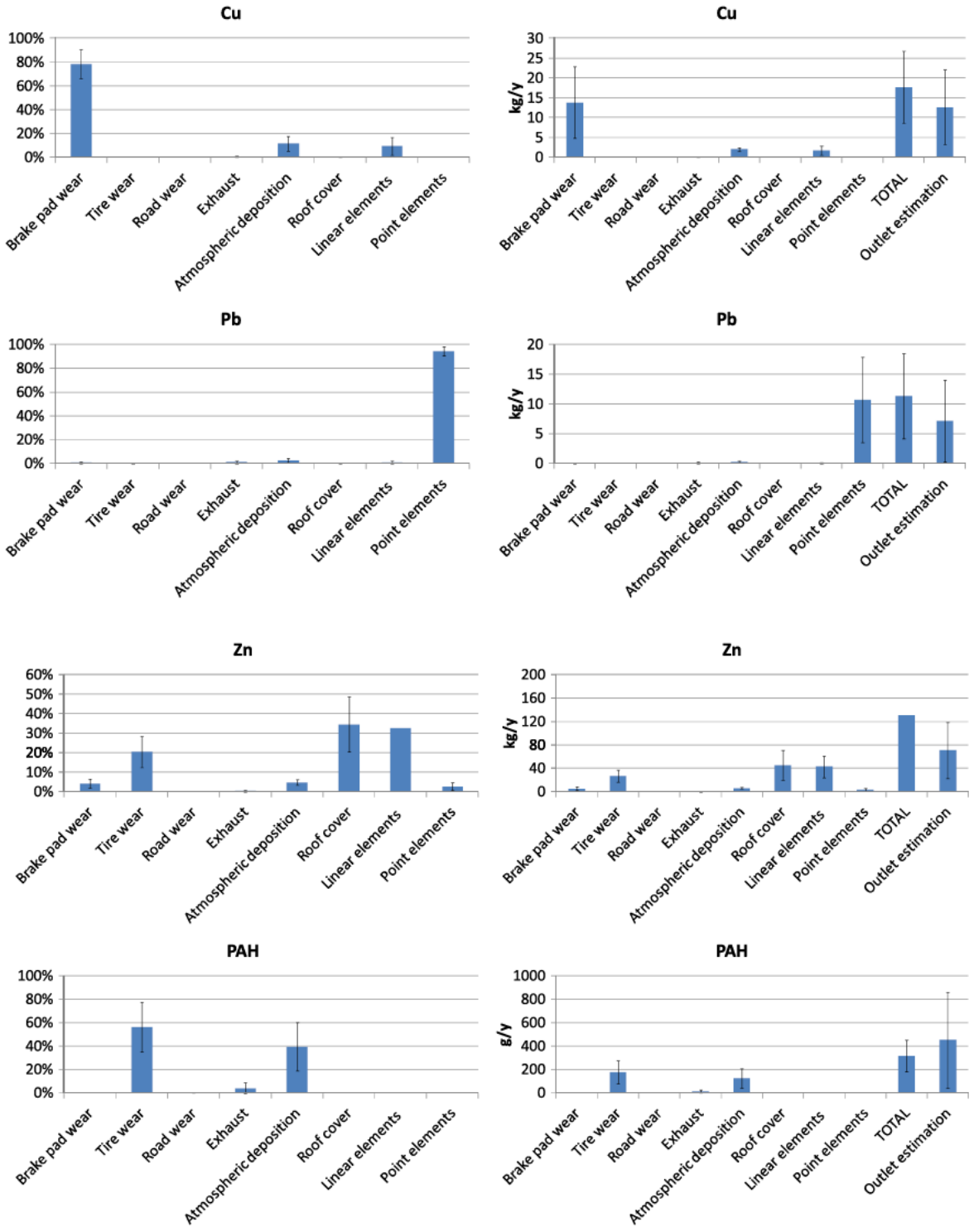

Figure 4 Relative contribution (left) and total catchment emissions (right) of the different sources for Cu, Pb, Zn and PAH. Error bars represent a ±σ interval

For Cu the largest source is brake pad wear (79%), followed by atmospheric deposition (12%) and linear elements (9%). Thus, activity-related sources contribute for more than 90% to the total Cu emission in Sucy. Despite the uncertainties, the dominance of brake pad wear and, more in general, of activity-related sources, is stable. However the contribution of gutters and downspouts is remarkable: in Sucy only about 3% of the linear elements are in copper. In other urban areas, copper is a more common material for this use and the contribution of

linear roof accessories can be the largest one. It is the case, for example, of the city of Lausanne studied by Chèvre et al. (2011): they found that the main sources of Cu are trolleybus catenaries, absent in our catchment, and roofs. Brake pad emissions represent only 16% of those from roofs, an inverted proportion compared to our results. Davis et al. (2001), on a hypothetical American urban area, conclude on a dominance of brake pad wear (47%) followed by buildings (31%) and atmospheric deposition (21%). A deeper comparison with these researches on absolute values is not possible because no data on the active area considered is given. However, the observations made are sufficient to conclude that brake pad wear is always a significant source of Cu in urban runoff, while other main sources strongly depend on specific features of the catchments (presence of tramways, frequency of copper elements in buildings).

For Pb 94% of the emissions are produced by the lead watertight joints and valleys used in roofs. The other sources are mainly traffic related (exhaust, atmospheric deposition, brake pad wear). As for Cu, this ordering is stable despite the uncertainties. Thévenot et al. (2007), using measurements from 1997, estimated a balance of lead sources in a small dense catchment in central Paris, and obtained total annual fluxes six to seven times higher than what founded here (1.58 kg/(ha·y)). However, the authors consider that this estimation should be lowered according to important reduction of lead emissions in the last decade and that in the ancient buildings of the studied catchment the use of lead elements in roofs was particularly high. In terms of sources, they found that 73% of lead was originated by roof runoff, 23% by streets and the remaining from courtyards. Considering the decrease in traffic emissions and atmospheric deposition of Pb in recent years, these ratios are consistent with our results. The dominance of building emissions demonstrates, on the one hand, the effectiveness of the regulatory efforts of the last decades to reduce lead emissions from road traffic. On the other hand, it shows that if lead emissions to the atmosphere have been cut down, they are still significant for the water compartment because of building materials. Although regulations addressed also construction practices, the replacement of lead elements with other materials will take decades, and for this time emissions to stormwater will continue.

Zn does not show single sources prevailing over the others, although building materials (roof cover plus linear elements) account for 70% of the total emissions and activity-related sources account for the remaining 30%. The ordering of specific sources is impossible because of the uncertainties. However it is remarkable that in an urban area with uncommon zinc-emitting roofs (3.5%) their contribution is about one third of the total emissions. It is possible that the procedure applied for estimating zinc-emitting roofs drove to an overestimation because of the presence of non-identified metal roofs, but for areas including relevant fractions of zinc roofs, this source will easily constitute the most relevant one. This is the case in the catchment studied by Thévenot et al. (2007): half of the roof area is in zinc and roofs account for 86% of the total Zn emissions (10.6 kg/(ha·y)) while streets for 12% with 1.44 kg/(ha·y). This last number is comparable to our result of 0.7 kg/(ha·y) (sum of the traffic-related sources) and the difference can be explained by the higher concentration of activities and atmospheric pollution in central Paris than in Sucy.

For PAH the largest sources are represented by tire wear (56%) and atmospheric deposition (40%) while exhaust emissions to the ground account only for 4%. Among the two largest sources, uncertainties make impossible to decide the largest one. In a research on an urban/business catchment in Le Havre, France, Motelay-Massei et al. (2006) measured absolute values for PAH atmospheric deposition (2090±830 mg/(ha·y)) close to our estimations. However, they conclude that this contribution accounts for only 4% of the total PAH content in runoff, estimated in 51450±3220 mg/(ha·y). They attribute the remaining 96% mainly to street deposits. The much higher estimation of the total flux by these authors can depend on catchment specificities or on the presence of point sources, but suggests further investigations about unrecognized potential non-point sources. Despite this discordance both results underline how some traffic-related sources which are poorly relevant for atmospheric pollution can be the most significant for the water compartment.

The comparison with the outlet estimation tends to confirm the validity of the analysis. Considering the uncertainty in both measurements and source analysis, the two estimations are always compatible. The mean values show a trend: for the three metals (Cu, Pb, Zn) the source analysis provides results always higher than the measurements at the outlet. The ratios between the two estimations are all comprised between 1.4 and 1.85. This stable reduction between catchment emissions and outflow can be interpreted as the effect of processes like sedimentation in the sewer system. For PAH the ratio between the two estimations is inverted: the result of the source analysis is 30% smaller than the outlet estimation. Although uncertainties are particularly significant for PAH, this opposite behavior of PAH as compared with metals suggests that some supplementary sources of PAH can exist in the catchment or in the sewer system.

The analysis of the uncertainties offers directions on how to improve the quantification of each pollutant. For pollutants having a single main source identified, this single source is clearly the focus. It is the case for copper and lead. For the first, principally emitted by brake pads, the main uncertainty resides in the Cu content of pads. A sensitivity analysis showed that halving the uncertainty of this parameter could reduce the uncertainty of the total Cu emissions from 52% to 37%. A similar halving of uncertainty, for instance, for the total traffic load, could reduce uncertainty only to 51%. For lead, depending on roof point elements, it could be useful to enlarge the sample of buildings used for surface estimation: halving the uncertainty on the total surface of lead elements could reduce the uncertainty of total Pb emissions from 63% to 46%, while halving the uncertainty on emission factors could reduce uncertainty to 53%. For the other pollutants, which have several main sources, reasoning should be based on opportunities: for example, extending the sample of buildings to improve Pb estimations could be beneficial also for the estimation of linear elements and thus for Zn emissions. Similarly, an improvement in the characterization of tire average content and wear could improve estimations of both Zn and PAH.

5. Conclusions

In this research a methodology was proposed for the quantification of non-point sources of urban runoff contamination. The procedure, consisting in an iterative decomposition of complex estimations into simpler ones, is not radically different from what is already implicitly used in many SFA focused on sources of pollutants. However its explicit formulation allows a parallel treatment of uncertainties, which is a major methodological improvement as compared with existing studies. In particular, even if uncertainties remain important they are estimated in a transparent, verifiable way.

The methodology was applied to the estimation of sources of Cu, Pb, Zn and PAH in a residential catchment in the Paris region. This example has not only the purpose of clarifying the procedure, but also of illustrating procedures applicable in other situations. Annual traffic load over the catchment was estimated on the basis of a few traffic measurements and of a generic topographical database: this procedure, simpler than detailed traffic modeling, can be easily applied for the estimation of annual flows of pollutants from road traffic. In fact, even if this procedure can be too approximated for other uses, in a context of high uncertainties its results demonstrated a sufficient accuracy. Similarly, we presented a sampling procedure to estimate the extent of metallic elements in roofs (linear and point accessories). This procedure proved to be useful to analyze this source of pollutants often neglected. The sample used was, as suggested by Sellami et al. (2013), of 4% of the buildings population: this sample size was sufficient to well characterize frequent features like zinc gutters but resulted too small for more uncommon elements like lead joints. Together with these two procedures to estimate the *extent* of pollution sources, we suggested a method to assess the *emission factors* and their uncertainty on the basis of literature reviews and of other procedures providing mixed quantitative and qualitative information. We applied this method to obtain up-to-date emission factors for the considered pollutants, which can be reused in other applications.

Specific results on the studied catchment are that human activities are the main sources for Cu (brake pad wear) and PAH (tire wear), while land-cover materials are responsible for most of Pb (roof point elements) and Zn (roof cover and linear elements) pollution. These results can be useful to define mitigation strategies.

In terms of research perspective the analysis of uncertainties showed that, with some generality, the estimation of activity-related sources could be improved by more detailed researches on emission factors. The extent of these sources seems reasonably known using GIS data and usual measurements or statistics, available for most catchments. It is not the same for land-cover related emissions: even if the characterization of emission factors should be improved, the main issue for quantifying these sources is the determination of their extent. Today, methods for fast characterization of materials used in buildings and infrastructures, including small but frequent and highly emitting elements, are poorly developed. A further difficulty is that materials employed in buildings often depend on local traditions, regulations and other specific conditions. As a consequence, the development of generic ratios or average values for urban typologies seems highly challenging and requires deep analyses.

Acknowledgements

This study was realized in the framework of the INOGEV research program. The program is funded by the French National Research Agency. The authors thank the OPUR program.

References

Aatmeeyata, Sharma, M. (2010) Contribution of Traffic-Generated Nonexhaust PAHs, Elemental Carbon, and Organic Carbon Emission to Air and Urban Runoff Pollution. *Journal of Environmental Engineering*, *136*(12), 1447-1450.

Abu-Allaban M., Gillies J.A., Gertler A.W., Clayton R., Proffitt D. (2003) Tailpipe, resuspended road dust, and brake-wear emission factors from on-road vehicles. *Atmospheric Environment* 37, pp. 5283–5293.

ANSES (2011) Connaissances relatives aux usages du bisphénol A. Knowledge on the uses of bisphenol A. In French. Agence nationale de sécurité sanitaire de l'alimentation, de l'environnement et du travail. September 2011. Available online:

http://www.anses.fr/sites/default/files/documents/CHIM-Ra-BisphenolA.pdf

Autorité de la concurrence (2012) Avis n° 12-A-21 du 8 octobre 2012 relatif au fonctionnement concurrentiel des secteurs de la réparation et de l'entretien de véhicules et de la fabrication et de la distribution de pièces de rechange. Notice n° 12-A-21 of the 8th of October 2012 about the competitive functioning of the sectors of vehicles repairs and maintenance and of the production and distribution of spare parts. In French. Available online:

www.autoritedelaconcurrence.fr/pdf/avis/12a21.pdf

Ayrault S, Senhou A., Moskura M., Gaudry A. (2010) Atmospheric trace element concentrations in total suspended particles near Paris, France. *Atmospheric Environment* 44, 3700-3707.

Azimi S., Ludwig A., Thévenot D.R., Colin J.-L. (2003) Trace metal determination in total atmospheric deposition in rural and urban areas. *Science of the Total Environment* 308, 247– 256.

Azimi S., Rocher V., Muller M., Moilleron R., Thevenot D.R. (2005) Sources, distribution and variability of hydrocarbons and metals in atmospheric deposition in an urban area (Paris, France). *Science of the Total Environment* 337, 223– 239.

Benedetti L., Dirckx G., Bixio D., Thoeye C., Vanrolleghem P., (2006) Substance flow analysis of the wastewater collection and treatment system. *Urban water journal* 3(1), 33-42.

Bjorklund K. (2010) Substance flow analyses of phthalates and nonylphenols in stormwater. *Water Science & Technology* 62.5 1154-1160.

Blanchoud H., Farrugia F., Mouchel J.M. (2004). Pesticide uses and transfers in urbanised catchments. *Chemosphere*, 55, pp. 905–913.

Boonyatumanond R., Murakami M., Wattayakorn G., Togo A., Takada H. (2007) Sources of polycyclic aromatic hydrocarbons (PAHs) in street dust in a tropical Asian mega-city, Bangkok, Thailand. *Science of the Total Environment, 384*(1), 420-432.

Botta F., Fauchon N., Blanchoud H., Chevreuil M., Guery B. (2012). Phyt'Eaux Cités: Application and validation of a programme to reduce surface water contamination with urban pesticides. *Chemosphere*, Volume 86, Issue 2, Pages 166-176.

Brunner, P. H. and H. Rechberger (2004) Practical hand-book of material flow analysis. CRC Press.

Budai P. and Clement A. (2011) Refinement of national-scale heavy metal load estimations in road runoff based on field measurements. *Transportation Research Part D: Transport and Environment, 16*(3), 244-250.

Burkhardt M., Zuleeg S., Vonbank R., Schmid P., Hean S., Lamani X., Bester K., Boller M. (2011). Leaching of additives from construction materials to urban storm water runoff. *Water Science and Technolog*, 63, 1974–1982

Cencic O. and Rechberger H. (2008). Material flow analysis with software STAN. Journal of *Environmental Engineering and Management*, 18(1), 3-7.

Chèvre N., Guignard C., Rossi L., Pfeifer H.-R., Bader H.-P., Scheidegger R. (2011). Substance flow analysis as a tool for urban water management, *Water Science and Technology* 63.7, 1341-1348.

CITEPA (2012). National inventories of air emissions in France : organisation and methodology. 9th edition. Centre Interprofessionnel Technique d'Etudes de la Pollution Atmosphérique (CITEPA), February 2012.

Cui Q., Brandt N., Sinha R., Malmström M.E. (2010). Copper content in lake sediments as a tracer of urban emissions: Evaluation through a source–transport–storage model. *Science of The Total Environment*, 408(13), 2714-2725.

Davis A. P., Shokouhian M., Ni S. B. (2001) Loading estimates of lead, copper, cadmium, and zinc in urban runoff from specific sources. *Chemosphere*, 44(5), 997-1009.

Davis B., Birch G. (2010) Comparison of heavy metal loads in stormwater runoff from major and minor urban roads using pollutant yield rating curves. *Environmental Pollution*, *158*(8), 2541-2545.

de Leeuw F. A., van Zantvoort E. D., Sluyter R. J., & van Pul W. A. J. (2002) Urban Air Quality Assessment Model: UAQAM. Environmental Modeling and Assessment, 7(4), 243-258.

DGEMP (2006) Consommations de carburant des voitures particulières en France 1988-2005. Fuel consumption by private cars in France 1988-2005. In French. Ministère de l'économie des finances et de l'industrie. Direction Générale de l'Énergie et des Matières Premières. Available online: www.statistiques.developpement-durable.gouv.fr/fileadmin/documents/Themes/Energies_et_climat/Consommations_par_secteur/Transport/consom_carbu_05.pdf

Denier van der Gon H.A.C., Hulskotte J.H.J., Visschedijk A.J.H., Schaap M. (2007) A revised estimate of copper emissions from road transport in UNECE-Europe and its impact on predicted copper concentrations. *Atmospheric Environment*, 41 (38), pp. 8697–8710.

Deutsch, J.-C., Desbordes, M. (1981) Study of runoff pollution for urban planning. In : 2nd International Conference on Urban Storm Drainage, Urbana, Illinois USA, 14-19 June 1981.

Drapper D., Tomlinson R., and Williams P. (2000) Pollutant Concentrations in Road Runoff: Southeast Queensland Case Study. *Journal of Environmental Engineering*, 126(4), 313–320.

Energy Information Administration (2013) International Energy Outlook 2013. EIA, Department of Energy, U.S. Government: Washington, D.C.

Fallahshorshani M., André M., Bonhomme C., Seigneur C. (2012) Coupling traffic, pollutant emission, air and water quality models: Technical review and perspectives. *Procedia - Social and Behavioral Sciences* 48, 1794 – 1804.

Fallah Shorshani M., Bonhomme C., Petrucci G., André M. Seigneur C. (2013) Road traffic impact on urban water quality: a step towards integrated traffic, air and stormwater modelling. *Environmental Science and Pollution Research*. Available online, DOI: 10.1007/s11356-013-2370-x

Fenger J. (1999) Urban air quality. *Atmospheric environment*, 33(29), 4877–4900.

Garg B. D., Cadle S. H., Mulawa P. A., Groblicki P. J., Laroo C., & Parr G. A. (2000) Brake wear particulate matter emissions. *Environmental Science & Technology*, *34*(21), 4463-4469.

Gasperi J., Sebastian C., Ruban V., Delamain M., Percot S., Wiest L., Mirande C., Caupos E., Demare D., Diallo Kessoo M., Saad M., Schwartz JJ., Dubois P., Fratta C., Wolff H., Moilleron R., Chebbo G., Cren C., Millet M., Barraud S., Gromaire MC. (2013) Micropollutants in urban stormwater: occurrence, concentrations, and atmospheric contributions for a wide range of contaminants in three French catchments. *Environmental Science and Pollution Research*.

Gilbert J.K., Clausen J.C. (2006) Stormwater runoff quality and quantity from asphalt, paver, and crushed stone driveways in Connecticut. *Water Research*, Volume 40, Issue 4, Pages 826–832.

Göbel, P., Dierkes, C., & Coldewey, W. G. (2007) Storm water runoff concentration matrix for urban areas. *Journal of contaminant hydrology*, *91*(1), 26-42.

Gromaire-Mertz M. C., Garnaud S., Gonzalez A., Chebbo G. (1999) Characterisation of urban runoff pollution in Paris. *Water Science and Technology*, 39(2), 1-8.

Hansen E. and Lassen C. (2002) Experience with the Use of Substance Flow Analysis in Denmark. *Journal of industrial ecology* 6 (3-4).

Hjortenkrans, D. S., Bergbäck, B. G., Häggerud, A. V. (2007) Metal emissions from brake linings and tires: case studies of Stockholm, Sweden 1995/1998 and 2005. *Environmental science & technology*, *41*(15), 5224-5230.

Hulskotte J. H. J., van der Gon H. A C D., Visschedijk A. J. H., & Schaap M. (2007) Brake wear from vehicles as an important source of diffuse copper pollution. *Water Science & Technology*, *56*(1), 223-231.

IGN (2009) BD TOPO. Descriptif de contenu. BD TOPO, Content description. In French. Version 2, Institut Géographique National (IGN), France.

INERIS (2000) Hydrocarbures Aromatiques Polycycliques dans l'air ambient (HAP). PAH in ambient air. In French. Report. Institut National de l'Environnement Industriel et des Risques (INERIS), Laboratoire central de surveillance de la qualité de l'air.

JCGM (2008) Evaluation of measurement data — Guide to the expression of uncertainty in measurement. Joint Committee for Guides in Metrology, Working group 1, First edition 2008, corrected version 2010, 134 p. Available online:

www.bipm.org/utils/common/documents/jcgm/JCGM_100_2008_E.pdf

Joumard R., André J.M., Rapone M., Zallinger M., Kljun N., André M. et al. (2007) Emission factor modelling and database for light vehicles. Deliverable 3 of the Artemis project. LTE, INRETS, France.

Kennedy P., Gadd J. (2003) Preliminary examination of trace elements in tyres, brake pads, and road bitumen in New Zealand., Prepared for Ministry of Transport, New Zealand.

Kupiainen K. (2007) Road dust from pavement wear and traction sanding. Finnish Environment Institute. Monographs of the *Boreal Environment Research* 26.

Kwonpongsagoon S., Bader H.-P., Scheidegger R. (2007) Modelling cadmium flows in Australia on the basis of a substance flow analysis. *Clean Technologies and Environmental Policy*, Volume 9, Issue 4, pp 313-323.

Lamprea K., Percot S., Ruban V., Maro D., Roupsard P., Millet M. (2012) Characterization of atmospheric deposition in a small suburban catchment. *Urban Environment*, Alliance for Global Sustainability Bookseries, Vol. 19, pp. 131-140.

Lamprea-Bretaudeau K., Gromaire M.C. (2014) Potentiel d'émission d'alkylphénols et de bisphénol A par lessivage des matériaux de construction et consommables automobiles. Emission potential of alkylphenols and bisphenol A by washoff of building materials and car equipment. In French. Rapport final de sous-tâche, tâche 3, projet ANR-09-VILL-0001-01 INOGEV, 107 p.

Legret M., Pagotto C. (1999) Evaluation of pollutant loadings in the runoff waters from a major rural highway, *Science of The Total Environment*, 235(1–3), 143-150.

Legret M. (2001) Pollution et impact d'eaux de ruissellement de chaussées. Pollution and impact of road runoff. In French. Etudes et recherches des Laboratoires des Ponts et Chaussées. LCPC, 109 pp.

Lindgren, Å. (1998) Road construction materials as a source of pollutants. PhD Thesis, Division of Traffic Engineering, Luleå University of Technology, Sweden.

Luhana L., Sokhi R., Warner L., Mao H, Boulter P., McCrae I., Wright J and Osborn D.(2004) PARTICULATES - Characterisation of Exhaust Particulate Emissions from Road Vehicles, Deliverable 8, Measurement of non-exhaust particulate matter, University of Hertfordshire, UK.

Malawska M. and Wilkomirski B. (2001) An Analysis of Soil and Plant (Taraxacum Officinale) Contamination with Heavy Metals and Polycyclic Aromatic Hydrocarbons (PAHs) In the Area of the Railway Junction Iława Główna, Poland. *Water, Air, and Soil Pollution*, Volume 127, Issue 1-4, pp 339-349.

Månsson N., Sörme L., Wahlberg C., Bergbäck B. (2008) Sources of Alkylphenols and Alkylphenol Ethoxylates in Wastewater - A Substance Flow Analysis in Stockholm, Sweden. *Water air soil pollution* 8, 445-456.

Maruejols L., Lu X., Young D. (2011) A comparison of energy related characteristics of residential dwellings and technologies across Canada and the US. Canadian Building Energy End-Use Data and Analysis Centre (CBEEDAC), Department of Economics, University of Alberta, Canada.

Morf, L., Buser, A., Taverna, R. (2007) Dynamic Substance Flow Analysis Model for Selected Brominated Flame Retardants as a Base for Decision Making on Risk Reduction Measures (FABRO). NRP50. Final report. 165 p. Available online at: www.geopartner.ch/upload/FABRO_2007.pdf

Morf L.S., Buser A.M., Taverna R., Bader H.-P., Scheidegger R. (2008) Dynamic Substance Flow Analysis as a Valuable Risk Evaluation Tool - A Case Study for Brominated Flame Retardants as an Example of Potential Endocrine Disrupters. *CHIMIA*, Volume 62, Number 5, pp. 424-431.

Motelay-Massei A., Garban B., larcher K. T., Chevreuil M., Ollivon, D. (2006) Mass balance for polycyclic aromatic hydrocarbons in the urban watershed of Le Havre (France): Transport and fate of PAHs from the atmosphere to the outlet. *Water Research,* 40, 1995 – 2006.

Pagotto C. (1999) Etude sur l'émission et le transfert dans les eaux et les sols des éléments traces métalliques et des hydrocarbures en domaine routier. Study on the emission and transfer in water and soils of metallic trace elements and hydrocarbons in road settings. In French. PhD thesis. Université de Poitiers, France.

Robert-Sainte P., Gromaire M. C., De Gouvello B., Saad M., Chebbo G. (2009) Annual metallic flows in roof runoff from different materials: test-bed scale in Paris conurbation. *Environmental science & technology*, *43*(15), 5612-5618.

Roustan Y. (2005) Modélisation de la dispersion atmosphérique du mercure, du plomb et du cadmium à l'échelle européenne. Modeling of the atmospheric dispersion of mercury, lead and cadmium at the European scale. In French. PhD thesis, École Nationale des Ponts et Chaussées, Paris, France.

Rule K. L., Comber S. D. W., Ross D., Thornton A., Makropoulos C. K., & Rautiu R. (2006) Diffuse sources of heavy metals entering an urban wastewater catchment. *Chemosphere*, 63(1), 64-72.

Sadiktsis I., Bergvall C., Johansson C., Westerholm R. (2012) Automobile Tires – A Potential Source of Highly Carcinogenic Dibenzopyrenes to the Environment. *Environmental science & technology*, *46*(6), 3326-3334.

Sanders P. G., Xu N., Dalka T. M., Maricq M. M. (2003) Airborne brake wear debris: size distributions, composition, and a comparison of dynamometer and vehicle tests. *Environmental science & technology*, *37*(18), 4060-4069.

Saporta G. (1990) Probabilités, analyse des données et statistiques. Probability, data analysis and statistics. In French. Paris, Editions technip.

Schauer C., Niessner R., and Pöschl U. (2003) Polycyclic Aromatic Hydrocarbons in Urban Air Particulate Matter: Decadal and Seasonal Trends, Chemical Degradation, and Sampling Artifacts. *Environmental Science and Technology* 37 (13), pp 2861–2868.

Sellami E., de Gouvello B., Gromaire M.C., Chebbo G. (2013) Evaluation of roofing materials emissions at the city scale: Statistical approach for computing roofing area distribution. In: Novatech 2013, Lyon, 23-27/6/2013.

Sommer H., Sieker H., Jin Z., Ahlman S. (2008) Source and Flux Modelling with STORM-SEWSYS. In: 11th International Conference on Urban Drainage, Edinburgh.

Sörme L., Lagerkvist R. (2002) Sources of heavy metals in urban wastewater in Stockholm. *Science of The Total Environment*, 298(1–3), 131-145.

Sternbeck J., Sjodin A., Andréasson K. (2002) Metal emission from road traffic and the influence of resuspension-results from two tunnel studies. *Atmospheric Environment* 36, 4735-4744.

Takada H., Onda T., Ogura N. (1990) Determination of polycyclic aromatic hydrocarbons in urban street dusts and their source materials by capillary gas chromatography. *Environmental Science and Technology*, 24, 1179–1186.

Tangsubkul N., Moore S., Waite T.D. (2005) Incorporating phosphorus management considerations into wastewater management practice. *Environmental Science & Policy* 8, 1–15.

Terekhanova, T. A., Helm, B., Tränckner, J., & Krebs, P. (2012) IWRM decision support with material flow analysis: consideration of urban system input. *Water Science & Technology*, 66(11), 2432-2438.

Thévenot D.R., Moilleron R., Lestel L., Gromaire M.-C., Rocher V., Cambier P., Bonté P., Colin J.-L., de Pontevès C., Meybeck M. (2007) Critical budget of metal sources and pathways in the Seine River basin (1994–2003) for Cd, Cr, Cu, Hg, Ni, Pb and Zn. *Science of the total environment*, 375(1), 180-203.

Thorpe A., Harrison R. M. (2008) Sources and properties of non-exhaust particulate matter from road traffic : a review. *Science of The Total Environment* 400, 270-282.

Val-de-Marne (2010) Trafic routier en Val-de-Marne. Road traffic in Val-de-Marne. Edition juin 2010. Conseil général du Val-de-Marne, observatoire des déplacements.

van Bohemen H.D. and W.H. Janssen van de Laak (2003) The Influence of Road Infrastructure and Traffic on Soil, Water, and Air Quality. *Environmental Management* Vol. 31, No. 1, pp. 50 – 68.

van der Swaluw E., Asman W.A.H., van Jaarsveld H., Hoogerbrugge R. (2011) Wet deposition of ammonium, nitrate and sulfate in the Netherlands over the period 1992–2008. *Atmospheric Environment*, Volume 45, Issue 23, Pages 3819-3826.

Van De Voorde A., Lorgeoux C., Chebbo G., Gromaire M. C. (2011) Roof maintenance impacts on roof runoff quality in France. In: Proceedings of the 12th International conference on Urban Drainage, Porto Alegre, Brazil, 10-15 September 2011.

van Metre P. C., Mahler B. J. (2003) The contribution of particles washed from rooftops to contaminant loading to urban streams. *Chemosphere*, 52(10), 1727-1741.

von Uexküll O., Skerfving S., Doyle R., Braungart M. (2005) Antimony in brake pads-a carcinogenic component?, *Journal of Cleaner Production*, 13(1), 19-31.

Wang Y. F., Huang K. L., Li C. T., Mi H. H., Luo J. H., Tsai P. J. (2003) Emissions of fuel metals content from a diesel vehicle engine. *Atmospheric Environment*, *37*(33), 4637-4643.

WEAREM (2010) Wear particles from road traffic - a field, laboratory and modelling study. Final report. IVL Swedish Environmental Research Institute Ltd. Available online : www20.vv.se/fud-resultat/Publikationer_000801_000900/Publikation_000871/WEAREM%20Final%20Report%20June%202010.pdf

Westerlund K-G. (2001) Metal emissions from Stockholm traffic-wear of brake linings. Report 3:2001. Available online: www.slb.mf.stockholm.se/slb/rapporter/pdf/metal_emissions2001.pdf

Westerlund C. (2007) Road runoff quality in cold climates. PhD thesis. Lulea University of Technology.

WG-AEN (2006) Good Practice Guide for Strategic Noise Mapping and the Production of Associated Data on Noise Exposure, Final draft, version 2. European Commission Working Group Assessment of Exposure to Noise (WG-AEN).

Wik A., Dave G. (2009) Occurrence and effects of tire wear particles in the environment – A critical review and an initial risk assessment. *Environmental Pollution* 157, 1-11.

Wittmer I.K., Bader H.P., Scheidegger R., Singer H., Lück A., Hanke I., Carlsson C., Stamm C. (2010) Significance of urban and agricultural land use for biocide and pesticide dynamics in surface waters. *Water Research*, 44 (9), pp. 2850–2862.

Yang H.H., Chiang C.F., Lee W.J., Hwang K.P., Wu E.M.Y. (1999) Size distribution and dry deposition of road dust PAHs. *Environment International*, *25*(5), 585-597.

Ying Q., Lu J., Kleeman M. (2009) Modeling air quality during the California Regional PM10/PM2.5 Air Quality Study (CPRAQS) using the UCD/CIT source-oriented air quality model – Part III. Regional source apportionment of secondary and total airborne particulate matter. *Atmospheric Environment*, Volume 43, Issue 2, Pages 419-430.